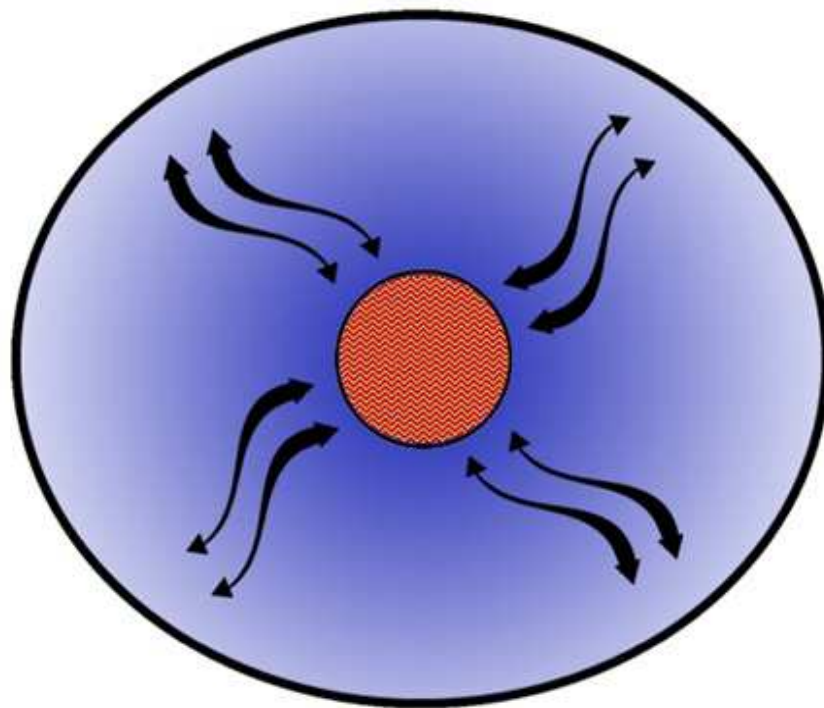


**AUTOLOGOUS BONE TISSUE ENGINEERING  
STRATEGIES ENVISIONING THE REGENERATION OF  
CRITICAL SIZE DEFECTS USING CELL-SEEDED  
SCAFFOLDS AND A NEWLY DEVELOPED PERFUSION  
BIOREACTOR.**



LEANDRO GARDEL

TESE DE DOUTORAMENTO EM CIÊNCIAS VETERINÁRIAS

2012



LEANDRO GARDEL

**AUTOLOGOUS BONE TISSUE ENGINEERING STRATEGIES  
ENVISIONING THE REGENERATION OF CRITICAL SIZE  
DEFECTS USING CELL-SEEDED SCAFFOLDS AND A NEWLY  
DEVELOPED PERFUSION BIOREACTOR.**

Tese de Candidatura ao grau de Doutor em Ciências Veterinárias, submetida ao Instituto de Ciências Biomédicas Abel Salazar da Universidade do Porto.

Orientador–Doutor Rui Luís Reis

Categoria–Professor Catedrático

Afiliação–Departamento de Engenharia de Polímeros da Universidade do Minho

Co-orientador–Doutor Luís Alvim Serra

Categoria–Professor Catedrático Convidado

Afiliação–Faculdade de Medicina do Porto

Co-orientador–Doutora Manuela Estima Gomes

Categoria–Professora Assistente Convidada MIT-Portugal

Afiliação–Departamento de Engenharia de Polímeros da Universidade do Minho

É AUTORIZADA A REPRODUÇÃO PARCIAL DESTA TESE APENAS PARA EFEITOS DE INVESTIGAÇÃO, MEDIANTE DECLARAÇÃO ESCRITA DO INTERESSADO, QUE A TAL SE COMPROMETE

DATA:

ASSINATURA: \_\_\_\_\_

\_\_\_\_\_

LEANDRO GARDEL

TO ALL THAT SOMEHOW  
CONTRIBUTED TO THIS THESIS  
AND MY FAMILY



# ACKNOWLEDGEMENTS

In the last few years had the privilege of knowing and working with many exceptional and talented people that contributed to the accomplishment of the work described in this thesis. To them, I would like to deeply express my gratitude and dedicate this thesis.

My first acknowledgments are made to my supervisor Prof. Dr. Rui Reis which gave me the privilege of being a part of the 3B's Group some years ago. During this period he always transmitted to me motivation and as natural leader showed me that it is always possible to do better. His accomplishments, professionalism and leadership are motivation and make me feel privileged by working under his supervision.

To Prof<sup>a</sup>. Dr<sup>a</sup>. Manuela Gomes, my co-supervisor, for her knowledgeable and careful supervision of my work. She showed always to be available and, above all, she constantly gave me important advices and inputs that resulted in the improvement of my work. I'm also thankful to Prof<sup>a</sup> Manuela for the time that she patiently lost with me explaining me how to overcome my limitations and doubts.

To Prof. Dr. Luís Alvim Serra, my co-supervisor, for guiding my scientific work and help. I really enjoyed all our discussions around orthopedics science. I also acknowledge the way Prof. Luís received me at the department of the orthopedics-Santo António General hospital, during this last ten years. I'm sincerely grateful.

I would also like to express my gratitude to Prof. Dr. António Pereira and Prof. Dr. António Fonseca, my directors in the ICBAS-UP.

I also thank Prof.<sup>a</sup> Dr<sup>a</sup>. Isabel Malheiro, Prof<sup>a</sup> Dr<sup>a</sup> Beatriz Porto and team (Rosa, Lara and Filipa) for giving me the opportunity to develop part of my thesis in cytogenetic laboratory. ICBAS-UP.

I would also like to express my gratitude to Prof. Dr. António Oliveira director of orthopedics services of General Hospital of Santo António. ICBAS-UP.

I also thank Prof. Dr Eduardo Rocha and your team (Fernanda and Célia) for giving me the opportunity to carry out part of my thesis in Histology laboratory. ICBAS-UP.

I'm especially grateful to my department colleagues Prof. Dr. Augusto Matos, Prof<sup>a</sup>. Dr<sup>a</sup>. Ana Lúcia, Prof. Dr. Plabo Payo, Prof<sup>a</sup> Dr<sup>a</sup> Cláudia Baptista, and Prof. Dr Miguel Farias.

I want show my deepest gratitude to Maria Afonso, at the beginning of project my student, today my colleague (DVM) for his precious help in revising the English of all the work of this thesis, thank you.

To Prof<sup>a</sup> Carla Gomes for you help in statistical analysis, thank you.

I would like to dedicate a special thank two people (friends) without them this thesis would have been very difficult mission to accomplish, the technical experts Sr. Carlos Frias (U.Porto) and Sr. Marques (U.Minho), a big thank for your help, ideas and availability.

I want to thank all the ICBAS staff who in one way or another during these years helped me, Dr<sup>a</sup> Jorge; Dr<sup>a</sup> Joana, Dr<sup>a</sup> Liliana, D. Maria do Ceú (could not forget), Costa e Silva, Eng<sup>a</sup> Ana, D. Vitória, Carla, Verónica, Madalena (AEICBAS), Lena (reprographic), João e Joana Carvalheiro, hope I'm not forgetting anyone.

I would like to dedicate a special thank to 3B's people João Oliveira, Tommaso Rada, Pedro Costa, Márcia Rodrigues, Ana Dias, Dennis Link, Alexandra Marques, Ana Frias, Miguel Oliveira, Tírcia Santos, Mariana Cerqueira, Albino Martins, Isabel Leonor, João Requicha, Rógerio Pirraço, Wojtek and Simone Silva.

I would like to dedicate a special thanks to the worldwide spread 3B's colleagues.

I cannot forget and express particular gratitude to the all members of the 3B's management team.

I should also acknowledge the Portuguese Foundation for Science and technology (FCT) for my PhD grant SFR/BD/66714/2009.



By last, my final words go out to my family, my lovely wife Gabriela and my lovely children Vítor and Rafael. For your love, patience, dedication and for letting I am part of their lives. You are the inspiration that makes me have a happy life. I dedicate this thesis to you.



## SHORT CURRICULUM VITAE

Leandro S. Gardel was born in Niterói, Rio de Janeiro, Brasil, His background includes a five-years graduation in Veterinary Medicine in 1993, University Federal Rural of Rio de Janeiro, Brasil and he started his career in Portugal, as a Lecture/Assistant Researcher in 1996, in the College of Veterinary Medicine of the University of Trás os Montes e alto Douro (UTAD), working in area of Surgery and Anaesthesiology Veterinary, In 1998, Leandro Gardel assumed the same position at the College of the Veterinary Medicine of University of Porto- ICBAS, where he also had the opportunity to supervise several students/trainees. In 2003 defended the thesis entitled:” Repair of fractures femurais oblique in dogs” a review work, integrated in the evaluation of pedagogical and scientific capacity to that allowed him to become Assistant Professor. In the same year he started his research work in 3B’s Research Group-Biomaterials, Biodegradables, Biomimetics, of the University of Minho (Supervised by Prof. Rui Reis and Prof<sup>a</sup>. Manuela Gomes) and in 2005 he enrolled as a PhD student of University of Porto, developing his research work at the 3B’s Group-Headquarters of the European Institute of Excellence on Tissue Engineering and Regenerative Medicine in collaboration of University of Porto- ICBAS and General Hospital of Santo António – University of Porto- ICBAS. His main research topics are related to bone tissue engineering strategies, namely, adult stem cells isolation and differentiation from different sources and design of dynamic bioreactors to obtain highly in vivo functional tissue engineered substitutes. Currently, Leandro Gardel is responsible for the Orthopedics Surgery service of the Hospital Veterinary Medicine of ICBAS (UP VET). Leandro S. Gardel is author and co-author papers international referred journals, one European patent application (Patent pending), communications (oral presentation) and poster presentation at Worlds and European Congres

# LIST OF PUBLICATIONS

The work performed during this PHD resulted in the following publications

## **PATENT PENDING**

Gardel, LS. Gomes ME, Reis RL. PTC: Bi-Diretctional Continuous Perfusion Bioreactor for Tri-Dimensional Culture of Mammal Tissue Substitutes (A4TEC) Association for the Advancement of Tissue Engineering Cell Based Technologies & Therapies. Nº: 104278; Date: 04 of December 2008.

## **PAPERS INTERNATIONAL JOURNAL WITH REFEREES**

Gardel LS, Dias A, Link D, Serra LA Gomes ME, Reis RL. Development of a novel bidirectional continuous perfusion bioreactor (BCPB) for culturing cells in 3D scaffolds. *Histology and Histopathology Cellular and Molecular Biology*, 26, 2011. (supplement 1) : 70-71.

## **ORAL COMMUNICATIONS IN INTERNACIONAL CONFERENCES**

Gardel LS; Afonso M, Frias, C, Correia-Gomes C, Serra LA, Gomes ME, Reis RL Osteogenic properties of osteoblast-like cells loaded on starch poly(caprolactone) dishes perfused on a new perfusion bioreactor system in a goat critical sized tibial defect. 16th ESVOT Congress, Bologna, Italy, September, 2012

Gardel LS, Dias A, Link D, Serra LA Gomes ME, Reis RL. Development of a novel bidirectional continuous perfusion bioreactor (BCPB) for culturing cells in 3D scaffolds. TERMIS EU 20011, Annual Meeting, Granada, Spain, June, 2011.

Gardel LS, Frias C Afonso M, RadaT, Serra LA Gomes ME. Reis, RL. A regenerative Medicine Aproach for the Treatment of Large Gap on Bone Fracture in the Cat Using Mesenchimal Stem Cells: A Case Report. 3rd World Veterinary Orthopaedic Congress, ESVOT-VOS, 15th ESVOT Congress, Bologna, Italy, September, 2010

Gardel LS, Frias C, Afonso M, Rada T, Serra LA, Gomes ME, Reis RL .Autologous stem Cell Therapy (ASCT) for the treatment of bone fractures in cat: A case report. World Conference on Regenerative Medicine and Veterinary Stem Cell Consortium, Germany, Leipzig, October, 2009.

#### **POSTER PRESENTATION IN INTERNACIONAL CONFERENCES**

Gardel LS, Dennis P. Link, Ana F. Dias, Manuela E. Gomes, Rui L. Reis. Development of an continuous perfusion bi-directional bioreactor for large-sized constructs. 2nd IBB Scientific Meeting, Braga, Portugal, October 2010

#### **PAPERS INTERNATIONAL JOURNAL WITH REFEREES**

Link D, Gardel LS, Correlo VM, Gomes ME, Reis RL. Osteogenic properties of osteoblast-like cells loaded on starch poly( $\epsilon$ -caprolactone) fiber meshes in a rat critical-sized cranial defect. *Histology and Histopathology Cellular and Molecular Biology*, 26,2011. (supplement 1): 386.

Oliveira, JT, Gardel, LS, Rada, T, Martins L, Gomes ME, Reis RL. Injectable gellan gum hydrogels with autologous cells for the treatment of rabbit articular cartilage defects. *J Orthop Res.* 28, 2010. (9):1193-9.

Costa, PF, Gardel, LS, Rada, T, Gomes ME and Reis RL, Stimulating adult stem cells from different origins for bone TERM approaches, *Experimental Pathology and Health Sciences*, 2, 2008. (1): 45.

#### **ORAL COMMUNICATIONS IN INTERNACIONAL CONFERENCES**

M. Afonso, L. Gardel Stem cell therapy for the treatment of canine osteoarthritis: application in four patients. 16th ESVOT Congress, Bologna, Italy, September, 2012

Link D, Gardel LS, Correlo VM, Gomes ME, Reis RL. Osteogenic properties of osteoblast-like cells loaded on starch poly ( $\epsilon$ -caprolactone) fiber meshes in a rat critical-sized cranial defect. TERMIS EU 20011, Annual Meeting, Granada, Spain, June, 2011.

Oliveira JT, Gardel LS, Martins L, Santos TC, Rada T, Silva MA, Malafaya PB, Marques AP., Gomes ME, Sousa RA, Castro AG, Neves NM, Reis RL The Use of Gellan Gum Hydrogels for Cartilage Tissue Engineering Applications: In vitro characterization and In vivo evaluation. ICRS - 8th World Congress of the International Cartilage Repair Society. Biscayne Bay Miami, FL, USA. May, 2009.

Oliveira JT, Gardel LS, Martins L, Rada T, Gomes ME, Reis RL. Injectable Gellan Gum Hydrogels With Encapsulated Adipose Derived Cells For Cartilage Tissue Engineering Applications: Performance In A Rabbit Knee Defect, 3rd International Meeting of the Portuguese Society for Stem Cells and Cell Therapies (SPCE-TC, University of Algarve, Faro, Portugal. ), April, 2008.

Costa P., Gardel LS, Rada T, Gomes ME, Reis RL. Stimulating adult stem cells from different origins for bone TERM approaches, IX International Symposium on Experimental Techniques, UTAD, Vila Real, Portugal. October, 2008.

Rada T, Gardel LS, Serra LA, Gomes ME,. Reis RL. A novel cell-specific isolation method for Adipose derived Stem cell. In: 1st Annual International Meeting of the Portuguese Society for Stem Cells and Cell Therapies, Madeira, Portugal, May, 2006.

#### **POSTER PRESENTATION IN INTERNACIONAL CONFERENCES**

Oliveira JT, Gardel LS, Martins L, Santos TC, Rada T, Silva MA, Malafaya PB, Marques AP, Gomes ME, Sousa RA, Castro AG, Neves NM, Reis RL. The Use of Gellan Gum Hydrogels for Cartilage Tissue Engineering Applications: *In vitro* characterization and *In vivo* evaluation. 8th World Congress of the International Cartilage Repair Society (ICRS), Miami, Florida, United States (*electronic poster presentation*), May 2009.

Oliveira JT, Gardel LS, Serra LA, Gomes ME,. Reis RL .Adipose Tissue Derived Cells and Articular Chondrocytes Combined with Injectable Gellan Gum Hydrogels in the Treatment of Full Thickness Articular Cartilage Defects in Rabbits. 6th Annual Meeting of the International Federation of Adipose Therapeutics and Science (IFATS 08), Toulouse, France. October 2008.

## ABSTRACT

Bone is a dynamic living tissue and thus, upon trauma, it continuously undergoes absorption, reconstruction and remodelling. However, in the case of severe bone lesions, this repairing mechanism might fail, leading to a biomechanical failure of the tissue. In such clinical situations, tissue engineering offers the ultimate possibility of providing alternative successful therapies for the regeneration of injured bone tissue, through the creation of a functional tissue substitute in vitro. This is generally achieved through a specific interplay between cells and supportive materials – scaffolds, which can be further modulated by the culturing system used. A major challenge in the translation of such tissue engineered bone substitutes to viable clinical treatments consists in the need to grow large, fully viable grafts that are several centimetres in size that can be used for the regeneration of large critical size defects. The use of flow perfusion bioreactors has shown evident advantageous over static culturing, as these systems usually allow a more efficient transfer of nutrients and oxygen, enabling a uniform distribution of cell seeded on the 3D scaffold, thus stimulating the development of homogeneous tissue for subsequent implantation. Some of these systems have also demonstrated the ability to provide mechanical stimulus to cell – seeded scaffolds, leading to higher functionality of the resulting constructs. However, up to now, these studies have focused on culturing small constructs, which do not address the clinical need for developing grafts that can be used in the regeneration of bone critical sized defects

The main objective of this thesis was to study the importance of scaffolds and cells in the regeneration of critical size defects and to develop a new flow perfusion bioreactor enabling to culture large sized defects with improved functionality for the treatment of large bone defects. Therefore, the main specific objectives proposed for this thesis were:

- Studying the importance of the scaffold material and autologous stem cells obtained from the bone marrow in the regeneration of critical sized orthotopic defects.
- Development of a new flow perfusion bioreactor system enabling the culture of 3D-scaffold with large dimensions, up to 120 mm in length and 60 mm in diameter, allowing maintenance of cell viability/functionality in the interior of the scaffold, and also enabling mechanical stimulation through fluid flow induced shear stresses.

- Analysing the feasibility of the developed bioreactor, studying the behaviour of the three dimensional starch-based scaffolds seeded with bone marrow MSCs and cultured under static and flow perfusion culturing conditions.
- Assessing the influence of three dimensional cell-scaffold constructs *in vitro* cultured in the newly developed bioreactor on the regeneration of bone critical sized defects performed in a large animal model
- Studying the use of bone marrow stromal cells (from rat, goat and cat) as a reliable cell source for bone tissue engineering application, as they can be readily available and obtained by simple harvesting procedures from the same patient, avoiding the risk of disease transmission and/or immune rejection. These cells can be used in tissue engineering strategies but also in other regenerative medicine approaches, such as the direct implantation into a tissue defect to stimulate healing

Under the scope of this thesis it was created, designed, built, developed and optimized a Bi-Directional Continuous Perfusion Bioreactor (patent pending) that enables culturing three dimensional cell-scaffold constructs of large dimensions, for the reconstruction of critical size defects for bone tissue engineering. The feasibility of the system was demonstrated by the functionality of the tissue engineering constructs obtained under *in vitro* culturing conditions provided by the bioreactor, that allows to mitigate diffusion limitations typical of static culturing and simultaneously provide physiological-like stimulus to the seeded cells.

The 3D scaffolds studied in this thesis, namely fiber mesh based on a biodegradable polymeric blend of starch with polycaprolactone (SPCL) were able to promote adhesion, proliferation and differentiation of marrow stromal cells (of different animal species) towards the osteoblastic phenotype, particularly when cultured under flow perfusion conditions. Furthermore, the *in vivo* studies demonstrated that these 3D scaffolds, play an important role both in the formation of bone tissue and neovascularisation, conditions important for the development and sustainability of cell-scaffolds of large dimensions, but also provided an excellent biomechanical environment for the regeneration of critical sized defects. In summary, the culture of an appropriate scaffold material with bone marrow cells, cultured in the new bioreactor herein developed may provide an important step forward in the development of bone tissue engineered grafts of large dimensions that are highly in demand in the orthopedical clinical field.



## RESUMO

O osso é um tecido dinâmico que, quando traumatizado, sofre um processo contínuo de absorção, reconstrução e remodelação. Contudo, no caso de lesões ósseas severas, este mecanismo de regeneração pode falhar, levando à falência biomecânica do tecido. Nestas situações, a engenharia de tecidos oferece uma solução terapêutica alternativa, capaz de levar à regeneração do tecido ósseo danificado através da criação *in vitro* de um substituto de tecido funcional. Isto é conseguido através da interação entre células e um material de suporte tridimensional (“*scaffold*”), que podem ser posteriormente modulados através do sistema de cultura usado. Um dos maiores desafios para a translação clínica destes materiais híbridos (constituídos pelos *scaffolds* e células) produzidos por metodologias de engenharia de tecidos, é a necessidade da produção de materiais híbridos de grande dimensão (vários cm) totalmente viáveis para a regeneração de defeitos de tamanho crítico. A utilização de biorreatores de perfusão de fluxo permite uma maior eficácia na transferência de nutrientes e oxigénio e possibilita uma distribuição uniforme das células no biomaterial de suporte tridimensional levando assim, à estimulação do desenvolvimento de tecido homogêneo para subsequente implantação. A utilização deste tipo de bioreactores tem-se revelado vantajosa quando em comparação com sistemas de cultura estática sendo que, alguns destes sistemas demonstram serem também capazes de proporcionar estímulos mecânicos às células semeadas no biomaterial de suporte tridimensional, proporcionando uma maior funcionalidade dos materiais híbridos obtidos. Até ao momento, estes estudos têm-se focado na cultura de *scaffolds* de reduzida dimensão, que não permitem a sua utilização clínica na regeneração de defeitos ósseos de dimensão crítica.

O principal objetivo desta tese consiste em estudar a importância dos *scaffolds* e das células na regeneração de defeitos de dimensão crítica e desenvolver um novo biorreator de perfusão de fluxo que possibilite a cultura de *scaffolds* de grandes dimensões conducentes ao tratamento de defeitos ósseos de dimensões críticas. Assim, os principais objetivos específicos desta tese foram:

- Estudar a importância do material do biomaterial de suporte tridimensional e das células estaminais autólogas obtidas por aspiração da medula óssea na regeneração de defeitos ósseos ortotópicos de tamanhos críticos.

- Desenvolver um novo bioreactor de perfusão de fluxo que possibilite a cultura de biomaterial de suporte tridimensional de grandes dimensões (até 120 mm de comprimento e 60 mm de diâmetro), que permita a manutenção da viabilidade/funcionalidade celular no interior do biomaterial de suporte tridimensional e possibilitar estímulos mecânicos, através das forças de tensão de corte induzidas pela perfusão do meio de cultura.
- Analisar a funcionalidade do biorreator desenvolvido através do estudo do comportamento de *scaffolds* baseados numa mistura polimérica de amido de milho e policaprolactona (*starch/polycaprolactone* - SPCL), e semeados com células estaminais mesenquimatosas, originárias da medula óssea, após cultura no bioreactor de perfusão de fluxo ou cultura em condições estáticas.
- Avaliar a influência dos materiais híbridos constituídos pelo *scaffolds* e células após cultura *in vitro* no novo biorreator, na regeneração em defeitos ósseos de tamanho crítico, através da implantação em modelos animais de grande porte (cabra).
- Estudar a utilização da medula óssea (de rato, cabra e gato) enquanto fonte segura de células estaminais para aplicações em engenharia de tecido ósseo, uma vez que estão disponíveis em quantidades interessantes e podem ser obtidas através de procedimentos de recolha simples a partir do próprio paciente, evitando assim o risco de transmissão de patologias e/ou rejeição imune. Estas células podem ser usadas em estratégias de engenharia de tecidos mas também noutras técnicas de medicina regenerativa, como é o caso da implantação direta em defeitos tecidulares para estimulação da cicatrização óssea.

No âmbito desta tese, foi criado, desenhado, construído, desenvolvido e otimizado um Biorreator de Perfusão Contínua Bi-direcional (patente pendente) que permite a cultura de *scaffolds* de grandes dimensões para a reconstrução de defeitos de tamanho crítico na área da engenharia de tecidos ósseos. A viabilidade do sistema foi demonstrada pela funcionalidade das estruturas de engenharia de tecidos obtidas em condições de cultura *in vitro* proporcionadas pelo biorreator que permite mitigar as limitações de difusão típicas de sistemas de cultura estática fornecendo, simultaneamente, um estímulo às células em cultura, semelhante ao existente em condições fisiológicas.

Os biomateriais de suporte tridimensional estudados nesta tese, nomeadamente a malha de fibra baseada numa mistura polimérica biodegradável de amido de milho com policaprolactona (SPCL), possibilitaram a adesão, proliferação e diferenciação de células medulares estromais (de diferentes espécies animais) em células de fenótipo osteoblástico, particularmente quando submetidas a condições de cultura em perfusão de fluxo. Paralelamente, o estudo *in vivo* demonstrou que estes biomateriais de suporte tridimensional têm um importante papel não só na formação de tecido ósseo e na neovascularização (condições importantes para o desenvolvimento e sustentabilidade de biomateriais de suporte tridimensional celulares de grandes dimensões) como também mostraram proporcionar um excelente ambiente biomecânico, fator importante no que diz respeito ao uso de biomateriais em defeitos de dimensão crítica. Em síntese, a cultura de biomateriais de suporte tridimensional apropriados, com células da medula óssea cultivadas neste novo biorreator pode providenciar um importante passo em frente no desenvolvimento de enxertos ósseos de grandes dimensões, desenvolvidos através de técnicas de engenharia de tecidos que constituem uma importante necessidade para o campo da ortopedia clínica.

# TABLE OF CONTENTS

Acknowledgements	IV
Short <i>Curriculum vitae</i>	VIII
List of publications	IX
Abstract	XII
Resumo	XIV
Table of contents	XVII
List of figures	XXIV
List of tables	XXVIII
List of abbreviations	XXIX
<b>SECTION 1</b>	<b>1</b>
CHAPTER I.	
GENERAL INTRODUCTION: Bone biology	
1.1. Introduction	3
1.2. Normal vascularization of bone	4
1.3. Structure and composition of bone tissue	4
1.3.1. Macroscopic organization of bone tissue	4
1.3.2. Microscopic organization of bone tissue	5
1.4. Cells of bone tissue	5
1.5. Biochemical composition of extracellular bone matrix	8
1.6. Functions of bone tissue	9
1.7. Remodelling of bone tissue	9
1.8. Biology of bone fracture healing	9
1.8.1. Inflammatory phase	10
1.8.2. Reparative phase	10
1.8.3. Remodelling phase	11
1.8.4. Primary bone healing	11
1.8.5. Secondary bone healing	11
1.8.6. Intramembranous bone formation	12
1.9. Bone regeneration	13
1.10. Bone mesenchymal stem cells (MSC)	13
1.11. Osteogenesis	15
1.12. Osteoinduction	17

1.13. Osteoconduction	17
1.14. Osteopromotion	18
References	20
CHAPTER II	27
REVIEW: Use of perfusion bioreactors and large animal models for long bone tissue engineering.	
Abstract	29
2.1. Introduction	30
2.2. Bioreactors for bone tissue engineering	31
2.3. Perfusion bioreactors	32
2.3.1. Perfusion bioreactors with individual culture chamber for culturing small dimension constructs	33
2.3.2. Single culture chamber perfusion bioreactors that enable culturing large sized constructs	42
2.4. Large animal models	47
2.4.1. Selection of appropriate animal models	47
2.4.2. Animal models in bone repair research	48
2.4.3. Ovine models	49
2.4.4. Caprine models	50
2.5. Critical/cylindrical size defects	51
2.6. Creation of the cylindrical critical size defects in large animals	52
2.7. Fixation of the cylindrical critical size defects in large animals	53
2.8. Conclusion	59
2.9. Acknowledgments	
References	61
<b>SECTION 2</b>	<b>75</b>
CHAPTER III	
MATERIALS AND METHODS	
3.1. Developed of a new Flow Perfusion Culture System	76
3.1.1. Design philosophy	76
3.1.2. Materials used in constituents parts	76
3.1.3. Design description	77

3.2. Scaffolds	81
3.2.1. Starch-poly ( $\epsilon$ -caprolactone)(SPCL) fiber-meshs scaffolds	81
3.3. Harvesting, isolation and culture of bone marrow mesenchymal stromal cells	83
3.3.1. Harvesting, isolation and culture of rat bone marrow stromal cells	83
(RBMSC's)	
3.3.2. Harvesting, isolation and culture of goat bone marrow stromal cells	84
(GBMSC's)	
3.3.2.1 Cryopreservation of cells	84
3.3.2.2 Replating cells after cryopreservation	85
3.3.3 Harvesting, isolation and culture of cat bone marrow stromal cells	85
(CBMSC's)	
3.4. Osteogenic differentiation	86
3.5 “ <i>In-Vitro</i> ” biological testing	86
3.5.1 Culture of Goat bone marrow stromal cells in SPCL constructs	86
3.5.1.1 Seeding GBMSC's onto SPCL constructs	86
3.5.1.2 Static culture	87
3.5.1.3 Bioreactor culture	87
3.6 “ <i>In-Vitro</i> ” characterization of the cultured cell-scaffolds constructs	88
3.6.1 Cell morphology – Scanning Electron Microscopy (SEM)	88
3.6.2 Cell viability assay	88
3.6.3 Cell proliferation assay	89
3.6.4 Determination of alkaline phosphatase activity in cells – scaffold	90
constructs	
3.6.5 Histological analysis	90
3.6.6 Light microscopy	90
3.6.7 Statistical analysis	91
3.7 “ <i>In-Vivo</i> ” studies	91
3.7.1 Rat animal model	91
3.7.1.1 Seeding rat bone marrow stromal cells in SPCL constructs	91
3.7.1.2 Characterization of DNA in cell-seeded meshes	91
3.7.1.3 Animal surgical procedures	92
3.7.2 Characterization of the samples retrieved from in vivo study performed	93
in a rat model	
3.7.2.1 Micro-CT analysis	93
3.7.2.2. Histology	93
3.7.2.3. Statistical analyses	93

3.7.3 Goat animal model	94
3.7.3.1 Cell seeding onto SPCL scaffolds	94
3.7.3.2 Static Culture Groups	94
3.7.3.3 Bioreactor culture groups	94
3.7.3.4 Animal surgical procedures	95
3.7.4 Characterization of the samples retrieved from in vivo study performed in a goat model	96
3.7.4.1 Digital radiography	96
3.7.4.2 Micro-CT	96
3.7.4.3 SEM	97
3.7.4.4 Histological analysis	97
3.7.4.5 Light microscopy	97
3.7.4.6 Statistical analysis	97
3.7.5 Cat animal model	98
3.7.5.1 Cells harvesting, culturing and implantation	98
3.7.5.2 Osteogenic differentiation - Determination of the alkaline phosphatase activity	98
3.7.5.3 Osteogenic differentiation- Alizarin red staining	99
3.7.6 Characterization performed upon cells implantation	99
3.7.6.1 Radiography	99
3.7.6.2 Determination of alkaline phosphatase activity in cat blood serum	99
References	100

## **SECTION 3** **103**

### CHAPTER IV

Osteogenic properties of starch poly ( $\epsilon$ -caprolactone) (SPCL) fiber meshes loaded with rat bone marrow stromal stem cells (RBMSCs) in a rat critical-sized cranial defect

Abstract	105
4.1. Introduction	106
4.2. Material and Methods	107
4.2.1 Scaffolds preparation	107
4.2.2 Cell isolation and seeding into scaffolds	108
4.2.3 Characterization of cell-seeded meshes	108
4.2.3.1 DNA quantification	108
4.2.4 Surgery	109
4.2.5 Characterization of the explants	110

4.2.5.1 MicroCT	110
4.2.5.2 Histology	111
4.2.6 Statistical analyses:	111
4.3 Results	111
4.3.1 In vivo experiment	112
4.3.1.1 General observations	112
4.3.1.2 MicroCT	112
4.3.1.3 Histology	114
4.4 Discussion	115
4.5 Conclusions	117
References	118
<b>SECTION 4</b>	<b>122</b>
CHAPTER V	
A novel bidirectional continuous perfusion bioreactor for mammalian tissue growth in 3D scaffolds.	
Abstract	124
5.1. Introduction	125
5.2 Materials and methods	126
5.2.1. Flow perfusion bioreactor design	126
5.2.2. Construction and functioning of the BCPB	127
5.2.3 Preliminary evaluation of the bioreactor functionality	129
5.2.3.1 Scaffolds design and preparation	129
5.2.3.2 Cell seeding of scaffolds	130
5.2.3.3 Bioreactor culture	131
5.2.4. –Characterization of cell-scaffolds constructs	131
5.2.4.1 Cell proliferation and viability analysis	131
5.2.4.2 Determination of alkaline phosphatases (ALP) activity of cells on scaffolds	132
5.2.4.3 Cell morphology analysis	132
5.2.4.4 Histological analysis	133
5.2.5 Statistical Analysis	133
5.3. Results	133
5.3.1 Alkaline phosphatases activity	133
5.3.2 Cell proliferation	134
5.3.3 Cellular viability	135



5.3.4 Cell Morphology	136
5.3.5 Histological analysis	137
5.4. Discussion	139
5.5. Conclusions	142
References	143
<b>SECTION 5</b>	<b>148</b>
CHAPTER VI	
Assessing the repair of critical size bone defects performed in a goat tibia model using tissue engineered constructs cultured in a bi-directional flow perfusion bioreactor	
Abstract	150
6.1. Introduction	151
6.2. Materials and methods	152
6.2.1 GBMSC's harvesting, isolation and culture	152
6.2.2 Scaffold design and preparation	153
6.2.3 Flow-perfusion bioreactor design	153
6.2.4 GBMSC's seeding onto SPCL scaffolds and bioreactor culture	154
6.2.4.1 Characterization of cell viability in seeded scaffolds	155
6.2.5 Animal surgical procedures	155
6.2.6 Characterization of explants from in vivo studies	157
6.2.6.1 Radiographic Analysis	157
6.2.6.2 Scanning Electron Microscopy (SEM) and Energy-Dispersive	158
X-ray Spectroscopy (EDS) analysis	
6.2.6.3 Micro-CT analysis	158
6.2.6.4 Histological analysis	159
6.2.7 Statistical analysis	159
6.3. Results	159
6.3.1 Cell adhesion and viability of scaffolds	159
6.3.2 Radiographic analysis	160
6.3.3 SEM analysis	162
6.3.4. Micro-CT analysis	165
6.3.5 Histological analysis	166
6.4. Discussion	169
References	172

<b>SECTION 6</b>	<b>176</b>
CHAPTER VII	
Autologous stem cell therapy for treatment of a tibial fracture gap in a cat. A case report.	
Abstract	178
7.1. Introduction	179
7.2. Case report	180
7.3. Results	182
7.4. Conclusion	186
Reference	187
<b>SECTION 7</b>	<b>190</b>
CHAPTER VIII	
8.1- General Discussion	192

# LIST OF FIGURES

## SECTION 1

### CHAPTER I. GENERAL INTRODUCTION: Bone biology

- Figure1.1.** Schematic representation of the principal source of adult stem cells. 14  
Adapted from:(57)
- Figure1.2.** Schematic representation of the osteogenic lineage. Adapted from:(57) 16
- Figure1.3.** Schematic representation of an ideal bone graft. Adapted from:(57) 19

## SECTION 2

### CHAPTER III: MATERIALS AND METHODS

- Figure3.1.** Design of the cellular culture chamber with the scaffold and culture medium. 78
- Figure3.2.** Overview of the design of the BCPB. 79
- Figure3.3.** Two parts of extremities of the cellular chamber culture. 79
- Figure3.4.** Coaxial perforated tube in polycarbonate or stainless steel and scaffold. 80
- Figure3.5.** Scaffold size of the same size of the perforations in the tube. 80
- Figure3.6.** Overview of the BCPB circular flow system. 81
- Figure3.7.** Schematic representation of the SPCL fiber-meshes scaffolds. 87

## SECTION 3

### CHAPTER IV: Osteogenic properties of starch poly( $\epsilon$ -caprolactone) (SPCL) fiber meshes loaded with rat bone marrow stromal stem cells (RBMSCs) in a rat critical-sized cranial defect

- Figure4.1.** Surgical approach and implantation of the scaffold. 110
- Figure4.2.** Implant characterization and SEM picture before implantation after 1 day of culturing. 111
- Figure4.3.** MicroCT reconstructions of the various implant formulations. 113
- Figure4.4.** MicroCT quantification of the new bone formation of the various implant formulations. 113
- Figure4.5.** Histological sections stained with hematoxylin and eosin (first two rows) and Masson's trichrome (bottom row) of SPCL fiber meshes loaded with MSCs after four (A) and eight (B) weeks of implantation. Four (C) and eight (D) weeks of implantation of SPCL fiber meshes and empty controls 114

(E) after eight weeks were stained as well. C = cranial bone; F = fibrous tissue; N = newly formed bone; S = SPCL fibers

## SECTION 4

### CHAPTER V: A novel bidirectional continuous perfusion bioreactor for mammalian tissue growth in 3D scaffolds.

<b>Figure5.1.</b> A) Coaxial perforated tube in polycarbonate and scaffold. B) Scaffold positioned in the tube.	127
<b>Figure5.2.</b> A) Representation of the cell culture chamber with the scaffolds inserted in the perforated tube and filled with medium culture. B) Picture of the complete BiDirectional Continuous Perfusion Bioreactor (BCPB) system under operation in a CO <sub>2</sub> incubator.	128
<b>Figure5.3.</b> Schematic representation of the flow system “circuit” that is associated with the continuous bi-directional flow bioreactor	129
<b>Figure5.4.</b> Schematic representation of the SPCL fiber-mesh scaffolds samples used in this study.	130
<b>Figure5.5.</b> ALP activity in static and flow culture (A), and maximum and minimum ALP activity values expressed (B).	134
<b>Figure5.6.</b> DNA concentration in static and flow culture (A) and maximum and minimum DNA concentration values expressed (B).	135
<b>Figure5.7.</b> MTS quantification in static and flow culture.	136
<b>Figure5.8.</b> A) Cells in the interior of the scaffolds in day 0, x1000.	136
<b>Figure5.9.</b> A) Cells in the interior of the scaffolds in day 14 flow, x 200. B) Day 14 flow, x1000.	137
<b>Figure5.10.</b> A) Cells in the interior of the scaffolds in day 21 flow, x200.B) Day 21 flow, x1000.	137
<b>Figure5.11.</b> A) Cells in the interior of the scaffolds in day 14 static, x200.B) Day 21 static, x1000.	137
<b>Figure5.12.</b> Sections of cell-scaffolds constructs cultured in the bioreactor and stained with H&E: (A) 14 days; (B) 21 days of culture. S: Scaffold.	138
<b>Figure5.13.</b> Sections of cell-scaffolds constructs cultured in static conditions and stained with H&E: (A) 14 days; (B) 21 days of culture. S: Scaffold.	138
<b>Figure5.14.</b> Graphical representation of the scaffolds volume cultured in several bioreactors reported in literature, as compared to the newly developed BCPB.	140

## SECTION 5

### CHAPTER VI: Assessing the repair of critical size bone defects performed in a goat tibia model using tissue engineered constructs cultured in a bi-directional flow perfusion bioreactor

- Figure6.1.** Schematic representation of the SPCL fiber-meshes stacked into a scaffold of critical sized defect dimensions 153
- Figure6.2.** (A) Bone fragment removed together with the periosteum; (B) Osteosynthesis material applied to the tibia; (C) Implantation of the biomaterial in tibia bone and fixation with osteosynthesis material; (D) Empty defect (control group). 156
- Figure6.3.** X-ray obtained immediately after surgery, showing the correct positioning of the bone fixation device. (A) Control group (empty defect); (B) Static group; (C) Bioreactor group. In B and C images it is possible to visualize radiographically the cells-scaffolds constructs implanted within the defect. 157
- Figure6.4.** (A) Boxplot of MTS quantification from all groups, day 0;(B) Boxplot of DNA quantification from all groups, day 0;(C) SEM photomicrographs obtained from cell seeded SPCL samples at day 0. 160
- Figure6.5.** Radiographs obtained after 6 weeks of implantation: (A) Control- empty defect (B) Static group (C) Bioreactor group. 160
- Figure6.6.** Radiographs obtained after 12 weeks of implantation: (A) Control-empty defects weeks; (B) Static; (C) Bioreactor. 161
- Figure6.7.** Radiographs obtained after implantation: (A) Static 6/ weeks group;(b) Static/12 weeks group; (C) Bioreactor/6 weeks group; (D) Bioreactor/12 weeks group. 162
- Figure6.8.** SEM photomicrographs of the cell-scaffolds constructs retrieved upon implantation: (A) Static 6 weeks [A1 (x200),A2 (x500),A3 (x1000)]; (B) Static 12 weeks [B1 (x200),B2 (x500),B3 (x1000)]; (C) Bioreactor 6 weeks [C1(x200),C2(x500),C3(x1000)] and (D) Bioreactor 12 weeks (D1 (x200),D2 (x500),D3 (x1000)]. 163
- Figure6.9.** EDS spectra for Bioreactor 6 weeks group (A), Bioreactors 12 weeks group (B), Static 6 weeks group (C) and Static 12 weeks group (D). 164
- Figure6.10.**  $\mu$ -CT 3D virtual models images of the region corresponding to the bone interfaces with SPCL-Cells constructs. A) Interface between proximal fragment and scaffolds bioreactor 6 weeks group; B) Interface between distal fragment and scaffolds bioreactor 6 weeks group; C) Interface between proximal fragment and scaffolds bioreactor 12 weeks group and D) Interface among distal fragment and scaffolds bioreactor 12 weeks group. 166

<b>Figure6.11.</b> Light microscopy images of cell-scaffolds sections corresponding to the bioreactor groups after 6 weeks implantation (HE (A) and MT (B) and static groups after 6 weeks implantation ( H&E(C) and MT(D). Bone (B); Matrix Deposition (MD); Fibrous Tissue (FT); Revascularization (R); Neovascularization (NV); SPCL fiber-meshs (S).	167
<b>Figure6.12.</b> Light microscopy images of cell-scaffolds constructs sections corresponding to bioreactor groups after 12 weeks implantation (HE (E) and MT (F), and static groups after 12 weeks of implantation. Bone (B); Bone Marrow (BM); Matrix Deposition (MD); Revascularization(R); Neovascularization(NV); SPCL fiber-meshs (S).	168

## **SECTION 6**

### **CHAPTER VII: Autologous stem cell therapy for treatment of a tibial fracture gap in a cat. A case report**

<b>Figure7.1.</b> Craneo-caudal radiography projections of the affected limb, where it is observed a lateral displacement in the axial focus of fracture.	180
<b>Figure7.2.</b> Syringe containing the cells suspension, used for the application of the cells in fracture gap.	181
<b>Figure7.3.</b> ALP activity in cells cultured in vitro, in osteogenic medium, at the day of implantation (after expansion for 2 weeks in osteogenic medium) and at 7 and 21 days of subsequent culturing.	183
<b>Figure7.4.</b> Alizarin red staining of the cat bone marrow cells after 3 weeks of in vitro culture in osteogenic medium	183
<b>Figure7.5.</b> ALP activity in blood serum of the cat, measured at the day of the application of the cells (day 0) and 7 and 21 days after application.	184
<b>Figure7.6.</b> Craneo-caudal radiographic projections obtained at: (A) day 0 (day of cells application); (B) after 1 weeks of cells application in the fracture site; (C) after 3 weeks of cells application in the fracture site.	185
<b>Figure7.7.</b> Craneo-caudal and latero-medial radiographic projections showing a medial deviation and recurvatum deformity of the tibial bone after eighteen months of follow-up.	186

# LIST OF TABLES

## SECTION 1

**CHAPTER II: REVIEW: Use of perfusion bioreactors and large animal models for long bone tissue engineering.**

**Table 2.1.** Summary table on research studies describing the development/use of perfusion bioreactor of individual culture chambers in bone tissue engineering. 34

## LIST OF ABBREVIATIONS

### A

AdBMP7 adenoviral vector containing the bone morphogenetic protein 7 gene

AA ascorbic acid

ALP alkaline phosphatase

AO orthopaedic association foundation

$\alpha$  MEM alpha modified eagle medium .

### B

b-TCP b-tricalcium phosphate

BCP biphasic calcium phosphate

BCPB bi-directional continuous perfusion bioreactor

BM bone marrow

BMSCs bone marrow stromal cells

BMP-2 bone morphogenetic protein 2

BSP bone sialoprotein

BPT Thermoplastic Elastomer Tubing

### C

CaCO<sub>3</sub> calcium carbonate

CaP calcium phosphate

°C celsius degree

CG collagen-GAG

cm<sup>2</sup> square centimeter

cm<sup>3</sup> cubic centimeter

Col I collagen type I



Col II	collagen type II	EO	ethylene oxide
CO <sub>2</sub>	dioxide carbon	ESF	external skeletal fixator
CT	computed tomography	<b>F</b>	
cm <sup>2</sup>	square centimeter	FBS	Foetal bovine serum
cm <sup>3</sup>	cubic centimeter	FDA	food and drug administration
C3H10T1/2	cell line	FGF-2	fibroblast growth factor 2
<b>D</b>		FTIR	fourier transform infra-red
DCP	dynamic compression plate	<b>G</b>	
DEX	dexamethasone	GAGs	glycosaminoglycans
DMEM	dulbecco's modified eagle's medium	GBR	guided bone regeneration
DMSO	glycerol or dimethyl sulfoxide	GFP	Green fluorescent protein
DNA	deoxyribonucleic acid	GMCs	goat marrow stromal cells
<b>E</b>		GBMCs	goat bone marrow mesenchymal cells
ECM	extracellular matrix		
EDS	energy dispersive spectrometer		

		kPa	kilopascal unit
GMP	good manufacturing practices		
		<b>L</b>	
<b>H</b>		LC-DCP	limited contact dynamic compression plate
HASi	triphasic ceramic-coated HA		
		LCP	locking compression plate
hASCs	human adipose-derived stem cells		
HE	hematoxylin & Eosin	<b>M</b>	
Hz	hertz	MATE	mechanoactive transduction and evaluation bioreactor
hMSC	human mesenchymal stem cells		
		Micro-CT	micro-computed tomography
hFOB 1.19	Human fetal osteoblasts		
		MC3T3-E1	mouse immature osteoblast-like cell line
hTERT	human telomerase catalytic subunit		
		mM	milimolar
<b>I</b>			
		mm	milimeters
IGF-1	insulin growth factor-1		
		mm <sup>3</sup>	cubic milimeters
<b>K</b>			
		ml	mililiters
Kg	kilograms	min	minutes

MRI	magnetic resonance imaging	<b>O</b>	
MSCs	mesenchymal stem cells	OC	osteocalcin
		OP	osteopontin
MT	Masson Trichrome	OP-1	osteogenic protein-1
MTS/MTT	3-(4,5-dimethylthiazol- 2-yl)-5-(3- carboxymethoxyphen- yl)-2(4-sulphophenyl)- 2H tetrazolium	O <sub>2</sub>	Oxigene
		<b>P</b>	
μg	micrograms	PA	peptide–amphiphile
μl	microliters	PBS	phosphate-buffered saline
μm	micrometers	PCL	polycaprolactone
<b>N</b>		PET	poly (ethylene- terephthalate)
N	Newton	PGA	poly (glycolic acid)
NADPH	nicotinamide adenosine dinucleotide phosphate	PLGA	poly (DL-lactic-co- glycolic acid)
NADP	nicotinamide adenine dinucleotide	pH	potencial of hydrogen
NHPs	nonhumans primates	PRP	platelet rich plasma
		pNP	<i>p</i> -nitrophenol

E <sub>2</sub>	Prostaglandin E <sub>2</sub>		
<b>R</b>		T-CUP	tissue culture under perfusion
RBMCs	rat bone marrow mesenchymal cells	TERM	tissue engineering and regenerative medicine
RGD	Arg–Gly–Asp peptides	TGF-β1	Transforming growth factor beta1
rhTGFbeta-3	recombinant human transforming growth factor-beta 3	TPS system	tubular perfusion
RT-PCR	reverse transcription polymerase chain reaction	2D	two dimensional
RNA	ribonucleic acid	3D	three dimensional
<b>S</b>		<b>U</b>	
SEM	scanning electron microscopy	UTN	universal tibial nail
SPCL	starch-poly(ε-caprolactone)	UV	ultraviolet
<b>T</b>		<b>V</b>	
TMJ joint	temporomandibular joint	VEGF	vascular endothelial growth factor
TCP	tricalcium phosphate cylinders	<b>X</b>	
		X-rays	X-rays imagens

## **SECTION 1**

### **Chapter I**

## **GENERAL INTRODUCTION**



# Bone Biology

## 1.1 Introduction

The embryologic mechanisms of bone formation entail an orchestration of cellular humoral and mechanical factors resulting in the formation of skeletal bony tissues. Bone is a connective tissue with cells and fibres which are embedded in a hard substance that protects and supports it. In addition to these mechanical functions, bones serve an important chemical function, providing a reservoir for mineral homeostasis (1, 2). Bone consists of several functionally distinct regions: At the articulating surfaces is the articular cartilage; Surrounding the entire bone is a membranous structure, the periosteum; Lining the area enclosing the cartilage (capsule) of the joints and also lining tendons sheaths are the synovial membranes, providing nutrition and lubrication to the articular cartilage while serving as a protective barrier; The woven lamellar, cancellous bone lies below the physis in a metaphysis, and the compact, cortical bone surrounds a marrow cavity in the diaphyseal region(2). Bone is a dynamic tissue that, throughout life, is renewed and remodelled. It has a unique structure that provides a great tensile strength with the least amount of weight when compared to any other tissue, having the ability to adapt its internal structure to changes that might happen in the load environment (3). Structurally, bone is a dense material, or matrix, in which, as rule, spidery cells called osteocytes are embedded. The matrix is composed of collagen fibers, crystals of a calcium-phosphate complex, and a ground substance, or cement, containing mucopolysaccharides, among many other components. The nucleated body of each osteocyte occupies a small cavity, or lacuna, in the matrix; and the long, branching, cytoplasmic processes lie in fine tunnels, or canaliculi, which radiate from the lacuna.

Canaliculi from neighbouring lacunae anastomose freely; thus, bone is characteristically permeated throughout by an extremely rich system of communicating cavities and canals (4). Bone is a unique tissue that gives mechanical support to the body. It is a major reservoir of calcium and bone marrow, which produces the blood cells. Cells present in bone are the supporting cell, termed osteoblasts and osteocytes, and remodelling cells called osteoclasts. Osteoblasts are the skeletal cells responsible for synthesis, deposition, and mineralization of bone. Osteocytes are derived from osteoblasts. After secreting osteoid and mineral salts, osteoblasts become isolated in a cavity of bone matrix and become an osteocyte. Osteoclasts are constantly eroding deposited bone, while osteoblasts are constantly replacing osteoid and minerals.

In this way, bone is a dynamic tissue that is being formed and broken down in a continuous cycle in response to physical and hormonal factors (5, 6).

## 1.2 Normal Vascularization of Bone

In 1691, Clopton Havers described in his book how a large nutrient artery pierces the shaft of long bones and ramified in bone marrow. He presumed that an oily medullary substance was expelled into a system of straight pores within the bone, these pores becoming known as Haversian canals. It is now well accepted that the nutrient artery penetrating the nutrient foramen, divides into ascending and descending branches of the medullary artery and these are the main source of centrifugal blood flow in the cortical bone of long bones. The medullary blood vessels arborize and anastomose with both the metaphyseal vessels as well as the periosteal vessels in regions of the strong soft tissue attachment. This allows increased compensatory blood flow from the anastomosing supply should one system, such as the medullary supply be knocked out(7).

In Compact bones the vascularisation is performed between the afferent and efferent systems and function as the vascular lattice where critical exchange between the blood and surrounding living tissue occurs.

Cortical canal of Havers and Volkmann and the minute canaliculi make this system, which convey blood supply to the osteocytes(7).

## 1.3 Structure and composition of bone tissue

All bones – long, flat, intramembranous, woven and compact- are specialized forms of connective tissues, and their form and function, like those of other connective tissues, depend on the arrangement and interactions of the elements of the extracellular bone matrix that distinguishes it from other connective tissue matrices and enables it to perform its unique functions(2).

### 1.3.1 Macroscopic organization of bone tissue

Macroscopically, bone is considered to be a non-homogenous, porous (porosity varying from 5 to 95%) and anisotropic tissue (8).

Two main forms of bone may be seen in vertebrate organisms: woven bone (immature bone with randomly arranged collagen fibres in the osteoid, produced when osteoblasts rapidly produce osteoid) and lamellar bone (composed of regular parallel bands of collagen). The woven bone, which is rapidly formed, will eventually be remodelled and will form lamellar bone, a stronger type of bone (9, 10).



In the mature skeleton two types of lamellar bone may be found: cortical bone and medullary bone.

Compact or cortical bone (5-10% porosity) forms the walls of the diaphysis, it consists of parallel columns that individually are made of concentric lamellae disposed around Haversian channels (central channel with blood and lymphatic vessels and nerves, also called osteons) which, on their turn, connect with other Haversian channels and with periosteum and endosteum through Volkmann's channels. The limits between osteons and surrounding bone are called cement lines.

Medullary bone or cancellous bone (50-95% porosity) occupies part of the central cavity of the bone and consists of trabeculae (a network of fine plates) which are separated by spaces that intercommunicate containing the medullary blood supply and filled mostly by fat tissue. An adult long bone, as for example the humerus or the femur, in a longitudinal cut consists of two enlarged ends called epiphyses which are connected by a hollow cylindrical shaft named diaphysis. Between these, lies a very important cancellous type of bone named metaphysis that contains important hematopoietic elements. Separating the epiphysis from metaphysis, we can distinguish a vital element for immature bone known as growth plate, which is responsible for the longitudinal lengthening of long bones(9, 10).

### **1.3.2 Microscopic organization of bone tissue**

Bone is composed of cells and an extracellular matrix predominantly collagenous called osteoid and it mineralizes after the deposition of calcium hydroxyapatite, which makes bone strong and rigid (10).

### **1.4 Cells of bone tissue**

There are three principal cell types in all bones: osteoblasts, osteocytes, and osteoclasts.

Osteoblasts synthesize and mediate the mineralization of osteoid and are found lined along the bone surface (where new bone is deposited), ranging from columnar to squamous shape, the nucleus is located in the basal region and the cytoplasm is basophilic with abundant endoplasmic reticulum. They are found on the surface of bone-forming regions, known as Haversian systems, which surround blood vessels within the matrix of woven bone (2). These cells are of mesenchymal origin and are of great importance in various functions:

Matrix synthesis – being responsible for producing all matrix components and matrix mineralization – it is believed that initiation of mineralization is under control of the osteoblast within matrix vesicles (whose function is to destroy inhibitors of mineralization and to concentrate precipitates and crystals of calcium and phosphorus) facing the bone-forming surface (9, 10).

Initiation of resorption – receptors that activate osteoclastic bone resorption are found on osteoblasts: hormones (PTH, for example) and cytokines that stimulate this process bind to osteoblasts. In the particular case of parathyroid hormone these receptors located on the cell membrane of osteoblasts induce an increase in intracellular cAMP that will phosphorylate intracellular proteins consequently activating a physiological response (PTH will cause osteoblasts to round up and separate from one another and will also activate the release of collagenases that will then destroy the thin and unmineralized layer of collagen allowing osteoclasts to gain access to bone surface through gaps formed by this osteoblastic separation and destruction of the collagen layer). Communication with osteocytes (osteoblast-osteocyte network) – osteoblasts are able to send cytoplasmic projections into the matrix during the synthesis of the latter. Some of these projections extend through canaliculi and then from lining cells to the osteocytes and from osteocyte to osteocyte, forming gap junctions that allow small molecules and also ions to travel between these cells. Osteocytes are inactive osteoblasts trapped inside formed bone and are able to assist in the nutrition of the bone. These are the principal cell type in mature bone and they reside in *lacunae*, microscopic holes in the bone. These cells are able to send cytoplasmic projections that are able to penetrate through the bone in canaliculi and gap junctions are present where the cell contacts processes of an adjacent bone. The long cellular projections are able to shorten and lengthen and this activity possibly allows the movement of pulsatile fluid flow through lacunae and canaliculi in order to transfer metabolites (10, 11). Osteocytes and bone-lining cells are presently thought to be the primary mechanosensory cells responsible for interpreting mechanical forces in bone tissue and translating them to osteoblasts and osteoclasts for bone remodelling (12-14).

Multiple investigators report evidence supporting the key mechanosensory role of osteocytes in bone formation as detected by changes in matrix protein expression, and production of nitric oxide (NO) and prostaglandin E2 (PGE2), a potent stimulator for bone formation (14, 15).

The osteocytes trapped deeper in the bone are older than the more superficial ones. Osteocytes play a role in the homeostasis of calcium and that changes in their metabolic activity are able to solubilise small amounts of mineral in the lacunar walls. Osteocytes are the most abundant differentiated cells. Numerous of these cells are released from the *lacunae* when osteoclast resorption is occurring (10, 11).

Osteoclasts are large phagocytic cells (20 to 100  $\mu\text{m}$  in diameter) that have the capacity to erode the bone, and which are important in the process of bone turnover and refashioning. These cells are originated from the monocyte-macrophage system. Preosteoclasts are mononucleated cells that when activated will fuse with cells alike and when after accessing the bone surface, they differentiate further finally becoming multinucleated (15 to 30 nuclei per cell) osteoclasts. The activated osteoclasts have ruffled borders (is a resorbing organelle, and it is formed by fusion of intracellular acidic vesicles with the region of plasma membrane facing the bone (16) and secrete acid and lysosomal enzymes are directly responsible for removing the mineral and matrix bone (17, 18). After enzymatic and acid digestion (acid phosphatase, collagenase, cathepsins and neutral proteases) of the bone matrix the erosion lacune (Howship's lacuna) is formed(2).Differences in mode of degradation have been observed as well. Calvarial (flat bone) osteoclasts use cysteine proteinases as well as matrix metalloproteinases (MMPs) to degrade the bone matrix, whereas resorption by long bone osteoclasts is accomplished mainly by cysteine proteinases (19, 20). This lacuna will remain even after the osteoclast is gone, which indicates prior areas of bone resorption.

Osteoclasts are also found as part of cellular complexes involved in bone remodeling and these cells are responsible for the release and activation of TGF-beta, and of mineral and protein components of bone, participating in the maintenance of blood calcium homeostasis by responding to parathyroid (which stimulates osteoclastic resorption and the release of calcium ions from the bones) and calcitonin (acts as a mitogenic agent on pre-osteoblastic cell lineage) (10).

Interleukine 1 (*in vitro* induces bone resorption and osteoclast-like cell formation in human and murine marrow cultures; in *in vivo* studies induced hypercalcemia and growth and differentiation of the earliest identifiable osteoclast precursor – CFU-GM), IL - 6 (controversial role, potentiates the effect of PTH on calcium homeostasis and bone resorption *in vivo*) and IL-11 (effects on osteoclast differentiation), M-CSF (important role on osteoclast development), TGF- $\alpha$  (proliferative factor, stimulates the growth of early osteoclast precursors), TNF- $\alpha$  and  $\beta$  (stimulate the formation of osteoclast like multinucleated cells in human marrow cultures, increase bone resorption, enhance the effect of IL-1) are soluble factors that increase osteoclast activity. TGF- $\beta$  (modulates

osteoclastic bone resorption, migration and differentiation, inhibiting bone resorption) IFN- $\gamma$  (inhibitor of bone resorption *in vitro*, suppresses formation of and maturation of osteoclasts), IL-4 (high levels may inhibit bone formation and bone resorption), IL-18 (inhibits osteoclastic formation *in vitro*), nitric oxide (produces rapid contraction and detachment of osteoclasts in cell surfaces, inhibits bone resorption), sex steroids (estrogen inhibits osteoclast formation), and osteoprotegerin (disrupts an F-actin ring inhibiting osteoclastogenesis and bone resorption) inhibit osteoclastic activity (21). Bone lining cells consist of inactive osteoblasts not buried in new bone. After bone formation stops, these cells will remain on bone surface and will only be re-activated after chemical, mechanical stimuli or both (9, 22).

### 1.5 Biochemical composition of extracellular bone matrix

The mature compact bone is made of approximately 65% inorganic salts and 35% organic matrix (1, 23). Of this organic component, about 90% is collagen (specially type I fibers), the protein which gives strength to the bone; in mature bone collagen fibers are organized in concentric layers in osteons (cortical bone) or parallel the rounding surfaces of trabeculae (cancellous bone). The remaining 10% is made of ground substance proteoglycans (essentially chondroitin sulphate and hyaluronic acid forming aggregates) which besides controlling the content in water of the bone, are also supposed to be involved in the regulation of the formation of collagen fibers for ulterior mineralization of the matrix and non-collagen molecules which are supposed to be involved in the regulating the bone mineralization (osteocalcin – which is involved in binding calcium; osteonectin – which may have a bridging function between the mineral component and collagen; sialoproteins and other molecules) (8, 10). Differences in the organic matrix were observed in a study where cortical bone (midshaft of tibia) was compared with trabecular bone (lumbar spine), showing trabecular bone to have more osteonectin but less osteocalcin than cortical bone (24).

The inorganic component consists of hydroxiapatite crystals which are deposited within the collagen fiber network. The principal salts in bone are: Ca, CO<sub>3</sub>, PO<sub>4</sub>, and OH. There are also substancial amounts of Na, Mg and Fe present in bone, which is also considered a “storehouse” for calcium and phosphorus (23). Although only one percent of the amount of calcium-phosphorus existing in the matrix can be rapidly deployed in ion (22)The inorganic component of bone controls the compression strength and stiffness, whereas the collagen is believed to contribute to the ultimate strength and toughness of bone (25-27).

## 1.6 Functions of bone tissue

The most evident functions of bone tissue are obviously to support to the body organs and tissues, so that it maintains its basic structure, and to enable movement/locomotion. Moreover bones provide attachment points for the muscles, transmitting forces from one part of the body to another under controlled strain and to protect vital organs and structures (8). Within the bone it is found the bone marrow, an essential structure for hematopoiesis and immune function. In addition to this, bone also plays a function in mineral, specially calcium, homeostasis (this feature is however rather small when compared to other organs such as the kidney) (10).

## 1.7 Remodelling of bone tissue

The remodelling process consists in the activation of resorption -proteases that dissolve bone matrix and acid that will release bone mineral into the extracellular space beneath the ruffled border are secreted by osteoclasts (21) followed by formation of new bone. Theoretically, the total amount of new bone replaced is equal to the total amount of removed bone (so that the volume difference is equal to zero). This process allows that microfractures and other small damages suffered with time are removed and replaced with new tissue(9).

Bone remodelling only happens in the internal surface of trabecular surfaces (cancellous bone) and of Haversian systems (cortical bone). The process is not performed individually by each different cell type, but actually by “basic multicellular units” (BMUs) which are groups of organized cells that operate replacing old bone by new bone in a discrete fashion, in a sequence that usually follows a similar pattern: activation – resorption – formation(28).

## 1.8 Biology of bone fracture healing

Fracture healing represents a complex series of responses including inflammation, wound repair, developmental responses and bone remodelling. Biologically, fracture healing has been classically divided into several stages, which include haematoma formation, inflammation, angiogenesis, cartilage formation, endochondral ossification and remodelling. The early stages are all non-specific to bone repair in that they are wound repair phenomena, common to soft tissue injury also. The specific bone repair phenomena include endochondral and intramembranous ossification and bone remodelling.

Basically, there are three stages in the process of post-fracture bone healing, which are similar to what occurs in other tissues.

### **1.8.1 Inflammatory Phase**

After a trauma to the bone, which results in a fracture, the periosteum and the muscles around the bone are torn and many blood vessels are damaged. The hematoma (which will later organize itself and will serve as a fibrin scaffold for repair cells to perform their function) accumulates inside the medullary canal, between fracture ends and beneath elevated periosteum. This vascular damage will deprive osteocytes of nutrition which will cause their death. Thus, the edges of the fractures are dead. The presence of necrotic material in large quantities leads to an intense acute inflammatory response characterized by vasodilatation, plasma exudation and acute edema. Inflammatory cells, polymorphonuclear leukocytes and macrophages will then migrate to the region(22).

### **1.8.2 Reparative Phase**

The cells directly involved in this process are pluripotent cells of mesenchymal origin. During this period the gap fracture is filled with bony like material and the revascularization of bone fragments occurs by a temporary formation of an extraosseous blood supply by connecting the surrounding soft tissues to the bone fragments and by establishment of a centripetal flow circulation.

Under natural circumstances, the periosteal vessels will contribute to the majority of capillary buds early in bone healing, with the medullary artery being of greater importance later in the process. As soon as the intramedullary blood supply is re-established the afferent vascular system returns to its normal pattern. All tissues require microvasculature to heal beyond scar, with the exception of cartilage, which makes microvasculature a good indicator of bone healing (29).

It is known that the microenvironment around the fracture gap is acid, and this may stimulate the cell behaviour during this phase. Over time, as the reparative phase occurs, the pH will return to a slightly alkaline level. The hematoma, which provides some mechanic support on the site, tends to be invaded by granulation tissue composed mostly by fibrous tissue and cartilage known as fibrous callus. This process enhances the stability in the fracture ends leading to the next phase called mineralized callus. This occurs when there is a high quantity of collagen which leads to deposition of calcium hydroxyapatite crystals (30).

This deposition process tends to be highly organized and ends when the union of the fracture ends is safely achieved. During this phase it is very important that too stressful forces are absent of the fracture ends due to the need of an oxygen rich environment which otherwise can delay de union(22).

### **1.8.3 Remodelling Phase**

The last phase in bone healing consists in the replacement of woven bone by longitudinal haversian systems in the fracture gap. This phase may occur for several years as evidenced by radioisotope studies that show that increased activity in a bone that has suffered a fracture may last for 6 to 9 years in human tibial fracture. The mechanism that controls this cell behaviour is believed to be electric: after stress, electro-positivity will occur on the convex bone surface (associated with osteoclastic activity) and electro-negativity on the concave surface (associated with osteoblastic activity), producing current (piezoelectric effect). The resorption unit (which consists of osteoclasts that resorb bone and osteoblast that lay down new haversian systems) is the cellular module that controls remodelling).Two patterns are recognizable in bone healing: primary and secondary healing (9, 30).

### **1.8.4 Primary bone healing**

Primary healing happens when strain across the gap is less than 2% and can occur in two different ways: under small fracture gaps, by direct bridging of the fracture gap by haversian or, more commonly, in a process called “gap healing”, which consists in the woven bone being directly laid into the gap by osteoblasts followed by remodelation by haversian bone (30).

This process involves attempts by bone cortex to re-establish new haversian systems by formation of “cutting cones” (remodelling units) in order to restore continuity of bone. During this process there is no formation of bone callus (31).

### **1.8.5 Secondary bone healing**

Secondary healing occurs with the formation of a fracture callus by involving a combination of intramembranous (involving the formation of bone directly – without forming cartilage – from pluripotential mesenchymal and osteoprogenitor cells. The callus formed is a hard callus) and endochondral ossification (involving the recruitment, proliferation and differentiation of mesenchymal cells into cartilage followed by

calcification and replacement by bone tissue. This process provides the formation of a soft callus, an early bridging callus that stabilizes the fragments formed after trauma (31, 32).

The indirect bone healing occurs when there is an unstable environment that produces motion in the fracture ends or these are too distant to allow lamellar bone formation in a direct way. The degree of movement or strain defines the capability and conditions of bone healing and starts always with a soft callus that progress to mineralization. The gaps between the fractures ends are filled initially with hematoma (formed by the local ruptured vessels and turned tissues). The role of the hematoma is still controversial since some investigators believe that it should be removed to accelerate de bone healing and others support the fact that it contains important factors and cells that provide the development of the granulation tissue. These together produce some mechanical stability which is crucial for the next phases. With time these tissues tend to be replaced by fibrous connective tissue and fibrous cartilage forming the soft callus. This together with lamellar bone deposition increases the local stability and leads to the fibrocartilaginous mineralization. The mineralization occurs from the base of the fracture ends to the middle of the bridge forming trabecular and woven bone known as hard callus. At this stage the degree of instability at the site dictates the capability and the exuberance of this type of callus formed. The granulation tissue in fractures ends with too much motion tends to involve a larger area leading to a consequent bigger callus. At the same time the mineralization occurs, resorption mechanisms can be observed on the initial bone. These occur due to the high osteoclast activity leading to resorption cavities which penetrate trough fragment ends and newly formed bone gap. Then theses spaces tend to be filled with new mesenchymal cells with high osteoblast population forming aligned lamellar bone. This last stage can be active from months to several years until perfect oriented mineralization is achieved (2, 30, 33).

### **1.8.6 Intramembranous bone formation**

In fractures with multiple bone fragments and sufficient local stability the initial phase consists in intramembranous bone formation. In these cases, bone is directly deposited on the fragments from the fracture site or in the bridging phase of much comminuted fractures. This type of bone formation is always combined with various steps of indirect bone healing process (30, 31).



## 1.9- Bone regeneration

The processes of bone repair are sufficient for effective and timely restoration of skeletal integrity for most fractures, when an appropriate mechanical environment exists or is created with internal fixation or coaptation. However, some situations require manipulation or augmentation of natural healing mechanisms to regenerate larger quantities of new bone than would naturally occur to achieve surgical goals. Specific situations that may require additional interventions include substantial loss of host bone from trauma or tumor resection, arthrodesis, or spinal fusion, non- or delayed unions, metabolic disease, arthroplasty, or insufficient healing potential of the host because of local or systemic disease or old age. Materials and strategies that are employed must duplicate and amplify the events of secondary bone union to achieve the desired results (34, 35). Bone can be regenerated through the following strategies: osteogenesis-- the transfer of cells; osteoinduction--the induction of cells to become bone; osteoconduction, providing a scaffold for bone forming cells or osteopromotion—the promotion of bone healing and regeneration by encouraging the biologic or mechanical environment of the healing or regeneration tissues (35). The most efficacious strategies use as many of the fundamental components of bone regeneration as possible, and each facet of bone regeneration relies upon mesenchymal stem cells (36, 37).

## 1.10- Bone mesenchymal stem cells (MSC)

Mesenchymal stem cells (MSCs) are an interesting candidate for cell-based therapeutics and regenerative medicine (38, 39). MSCs are a rare population of multipotential cells capable of differentiating into osteoblasts, chondrocytes, adipocytes, tenocytes and myoblasts (Figure 1.1) (5, 40-46). Their origin is either the cambium layer of periosteum or bone marrow, although other sources such as muscles, fat, and synovium provide a limited source (32, 45, 47).

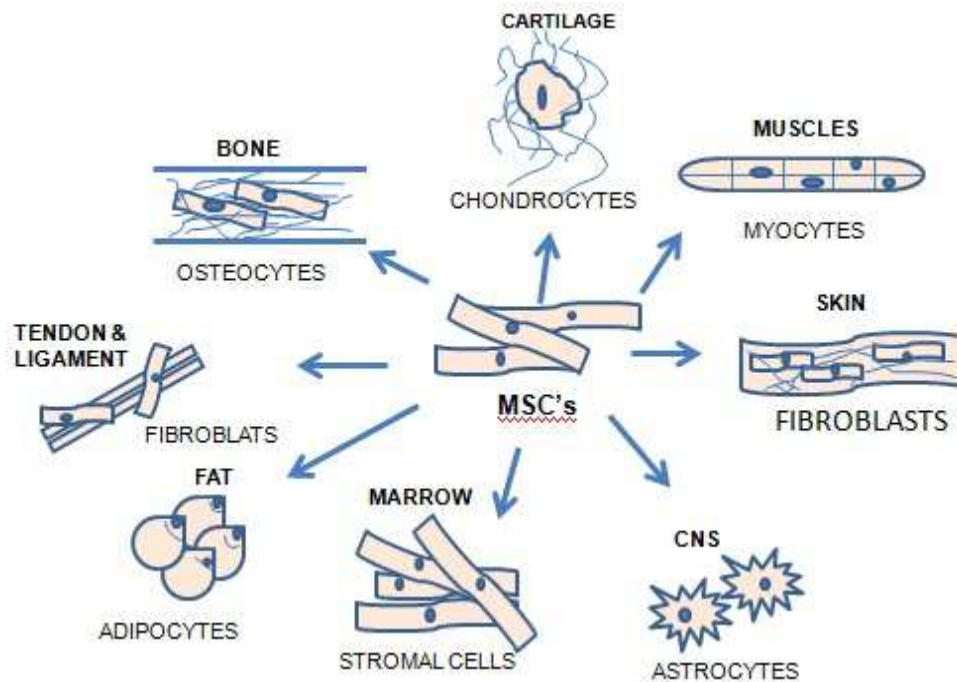


Figure 1.1. Schematic representation of the principal source of adult stem cells. Adapted from: (57)

Bone marrow and periosteum sources are richest in young age with numbers diminishing, but still present in old age. MSC number and biologic activity are greatest in metaphyseal bone and areas of thick and vascular periosteum, contributing to more robust healing at these locations (45, 46).

The study of MSC has primarily utilized those retrievable from bone marrow aspirate (47). Isolation techniques are generally based on the adherent properties of the MSC. Density gradient centrifugation is sometimes employed to separate nucleated MSC. As the cells are cultured, MSC adhere to the flask surface (40, 47). The non-adherent cells are removed with the culture medium when it is changed, concentrating the MSC. The cells are repeatedly passaged, expanding the cell population, until a pure culture is produced. The isolated cells are confirmed to possess osteogenic potential by various techniques (32, 48, 49).

In vitro experiments have demonstrated the formation of mineralized nodules, along with elevated production of alkaline phosphatase, osteopontin, bone sialoprotein, osteocalcin, types I and III collagen, and the generation of PTH and estrogen receptors, during the differentiation of MSC into osteoblasts (42, 50-52).

In view of this, various studies have already shown that culturing of osteoprogenitor cells from purified MSC in media supplemented with dexamethasone, ascorbic acid, and glycerophosphate initiates a development process that directs the cells into an osteoblastic differentiation pathway (42-44). The cells express bone matrix protein mRNAs and the deposition of a hydroxyapatite-mineralized extracellular matrix confirming that the cells isolated become bone forming cells (44, 47).

MSC can also maintain viability and multilineage potential after cryopreservation. Neither cryopreservation nor thawing negatively effects the growth or differentiation of MSCs (45). Therefore, MSC can be effectively isolated, culture expanded, preserved, and implanted. The osteogenic potential of marrow-derived MSCs has evoked widespread interest and been well defined, as evidenced by their ability to produce new bone after transplantation of MSCs in vivo (41, 42) by the direct conversion of MSCs to osteoblasts, without progression through a cartilaginous intermediate (47). Because bone healing and growth involve migration, proliferation, and differentiation of osteocompetent cells, a major improvement in materials used for bone repair and regeneration is achieved through loading of the scaffold prior to implantation, with osteocompetent cells. Subsequent bone formation would therefore not depend on the local recruitment of osteocompetent cells. It is thought that by delivering stem cells directly to the site, both the need for chemotaxis of osteoblast progenitor cells to the defect and the level of proliferation required to repair the bone were decreased (48).

### **1.11- Osteogenesis**

Bone formation requires the cellular machinery to fabricate its structural components. As such, no strategy of bone regeneration can neglect introduction of cells, and the most efficacious strategies nurture an early cellular environment (35). Autogenous cancellous bone grafts are best example of an osteogenic graft and are the “gold standard” for bone regenerative materials (Figure 1.2). Cancellous autograft provides a mixture of cells from fully differentiated osteoblasts lining the cancellous bone to undifferentiated MSC in the marrow components (32). MSC can respond to the local biologic and mechanical environment and differentiate into any cellular component needed in secondary bone union, therefore offer robust bone healing potential for a variety of situations.

However, the cells do not work alone but are combined with matrix and signals provided by the cancellous particles, yielding a mixture that contains other facets of bone regenerating strategy. Autogenous cancellous bone grafts are easily obtained from the iliac crest, greater tubercle of the humerus, wing of the ilium and sternum in veterinary medicine, from iliac crest in human medicine and are the mainstay of osteogenic material in orthopaedic surgery.

Harvesting bone graft requires a separate surgical site increasing surgical time and cost. Donor site morbidity is more common in humans (53, 54). The quantity of autogenous cancellous bone that can be harvested may be insufficient, especially in older or small patients, or when a very large amount of graft material is needed. Thus, although autogenous cancellous bone is principally ideal, substitutes are often needed. Another example of an osteogenic material is bone marrow (55, 56). Bone marrow aspirates contain MSC, cells already committed to osteogenic or chondrogenic lineage, and some biologically active proteins that stimulate bone regeneration in similar manner to naturally occurring fracture clot, many from platelet degranulation. However, use of bone marrow does not yield the magnitude of osteogenesis observed with cancellous bone for several reasons. Aspiration results in varying quality of bone marrow depending on technique and patient (55).

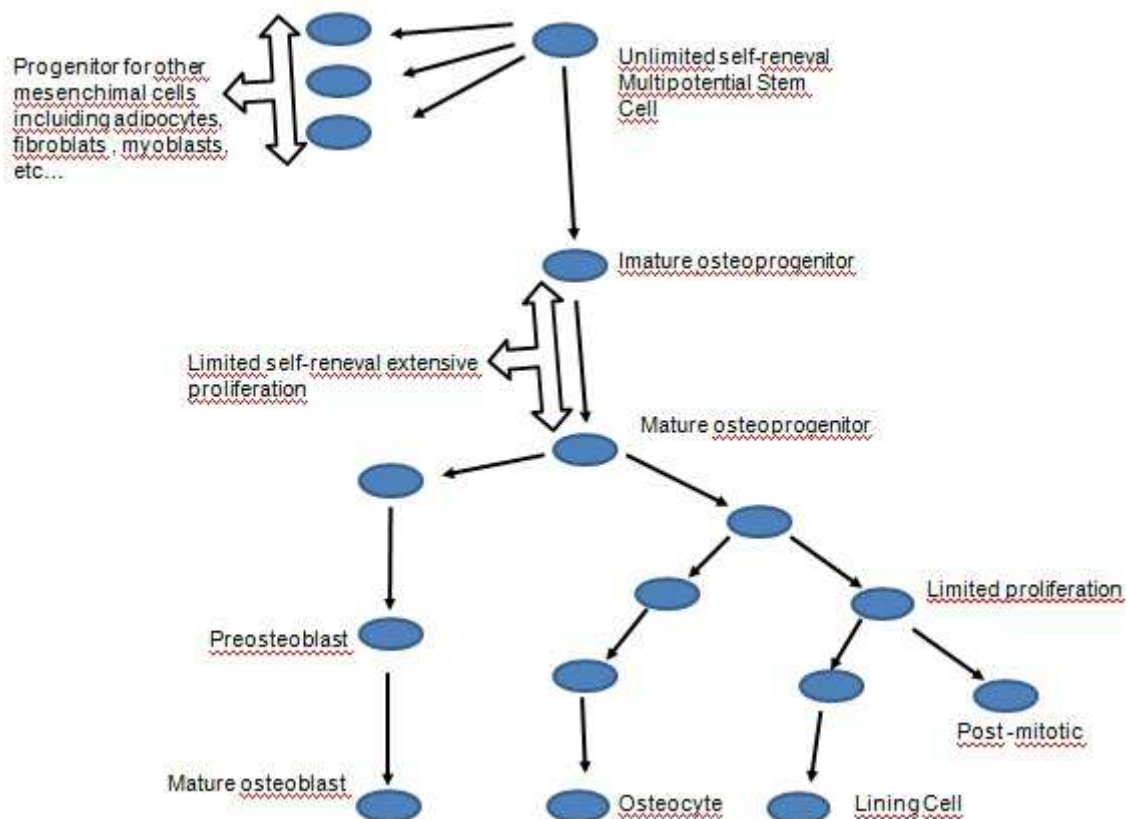


Figure 1.2. Schematic representation of the osteogenic lineage. Adapted from:(57)

### 1.12- Osteoinduction

Materials that have the capacity to induce bone formation when placed into a site where no bone formation will occur are termed osteoinductive (Figure 1.3) (35, 58, 59). These materials do not work alone, but recruit MSC or their progeny to infiltrate the material (chemoattraction and migration) then induce the multipotential cells to multiply and become cells that comprise the regenerating bony callus (proliferation and differentiation). The best known example of osteoinductive materials is demineralised bone matrix (DBM). By decalcifying bone (usually allogeneic) in a process that does not inactivate bone's biologically active components, organic matrix exposed along with a plethora of bone stimulatory cytokines trapped within the organic matrix during bone formation. These are naturally occurring initiators and mediators of bone healing, which are released when bone fractures. Bone morphogenetic proteins (BMP), the most specific family of bone inducing cytokines, are members of the transforming growth factor (TGF- $\beta$ ) superfamily of growth factors that include cartilage-derived growth factors, and other growth and differentiation factors. Although often referred to as a specific entity, the growth factors of DBM are a combination of biologically active cytokines, which may be chemotactic to MSC to follow certain osteoblastic or chondroblastic lineages, or stimulate replication of MSC or their progeny (58, 59).

### 1.13- Osteoconduction

A material that provides a scaffold for MSC and their progeny to migrate into, and proliferate within, is termed osteoconductive (Figure 1.3) (35). These are materials with a three-dimensional shape that offer an appropriate framework, surface characteristics for adherence of MSC, osteoblasts, osteocytes, chondroblasts and chondrocytes (60, 61), and interconnecting porosity for cellular proliferation and vascular ingrowth and thus may serve as temporary scaffolds for transplanted cells to attach, grow, and maintain differentiated functions (61-70). In any case, the role of the biomaterial is temporary, but rather crucial to the success of the strategy. Therefore, the selection of a scaffold material is both a critical and difficult choice (71). Specific examples of naturally occurring osteoconductive materials include autogenous cancellous bone, and some forms of DBM or deproteinized bone. Synthetic materials include metals, hydroxyapatite, collagen, tricalcium phosphate, apatitic calcium phosphate, calcium sulfates, porous coralline ceramics, bioactive glass, calcified triglycerides, or the polyhydroxy acid family of polymers (polylactide, polyglycolide), blends of corn starch (in amounts varying from 30 up to 50 %wt) with poly(ethylene vinyl alcohol) (SEVA-C), cellulose acetate (SCA), poly( $\epsilon$ -caprolactone) (SPCL) and poly-lactic acid (SPLA) (60, 61, 72, 73).

Bioabsorption and osteoconduction are quite variable between materials and because of their relatively passive role in bone regeneration; these materials have limited utility alone. Although bone can infiltrate and often replace many of these materials, they lack essential osteogenic and osteoinductive properties and rely on natural cellular activities of MSC or their progeny to infiltrate and provide their own biologic signals for proliferation and differentiation (60), but the criteria of biodegradability and non-brittle nature (ideally with tissue matching mechanical properties) excludes the use of all metals and most ceramics as scaffolds materials (74) and gives preference to biodegradable polymers for most of the applications within the tissue engineering and regenerative medicine field (71).

### **1.14- Osteopromotion**

A material or physical impetus that results in enhancement of regenerating bone is termed osteopromotive (Figure 1.3) (35). Osteopromotion can function at various stages during bone healing and provide different stimulatory signals to bone regenerating tissues. Osteopromotion differs from osteogenesis or osteoconduction as bone formation is enhanced without cells or a scaffold; however, osteopromotive stimuli alone cannot induce bone formation.

Osteopromotion can be achieved by introduction of substances or materials that enhance bone regeneration, or by physical or mechanical strategies that induce proliferation and differentiation of MSC and their progeny. The good example of an osteopromotive substance is platelet-rich plasma (PRP), which is produced by centrifugation of the blood yielding a suspension of concentrated platelets. Platelets function not only in hemostasis, but are essential for initiation of the healing process, including bone healing. The granules of platelets contain a rich source of growth factors including TGF- $\beta$ , platelet-derived growth factor (PDGF), vascular endothelial growth factor (VEGF), and insulin-like growth factor (IGF). TGF- $\beta$  is a potent chemotactic agent for MSC and supports differentiation of osteoblasts (73); PDGF and IGF I and II are potent mitogenic agents, and VEGF is a potent angiogenic agent (75). Platelets will release the contents of their granules on contact with fibrin or von Willebrand's factor (73). Cellular and humoral factors are essential mechanical factors cannot be neglected. MSC and their progeny respond aggressively to local mechanical forces and the local mechanical environment has a strong influence on cellular proliferation and differentiation. Developing fracture callus or areas of regenerating bone are subjected to physical forces.

If these forces result in physical disruption of regenerative tissues then bone healing cannot occur and non-union results; however, forces of lesser magnitude may have a physical effect on regenerating tissues without cell death. Compression of MSCs resulting in increasing pressure within the cell will encourage chondroblastic differentiation; however, low-to-moderate magnitudes of tensile strain and hydrostatic tensile stress may stimulate new bone formation. This occurs because of deformation or elongation of the cells including MSC and early osteoblastic and chondroblastic cells. Cellular deformation results in intracellular signals, which in turn encourage regenerating cells to proliferate and follow an osteoblastic lineage, provided the biologic environment and oxygen levels are suitable (76).

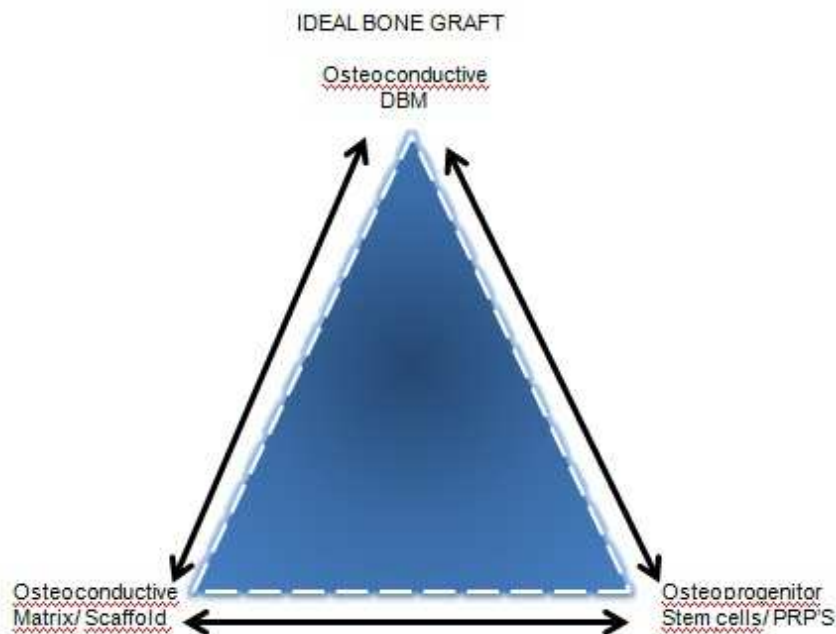


Figure 1.3. Schematic representation of an ideal bone graft. Adapted from:(57)

## References

1. Buckwalter, J.A., Glimcher, M.J., Cooper, R.R., Recker, R. Bone biology. I: Structure, blood supply, cells, matrix, and mineralization. Instr Course Lect 45, 1996,371.
2. Boskey, A.L. Connective Tissues of the Musculoskeletal System. In: Slatter D, ed. Textbook of Small Animal Surgery. 3rd ed: WB Saunders; 2003. pp. 1790.
3. Bagge, M. A model of bone adaptation as an optimization process. J Biomech 33, 2000,1349.
4. Moss, M.L. Studies of the acellular bone of teleost fish. I. Morphological and systematic variations. Acta Anat (Basel) 46, 1961,343.
5. Aubin, J.E. Bone stem cells. J Cell Biochem 30-31, 1998,73.
6. Bancroft, G.N., Mikos, A.G. Bone tissue engineering by cell transplantation. Tissue Engineering for Therapeutic Use 1222, 2001,151.
7. Rhinelander, F.W., Wilson, J.W. Blood supply to developing mature, and healing bone. In: Summer-Smith G, ed. Bone Clinical Orthopaedics A study in comparative osteology. Philadelphia: Wb saunders; 1982. pp. 81.
8. Doblare, M., Garcia, J.M., Gomez, M.J. Modelling bone tissue fracture and healing: a review. Eng Fract Mech 71, 2004,1809.
9. Olmstead, M.L. Structure and Healing of the Musculoskeletal System. In: Olmstead ML, ed. Small Animal Orthopedics. St. Louis, Missouri: Mosby; 1995. pp. 27.
10. Young, B., Lowe, J.S. Skeletal Tissues. Weather's Functional Histology: A text and colour atlas. 5th ed. Philadelphia: Elsevier Limited; 2006. pp. 189.
11. Suzuki, R., Domon, T., Wakita, M., Akisaka, T. The reaction of osteoclasts when releasing osteocytes from osteocytic lacunae in the bone during bone modeling. Tissue & Cell 35, 2003,189.
12. Burger, E.H., Klein-Nulend, J. Mechanotransduction in bone - role of the lacuno-canalicular network. Faseb J 13, 1999,S101.
13. Sikavitsas, V.I., Temenoff, J.S., Mikos, A.G. Biomaterials and bone mechanotransduction. Biomaterials 22, 2001,2581.
14. Klein-Nulend, J., Semeins, C., Burger, E., Plas, A.V.D., Ajubi, N., Nijweide, P. Response of isolated osteocytes to mechanical loading in vitro. In: Odgaard A, Weinans H, eds. Bone Structure and Remodeling. Singapore: World Scientific Publishing Co. Pvt. Ltd; 1994. pp. 37.
15. Ajubi, N.E., Klein-Nulend, J., Nijweide, P.J., VrijheidLammers, T., Alblas, M.J., Burger, E.H. Pulsating fluid flow increases prostaglandin production by cultured chicken osteocytes-a cytoskeleton-dependent process. . Biochem Biophys Res Commun 225, 1996,62.



16. Blair, H.C., Teitelbaum, S.L., Ghiselli, R., Gluck, S. Osteoclastic Bone-Resorption by a Polarized Vacuolar Proton Pump. *Science* 245, 1989,855.
17. Vaananen, H.K., Zhao, H., Mulari, M., Halleen, J.M. The cell biology of osteoclast function. *J Cell Sci* 113, 2000,377.
18. Suda, T., Takahashi, N., Udagawa, N., Jimi, E., Gillespie, M.T., Martin, T.J. Modulation of osteoclast differentiation and function by the new members of the tumor necrosis factor receptor and ligand families. *Endocr Rev* 20, 1999,345.
19. Shorey, S., Heersche, J.N., Manolson, M.F. The relative contribution of cysteine proteinases and matrix metalloproteinases to the resorption process in osteoclasts derived from long bone and scapula. *Bone* 35, 2004,909.
20. Everts, V., Korper, W., Jansen, D.C. Functional heterogeneity of osteoclasts: matrix metalloproteinases participate in osteoclastic resorption of calvarial bone but not in resorption of long bone. *Faseb J* 13, 1999,1219.
21. Roodman, G.D. Cell biology of the osteoclast. *Experimental Hematology* 27, 1999,1229.
22. Cruess, R.L., Dumont, J.R. Basic fracture Healing. In: Newton CD, Nunamaker DM, eds. *Textbook of Small Animal Orthopaedics*. Philadelphia: JB Lippincott; 1985. pp. 35.
23. Jee, W.S. Principles in bone physiology. *J Musculoskelet Neuronal Interact* 1, 2000,11.
24. Ninomiya, J.T., Tracy, R.P., Calore, J.D., Gendreau, M.A., Kelm, R.J., Mann, K.G. Heterogeneity of human bone. *Journal of Bone Miner Res* 5, 1990,933.
25. Wang, X.D., Bank, R.A., TeKoppele, J.M., Agrawal, C.M. The role of collagen in determining bone mechanical properties. *J Orthopaed Res* 19, 2001,1021.
26. Burr, D.B. The contribution of the organic matrix to bone's material properties. *Bone* 31, 2002,8.
27. Boivin, G., Bala, Y., Doublier, A., Farlay, D., Ste-Marie, L.G., Meunier, P.J., et al. The role of mineralization and organic matrix in the microhardness of bone tissue from controls and osteoporotic patients. *Bone* 43, 2008,532.
28. Serra, L.A. *Critérios fundamentais em fracturas e ortopedia*. Segunda ed: Lidel; 2001.
29. Winet, H. The role of microvasculature in normal and perturbed bone healing as revealed by intravital microscopy. *Bone* 19, 1996,S39.
30. Roush, J.K. Management of fractures in small animals. *Veterinary Clinics of North America* 35, 2005,1137.
31. Dimitriou, R., Tsiridis, E., Giannoudis, P.V. Current concepts of molecular aspects of bone healing. *Injury* 36, 2005,1392.

32. Yoo, J.U., Johnstone, B. The role of osteochondral progenitor cells in fracture repair. *Clin Orthop Relat Res*, 1998,S73.
33. Piermattei, D.L., Flo, G.L. Fractures: Classification, Diagnosis and Treatment. In: Brinker, Piermattei, Flo's, eds. *Handbook of Small Animal Orthopedics and Fracture Repair*. 4rd ed. Philadelphia: W.B. Saunders; 2006. pp. 30.
34. Cancedda, R., Dozin, B., Giannoni, P., Quarto, R. Tissue engineering and cell therapy of cartilage and bone. *Matrix Biol* 22, 2003,81.
35. Attawia, M., Kadiyala, S., Fitzgerald, K. Cell-based approaches for bone graft substitutes. In: (ed) LC, ed. *Bone Graft Substitutes*. West ConshohockenPA: ASTM International; 2001. pp. 126.
36. Bruder, S.P., Fox, B.S. Tissue engineering of bone - Cell based strategies. *Clin Orthop Rel Res*, 1999,S68.
37. Muschler, G.F., Midura, R.J. Connective tissue progenitors: practical concepts for clinical applications. *Clin Orthop* 2002,66.
38. Salgado, A.J., Oliveira, J.T., Pedro, A.J., Reis, R.L. Adult stem cells in bone and cartilage tissue engineering. *Curr Stem Cell Res Ther* 1, 2006,345.
39. Satija, N.K.G., G.U. Sharma, S. Afrin, F. Gupta, P. Verma, Y.K. Singh, V.K. Tripathi, R.P. Mesenchymal stem cells: molecular targets for tissue engineering. *Stem Cells Dev* Feb, 2007, 7.
40. Caplan, A.I. Mesenchymal Stem-Cells. *J Orthop Res* 9, 1991,641.
41. Goshima, J., Goldberg, V.M., Caplan, A.I. The osteogenic potential of culture-expanded rat marrow mesenchymal cells assayed in vivo in calcium phosphate ceramic blocks. *Clin Orthop Relat Res*, 1991,298.
42. Haynesworth, S.E., Goshima, J., Goldberg, V.M., Caplan, A.I. Characterization of cells with osteogenic potential from human marrow. *Bone* 13, 1992,81.
43. Caplan, A.I. The Mesengenic Process. *Clin Plast Surg* 21, 1994,429.
44. Jaiswal, N., Haynesworth, S.E., Caplan, A.I., Bruder, S.P. Osteogenic differentiation of purified, culture-expanded human mesenchymal stem cells in vitro. *J Cell Biochem* 64, 1997,295.
45. Bruder, S.P., Jaiswal, N., Haynesworth, S.E. Growth kinetics, self-renewal, and the osteogenic potential of purified human mesenchymal stem cells during extensive subcultivation and following cryopreservation. *J Cell Biochem* 64, 1997,278.
46. Pittenger, M.F., Mackay, A.M., Beck, S.C., Jaiswal, R.K., Douglas, R., Mosca, J.D., et al. Multilineage potential of adult human mesenchymal stem cells. *Science* 284, 1999,143.

47. Kadiyala, S., Jaiswal, N., Bruder, S.P. Culture-expanded, bone marrow-derived mesenchymal stem cells can regenerate a critical-sized segmental bone defect. *Tissue Eng* 3, 1997,173.
48. Bruder, S.P., Jaiswal, N., Ricalton, N.S., Mosca, J.D., Kraus, K.H., Kadiyala, S. Mesenchymal stem cells in osteobiology and applied bone regeneration. *Clin Orthop Relat Res*, 1998,S247.
49. Cooper, L.F., Harris, C.T., Bruder, S.P., Kowalski, R., Kadiyala, S. Incipient analysis of mesenchymal stem-cell-derived osteogenesis. *J Dent Res* 80, 2001,314.
50. Satomura, K., Nagayama, M. Ultrastructure of mineralized nodules formed in rat bone marrow stromal cell culture in vitro. *Acta Anat (Basel)* 142, 1991,97.
51. Lazarus, H.M., Haynesworth, S.E., Gerson, S.L., Rosenthal, N.S., Caplan, A.I. Ex-Vivo Expansion and Subsequent Infusion of Human Bone-Marrow-Derived Stromal Progenitor Cells (Mesenchymal Progenitor Cells) - Implications for Therapeutic Use. *Bone Marrow Transplant* 16, 1995,557.
52. Horwitz, E.M., Prockop, D.J., Fitzpatrick, L.A., Koo, W.W., Gordon, P.L., Neel, M., et al. Transplantability and therapeutic effects of bone marrow-derived mesenchymal cells in children with osteogenesis imperfecta. *Nat Med* 5, 1999,309.
53. Silber, J.S., Anderson, D.G., Daffner, S.D., Brislin, B.T., Leland, J.M., Hilibrand, A.S., et al. Donor site morbidity after anterior iliac crest bone harvest for single-level anterior cervical discectomy and fusion. *Spine* 28, 2003,134.
54. Joshi, A., Kostakis, G.C. An investigation of post-operative morbidity following iliac crest graft harvesting. *Br Dent J* 196, 2004,167.
55. Muschler, G.F., Nitto, H., Boehm, C.A., Easley, K.A. Age- and gender-related changes in the cellularity of human bone marrow and the prevalence of osteoblastic progenitors. *J Orthop Res* 19, 2001,117.
56. Muschler, G.F., Nitto, H., Matsukura, Y., Boehm, C., Valdevit, A., Kambic, H., et al. Spine fusion using cell matrix composites enriched in bone marrow-derived cells. *Clinical Orthop*, 2003,102.
57. Van den Dolder, J. Optimization of cell loading and culturing techniques [PhD Thesis Medical Center Nijmegen, Netherlands, 2003.
58. Kirker-Head, C.A., Gerhart, T.N., Armstrong, R., Schelling, S.H., Carmel, L.A. Healing bone using recombinant human bone morphogenetic protein 2 and copolymer. *Clin Orthop Relat Res*, 1998,205.
59. Kirker-Head, C.A. Potential applications and delivery strategies for bone morphogenetic proteins. *Adv Drug Deliv Rev* 43, 2000,65.
60. Bucholz, R.W. Nonallograft osteoconductive bone graft substitutes. *Clin Orthop Rel Res*, 2002,44.

61. Ishaug, S.L., Crane, G.M., Miller, M.J., Yasko, A.W., Yaszemski, M.J., Mikos, A.G. Bone formation by three-dimensional stromal osteoblast culture in biodegradable polymer scaffolds. *J Biomed Mater Res* 36, 1997,17.
62. Dunn, M.G., Avasarala, P.N., Zawadsky, J.P. Optimization of Extruded Collagen-Fibers for Acl Reconstruction. *J Biomed Mater Res* 27, 1993,1545.
63. Mikos, A.G., Sarakinos, G., Leite, S.M., Vacanti, J.P., Langer, R. Laminated 3-Dimensional Biodegradable Foams for Use in Tissue Engineering. *Biomaterials* 14, 1993,323.
64. Mooney, D.J., Kaufmann, P.M., Sano, K., Mcnamara, K.M., Vacanti, J.P., Langer, R. Transplantation of Hepatocytes Using Porous, Biodegradable Sponges. *Transplant Proc* 26, 1994,3425.
65. Mikos, A.G., Thorsen, A.J., Czerwonka, L.A., Bao, Y., Langer, R., Winslow, D.N., et al. Preparation and Characterization of Poly(L-Lactic Acid) Foams. *Polymer* 35, 1994,1068.
66. Rivard, C.H., Chaput, C.J., Desrosiers, E.A., Yahia, L.H., Selmani, A. Fibroblast Seeding and Culture in Biodegradable Porous Substrates. *J Appl Biomater* 6, 1995,65.
67. Thomson, R.C., Yaszemski, M.J., Powers, J.M., Mikos, A.G. Fabrication of biodegradable polymer scaffolds to engineer trabecular bone. *J Biomater Sci Polym Ed* 7, 1995,23.
68. Laurencin, C.T., Attawia, M.A., Elgendy, H.E., Herbert, K.M. Tissue engineered bone-regeneration using degradable polymers: The formation of mineralized matrices. *Bone* 19, 1996,S93.
69. Saad, B., Matter, S., Ciardelli, G., Uhlschmid, G.K., Welti, M., Neuenschwander, P., et al. Interactions of osteoblasts and macrophages with biodegradable and highly porous polyesterurethane foam and its degradation products. *J Biomed Mater Res* 32, 1996,355.
70. Minuth, W.W., Sittinger, M., Kloth, S. Tissue engineering: generation of differentiated artificial tissues for biomedical applications. *Cell Tissue Res* 291, 1998,1.
71. Gomes, M.E., Reis, R.L. Tissue engineering: Key elements and some trends. *Macromol Biosci* 4, 2004,737.
72. Reis, R.L., Mendes, S.C., Cunha, A.M., Bevis, M.J. Processing and in vitro degradation of starch/EVOH thermoplastic blends. *Polymer Internat* 43, 1997,347.
73. Fleming, J.E., Cornell, C.N., Muschler, G.E. Bone cells and matrices in orthopedic tissue engineering. *Orthop Clin North Am* 31, 2000,357.
74. Thomson, R.C., Wake, M.C., Yaszemski, M.J., Mikos, A.G. Biodegradable polymer scaffolds to regenerate organs. *Adv Polym Sci* 122, 1995,245.

75. Cassiede, P., Dennis, J.E., Ma, F., Caplan, A.I. Osteochondrogenic potential of marrow mesenchymal progenitor cells exposed to TGF-beta 1 or PDGF-BB as assayed in vivo and in vitro. *J Bone Miner Res* 11, 1996,1264.
76. Carter, D.R., Beaupre, G.S., Giori, N.J., Helms, J.A. Mechanobiology of skeletal regeneration. *Clin Orthop Rel Res*, 1998,S41.



## Chapter II

### **REVIEW: Use of perfusion bioreactors and large animal models for long bone tissue engineering**

This chapter is based on the following publication:

Gardel LS, Serra LA, Gomes ME, Reis RL. Use of Perfusion Bioreactors and Large Animal Models for Long Bone Tissue Engineering. 2012 submitted





## **Abstract**

Tissue engineering and regenerative medicine (TERM) strategies for generation of new bone tissue includes the combined use of autologous or heterologous mesenchymal stem cells (MSC) and three-dimensional (3D) scaffold materials serving as structural support for the cells, that develop into tissue-like substitutes under appropriate in vitro culture conditions. This approach is very important due to the limitations and risks associated with autologous as well as allogenic bone grafting procedures currently used. However, the cultivation of osteoprogenitor cells in 3D scaffolds presents several challenges, such as the efficient transport of nutrient and oxygen and removal of waste products from the cells in the interior of the scaffold. In this context, perfusion bioreactor systems are key components for bone TERM, as many recent studies have shown that such systems can provide dynamic environments with enhanced diffusion of nutrients and therefore perfusion can be used to generate grafts of clinically relevant sizes and shapes. Nevertheless, in order to determine whether a developed tissue-like substitute conforms to the requirements of biocompatibility, mechanical stability and safety, it must undergo rigorous testing both in vitro and in vivo. Results from in vitro studies can be difficult to extrapolate to the in vivo situation, and for this reason, the use of animal models is often an essential step in the testing of orthopedic implants prior to clinical use in humans. This review provides an overview of the concepts, advantages and challenges associated with different types of perfusion bioreactor systems, particularly focusing on systems that may enable the generation of critical size tissue engineered constructs. Furthermore, this review discusses some of the most frequently used animal models, such as sheep and goats, to study the in vivo functionality of bone implant materials, in critical size defects.

## 2.1- Introduction

The TERM field has expanded rapidly as new discoveries are made that render possible tissue replacement and regeneration. Considering the body's tissues biochemical, biophysical and hydrodynamic requirements, functional tissue engineering requires the development of new tools for *in vitro* tissue culture, in order to create a biotissue that can develop *in vivo* and replace damaged tissue (1, 2). Moreover, the increasing patient demand for tissue-engineered products and therapies requires technologies for large scale production of tissue substitutes with precise control of shape/size and high quality (3-6). Bioreactors can be defined as devices in which biological or biochemical processes, or both, are re-enacted under controlled conditions (for example, pH, temperature, pressure, oxygen supply, nutrient supply, and waste removal). Originally most bioreactors were developed to test biomaterials but some of them were also invented with the objective of enabling extracorporeal tissue growth (7). In fact, bioreactors might facilitate the aseptic growth of functional tissues and simultaneously offer several further advantages over culture in plates and flasks (8, 9). In addition, bioreactors can be custom designed for engineering tissues with complex three-dimensional geometry containing multiple cell types (10). The fact that physical stimuli can modulate cell function and tissue development has further motivated the development of biomechanically active stimulation systems to culture functional cell-tissues constructs *in vitro* by exposing them to physiologically relevant mechanical and/or hydrodynamic stimulation. The overall goal is to have systems that reliably and reproducibly form, store, and deliver functional tissues substitutes that can sustain function *in vivo*. In essence, the bioreactor needs to provide the appropriate physical stimulation to cells, continuous supply of nutrients (e.g. glucose, amino acids), biochemical factors and oxygen, diffusion of chemical species to the construct interior, as well as continuous removal of by-products of cellular metabolism (e.g. lactic acid) (11). In the absence of a vascular blood supply *in vitro*, nutrient delivery to cells throughout three-dimensional (3D) tissue-engineered constructs grown in static culture must occur by diffusion. As a result, thin tissues and tissues that are naturally avascular (e.g., cartilage) have been more readily grown *in vitro* than thicker, vascular tissues such as bone (12-14). The *ex vivo* generation of larger three-dimensional tissue substitutes particularly requires the development of enlarged devices and systems that allow cells to distribute within a wide three-dimensional space, and at the same time satisfy the physicochemical demands of culturing such large cell masses into a scaffold (6, 15).

Several international research groups have demonstrated the advantages of using culture systems that combine both hydrodynamic and mechanical stimulation during tissue development (16-21). The vast majority of these studies report on the development and use of perfusion bioreactors, which are mostly composed of a perfusion pump with one or more output channels where the flow can be controlled and connected to single or multiple cell culture chambers through silicone tubes which allow the exchange of gases (O<sub>2</sub>, CO<sub>2</sub>) between the culture medium and the environment. Most of these groups work for the development of new combinations of stem cells and materials constructs to obtain functional tissue-engineered constructs for bone regeneration. Thus, they are also interested in developing and evaluating their concepts in highly reproducible large segmental defects in preclinical large animal models. These studies should allow the development of methods to produce reliable data (biocompatibility, mechanical stability and safety), creating a real set of information to allow, in the near future, the use of tissue engineered constructs of large dimensions, specifically translating into the orthopedics surgical field. This is an essential step in the process of assessing newly developed bone grafts prior to clinical use in humans. Animal models allow the evaluation of materials in loaded or unloaded situations over potentially long time durations and in different tissue qualities and ages. While some animal models may closely represent the mechanical and physiological human clinical situation, it must be remembered that it is only an approximation, with each animal model having unique advantages and disadvantages (22). This review examines the existent literature concerning the use of perfusion bioreactors systems and large animal models to evaluate tissue engineered constructs of large dimensions.

## **2.2- Bioreactors for bone tissue engineering**

For tissue engineering purposes, dynamic culture bioreactors, such as spinner flasks (23, 24), rotating wall bioreactors (23, 25), and flow perfusion systems (19, 26), have shown promising results. In general, dynamic culture yields a much more homogeneous distribution of cells and matrix while systems enabling shear stresses applied by the medium flow may stimulate the cells to proliferate and differentiate. Furthermore, these systems enhance mass transport, ensuring continuous nutrition of cells and removal of waste products. The commonly used spinner flasks are low cost equipments, but the non-uniform media flow that is provided around scaffolds limits their use. The cells on the outer periphery of scaffolds are subjected to a turbulent flow, whereas the cells in the interior exhibit static molecular diffusion (27).

Similar drawbacks are seen in the rotating wall bioreactor. Some flow perfusion systems overcome the flow issues because medium is flushed directly through scaffolds (19, 26), thereby providing nutrient and stimuli throughout the entire volume of the scaffold (27). The design and performance of bioreactors is therefore of special relevance in recent and future tissue engineering strategies. Bioreactors that use a pump system to perfuse media directly through a scaffold are known as perfusion bioreactors (28). Perfusion bioreactors with defined mechanical stimulation functions are of special interest to optimize the *ex vivo* growth of the desired cell or scaffold constructs (7, 29). However, direct perfusion introduces a new level of complexity when scale-up is considered, and the engineering challenges may be significant (11).

Nutrition, chemotransport enhancement and mechanical stimulation (dynamic tension, compression or hydrodynamic forces) of cells or cell/scaffold constructs, control over environmental conditions, culture duration, on-line evaluation of biological variables and automation of bioprocesses should be considered for the development and use of bioreactors (1, 29-35). Moreover, bioreactors should be able to operate over long periods of time under aseptic conditions since maturation of a functional tissue substitute may take up to several weeks. Another important issue in the design of bioreactors is the monitoring of tissue growth. In fact, an advantage in the area would be the development and employment of techniques which could assess the integrity of the tissue non-invasively (11). Oxygen and nutrient need and its consumption by the cells, metabolite removal and fluid flow within the site have a dramatic impact on the growth and survival of enlarged constructs for tissue substitution, and when controlled can be used as major positive modulators in elaborated bioreactors. This would allow for a higher efficiency in the tissue engineering process, as well as a high degree of certainty in harvesting tissues within the pre-determined manufacturing specifications.

### **2.3- Perfusion bioreactors**

In addition to enhancing mass transport, perfusion bioreactor systems may be used to deliver controlled mechanical stimuli such as flow-mediated shear stresses and/or hydrodynamic forces to tissue constructs (36-38). Different perfusion bioreactors have been developed but most systems consist of a similar basic design consisting of a media reservoir, a pump, a tubing circuit, and perfusion chambers, columns or cartridges that hold the cell/scaffold constructs (39). Perfusion bioreactor systems have been developed to culture a variety of shapes and sizes of 3D bone tissue constructs (19, 25, 40-54).

In these systems, it is obvious that the flow-rate used for the medium perfusion is responsible to a great extent for the effects in the microenvironment of cells, i.e., for the magnitude of the shear stress sensed by the cells. Nevertheless, the local internal shear stress created by perfusion systems using hydrodynamic forces and experienced by the cells on three dimensional (3D) matrices is influenced not only by the medium flow rate but also by other parameters that have to be considered, for example, the porosity, the dimensions, the material and the geometry of the scaffold, the size, the anisotropy, and the degree of interconnectivity of pores, as well as the viscosity of the medium (55).

Nowadays, multidisciplinary efforts are being made to improve the size and quality of the bone substitutes that can be obtained in vitro. These efforts focus on the cell types used, scaffold structure/composition, and also on the cultivation in perfusion bioreactor systems with various designs. However, most studies on perfusion bioreactors describe systems that only enable culturing small scaffolds, which do not meet clinically relevant constructs size in the field of orthopedics defects regeneration. In the following sections, the main differences between two basic types of perfusion bioreactors (with individual culture chambers and single culture chamber) which enable to culture scaffolds with different dimensions, are described and discussed in the light of the current clinical need for larger engineered bone substitutes.

### **2.3.1- Perfusion bioreactors with individual culture chambers for culturing small dimension constructs**

In flow perfusion systems composed of individual chambers, usually the scaffolds are fitted in the culture chambers so that media cannot flow around it, thus perfusing media directly through the pores of the scaffold. The flow of medium through the scaffold porosity benefits cell differentiation by enhancing nutrient transport to the scaffold interior and by providing mechanical stimulation in the form of shear stresses (49, 56, 57). In fact, studies with perfusion systems have suggested that flow has many biological effects (27, 58-61), such as prostaglandin E2 release (62), osteogenic differentiation enhancement (49) and mineralized matrix production increase on bone marrow stromal osteoblasts seeded in 3D scaffolds (63). Research works using either custom-made or commercially available perfusion bioreactor systems are specified in Table 1.

Table 1 Summarizes research studies describing the development and/or use of perfusion bioreactors of individual culture chamber in the field of bone tissue engineering

Table1.Summary table on research studies describing the development/use of perfusion bioreactor of individual culture chambers in bone tissue engineering.

References	Perfusion Bioreactor (type)	Scaffolds material (shape)	Scaffolds volume	Cell type and density in scaffolds	Flow rate	Principal effects
25	6 chambers for cell/scaffolds samples	PLG 12.7X6mm	0.7600 cm <sup>3</sup>	Ratosteoblasts 1.900,000	0.030 ml/s	Proliferation =, ALP+, OC+
63		Titanium mesh 10 x0.8mm	0.1256 cm <sup>3</sup>	Rat MSC/ 500,000	Low 0.3 ml/min medium 1ml/min high 3 ml/min	Proliferation+, ALP +, Ca <sup>2+</sup> +, OP+
61		Titanium fiber mesh 10 X0.8mm	0,1256 cm <sup>3</sup>	Rat osteoblasts/ 500,000	0.5 ml/min	Proliferation +, ALP +, Ca <sup>2+</sup> +
40		SEVA-C and SPCL 8x2mm	0.1005 cm <sup>3</sup>	Rat MSC/ 500,000	0.3 ml/min	Proliferation +, gene expression of RUNX2 +, ALP=, OC=
64		Titanium mesh 8x0.8 mm	0.0402 cm <sup>3</sup>	Rat MSC 500,000	~0.3 ml/min(1 day) being increased to 1 ml/min.	Proliferation +, ALP +, Ca <sup>2+</sup> +, OP+
49		CPC 8x8 mm	0.4021 cm <sup>3</sup>	Rat MSC 1.500,000	~0.3 ml/min(1 day) being increased to 1 ml/min	Proliferation +, ALP+,OP +
65		Polystyrene 8mmx3mm	0.1507 cm <sup>3</sup>	Murine osteoblasts (MC3T3-E1) Diffrents density	0.15ml/mim oscillating flowd every 5 mim/2 hs. After unidirectional flow 0.15/min 8 hs.	perfusion seeding technique +, improve seeding efficiency +, cell spatial distribution+,proliferation+
66		PGA 8mmx3mm	0.1507 cm <sup>3</sup>	Rat MSC 500.000	0.15ml/mim oscillating flowd every 5 mim/2 hs. After unidirectional flow 0.15/min 8 hs.	ALP activity +,DNA + Ca <sup>+</sup> +.
67	Si-TCP 10x5mm	0.3962 cm <sup>3</sup>	hTERT-MSC 2.000,000	0.1ml/min	Proliferation+, ALP +, gene, OP +, BSP2 +, BMP2 +, Col1 -, RUNX2-,OC-expression of ALP +,	

56	8 chambers for cell/scaffolds samples	HDCB 6.4 x3mm	0.0965 cm <sup>3</sup>	Murine osteoblasts (MC3T3-E1) 2.000,000	perfusion rates of 1.0, 0.2, 0.1, and 0.01 ml/min	Proliferation +, gene expression of RUNX2 +, ALP=, OC=
59	Minucellss and Minutissue®	b-TCP 5x5x5mm	0.125 cm <sup>3</sup>	Rat osteoblasts 83,333	0.033ml/min	ALP + (in vitro/ in vivo), OC +, in vivo bone formation +
26	U-shaped glass tube, 2 scaffolds per tube	ChronOS™	0.2010 cm <sup>3</sup>	Human MSC 6E + 07 cells/cm <sup>3</sup>	1mm/s	MTT staining +, improvement in cell spatial uniformity
68		Porous hydroxyapatite ceramic 8mmx4mm	0.2010 cm <sup>3</sup>	Human MSC 4.8 ± 2.6x10 <sup>3</sup>	100µm/s	SEM +, BSP +, COL1 +, OP +, NGFR -, STRO-I -
27	Polycarbonate multiple perfusion cartridges (one scaffold per cartridge)	Collagen 11x1.5 mm, silk6x1.5mm	Collagen; 0.1425 cm <sup>3</sup> Silk: 0.0424 cm <sup>3</sup>	Human MSC Collagen: 500,000cells Silk:500,000	0.2 ml/min	Ca2 <sup>+</sup> +
53	Perfusion bioreactor multiple flow chambers(3 scaffolds per chamber)	PET16x1.2mm	2.4127 cm <sup>3</sup>	Human MSC 1.000.000	0.1 ml/min	DNA+ .SEM+,Van Kossa +, Lactate production +, Glucose consumption +, Osteogenic and adipocity differentiation+
70		PET16x1.2mm	2.4127cm <sup>3</sup>	Human MSC 800.000	0.1ml/min	Lactate production +, Glucose consumption +, ~9.4%gas phase oxygen
42		PET16x1.2mm	2.4127 cm <sup>3</sup>	Human MSC 1.000.000	0.1ml/min and 1.5 ml/min	ALP (0.1ml +, 1.5ml ++), Ca <sup>+</sup> (0.1ml +, 1.5ml ++), CFU-f(0.1ml ++, 1.5ml +), FN(0.1ml/min ++, 1.5ml/min =), HSP47(0.1ml =, 1.5ml +).
77		PET16x1.2mm	2.4127 cm <sup>3</sup>	Human MSC 1.540,000	0.2ml/min	ALP + Ca <sup>+</sup> +, BMP-2 +, ALP +, RUNX2 +, OC +
62	4 chambers for cell/scaffolds samples	CPC5x 3.5mm	0.0687 cm <sup>3</sup>	Murine osteoblasts (MC3T3) 100,000	0.025 ml/min. (4 h). After oscillating fluid flow( 40 ml/min)	PGE2 +, Proliferation =

73	6 flow wells chambers for cell/scaffolds samples	b-TCP 10x8mm	0.6283 cm <sup>3</sup>	Murine osteoblasts (MC3T3) 1.500,000	oscillatory perfusion	Proliferation +, ALP +, Ca <sup>2+</sup> +, cell Vitality+
44	6 radial chambers for cell/scaffolds samples	BCB 4x4mm	0.0502 cm <sup>3</sup>	Human MSC, low density 30.000,000, high density 60.000,000	100 µm/s(low-flow), 400µm/s (high flow)	cell distribution +, Col +, OP +, BSP2 +
48		BCB 4 x4mm	0.0502 cm <sup>3</sup>	Human adipose MSC 1.500,000	1.8ml/min	Proliferation =, cell Distribution +, Col +, OP +, BSP2 +
75	Minucellss and Minutissue®	BDBM 9x5mm	0.3180 cm <sup>3</sup>	Murine preosteoblast (MC3T3-E1), 50,000	18µl/min	Proliferation +, Vitality +
54	8 chambers for cell/scaffolds samples	Polyurethane 24x6mm	2.7143 cm <sup>3</sup>	Murine osteoblasts (MC3T3-E1) 10.857,200	1.0ml/min	Proliferation +, cellular Distribution+, vitality +
47	6 chambers for cell/scaffolds samples	PLGA 10x3mm	0.2356 cm <sup>3</sup>	hTERT-hMSCs 500000	0.2ml/min	Proliferation +,DNA +, ALP +, SEM +, Ca <sup>2+</sup> +, op +

Mathematical signs indicate the effects induced by the systems listed as compared to static culture :(+), positive effect ;(=), no effect ;(-), negative effect. BCP, biphasic calcium phosphate; BMP2, bone morphogenetic protein 2; HA, hydroxyapatite; PCL, polycaprolactone; PDMA, polydimethylsiloxane; PGE2, prostaglandin E2; PMMA, polymethylmethacrylate; RUNX2, runt-related transcription factor 2; SPCL, starch/polycaprolactone blend; SEVA-C, starch/ethylene vinyl alcohol blend; b-TCP, beta-tricalcium phosphate; OP, osteopontin, OC, osteocalcin; COL, Collagen; COL1, collagen1;BCB, bovine cancellous bone; BDBM, bovine; CFU, colony forming units; HSP-47, heat shock protein; PGA, Poly (glycolic acid); FN, fibronectin; hTERT-hMSCs, humam bone marrow-derived mesenchymal stem cells tranduced with humam telomerase catalytic subunit; PLGA, porous poly(lactic glycolic acid); MTT, [3(4,5- dimethylthiazol-2-yl)-2,5-diphenyltetrazolium bromide; SEM, Scanning electron microscopy; BSP, bone sialoprotein; NGFR nerve growth factor receptor; STRO-1, is a cell surface protein expressed by bone marrow stromal cells and erythroid precursors.

In 2001 Goldstein et al (25), compared a perfusion flow bioreactor to other systems that promote media convection, namely a spinner flask and a rotary vessel. For this purpose they used Poly (DL-lactic-co-glycolic acid) (PLGA) foam discs seeded with marrow stromal cells and cultured in the presence of dexamethasone and L-ascorbic acid, at a constant flow rate.



Cell numbers per foam were found to be similar with all culturing systems indicating that cell growth could not be enhanced by convection, but histological analysis indicated that the rotary vessel and the flow system produced a more uniform distribution of cells throughout the foams. Alkaline phosphatase (ALP) activity per cell was higher with culture in the flow system and spinner flask after 7 days, while no difference in osteocalcin (OC) activity per cell was observed among culturing methods after 14 days. Based on these results, the flow system appears to be the superior culturing method (25).

In 2002, Bancroft et al (63) reported the development of another flow perfusion bioreactor and investigated the effect of different flow rates, in rat bone marrow cells seeded into titanium fiber mesh scaffolds cultured in osteogenic media. Culturing seeded scaffolds at different flow rates for 16 days revealed a dose-dependent effect of flow perfusion rate on mineralized matrix production, matrix modeling, and cell matrix distribution. The latter was significantly higher in the flow perfusion cultures when compared with static culture (63). Van De Dolder et al, in 2003 (61), used the same bioreactor, biomaterial, culture medium and cells, to analyze the effect of flow perfusion (as compared to static conditions), at a constant flow rate, founding that this system can enhance the early proliferation, differentiation, and mineralized matrix production of rat bone marrow stromal cells(61).

The same bioreactor developed by Bancroft et al, in 2002 (63), was used in other studies, using different types of scaffolds, such as porous biphasic calcium phosphate ceramic scaffolds(49), Poly(L-lactic acid) nonwoven fiber mesh scaffolds (43), and starch polycaprolactone (SPCL) biodegradable fiber mesh scaffolds (40, 41). Furthermore, Holtorf et al, in 2005 (64), showed that using this system, even in the absence of dexamethasone supplement, rat BMSCs can differentiate into osteoblastic (64). Gomes et al, in 2003 (40) have also showed that rat BMSCs proliferation and differentiation are affected by the scaffold's porosity and architecture (40) and reported increased production and localization of TGF- $\beta$ 1, VEGF, BMP-2, and FGF-2 in constructs cultured under increase fluid flow rate(41). Based on the same bioreactor design, Alvarez-Barreto et al, in 2007 (65), developed and characterized an oscillatory flow-perfusion seeding technique, to improve seeding efficiency, cell spatial distribution and strength of cell adhesion. The technique consisted in the application of an oscillating flow for 2 h at 0.1 ml/min that is created by manually changing the direction of the pump every 5 min(65). This technique led to enhanced seeding efficiency and osteoblastic differentiation of rat BMSC cultured in poly (glycolic acid) (PGA) scaffolds (66). Bjerre and co-workers in 2008 (67), performed another modification of the same bioreactor. The modified system consists of 16 parallel flow chambers, each supplied by a common reservoir controlled by a peristaltic pump.

They analyzed the proliferation and differentiation of hMSC cultured on silicate-substituted tricalcium phosphate scaffolds at a constant flow rate as compared to static culture. Data obtained from ALP activity and RT-PCR analysis of bone markers after 14 days in flow culture demonstrated an increase in proliferation, differentiation and cell/matrix deposition (67).

The perfusion bioreactor from Minucells and Minutissue<sup>®</sup>, are one of the few commercially available culture systems and has a different design: there is not a recirculation of the culture medium as in most systems described; the culture medium is perfused through 12 culture chambers in one direction, each one supporting a single, tightly fitting scaffold and the container is maintained at 37°C by a thermo plat in room temperature, connected to another bottle (waste culture medium) where the flow ends. This system was used by Wang et al, in 2003 (59), to culture bone marrow-derived cell in porous ceramic scaffolds, using a constant flow rate. ALP and OC expression were increased in perfusion cultures when compared of static cultures (59).

Wendt et al, in 2003 (26) developed a bioreactor for automated cell seeding of 3D scaffolds by continuous perfusion of a cell suspension through the scaffold pores in oscillating directions. In this system, scaffolds are placed in chambers (one scaffold per chamber) that are positioned at the bottoms of two glass columns and connected through a U-shaped glass tube at their base. Flow is induced with the use of a vacuum pump and the flow rate regulated with a flow meter. The direction of flow is reversed when the fluid level in one column reaches an optical sensor placed near the top of each glass column. The sensor detects the cell suspension, actuating a pair of solenoid valves, switching the vacuum to the opposite column, and therefore reversing the direction of fluid flow. To assess the efficiency and uniformity of perfusion seeding of Polyactive foams ChronOS<sup>®</sup> seeded with bone marrow stromal cells (BMSCs), as compared to static and spinner flask cultures, they used quantitative biochemical and image analysis techniques. The results showed that perfusion seeding of cells into Polyactive foams were more homogeneously distributed throughout the scaffold volume and formed more homogeneously sized cell clusters when compared to other systems (26). Braccini et al, in 2005(68), used the same system, to study the effect on seeding, expansion, and differentiation of BMSCs into a 3D hydroxyapatite scaffolds and subsequent in vivo outcomes. When implanted ectopically in nude mice, the engineered constructs generated bone tissue more reproducibly, uniformly, and extensively than scaffolds loaded with 2D expanded BMSCs (68).

Zhao and Ma, in 2005 (53), modified a 3D perfusion bioreactor system developed previously by Ma et al, in 1999 (69), which is composed of three circulating loops. The main circulating loop includes culture chambers and a section of the flow path for continuous circulation of medium. The inoculation loop includes culture chambers and a section of the flow path used for inoculating cells into scaffolds. The replenishing loop consists of the fresh media container and the section of the flow path used for supplying fresh media to the system. The two inlets and two outlets in each chamber are connected to independent inlets from the computerized peristaltic pump that has eight independent channels. This system enables the recirculation of media and has two sampling ports at the inlet and outlet of each chamber. Furthermore it can accommodate multiple flow chambers, depending on the operational requirements. To examine the dynamic seeding efficiency, the author used non-woven poly (ethylene terephthalate) (PET) fibrous scaffolds cultured with human mesenchymal stem cells (hMSC). They observed an inverse correlation between flow rates for seeding operation and seeding efficiencies and analyses showed that after a long period of culture, higher cell densities of hMSCs were found in the bioreactor system (53). With the same method and biomaterial Zhao et al, in 2005 (70), studied the effects of the physiological oxygen environment on the intrinsic tissue development characteristics in the 3D scaffolds as compared to static conditions, using a mathematical modeling. Results show that the oxygen tension in the static culture is lower than that of the perfusion unit, where the cell density was 4 times higher (70). To demonstrate the effect of shear stress, Zhao et al, in 2007 (42), cultured porous 3D PET matrices with hMSC at different flow rates in the same bioreactor. The higher flow rate enhanced osteogenic differentiation potential at 14 days, and calcium deposition in the matrix after 20 days with osteogenic media (42).

A perfusion bioreactor was developed by Timmins and co-workers in 2007 (71), the tissue culture under perfusion (T-CUP), based on the concept of controlled and confined alternating motion of scaffolds through a cell suspension or culture medium, as opposed to pumping the fluid through the scaffolds. Different cell types as well as scaffold designs and compositions were tested. When freshly isolated human bone marrow nucleated cells seeded into ENGipore<sup>®</sup> ceramic scaffolds cultured for 19 days in the T-CUP resulted in stromal cell-populated constructs capable of inducing ectopic bone formation in nude mice (71).

Grayson et al, in 2008 (44), described a bioreactor system that enables cultivation of up to six tissue constructs simultaneously in individual chambers, using a radial channel with direct perfusion and imaging capability.

Fully decellularized bovine trabecular bone was used as a scaffold, seeded with hMSCs using different cellular densities and different flow rates (low and high). The results of the study indicated that, at the seeding densities evaluated, greater initial cell numbers do not necessarily result in increased bone formation.

The study also showed that flow rate of medium perfusion remains a significant parameter that allows a more uniform tissue development and supports higher cell densities within the constructs (44). Frohlich et al, in 2010 (48), using the same bioreactor showed that, human adipose-derived stem cells (hASCs), cultured in decellularized bone scaffolds, after 5 weeks of culture in osteogenic medium, presented significant increases in the construct cellularity and in the amounts of bone matrix components (48).

Costa et al, in 2008 (72), developed a perfusion bioreactor composed of 20 culture chambers, each one supporting a single, tightly fitting scaffold. A peristaltic pump controls the medium flow rate through the bioreactor, with silicon tubes directly connected to the system and to a medium reservoir (with recirculation flow). Using this system, a study was conducted using starch-polycaprolactone (SPCL) meshes statically seeded with goat bone marrow cells (gBMCs) and cultured in osteogenic medium for 7 and 14 days. The results showed enhanced cellular proliferation and differentiation by combination of fluid flow rate and flow inversion frequency during different culturing periods (72).

Sailon et al, in 2009 (54), developed a flow perfusion chamber bioreactor with 8 individual chambers to provide chemotransportation in thick scaffolds. Polyurethane scaffolds, seeded with murine preosteoblasts, were cultured. Flow-perfused scaffolds demonstrated increase in peripheral cell density and core density at day 8. This study established that thick (>6mm) 3D constructs are sustainable using a flow-perfusion bioreactor(54)

Yang and co-workers, in 2010 (47), developed a perfusion system that is composed of six culture cassettes, a multichannel cylinder pump and a medium reservoir. Each culture cassette contained a screw-top, a neoprene o-ring, and a screw-bottom with an internal cavity. The scaffold is press-fitted on a net in the internal cavity of the screw-bottom. Media flows from top to bottom through the scaffold. Flow through each cassette is driven by the cylinder pump with each culture cassette on its own independent pumping circuit. In the complete perfusion culture circuit, media is drawn from the common media reservoir, pumped through each culture cassette, and returned to the common media reservoir. The entire flow circuit is connected with silicon tubing.

Using hMSCs transduced with human telomerase catalytic subunit hTERT (hTERT-hMSCs) cultured in porous PLGA scaffolds under perfusion for 12 days at a flow rate of 0.5 ml/min, they demonstrated that the flow enhances osteogenic proliferation and differentiation of hTERT-hMSCs, when compared to static conditions (47).

An oscillatory perfusion bioreactor was fabricated by Du et al, in 2008 (73). The upper chamber consisted of six flow wells custom-machined in a block of Teflon. The base of each well was sealed with a silicon film. The scaffold is press-fitted to a silicon cassette that was then fixed into each well with an upper O-ring and steel cap with up-to-down pressure to ensure that the media would perfuse only through the scaffold and not flow in between the scaffold and cassette or between the cassette and well wall. The lower chamber is filled with sterilized water using a 30-mL syringe with gas removed from the gas outlet. The movement of the syringe back and forth is controlled by a continuous cycle syringe pump, forcing the silicon membranes to move up and down, thus driving the media in the flow wells to perfuse up and down through the scaffolds in an oscillatory manner. Results obtained with a mouse immature osteoblast-like cell line, MC 3T3- E1 seeded in porous beta-tricalcium phosphate (b-TCP) scaffolds suggested that the oscillatory flow condition not only allows a better seeding efficiency and homogeneity, but also facilitates uniform culture and early osteogenic differentiation (73). The same group designed a unidirectional perfusion system. A media bottle is set on each end of the perfusion chamber as both media reservoirs and gas bubble trappers. A gas-permeable bag is set in the circuit loop as a gas exchanger. The unidirectional media flow was driven by a pump. A couple of silicon tubes led from bottle 2 to the clean bench, so that the medium could be exchanged in a sterile environment without moving the whole complicated system. This system presents a recirculation flow, thus media is drawn from the media reservoir, pumped through the compartments, merged at the outlets of the chambers, and returned back to the media reservoir. The perfusion system with the scaffolds set inside is sterilized by ethylene oxide gas. To compare these two different types of perfusion systems developed, mouse osteoblast-like MC 3T3-E1 cells were 3D-cultured with porous ceramic scaffolds for 6 days under static and hydrodynamic conditions with either a unidirectional or oscillatory flow. In perfusion culture with the unidirectional flow, the proliferation was significantly higher than in the other groups but was very inhomogeneous. Only the oscillatory flow allowed osteogenic cells to proliferate uniformly throughout the scaffolds, and also increased the activity of ALP(35).

### **2.3.2- Single Culture Chamber perfusion Bioreactors that enable culturing large sized constructs**

As seen in the previous section, many research groups have developed bioreactors that perfuse cell seeded constructs, and that have demonstrated the beneficial effects of perfusion on cell survival, proliferation, differentiation and ECM formation in the scaffold. However, these studies focus on the construction of small-size tissue-engineered bone ranging from 0.04 to 2.7 cm<sup>3</sup> (25, 27, 40, 44, 48, 56, 57, 61-63, 67, 73-77). In this section we will describe some of the few available systems that may enable the culture of large dimension constructs.

According to published works there has been an increasing focus on the development of such bioreactors which are usually designed with a single cellular culture chamber. Hosseinkhani et al, in 2005 (50), developed a perfusion bioreactor in which the cell-seeded scaffolds are set in a sample holder, while the medium is flowed by a peristaltic pump at a linear flow velocity to perfuse the medium through the scaffold using a medium recirculation method and only one medium reservoir. The perfusion system is operated in a CO<sub>2</sub> incubator atmosphere. It was found that this system enabled improvement of MSCs proliferation and differentiation in collagen sponges reinforced with PGA fibers (50). Furthermore, in another study, it was shown that BMP-2 expression of rat MSCs impregnated with plasmid DNA encoding for BMP-2 was enhanced with perfusion culture (78). In a subsequent in vivo study, the collagen-PGA scaffolds of 12 mm diameter seeded with rat MSCs were implanted ectopically in Fischer male rats. Significant increase in ALP and OC expression at sites of implantation of constructs previously cultured in the perfusion system, was observed as compared to constructs obtained in static conditions (79).

Xie et al, in 2006 (80), described a bioreactor system that is composed of 3 parts: the driving part, the reservoir, and the tubing part. The driving part consists of up to eight 3-stop tubes which are fixed in an 8-channel pump head and driven by a peristaltic pump. The reservoir (only chamber) is a 75-cm<sup>2</sup> flask containing the perfusion medium. In the tubing part, there are 2 silicone tubes with one end penetrating through the plug cap into the flask as the inlet and outlet. To study the effects of flow shear stress and mass transport, respectively, on the construction of a large-scale tissue-engineered bone substitute, Li et al (45), used a critical-sized b-TCP cylinder scaffold (14mm in diameter and 30mm in length with a tunnel of the 3,5 mm in diameter and 25 mm in length) seeded with hBMSCs.

The results suggested that shear stress accelerates osteoblastic differentiation of hBMSCs while mass transport shown to increase differentiation among lower ranges (45, 80).

A direct semi-automated perfusion bioreactor system (single chamber) was developed by Janssen and his researchers (81). Goat bone marrow stromal cells (GBMSCs) were dynamically seeded/cultured in this system in volumes (10 cm<sup>3</sup>) of small-sized macroporous biphasic calcium phosphate (BCP) scaffolds. Cell load and distribution was shown using methylene blue block staining, and MTT staining was used to demonstrate the viability of the cells. Online oxygen measurements were correlated with proliferating GBMSCs. They conclude that this bioreactor enabled homogenous cell growth of GBMSCs (82). In posterior studies, the authors demonstrated that dynamically cultured GBMSCs grown on calcium phosphate ceramic produced bone when implanted into mice (51). Another study conducted in 2010 by the same group, concluded that this perfusion bioreactor system is capable of producing clinically relevant and viable amounts of human tissue-engineered bone that exhibit bone-forming potential after implantation in nude mice (81).

Jaasma et al, in 2008 (83), developed a flow perfusion chamber bioreactor consisting of a syringe pump, a scaffold chamber, and a media reservoir which are connected via gas-permeable, silicone tubing and tubing connectors. The scaffold is held in place within a silicone O-ring and between two machined polycarbonate pieces. The scaffold is maintained under approximately 10% compression using aluminium spacers and an O-ring inner diameter is larger than the flow path diameter through the polycarbonate pieces of the scaffold chamber. The scaffold chamber is designed to accommodate compliant scaffolds, but stiff scaffolds can also be used by adjusting the spacer height. The syringe pump is programmable to allow for the application of steady, pulsatile and oscillatory flow profiles, and can accommodate up to six 50-ml syringes, which allows for the simultaneous culture of six cell-seeded constructs. The authors used Collagen-GAG (CG) scaffold with 12,7mm in diameter and 3,5 mm of thickness MC 3T3-E1 cells and four scaffolds were cultured simultaneously, but each one in a different bioreactor. Flow analysis revealed that steady, pulsatile and oscillatory flow profiles were transferred from the pump to the scaffold. Comparing to static, bioreactor culture of osteoblast seeded CG scaffolds led to a decrease in cell number but stimulated an increase in the production of prostaglandin E2, an early-stage bone formation marker (83).

Other study examined the effect of short term flow perfusion bioreactor culture, prior to long-term static culture, in the same bioreactor developed by Jaasma et al, in 2008 (83). Human fetal osteoblasts (hFOB 1.19) were seeded onto CG scaffolds. Results show that the bioreactor and static culture control groups displayed similar cell numbers and metabolic activity. However, histologically, peripheral cell-encapsulation was observed in the static controls, whereas, improved migration and homogenous cell distribution was seen in the bioreactor groups. Osteogenic markers investigated displayed greater levels of expression in the bioreactor groups compared to static controls. They demonstrated that this flow perfusion bioreactor improved construct homogeneity by preventing peripheral encapsulation whilst also providing an enhanced osteogenic phenotype over static controls (84).

Barthold and other researches, in 2005 (85), constructed a perfusion chamber bioreactor (single chamber), to analyze and identify soluble factors such as the formation of l-lactate, lactate dehydrogenase, collagen I C-terminal propeptide, soluble ALP and OC during the culture of rabbit bone marrow mesenchymal stem cells to get detailed information about the differentiation of the osteogenic cells (85). This same bioreactor was used to test human trabecular bone cells seeded onto three different types of scaffolds (porous CaCO<sub>3</sub>, mineralized collagen, porous tricalcium phosphate), with 5mm in diameter and 3 mm thick, were used, stacking 9 samples that were simultaneously cultured in the bioreactor. The scaffolds were subsequently implanted in rat mandibles for 6 weeks. Scaffolds without cells and scaffolds cultured in static conditions were used as controls. Histomorphometric evaluation showed that neither seeding human trabecular bone cells nor the culturing technique increased the amount of early bone formation compared with the level provided by osteoconductive bone ingrowth from the defect edges(86).

To engineer anatomically correct pieces, Grayson and his researcher's (46) report that clinically sized, anatomically shaped, viable human bone grafts can be developed using hMSCs and a "biomimetic" scaffold-bioreactor system. They selected the temporomandibular joint (TMJ) condylar bone as their tissue model. Scaffolds were generated from fully decellularized trabecular bone by using digitized clinical images, seeded with hMSCs, and cultured with interstitial flow of culture medium. A bioreactor with a single chamber in the exact shape of a human TMJ was designed for controllable perfusion throughout the engineered construct. After 5 weeks of culture, tissue growth was evidenced by the formation of confluent layers of lamellar bone, a markedly increased volume of mineralized matrix, and the formation of osteoids (46).



Yeatts et al (87), developed a bioreactor- the tubular perfusion system (TPS) - consisting of a tubular growth chamber and medium reservoir connected via a tubing circuit. The medium's flow is driven by a Multichannel peristaltic pump at 3 ml/min for short-term studies and at either 3 or 10mL/min for the long-term studies. The circuit consists of silicone tubing that is connected using silver ion-lined microbial resistant tubing connector. The growth chamber consists of length silicone tubing. The growth chamber has 13cm in length and is packed with 30 cell seeded alginate beads. The tubing is placed in a cell culture CO<sub>2</sub> incubator atmosphere. hMSCs were encapsulated in alginate beads (a total of 30 samples of 4mm diameter per bioreactor) and medium was perfused through the growth chamber and around the tightly packed scaffolds enhancing nutrient transfer while exposing the cells to shear stress. Results demonstrate that bioreactor culture supports early osteoblastic differentiation of hMSCs as shown by ALP gene expression and increases in the gene expression levels of OC, OP, and bone morphogenetic protein(BMP)-2 (87).

Bertrand et al, in 2011 (88), build a single chamber perfusion bioreactor based on fluidized bed bioreactor concepts for culture of clinical size scaffolds. It consists of a vertical cylindrical polycarbonate chamber connected to a reservoir containing the culture medium in a closed loop arrangement. The connections between the bioreactor chamber and the reservoir and between the bioreactor and a peristaltic roller pump are made of silicone tubing, Multiple perfusion bioreactors such as this were operated during experiments, using 140 units of coral scaffolds (each 3x3x3mm<sup>3</sup>) for each bioreactor, and seeded with GFP-C3H10T1/2 cells. To establish the flow influence, an in vitro study was conducted with various flow rates. To investigate the osteogenic potential of bone constructs, an in vivo study was carried out using sheep MSCs which were then subcutaneously implanted. The best flow rate determined for this bioreactor and this scaffold was the 10ml/min and 8 weeks as following the subcutaneous implantation in sheep, all retrieved samples had areas of mineralized bone and osteoid, with osteocytes located inside the matrix and a film of osteoblasts coating the newly deposited bone (88).

Gardel et al, in 2011 (89), developed a single chamber Bidirectional Continuous Perfusion Bioreactor (BCPB ). The BCPB is composed by one vacuum and one peristaltic pump, connected through of a circular flow system which are connected via gas-permeable, silicone tubing and tubing connectors, and also for rotational engines located in specific places, aiming at creating shears stresses, due to the medium flow perfusion using different gradients of pressure, to induce mechanical stimulations to the cells seeded onto the scaffolds.

The passage of the flow from the interior to the exterior of the three-dimensional support or from the exterior to the interior of the three-dimensional support is carried out through the use of a rigid tube (polycarbonate) with perforations in its central part and that has the same length of the three-dimensional support (that can have variable dimensions). This tube, containing the scaffold, is connected to a circular system and is located coaxially inside of the culture chamber. This culture chamber has four exits/entrances and is tightly closed, by that same circular system, which allows the control of the flow and the gradient of pressure inside of the chamber and inside of the perforated tube. Therefore this system enables to control the perfusion rate and gradient of flow, in the interior of the cell-scaffold constructs in culture, and it allow to culture constructs of significant dimensions, as it enable the access of nutrients to the interior of the material and the removal of the metabolic products from the interior of this, enabling the maintenance of the cells the viability. To prove the feasibility of this perfusion system, preliminary in vitro studies using Starch/Polycaprolactone (SPCL) fibbers mesh scaffolds (with 16mm in diameter and 3 mm thickness with a concentric hole of 6mm), were seeded with goat marrow stromal cells with and stacked, completing a 42 mm thick construct. The samples were cultured for a period of 14 and 21 days of culture in the bioreactor at a flow rate of 1 ml/min, using static cultured constructs as controls. The results showed higher ALP activity levels in dynamic cultures (14 days of culture) than those obtained under static conditions. SEM and histological images showed cells occupying the interior of the scaffolds cultured in the bioreactor, while cells were predominantly on the surface of the GBMC–SPCL constructs in the static cultures (90).

In summary, the systems currently available for the culture of large sized constructs, described in this review, differ considerably with respect to ease of use, cost-effectiveness, and degree of additional osteogenic stimuli provided, as well as monitoring and manipulation options. Further optimization of these systems may be achieved by adapting specific stimuli and by combining biophysical and biochemical stimuli within one system. However, a major challenge will be the translation of such bioreactor-based concepts into clinically applicable designs, because this requires adapting current designs or developing new bioreactors that enable culturing constructs of large dimension for clinical use, in accordance with Good Manufacturing Practices (GMP).

## **2.4- Large Animal models**

### **2.4.1- Selection of appropriate Animal Models**

Desirable attributes of an animal model include demonstration of similarities with humans, both in terms of physiological and pathological considerations as well as being able to observe numerous subjects over a relatively short time frame (91, 92). When deciding on the species of animal for a particular model there are several factors that should be considered, namely cost to acquire and care for animals, availability, acceptability to society, tolerance to captivity and ease of housing. The welfare and housing of animals is usually covered by a Federal Animal Protection Act and may vary slightly between countries. The Animal Protection acts outline the minimum requirements in terms of housing dimensions, lighting, flooring etc. and must be complied with when undertaking an animal study. Other factors include low maintenance care, ease of handling, resistance to infection and disease, inter-animal uniformity, tolerance to surgery, adequate facilities, support staff and an existing database of biological information for the species, ease of adaptability to experimental manipulation, ecological consequences and ethical implications (22, 93).

More specifically, for studies investigating bone-implant interactions, an understanding of the species specific bone characteristics – such as bone microstructure and composition, as well as bone modelling and remodelling properties, are important when later extrapolating the results to the human situation. Finally the size of the animal must be considered to ensure that it is appropriate for the number and size of implants chosen (22).

Within a field of study, no single animal model will be appropriate for all purposes, nor can a model be dismissed as inappropriate for all purposes. Furthermore, multiple model systems are likely required to establish a broad body of knowledge (94). International standards established regarding the species suitable for testing implantation of materials in bone, state that dog, sheep, goat, pig are suitable large animal models. At least two of each of the species mentioned above should be used for assessing each treatment at each implantation period. Long term implantation periods for these species are given as 12, 26, 52 and 78 weeks (22).

### **2.4.2-Animal models in bone repair research**

Animal models in bone repair research include representations of normal fracture healing, segmental bone defects, and fracture non-unions in which regular healing processes are compromised with the presence of a critical-sized defect site (95). In critical-sized segmental defect models bridging of the respective defect does not occur despite a sufficient biological microenvironment, due to the removal of critical amounts of bone substance. In contrast, in a true non-union deficient signaling mechanism, biomechanical stimuli or cellular responses may prevent defect healing rather than the defect size (96). Bone composition and biology of dog, sheep, goat, and pig are very similar to those of humans. Reviews of the literature comparing bone structure, composition, and biology in these animals identify modest differences in cancellous and cortical bone density at various sites, magnitude of sexual dimorphism, the age at which peak bone mass is achieved, and the rate and extent to which haversian remodeling replaces plexiform lamellar bone in the cortex of long bone (97). However, these points of variation do not provide evidence that any one of these animals provides a better match for human bone biology than the other (98). In a variety of study designs, pigs are considered the animal of choice and were described as a highly representative model of human bone regeneration processes in respect to anatomical and morphological features, healing capacity and remodeling, bone mineral density and concentration (99, 100). Pigs tend to be least used (101), likely due to difficult temperament, anatomically short and thick long bones, and large size.

The short bones do not allow for large gap defects because adequate fixation is difficult to achieve (98), which leads to the the need for special implants, as one cannot use implants designed for human use (96). Non human Primates (NHPs) are sometimes held up as the model of choice for prediction of clinical performance for bone repair and regeneration methods. This supposition is based on arguments of evolutionary proximity and similar structural anatomic, endocrine, digestive, and dietary features and immunology. Of the three common NHP species, only the baboon approaches the skeletal size range that humans share with large canines, sheep, and goats. NHPs are very expensive and present husbandry challenges that preclude models involving intensive wound assessment, management, or immobilization. Although NHPs do not have companion animal status, arguments of perceived evolutionary affiliation raise social and ethic questions related to increasing their use in research (98).

Dogs are used most due to a rich background of prior experience, ease of husbandry, and accessibility. A large literature characterizing canine models supports continued preferential use of dogs in many settings, particularly in bone marrow biology and transplantation immunology (102-108). The use of dogs is being challenged, however, by social concerns regarding the dog as a companion animal (98). Although, the use of dogs as experimental models has significantly decreased mainly due to ethical issues, between 1998 and 2008 approximately 9% of articles published in leading orthopedic and musculoskeletal journals described dogs as animal models for fracture healing research (101). Mature sheep and goats possess a body weight comparable to adult humans and long bone dimensions enabling the use of human implants (109). Sheep are readily available and docile, but can be frail and less resilient, particularly when not in a group. Goats, similar in size and skeletal anatomy to sheep, have a thinner coat and less muscular bulk, and are more tolerant of stress and isolation (98). The mechanical loading environment occurring is well understood (110, 111). Since no major differences in mineral composition (112) are evident and both metabolic and bone remodelling rates are akin to humans (113), sheep and goats are considered a valuable model for human bone turnover and remodeling activity (96, 114), making them an increasingly viable alternative for bone research (98).

### **2.4.3 Ovine models**

Ovines are a convenient large animal model for biomedical research because of ease of handling and housing, animal cost and acceptance to society as a research animal (115). Sheep are long boned, and allow the use of many systems of internal fixation. Sheep are readily available and docile, but can be frail and less resilient, particularly when not in a group (98).

They are a less expensive animal model versus other species, and their size is conducive to the insertion of prosthetic implants comparable to those implanted in humans. The age of the animals, the timing of the study, and the duration of the experiment have to be considered in sheep versus other species. The use of a few widely accepted standardized sheep breeds would make interlaboratory comparisons easier, and disclosure of reproductive and dietary histories could further aid our understanding of the efficacy of this animal model (97). The number of sheep used in orthopedic research is increasing in the last decade involving fractures, osteoporosis, bone-lengthening and osteoarthritis, in comparison with companion animals (116).

This increase in usage may be related to the ethical issues and negative public perception of using companion animals for medical research (22). Adult sheep offer the advantage of having a more similar body weight to humans and having long bones of dimensions suitable for the implantation of human implants and prostheses (109). Sheep are described as having a predominantly primary bone structure in comparison with the largely secondary bone of humans. Age related changes in bone structure are also described; adult sheep have a plexiform bone structure comprising a combination of woven and lamellar bone within which vascular plexuses are sandwiched. Secondary, Haversian (osteonal) remodelling in sheep is more prevalent in old sheep. Aging results in secondary haversian remodeling that becomes more extensive at specific locations such as the posterior aspect of long bones and in ribs (97). Haversian canal distribution has been shown to be less dense in ovine bone than in human bone (117) and has been described as not uniformly distributed (22). Differences in bone density exist between the human and sheep, whereby sheep bone shows a significantly higher density and subsequently greater strength. Bone location must be considered when contemplating differences between human and sheep bones. In terms of mineral composition humans and animals do not show significant differences (22).

Despite the differences in bone structure being recognized, studies show that sheep are a valuable model for human bone turnover and remodelling activity (114). As found in other species, it is likely that bone location may also alter bone composition and turnover in the sheep (22).

#### **2.4.4 Caprine models**

As previously mentioned, goats are similar in size and skeletal anatomy to sheep but have a thinner coat and less muscular bulk, and are more tolerant to stress and isolation (98). Goats are generally classified as gentle, inquisitive, placid, and easy to handle, as well as clean and hardy in nature (97), making them an increasingly viable alternative for bone research (98).

Like sheep, goats are considered food producing animals and thus also have the advantage of less critical public perception when used for research, than companion animals. When compared to other species, sheeps and goats are reported to be more tolerant to environmental conditions. (118). Histologically, the tibial cortical bone of goats does not have homogeneously distributed Haversian systems (concentrically oriented lamellar bone containing a centrally located blood vessel, also known as osteons).

Similar to the sheep, where the Haversian systems are non-uniformly distributed throughout individual bones, in the goat, the Haversian systems are located primarily in the cranial, cranio-lateral and medial sectors of the tibial diaphysis, while the caudal sector is mainly comprised of lamellar bone (where the collagen fibres are arranged in sheets and do not contain a central blood vessel) (119). Liebschner, in 2004 (91) shown that while there are small differences in the apparent and ash density between the goat and humans, these differences are probably not as significant as the differences found between anatomic sites of the same species(91). The mineral composition of bone does not vary significantly across species and therefore one could conclude that this also holds true for the goat (22). Goat has a metabolic rate and bone remodeling rate similar to that of human's presenting a suitable animal model for testing human implants and materials as they are considered (113, 120). However, the rate at which a bone graft is revascularised and converted into a vital trabecular structure is found to be faster in the goat, occurring at approximately 3 months in comparison to 8 months in humans. There is little information comparing the utility of goats versus sheep for implant-related studies. Therefore the choice of which small ruminant to use most likely depends on availability and other factors (22).

## **2.5- Critical/cylindrical size defects**

Critical-sized defects are defined as “the smallest sized intraosseous wound in a particular bone and animal species that will not heal spontaneously during the lifetime of the animal” (96, 121, 122) or as a defect which shows less than 10 percent bony regeneration during the lifetime of the animal (96, 123). However, this has been re-defined as segmental bone deficiencies of a length exceeding 2–2.5 times the diameter of the affected bone (96, 124, 125).

A critical defect in long bones, however, can hardly be defined by size only. The phenomenon of regeneration is also influenced by species, anatomic location, associated periosteum and soft tissue, and biomechanical conditions, as well as age, metabolic and systemic influences, and related injuries affecting defect healing (96, 121, 124).

Congenital abnormalities, cancer resections, non unions or traumatic incidents are very common both in human and inveterinary traumatology, and as suggested above, these problems do not heal or regenerate spontaneously. In fact, the currently available therapies that are usually used in such clinical scenarios, mostly consisting on the use of auto or allografts, present several disadvantages.

Tissue engineering, using scaffolds and stem cells offer the potential to overcome such limitations. Therefore, it is important that studies on scaffolds development for such applications envision the need for obtaining constructs with a cylindrical shape, as long bones show anatomically a cylindrical shape, and thus facilitating the translation to clinical settings. The composition of the defect generally includes periosteum, cortical bone, and endosteum. After suture, the opening of the defect is bounded by overlying muscle or fat. The base of the defect may be cancellous bone and marrow, cortical bone, or muscle/fat, depending on defect length and orientation within the long bone. In general, defects in the metaphysis of young large animals will be comprised of highly vascular hematopoietic marrow. However, marrow in defects in the diaphysis will generally be fatty or yellow marrow, which is still vascular, but far less cellular. Advancing age in animals will also increase the ratio of fatty to hematopoietic marrow, changing the biological environment of the graft site. Soft tissue encroachment does not compromise bone formation in most cylindrical defects. Regardless, cylindrical critical defects can be very sensitive to detecting differences in efficacy between osteoconductive scaffold materials as well as the effects of bioactive factors and cell transplantation. The uniform radial geometry of cylindrical defects also provides the potential for control and modeling of biological gradients relevant to bone regeneration.

Due to the pattern of diffusion and vascular ingrowth that must be oriented from the periphery to the center of the defect, cylindrical defects are particularly well suited for time-oriented studies of mass transport (e.g., the influence of diffusion, cellular metabolic demand, local oxygen delivery or generation, or gradients in the delivery of bioactive factors), degradation rate of implants, cell transplantation (survival and migration) and variables modulating the rate of bone or tissue ingrowth or vascular invasion into an implant (98).

## **2.6- Creation of the cylindrical critical size defects in large animals**

Osteotomy approach techniques are used for the creation of cylindrical critical size defects and can be performed by using a CO<sub>2</sub> Laser (126, 127), Oscillating saw (124, 128-136), Gigli saw (137, 138), treaded saw (139) and a chisel/ osteotome (140-142). The edges of the defect are usually cut straight with less trauma but there are advantages and disadvantages in the choice of each technique.



The CO<sub>2</sub> laser produces a cut with little trauma, it's the most accurate to perform the osteotomy but quite expensive. Kuttner et al (127), demonstrated that bone healing is similar and undelayed after both laser and oscillating saw. For practical applications, precise control of the depth of laser cutting and easier manipulation of the osteotome is required (127). The oscillating saw makes a straight cut without causing trauma to surrounding soft tissue and bone thermal necrosis caused by cutting blade unit can be avoided by a continuous irrigation of saline solution at the time of the cut; the technique of holding the cutting is easy and fast and cheaper when compared with the CO<sub>2</sub>, but more expensive when compared with the manual saws. Manual saws are much cheaper than all others, but require physical strength to make the cut and the start of this may not be accurate due to the difficulty of supporting the saw on the rounded and smooth bone surface, and care must be taken not to cause damage to surrounding soft tissues. The chisel (osteotomes) techniques require a hammer to be performed, and is not the best choice to perform an osteotomy in a long bone as it may cause jagged cuts in the bone surface.

## **2.7- Fixation of the cylindrical critical size defects in large animals**

To simulate human in vivo conditions as closely as possible, a variety of large cylindrical critical size defect models, mainly in sheep and goat, have been developed in the last decade to investigate the influence of different types of bone grafts on bone repair and regeneration. The method of fixation is an important variable to be studied in large cylindrical critical size defect models. Fixation should not only reflect what occurs in the clinic but also provide sufficient rigidity to support bone healing (143). The method of fixation is more important for defects within weight-bearing bones than the nonweight-bearing bones (144). At present, most long bone defect models use bone plates, interlocking intramedullary nails and external fixator to fix the defect, thus reflecting the situation within the clinic (143). Sufficient reduction and stability can be achieved by bone plates even in complicated fractures (145). Bone plate osteosynthesis is performed using standard instrumentation, differing according to the size of the implant and the type of plate fixation.

Most studies on bone tissue engineering using caprine and ovine models are performed in the diaphyseal bone (tibia, femur) requiring the use of cortical screws that are a very efficient devices for fixing a splinting device such as a plate.

The goal is to achieve as much contact area as possible in a sufficiently stable implant of minimal size; it is recommended that the screw diameter should not exceed 40% of the diameter of the bone. There are a number of different sizes of cortex screws available to enable fixation of bones of different diameters. Newly developed screws for use in humans, such as self-tapping screws, monocortical screws and those used in locking systems, are likely to find an increasing application in animal models. Various types of bone plates are available in the market for use as bone fixation methods, such as dynamic compression plates (DCP), limited contact dynamic compression plates (LC-DCP), locking compression plates (LCP), non dynamic compression plates and reconstruction plates. For sheep and goat weighing between 15 and 45 kg, plates with screws of 3.5 and 4.5 mm are used, but for weights superior of these values the use of screws 5.5 mm should be considered. However, conventional bone plates can result in histologically and radiologically verifiable bone loss, which has been attributed to stress protection (Wolff's law). An increase in cortical bone porosity proximate to the plate soon after bone plate osteosynthesis has been observed. This porosity is explained by impaired vascular perfusion underneath the plate due to high compression forces between plate, periosteum, and bone (96, 146). New plate systems were developed where load and torque transmission act through the screws (interlocking screws), the stabilization system acts like an external skeletal fixator (ESF) making a total plate–bone contact unnecessary to achieve stable fixation (96). The plates can be placed in three different functions: compression mode (the plate creates an axial compression), neutralization mode (the plate protects the interfragmentary compression), biological mode (the plate acts as a splint to maintain the correct length of the bone and the normal spatial alignment of the joints proximal and distal to the fracture).

For example, to study the effects of different bioceramics during bone repair of a tibial defect model in sheep of 16 mm length, Gao et al (147), implanted biocoral and tricalcium phosphate cylinders (TCP). The defects were stabilized medially using two overlapping contoured autocompression plates of 4 mm thickness (8 and 6 holes) and cortical screws (147). However, this method of fixation is not commonly used in the clinical practice.

A DCP stainless steel plate was used by Kirk-Head et al (148), for the stabilization of a 25 mm long mid-diaphyseal critical size defect in long bone of the sheep, in order to observe the use of recombinant human BMP-2 and a poly [D, L-(lactide-co-glycolide)] in 1 year of the long-term healing (148).

Several studies selected this as a method of fixation bone plate for osteosynthesis. Wefer et al (149), used as a method of fixing an anterolateral plate to implant a porous hydroxyapatite scaffold in a 20 mm critical size defect in the sheep long bone, to develop and test a scoring system based on real-time ultrasonography (149). Meinel et al (149), performed a non-critical 10 mm segmental tibia defect using for stabilization a 3,5 mm of 11 hole DCP plate, to study the treatment of bone defects by releasing of the insulin-like growth factor(IGF-1) from biodegradable poly(lactide-co-glycolide) microspheres (150). To evaluate a synthetic calcium phosphate multiphase biomaterial, Mastrogiacomo et al (151), created a 48 mm tibial defect model in sheep and stabilized with a 4.5 mm neutralizing plate (151). However, Reichert et al (96), in their review article reported that they observed bent plates and axial deviations in presented X-ray and CT images, and concluded that the chosen fixation, performed by Mastrogiano et al, seemed insufficient in this study (96). Teixeira et al (152), created a tibial critical size defects of 35 mm size, being the bone defects in the diaphysis of the sheep stabilized with a titanium bone plate (103 mm in length, 2 mm thickness, and 10 mm width), but as reported by the authors, plate bending occurred in 42% of the animals most likely caused by insufficient thickness of the fixation device (152). To demonstrate that the compartmentalization of tissues may have an important role in bone regeneration in long-bone defects, Klaue et al (153), created a foreign-body membrane with a temporary poly-methylmethacrylate spacer with the same critical size of the defect created (30 mm) on mid-diaphyseal of the sheep femurs and stabilized with an 8-hole, 4.5 mm low covering dynamic-compression plate (LC-DCP). The obtained results suggested that regeneration of bone can be enhanced by compartmentalisation of the bone defect (153). To study the different immunological characteristics between Human and ovine MSCs, Niemeyer et al (134) , applied a xenogenic transplant (human MSCs) and an autologous transplant (ovine MSCs) to a sheep animal model. For this purpose, they performed a critical size defect of 30 mm on the tibial diaphysis and stabilized it with a seven-hole locking compression plate and self-taping screw.

The results demonstrated that the xenogenic transplantation of human MSCs led to poorer bone regeneration than the autologous transplantation of ovine MSCs. Nevertheless, no local or systemic rejection reactions could be observed after xenogenic transplantation of human MSCs (134). To investigate whether MSCs and osteogenic protein-1 (OP-1) can improve allograft integration, Bella et al (154), performed a 30 mm full-size bone defect in the mid-diaphysis of the metatarsal bone of a sheep and stabilized with a seven-hole titanium dynamic compression plate (3.5 mm wide, 10,5 mm long). The results demonstrated that the association of MSCs and OP-1 improve bone allograft integration promoting an almost complete bone restoring when compared to other groups: allograft alone (control group), MSC group, OP-1 group (154).

A locked intramedullary nail is a stainless steel or titanium nail that is placed within the medullary cavity and is locked to the bone by screws or bolts that cross the bone and pass through holes in the nail. They are available in several diameters and can be locked with screws or bolts of 4.5 or 3.5 mm diameter and are the most suitable for use in ovine and caprine models. Locked intramedullary nails resist bending, axial, and rotational forces because they are locked with either bone screws or locking bolts. These are most effectively used to stabilize mid-diaphyseal fractures of the femur and tibia in animal models used in tissue engineering approaches and in the last decade several researchers have used this method for orthopedic fixation in their studies. To establish a new critical bone defect model of 30 mm, den Boer et al (114), used an interlocking intramedullary nail (AO<sup>®</sup> unreamed humeral nail); the defect (30mm length) was inflicted on sheep tibiae and bone healing was quantified through X-ray absorptiometry (114). A study conducted by Bloemers et al (155), indicated that new calcium phosphate based materials might be a potential alternative for autologous bone grafts. To conduct this study, they used a segmental tibial defect (30 mm) in sheep fixed by an AO<sup>®</sup> unreamed interlocking titanium tibial nail (155). To see the effect of platelet rich plasma (PRP) on new bone formation in a 25 mm diaphyseal tibial defect in sheep, Sarkar et al (156), stabilized the defect with intramedullary nail with locking screws on the proximal and distal surface and added stainless steel plate applied medially (156).

The effect of chondroitine sulphate on bone remodelling and regeneration was investigated by Schneiders et al (157), for which they performed a 30 mm tibial mid-diaphyseal defect site and reconstructed it using hydroxyapatite/collagen cement cylinders. The stabilization was achieved by insertion of a universal tibial nail (UTN, Synthes<sup>®</sup>, Bochum) (157).

To investigate the feasibility of BMSCs on coral scaffold infected with adenoviral vector containing the BMP-7 gene (AdBMP7), Zhu et al (136), performed a segmental bone defect of the 25 mm in length at the mid-portion of the femoral diaphysis of the goat, and stabilized this defect with an internal fixation rod and interlocking nails (136).

The interlocking intramedullary nail can be applied in two different ways, either static or dynamic compression. depending on the number of screws to use and their positioning(distal or proximal), the outcome of animal experiments and clinical retrievals strongly suggested that, particularly the mechanical load, has a positive effect on bone graft incorporation (158-160).

To prove this, Bullens et al (135), studied if a static or dynamic mode of nail fixation influenced the healing of segmental defect reconstructions in long bones. In this study, 35 mm critical size defects in goat femurs, were reconstructed using a cage filled with firmly impacted morsellised allograft mixed with a hydroxyapatite paste (Ostim<sup>®</sup>). All reconstructions were stabilized with an interlocking intramedullary stainless steel unreamed femur nail and AO<sup>®</sup> locking screws. Authors found that healing of these defects was not significantly influenced by the mode of fixation of the nail in this animal model (135). To analyze the efficacy of allogeneic mesenchymal precursor cells in the repair of sheep tibial segmental defects, Field et al (161) created 30 mm defects and stabilized them with a locking intramedullary nail and allowed to heal over a nine-month-period. The group treated with allogeneic cells and scaffolds displayed a significantly greater level of callus formation and rate of bone apposition in the defect, compared to the scaffolds without cells (161).

External skeletal fixation (ESF) and circular external fixation (Ilizarov model) are two types of the bone fixation which have been more widely used in large animals studies, offering versatility and smooth application. In fact, They offers major advantages over “conventional methods” in the management of fractures caused by the creation of critical-size defects, as the fact that they are relatively easy to apply, maintaining limb use and joint mobility, are well tolerated by patients, have a low cost when compared to plate systems, and involve a relatively low risk procedure.

In addition, external fixators are associated to minimal intra-operative trauma and the surrounding soft tissues are only marginally affected. The linear external fixators are composed of bars and clamps that can vary in amount depending on the type to be applied (type I frame, type II frame and type III frame), being the type III frame the most strong of all. The distal and proximal bone fragments should be secured with at least two pins at each end, and the conformation of these pins can be, smooth pin, negative and positive threaded pins. One of the most common complications with linear external fixators is the pin loosening often resulting in pin track infections, but this complication can be eliminated with the use of positive threaded pins. The linear external fixation has been selected by some research groups as a method of bone fixation to be implemented. For example, to study the effect of bioresorbable polylactide membranes, applied alone and/or in combination with autologous bone graft, in bone healing, Gugala et al (162) performed a critical defect of 40 mm in sheep tibia and stabilized with an AO® external fixator type II frame. Only in groups where the defect was filled with autogenous cancellous bone graft and covered with a membrane, defect healing was observed (162).

Maissen et al (163) studied the influence of rhTGFbeta-3 loaded on a poly (L/DL-lactide) carrier, as compared to the carrier only, autologous cancellous bone graft, and to untreated defects, on mechanical and radiological parameters of a healing bone defect in the sheep tibia. An 18 mm long defect was fixed with a unilateral (type I frame) external fixator and the results showed significant differences between the groups, indicating the autologous cancellous bone graft bone graft treatment performed better than the others group (163).

Based on its design and configuration, circular fixators are indicated for the treatment for lengthening or shortening bone, limb deformities, arthrodesis, non-union and fractures by presenting greater rigidity and versatility, but few researchers choose this method for bone fixation in their studies in large animals models. Recently, Liu et al (164), reported on the use of highly porous b-TCP scaffolds to repair 26 mm long goat tibial defects, stabilized using a circular external fixator. Study groups included defects treated with b-TCP ceramic cylinder loaded with osteogenically induced autologous bone marrow stromal cells, beta-TCP ceramic cylinder without cells and defects left untreated. X-ray, micro-computed tomography and histological analysis performed at 32 weeks post-implantation showed that the porous beta-TCP ceramic cylinder loaded with cells led to was significantly better results than all the other groups (164).

## 2.8- Conclusions

Bone Tissue Engineering and Regenerative Medicine (TERM) has the potential to become a real alternative to autologous bone grafts, but before this can happen it is necessary to solve the problem of homogeneously supplying oxygen and nutrient to cells within a large scaffold. Several bioreactors have been developed that hold potential to improve mass transfer in large cellular scaffold constructs and to apply favorable mechanical stimuli, thus facilitating the cellular viability, proliferation and differentiation. One of the major breakthroughs was the development of the perfusion bioreactor system that increase the mass transfer of cellular scaffolds not only at the periphery but also within its the interior of scaffolds, increasing cellular proliferation and osteogenic differentiation. A significant volume of work was reported in this review, related to the use of perfusion bioreactor systems for bone tissue engineering. However, most perfusion bioreactors described herein do not enable the culture of large constructs. Thus, additional efforts are required to develop improved design for the successful culture of large scaffolds to be used in clinical settings.

Given the amount of research conducted on many bioreactor systems, the next obvious step should t be the evaluation of constructs developed in perfusion bioreactors, using large animal models and critical size defects, to enable easier translation of outcomes to the clinical scenario. However, little work has been reported using perfusion bioreactor cultured bone tissue engineering constructs implanted in critical size defects animal models. Therefore, the selection of an experimental model, to access the feasibility of a determined tissue engineering concept, is critical to the success of the preclinical studies and must be considered in the light of the proposed ideas to be tested. The rapid progression of this research area and the great number of novel developments must be supported by systematic assessment based on clinical practicability and experience, the knowledge of basic biological principles, medical needs and commercial practicality. Preferentially, an animal model should match the clinical setting that it is to reflect, both in terms of creation of the defect and the cells or scaffolds that will be used for repairing it. It is clear that each of the species discussed here demonstrate unique advantages and disadvantages in terms of their appropriateness as a model for demonstrating the response of bone tissue to an implant material. Considerations should include the species and the type of defect (location, size, method of creation and repair, and fixation) as well as the post operation care and monitoring.

Although there is no ideal animal model, a deep understanding of the differences of bone (macroscopic, microscopic and remodeling attributes) are likely to improve the choice of model and interpretation of these in vivo studies. Probably, a combination of different animal models for different strategies may be more realistic. However, to allow comparison between different studies is fundamental that animal models, methods of orthopedic fixation, surgical procedures and devices for measuring qualitatively, quantitatively and objectively the samples are standardized to achieve a reliable data pool as a base for future lines of research in TERM. New horizons are opened in TERM, whether clinicians, surgeons, scientists, and entrepreneurs begin to work in multidisciplinary teams. These progresses will aid in ensuring that TERM fulfills the expectations for revolutionizing medical care.



## References

1. Young, R.G., Butler, D.L., Weber, W., Caplan, A.I., Gordon, S.L., Fink, D.J. Use of mesenchymal stem cells in a collagen matrix for Achilles tendon repair. *J Orthop Res* 16, 1998,406.
2. Awad, H.A., Butler, D.L., Boivin, G.P., Smith, F.N.L., Malaviya, P., Huibregtse, B., et al. Autologous mesenchymal stem cell-mediated repair of tendon. *Tissue Eng* 5, 1999,267.
3. Langer, R., Vacanti, J.P. *Tissue Engineering*. *Science* 260, 1993,920.
4. Nerem, R.M., Sambanis, A. *Tissue engineering: from biology to biological substitutes*. *Tissue Eng* 1, 1995,3.
5. Wu, F., Dunkelman, N., Peterson, A., Davisson, T., De la Torre, R., Jain, D. Bioreactor development for tissue-engineered cartilage. *Ann N Y Acad Sci* 875, 1999,405.
6. Griffith, L.G., Naughton, G. *Tissue engineering - Current challenges and expanding opportunities*. *Science* 295, 2002,1009.
7. Meyer, U., Szulczewski, D.H., Moller, K., Heide, H., Jones, D.B., Gross, U., et al. Attachment Kinetics and Differentiation of Osteoblasts on Different Biomaterials. *Cells and Mater* 3, 1993,129.
8. Ratcliffe, A., Niklason, L.E. *Bioreactors and bioprocessing for tissue engineering*. *Ann N Y Acad Sci* 961, 2002,210.
9. Pei, M., Solchaga, L.A., Seidel, J., Zeng, L., Vunjak-Novakovic, G., Caplan, A.I., et al. Bioreactors mediate the effectiveness of tissue engineering scaffolds. *Faseb J* 16, 2002,1691.
10. Williams, C., Wick, T.M. *Perfusion Bioreactor for small diameter tissue-engineered arteries*. *Tissue Eng* 10, 2004,930.
11. Korossis, S.A.B., F. Kearney, J.N. Fisher, J. Ingham, E. . *Bioreactors in Tissue Engineering*. In: *Topics in Tissue Engineering* Eds N Ashammakhi & RL Reis 2005. pp.1.
12. Freed, L.E., Marquis, J.C., Nohria, A., Emmanuel, J., Mikos, A.G., Langer, R. Neocartilage formation in vitro and in vivo using cells cultured on synthetic biodegradable polymers. *J Biomed Mater Res* 27, 1993,11.
13. Freed, L.E., Marquis, J.C., Vunjaknovakovic, G., Emmanuel, J., Langer, R. *Composition of Cell-Polymer Cartilage Implants*. *Biotechnol and Bioeng* 43, 1994,605.
14. Vunjak-Novakovic, G., Freed, L.E., Biron, R.J., Langer, R. *Effects of mixing on the composition and morphology of tissue-engineered cartilage*. *J Am Inst Chem Eng* 42, 1996,850.

15. Wu, W., Feng, X., Mao, T.Q., Feng, X.H., Ouyang, H.W., Zhao, G.F., et al. Engineering of human tracheal tissue with collagen-enforced poly-lactic-glycolic acid non-woven mesh: A preliminary study in nude mice. *Br J Oral Maxillofac Surg* 45, 2007,272.
16. Schreiber, R.E., Dunkelman, N.S., Naughton, G., Ratcliffe, A. A method for tissue engineering of cartilage by cell seeding on bioresorbable scaffolds. *Ann N Y Acad sci* 875, 1999,398.
17. Grande, D.A., Halberstadt, C., Naughton, G., Schwartz, R., Manji, R. Evaluation of matrix scaffolds for tissue engineering of articular cartilage grafts. *J Biomed Mater Res* 34, 1997,211.
18. Chromiak, J.A., Shansky, J., Perrone, C., Vandeburgh, H.H. Bioreactor perfusion system for the long-term maintenance of tissue-engineered skeletal muscle organoids. *In Vitro Cell Dev Biol Anim* 34, 1998,694.
19. Bancroft, G.N., Sikavitsas, V.I., Mikos, A.G. Design of a flow perfusion bioreactor system for bone tissue-engineering applications. *Tissue Eng* 9, 2003,549.
20. Goncalves, A., Costa, P., Rodrigues, M.T., Dias, I.R., Reis, R.L., Gomes, M.E. Effect of flow perfusion conditions in the chondrogenic differentiation of bone marrow stromal cells cultured onto starch based biodegradable scaffolds. *Acta Biomater* 7, 2011,1644.
21. Gomes, M.E., Holtorf, H.L., Reis, R.L., Mikos, A.G. Influence of the porosity of starch-based fiber mesh scaffolds on the proliferation and osteogenic differentiation of bone marrow stromal cells cultured in a flow perfusion bioreactor. *Tissue Eng* 12, 2006,801.
22. Pearce, A.I., Richards, R.G., Milz, S., Schneider, E., Pearce, S.G. Animal models for implant biomaterial research in bone: A review. *European Cells Mater* 13, 2007,1.
23. Sikavitsas, V.I., Bancroft, G.N., Mikos, A.G. Formation of three-dimensional cell/polymer constructs for bone tissue engineering in a spinner flask and a rotating wall vessel bioreactor. *J Biomed Mater Res* 62, 2002,136.
24. Mygind, T., Stiehler, M., Baatrup, A., Li, H., Zoua, X., Flyvbjerg, A., et al. Mesenchymal stem cell ingrowth and differentiation on coralline hydroxyapatite scaffolds. *Biomaterials* 28, 2007,1036.
25. Goldstein, A.S., Juarez, T.M., Helmke, C.D., Gustin, M.C., Mikos, A.G. Effect of convection on osteoblastic cell growth and function in biodegradable polymer foam scaffolds. *Biomaterials* 22, 2001,1279.
26. Wendt, D., Marsano, A., Jakob, M., Heberer, M., Martin, I. Oscillating perfusion of cell suspensions through three-dimensional scaffolds enhances cell seeding efficiency and uniformity. *Biotechnol and Bioeng* 84, 2003,205.

27. Meinel, L., Karageorgiou, V., Fajardo, R., Snyder, B., Shinde-Patil, V., Zichner, L., et al. Bone tissue engineering using human mesenchymal stem cells: Effects of scaffold material and medium flow. *Ann Biomed Eng* 32, 2004,112.
28. Yeatts, A.B., Fisher, J.P. Bone tissue engineering bioreactors: Dynamic culture and the influence of shear stress. *Bone* 48, 2011,171.
29. Depprich, R., Handschel, J., Wiesmann, H.P., Jasche-Meyer, J., Meyer, U. Use of bioreactors in maxillofacial tissue engineering. *Br J Oral Maxillofac Surg* 46, 2008,349.
30. Vandenberg, H.H., Hatfaludy, S., Karlisch, P., Shansky, J. Mechanically Induced Alterations in Cultured Skeletal-Muscle Growth. *J Biomech* 24, 1991,91.
31. Buschmann, M.D., Gluzband, Y.A., Grodzinsky, A.J., Hunziker, E.B. Mechanical Compression Modulates Matrix Biosynthesis in Chondrocyte Agarose Culture. *J Cell Sci* 108, 1995,1497.
32. Eschenhagen, T., Fink, C., Remmers, U., Scholz, H., Wattchow, J., Weil, J., et al. Three-dimensional reconstitution of embryonic cardiomyocytes in a collagen matrix: a new heart muscle model system. *Faseb J* 11, 1997,683.
33. Carver, S.E., Heath, C.A. Semi-continuous perfusion system for delivering intermittent physiological pressure to regenerating cartilage. *Tissue Eng* 5, 1999,1.
34. Matthews, J.B., Mitchell, W., Stone, M.H., Fisher, J., Ingham, E. A novel three-dimensional tissue equivalent model to study the combined effects of cyclic mechanical strain and wear particles on the osteolytic potential of primary human macrophages in vitro. *Proc Inst Mech Eng Part H- J Eng Med* 215, 2001,479.
35. Du, D., Furukawa, K.S., Ushida, T. 3D culture of osteoblast-like cells by unidirectional or oscillatory flow for bone tissue engineering. *Biotechnol and Bioeng* 102, 2009,1670.
36. Freed, L.E., Vunjaknovakovic, G. Cultivation of Cell-Polymer Tissue Constructs in Simulated Microgravity. *Biotechnol and Bioeng* 46, 1995,306.
37. Vandenberg, H., DeTatto, M., Shansky, J., Lemaire, J., Chang, A., Payumo, F., et al. Tissue-engineered skeletal muscle organoids for reversible gene therapy. *Hum Gene Ther* 7, 1996,2195.
38. Kim, S.S., Utsunomiya, H., Koski, J.A., Wu, B.M., Cima, M.J., Sohn, J., et al. Survival and function of hepatocytes on a novel three-dimensional synthetic biodegradable polymer scaffold with an intrinsic network of channels. *Ann Surg* 228, 1998,8.

39. Bilodeau, K., Mantovani, D. Bioreactors for tissue engineering: Focus on mechanical constraints. A comparative review. *Tissue Eng* 12, 2006,2367.
40. Gomes, M.E., Sikavitsas, V.I., Behraves, E., Reis, R.L., Mikos, A.G. Effect of flow perfusion on the osteogenic differentiation of bone marrow stromal cells cultured on starch-based three-dimensional scaffolds. *J Biomed Mater Res Part A* 67A, 2003,87.
41. Gomes, M.E., Bossano, C.M., Johnston, C.M., Reis, R.L., Mikos, A.G. In vitro localization of bone growth factors in constructs of biodegradable scaffolds seeded with marrow stromal cells and cultured in a flow perfusion bioreactor. *Tissue Eng* 12, 2006,177.
42. Zhao, F., Chella, R., Ma, T. Effects of shear stress on 3-D human mesenchymal stem cell construct development in a perfusion bioreactor system: Experiments and hydrodynamic modeling. *Biotechnol and Bioeng* 96, 2007,584.
43. Sikavitsas, V.I., Bancroft, G.N., Lemoine, J.J., Liebschner, M.A.K., Dauner, M., Mikos, A.G. Flow perfusion enhances the calcified matrix deposition of marrow stromal cells in biodegradable nonwoven fiber mesh scaffolds. *Ann Biomed Eng* 33, 2005,63.
44. Grayson, W.L., Bhumiratana, S., Cannizzaro, C., Chao, P.H.G., Lennon, D.P., Caplan, A.I., et al. Effects of Initial Seeding Density and Fluid Perfusion Rate on Formation of Tissue-Engineered Bone. *Tissue Eng Part A* 14, 2008,1809.
45. Li, D.Q., Tang, T.T., Lu, J.X., Dai, K.R. Effects of Flow Shear Stress and Mass Transport on the Construction of a Large-Scale Tissue-Engineered Bone in a Perfusion Bioreactor. *Tissue Eng Part A* 15, 2009,2773.
46. Grayson, W.L., Frohlich, M., Yeager, K., Bhumiratana, S., Chan, M.E., Cannizzaro, C., et al. Engineering anatomically shaped human bone grafts. *Proc Natl Acad Sci U S A* 107, 2010,3299.
47. Yang, J.F., Cao, C., Wang, W., Tong, X.M., Shi, D.Y., Wu, F.B., et al. Proliferation and osteogenesis of immortalized bone marrow-derived mesenchymal stem cells in porous polylactic glycolic acid scaffolds under perfusion culture. *J Biomed Mater Res Part A* 92A, 2010,817.
48. Frohlich, M., Grayson, W.L., Marolt, D., Gimble, J.M., Kregar-Velikonja, N., Vunjak-Novakovic, G. Bone Grafts Engineered from Human Adipose-Derived Stem Cells in Perfusion Bioreactor Culture. *Tissue Eng Part A* 16, 2010,179.
49. Holtorf, H.L., Sheffield, T.L., Ambrose, C.G., Jansen, J.A., Mikos, A.G. Flow perfusion culture of marrow stromal cells seeded on porous biphasic calcium phosphate ceramics. *Ann Biomed Eng* 33, 2005,1238.
50. Hosseinkhani, H., Inatsugu, Y., Hiraoka, Y., Inoue, S., Tabata, Y. Perfusion culture enhances osteogenic differentiation of rat mesenchymal stem cells in collagen sponge reinforced with poly( glycolic acid) fiber. *Tissue Eng* 11, 2005,1476.

51. Janssen, F.W., Oostra, J., van Oorschot, A., van Blitterswijk, C.A. A perfusion bioreactor system capable of producing clinically relevant volumes of tissue-engineered bone: In vivo bone formation showing proof of concept. *Biomaterials* 27, 2006,315.
52. Yu, X.J., Botchwey, E.A., Levine, E.M., Pollack, S.R., Laurencin, C.T. Bioreactor-based bone tissue engineering: The influence of dynamic flow on osteoblast phenotypic expression and matrix mineralization. *Proc Natl Acad Sci U S A* 101, 2004,11203.
53. Zhao, F., Ma, T. Perfusion bioreactor system for human mesenchymal stem cell tissue engineering: Dynamic cell seeding and construct development. *Biotechnol and Bioeng* 91, 2005,482.
54. Sailon, A.M., Allori, A.C., Davidson, E.H., Reformat, D.D., Allen, R.J., Warren, S.M. A novel flow-perfusion bioreactor supports 3D dynamic cell culture. *J Biomed Biotechnol* 2009, 2009,873.
55. Rauh, J., Milan, F., Gunther, K.P., Stiehler, M. Bioreactor Systems for Bone Tissue Engineering. *Tissue Eng Part B Rev* 17, 2011,263.
56. Cartmell, S.H., Porter, B.D., Garcia, A.J., Guldberg, R.E. Effects of medium perfusion rate on cell-seeded three-dimensional bone constructs in vitro. *Tissue Eng* 9, 2003,1197.
57. Porter, B., Zael, R., Stockman, H., Guldberg, R., Fyhrie, D. 3-D computational modeling of media flow through scaffolds in a perfusion bioreactor. *J Biomech* 38, 2005,543.
58. Botchwey, E.A., Pollack, S.R., El-Amin, S., Levine, E.M., Tuan, R.S., Laurencin, C.T. Human osteoblast-like cells in three-dimensional culture with fluid flow. *Biorheology* 40, 2003,299.
59. Wang, Y.C., Uemura, T., Dong, R., Kojima, H., Tanaka, J., Tateishi, T. Application of perfusion culture system improves in vitro and in vivo osteogenesis of bone marrow-derived osteoblastic cells in porous ceramic materials. *Tissue Eng* 9, 2003,1205.
60. Batra, N.N., Li, Y.J., Yellowley, C.E., You, L.D., Malone, A.M., Kim, C.H., et al. Effects of short-term recovery periods on fluid-induced signaling in osteoblastic cells. *J Biomech* 38, 2005,1909.
61. van den Dolder, J., Bancroft, G.N., Sikavitsas, V.I., Spauwen, P.H.M., Jansen, J.A., Mikos, A.G. Flow perfusion culture of marrow stromal osteoblasts in titanium fiber mesh. *J Biomed Mater Res Part A* 64A, 2003,235.
62. Vance, J., Galley, S., Liu, D.F., Donahue, S.W. Mechanical stimulation of MC3T3 osteoblastic cells in a bone tissue-engineering bioreactor enhances prostaglandin E2 release. *Tissue Eng* 11, 2005,1832.

63. Bancroft, G.N., Sikavitsas, V.I., van den Dolder, J., Sheffield, T.L., Ambrose, C.G., Jansen, J.A., et al. Fluid flow increases mineralized matrix deposition in 3D perfusion culture of marrow stromal osteoblasts in a dose-dependent manner. *Proc Natl Acad Sci U S A* 99, 2002,12600.
64. Holtorf, H.L., Jansen, J.A., Mikos, A.G. Flow perfusion culture induces the osteoblastic differentiation of marrow stromal cell-scaffold constructs in the absence of dexamethasone. *J Biomed Mater Res Part A* 72A, 2005,326.
65. Alvarez-Barreto, J.F., Linehan, S.M., Shambaugh, R.L., Sikavitsas, V.I. Flow perfusion improves seeding of tissue engineering scaffolds with different architectures. *Ann Biomed Eng* 35, 2007,429.
66. Alvarez-Barreto, J.F., Landy, B., VanGordon, S., Place, L., DeAngelis, P.L., Sikavitsas, V.I. Enhanced osteoblastic differentiation of mesenchymal stem cells seeded in RGD-functionalized PLLA scaffolds and cultured in a flow perfusion bioreactor. *J Tissue Eng Regen Med* 5, 2011,464.
67. Bjerre, L., Bunger, C.E., Kassem, M., Mygind, T. Flow perfusion culture of human mesenchymal stem cells on silicate-substituted tricalcium phosphate scaffolds. *Biomaterials* 29, 2008,2616.
68. Braccini, A., Wendt, D., Jaquierey, C., Jakob, M., Heberer, M., Kenins, L., et al. Three-dimensional perfusion culture of human bone marrow cells and generation of osteoinductive grafts. *Stem Cells* 23, 2005,1066.
69. Ma, T., Yang, S.T., DA., K. Development of an in vitro human placenta model by the cultivation of human trophoblasts in a fiber-based bioreactor system. *Tissue Eng* 5, 1999, ,91.
70. Zhao, F., Pathi, P., Grayson, W., Xing, Q., Locke, B.R., Ma, T. Effects of oxygen transport on 3-D human mesenchymal stem cell metabolic activity in perfusion and static cultures: Experiments and mathematical model. *Biotechnol Prog* 21, 2005,1269.
71. Timmins, N.E., Scherberich, A., Fruh, J.A., Heberer, M., Martin, I., Jakob, M. Three-dimensional cell culture and tissue engineering in a T-CUP (Tissue Culture Under Perfusion). *Tissue Eng* 13, 2007,2021.
72. Costa, P.F., Martins, A., Neves, N.M., Gomes, M.E., Reis, R.L. A novel bioreactor design for enhanced stem cells proliferation and differentiation in tissue engineered constructs. *Tissue Eng Part A* 14, 2008,802.
73. Du, D.J., Furukawa, K., Ushida, T. Oscillatory perfusion seeding and culturing of osteoblast-like cells on porous beta-tricalcium phosphate scaffolds. *J Biomed Mater Res Part A* 86A, 2008,796.

74. Porter, B.D., Lin, A.S., Peister, A., Hutmacher, D., Guldberg, R.E. Noninvasive image analysis of 3D construct mineralization in a perfusion bioreactor. *Biomaterials* 28, 2007,2525.
75. Volkmer, E., Drosse, I., Otto, S., Stangelmayer, A., Stengele, M., Kallukalam, B.C., et al. Hypoxia in static and dynamic 3D culture systems for tissue engineering of bone. *Tissue Eng Part A* 14, 2008,1331.
76. Sailon, A.M., Allori, A.C., Davidson, E.H., Reformat, D.D., Allen, R.J., Warren, S.M. A Novel Flow-Perfusion Bioreactor Supports 3D Dynamic Cell Culture. *J Biomed Biotechnol*, 2009.
77. Kim, J., Ma, T. Perfusion regulation of hMSC microenvironment and osteogenic differentiation in 3D scaffold. *Biotechnol Bioeng* 109, 2012,252.
78. Hosseinkhani, H., Inatsugu, Y., Hiraoka, Y., Inoue, S., Shimokawa, H., Tabata, Y. Impregnation of plasmid DNA into three-dimensional scaffolds and medium perfusion enhance in vitro DNA expression of mesenchymal stem cells. *Tissue Eng* 11, 2005,1459.
79. Hosseinkhani, H., Hosseinkhani, M., Tian, F., Kobayashi, H., Tabata, Y. Ectopic bone formation in collagen sponge self-assembled peptide-amphiphile nanofibers hybrid scaffold in a perfusion culture bioreactor. *Biomaterials* 27, 2006,5089.
80. Xie, Y.Z., Hardouin, P., Zhu, Z.N., Tang, T.T., Dai, K.R., Lu, J.X. Three-dimensional flow perfusion culture system for stem cell proliferation inside the critical-size beta-tricalcium phosphate scaffold. *Tissue Eng* 12, 2006,3535.
81. Janssen, F.W., van Dijkhuizen-Radersma, R., Van Oorschot, A., Oostra, J., de Bruijn, J.D., Van Blitterswijk, C.A. Human tissue-engineered bone produced in clinically relevant amounts using a semi-automated perfusion bioreactor system: a preliminary study. *J Tissue Eng Regen Med* 4, 2010,12.
82. Janssen, F.W., Hofland, I., van Oorschot, A., Oostra, J., Peters, H., van Blitterswijk, C.A. Online measurement of oxygen consumption by goat bone marrow stromal cells in a combined cell-seeding and proliferation perfusion bioreactor. *J Biomed Mater Res Part A* 79A, 2006,338.
83. Jaasma, M.J., Plunkett, N.A., O'Brien, F.J. Design and validation of a dynamic flow perfusion bioreactor for use with compliant tissue engineering scaffolds. *J Biotechnol* 133, 2008,490.
84. Keogh, M.B., Partap, S., Daly, J.S., O'Brien, F.J. Three hours of perfusion culture prior to 28 days of static culture, enhances osteogenesis by human cells in a collagen GAG scaffold. *Biotechnol and Bioeng* 108, 2011,1203.

85. Barthold, M., Majore, I., Fargali, S., Stahl, F., Schulz, R., Lose, S., et al. 3D-cultivation and characterisation of osteogenic cells for the production of highly viable bone tissue implants. In: Godia F FMe, ed. *Animal Cell Technology Meets Genomics*, Springer, . Dordrecht, Netherlands 2005. pp. 199.
86. Schliephake, H., Zghoul, N., Jager, V., van Griensven, M., Zeichen, J., Gelinsky, M., et al. Bone formation in trabecular bone cell seeded scaffolds used for reconstruction of the rat mandible. *Int J Oral Maxillofac Surg* 38, 2009,166.
87. Yeatts, A.B., Fisher, J.P. Tubular Perfusion System for the Long-Term Dynamic Culture of Human Mesenchymal Stem Cells. *Tissue Eng Part C Methods* 17, 2011,337.
88. Bertrand, D., Dominique, B.R., Karim, O., Mickael, D., Véronique, V., Morad, B., et al. A Perfusion Bioreactor for Engineering Bone Constructs: An In Vitro and In Vivo Study. *Tissue Eng Part C Methods* 17, 2011,505.
89. Gardel, L.S., Dias, A., Link, D.P., Serra, L.A., Gomes, M.E., Reis, R.L. Development of an novel bidirectional continuous perfusion bioreactor (BCPB) for culturing cells in 3D scaffolds. *Histology and Histopathology Cellular and Molecular Biology* 26, 2011,70.
90. Gardel, L., Dias, A., Link, D.P., Serra, L.A., Gomes, M.E., Reis, R.L. Development of a novel bidirectional continuous perfusion bioreactor (BCPB) for culturing cells in 3D scaffolds. Abstract presented at the Tissue Engineering & Regenerative Medicine International Society EU Annual Meeting, Granada, ES, 2011 Abstract no. 7.09.
91. Liebschner, M.A.K. Biomechanical considerations of animal models used in tissue engineering of bone. *Biomaterials* 25, 2004,1697.
92. Egermann, M., Goldhahn, J., Schneider, E. Animal models for fracture treatment in osteoporosis. *Osteoporos* 16, 2005,S129.
93. Davidson, M.K., Lindsey, J.R., Davis, J.K. Requirements and selection of an animal model. *Isr J Med Sci* 23, 1987,551.
94. Hazzard, D.G., Bronson, R.T., Mcclearn, G.E., Strong, R. Selection of an Appropriate Animal-Model to Study Aging Processes with Special Emphasis on the Use of Rat Strains. *J Gerontology* 47, 1992,B63.
95. Tseng, S.S., Lee, M.A., Reddi, H. Nonunions and the potential of stem cells in fracture-healing. *J Bone Joint Surg Am* 90A, 2008,92.
96. Reichert, J.C., Saifzadeh, S., Wullschleger, M.E., Epari, D.R., Schutz, M.A., Duda, G.N., et al. The challenge of establishing preclinical models for segmental bone defect research. *Biomaterials* 30, 2009,2149.
97. Reinwald, S., Burr, D. Review of nonprimate, large animal models for osteoporosis research. *J Bone Miner Res* 23, 2008,1353.



98. Muschler, G.F., Raut, V.P., Patterson, T.E., Wenke, J.C., Hollinger, J.O. The Design and Use of Animal Models for Translational Research in Bone Tissue Engineering and Regenerative Medicine. *Tissue Eng Part B Rev* 16, 2010,123.
99. Aerssens, J., Boonen, S., Lowet, G., Dequeker, J. Interspecies differences in bone composition, density, and quality: Potential implications for in vivo bone research. *Endocrinology* 139, 1998,663.
100. Thorwarth, M., Schultze-Mosgau, S., Kessler, P., Wiltfang, J., Schlegel, K.A. Bone regeneration in osseous defects using a resorbable nanoparticulate hydroxyapatite. *J Oral Maxillofac Surg* 63, 2005,1626.
101. O'Loughlin, P.F., Morr, S., Bogunovic, L., Kim, A.D., Park, B., Lane, J.M. Selection and development of preclinical models in fracture-healing research. *J Bone Joint Surg American Volume* 90A, 2008,79.
102. Stevenson, S., Hohn, R.B., Templeton, J.W. Effects of Tissue Antigen Matching on the Healing of Fresh Cancellous Bone Allografts in Dogs. *Am J Vet Res* 44, 1983,201.
103. Stevenson, S. The Immune-Response to Osteochondral Allografts in Dogs. *J Bone Joint Surg Am* 69A, 1987,573.
104. Welter, J.F., Shaffer, J.W., Stevenson, S., Davy, D.T., Field, G.A., Klein, L., et al. Cyclosporin A and tissue antigen matching in bone transplantation. Fibular allografts studied in the dog. *Acta Orthop Scand* 61, 1990,517.
105. Stevenson, S., Xiao, Q.L., Martin, B. The Fate of Cancellous and Cortical Bone after Transplantation of Fresh and Frozen Tissue-Antigen-Matched and Mismatched Osteochondral Allografts in Dogs. *J Bone Joint Surg Am* 73A, 1991,1143.
106. Bensusan, J.S., Davy, D.T., Goldberg, V.M., Shaffer, J.W., Stevenson, S., Klein, L., et al. The effects of vascularity and cyclosporin A on the mechanical properties of canine fibular autografts. *J Biomech* 25, 1992,415.
107. Stevenson, S., Shaffer, J.W., Goldberg, V.M. The humoral response to vascular and nonvascular allografts of bone. *Clin Orthop Relat Res*, 1996,86.
108. Zaucha, J.M., Zellmer, E., Georges, G., Little, M.T., Storb, R., Storer, B., et al. G-CSF-mobilized peripheral blood mononuclear cells added to marrow facilitates engraftment in nonmyeloablated canine recipients: CD3 cells are required. *Biol Blood Marrow Transplant* 7, 2001,613.
109. Newman, E., Turner, A.S., Wark, J.D. The Potential of Sheep for the Study of Osteopenia - Current Status and Comparison with Other Animal-Models. *Bone* 16, 1995,S277.
110. Taylor, W.R., Ehrig, R.M., Duda, G.N., Schell, H., Seebeck, P., Heller, M.O. On the influence of soft tissue coverage in the determination of bone kinematics using skin markers. *J Orthop Res* 23, 2005,726.

111. Taylor, W.R., Ehrig, R.M., Heller, M.O., Schell, H., Seebeck, P., Duda, G.N. Tibio-femoral joint contact forces in sheep. *J Biomech* 39, 2006,791.
112. Ravaglioli, A., Krajewski, A., Celotti, G.C., Piancastelli, A., Bacchini, B., Montanari, L., et al. Mineral evolution of bone. *Biomaterials* 17, 1996,617.
113. Anderson, M.L.C., Dhert, W.J.A., de Bruijn, J.D., Dalmeijer, R.A.J., Leenders, H., van Blitterswijk, C.A., et al. Critical size defect in the goat's os ilium - A model to evaluate bone grafts and substitutes. *Clin Orthop Relat Res*, 1999,231.
114. den Boer, F.C., Patka, P., Bakker, F.C., Wippermann, B.W., van Lingen, A., Vink, G.Q.M., et al. New segmental long bone defect model in sheep: Quantitative analysis of healing with dual energy X-ray absorptiometry. *J Orthop Res* 17, 1999,654.
115. Turner, A.S. Experiences with sheep surgery: Strengths and as an animal model for shoulder shortcomings. *J Shoulder and Elbow Surg* 16, 2007,158s.
116. Martini, L., Fini, M., Giavaresi, G., Giardino, R. Sheep model in orthopedic research: A literature review. *Comp Med* 51, 2001,292.
117. Hillier, M.L., Bell, L.S. Differentiating human bone from animal bone: A review of histological methods. *J Forensic Sci* 52, 2007,249.
118. Leung, K.S., Siu, W.S., Cheung, N.M., Lui, P.Y., Chow, D.H.K., James, A., et al. Goats as an osteopenic animal model. *J Bone Miner Res* 16, 2001,2348.
119. Qin, L., Mak, A.T.F., Cheng, C.W., Hung, L.K., Chan, K.M. Histomorphological study on pattern of fluid movement in cortical bone in goats. *Anat Rec* 255, 1999,380.
120. Spaargaren, D.H. Metabolic-Rate and Body-Size - a New View on the Surface Law for Basic Metabolic-Rate. *Acta Biotheor* 42, 1994,263.
121. Rimondini, L., Nicoli-Aldini, N., Fini, M., Guzzardella, G., Tschon, M., Giardino, R. In vivo experimental study on bone regeneration in critical bone defects using an injectable biodegradable PLA/PGA copolymer. *Oral Surg Oral Med Oral Pathol Oral Radiol Endod* 99, 2005,148.
122. Cacchioli, A., Spaggiari, B., Ravanetti, F., Martini, F.M., Borghetti, P., Gabbi, C. The critical sized bone defect: morphological study of bone healing. *Ann Fac Medic Vet di Parma* 26, 2006,97.
123. Gugala, Z., Gogolewski, S. Regeneration of segmental diaphyseal defects in sheep tibiae using resorbable polymeric membranes: A preliminary study. *J OrthopTrauma* 13, 1999,187.
124. Lindsey, R.W., Gugala, Z., Milne, E., Sun, M., Gannon, F.H., Latta, L.L. The efficacy of cylindrical titanium mesh cage for the reconstruction of a critical-size canine segmental femoral diaphyseal defect. *J Orthop Res* 24, 2006,1438.
125. Gugala, Z., Lindsey, R.W., Gogolewski, S. New approaches in the treatment of critical-size segmental defects in long bones. *Macromol Symp* 253, 2007,147.

126. Kuttenger, J.J., Stubinger, S., Waibel, A., Werner, M., Klasing, M., Ivanenko, M., et al. Computer-guided CO<sub>2</sub>-laser osteotomy of the sheep tibia: Technical prerequisites and first results. *Photomed Laser Surg* 26, 2008,129.
127. Kuttenger, J.J., Waibel, A., Stubinger, S., Werner, M., Klasing, M., Ivanenko, M., et al. Bone healing of the sheep tibia shaft after carbon dioxide laser osteotomy: histological results. *Lasers in Med Sci* 25, 2010,239.
128. Blokhuis, T.J., Wippermann, B.W., den Boer, F.C., van Lingen, A., Patka, P., Bakker, F.C., et al. Resorbable calcium phosphate particles as a carrier material for bone marrow in an ovine segmental defect. *J Biomed Mater Res* 51, 2000,369.
129. Sciadini, M.F., Johnson, K.D. Evaluation of recombinant human bone morphogenetic protein-2 as a bone-graft substitute in a canine segmental defect model. *J Orthop Res* 18, 2000,289.
130. Cook, S.D., Salkeld, S.L., Patron, L.P., Sargent, M.C., Rueger, D.C. Healing course of primate ulna segmental defects treated with osteogenic protein-1. *J Invest Surg* 15, 2002,69.
131. den Boer, F.C., Wippermann, B.W., Blokhuis, T.J., Patka, P., Bakker, F.C., Haarman, H.J.T.M. Healing of segmental bone defects with granular porous hydroxyapatite augmented with recombinant human osteogenic protein-1 or autologous bone marrow. *J Orthop Res* 21, 2003,521.
132. Arinzeh, T.L., Peter, S.J., Archambault, M.P., van den Bos, C., Gordon, S., Kraus, K., et al. Allogeneic mesenchymal stem cells regenerate bone in a critical-sized canine segmental defect. *J Bone Joint Surg Am* 85A, 2003,1927.
133. Brodke, D., Pedrozo, H.A., Kapur, T.A., Attawia, M., Kraus, K.H., Holy, C.E., et al. Bone grafts prepared with selective cell retention technology heal canine segmental defects as effectively as autograft. *J Orthop Res* 24, 2006,857.
134. Niemeyer, P., Schonberger, T.S., Hahn, J., Kasten, P., Fellenberg, J., Suedkamp, N., et al. Xenogenic Transplantation of Human Mesenchymal Stem Cells in a Critical Size Defect of the Sheep Tibia for Bone Regeneration. *Tissue Eng Part A* 16, 2010,33.
135. Bullens, P.H.J., Hannink, G., Verdonschot, N., Buma, P. No effect of dynamic loading on bone graft healing in femoral segmental defect reconstructions in the goat. *Injury* 41, 2010,1284.
136. Zhu, L., Chuanchang, D., Wei, L.Y., C. , Jiasheng, D., Lian, Z. Enhanced Healing of Goat Femur-Defect Using BMP7 Gene-Modified BMSCs and Load-Bearing Tissue-Engineered Bone. *J Orthop Res* 28, 2010,412.
137. Viateau, V., Guillemin, G., Bousson, V., Oudina, K., Hannouche, D., Sedel, L., et al. Long-bone critical-size defects treated with tissue-engineered grafts: A study on sheep. *J Orthop Res* 25, 2007,741.

138. Nair, M.B., Varma, H.K., Menon, K.V., Shenoy, S.J., John, A. Reconstruction of goat femur segmental defects using triphasic ceramic-coated hydroxyapatite in combination with autologous cells and platelet-rich plasma. *Acta Biomater* 5, 2009,1742.
139. Murakami, N., Saito, N., Horiuchi, H., Okada, T., Nozaki, K., Takaoka, K. Repair of segmental defects in rabbit humeri with titanium fiber mesh cylinders containing recombinant human bone morphogenetic protein-2 (rhBMP-2) and a synthetic polymer. *J Biomed Mater Res* 62, 2002,169.
140. Vogelin, E., Jones, N.F., Huang, J.I., Brekke, J.H., Lieberman, J.R. Healing of a critical-sized defect in the rat femur with use of a vascularized periosteal flap, a biodegradable matrix, and bone morphogenetic protein. *J Bone Joint Surg Am* 87A, 2005,1323.
141. Cheng, M.H., Brey, E.M., Allori, A., Satterfield, W.C., Chang, D.W., Patrick, C.W., et al. Ovine model for engineering bone segments. *Tissue Eng* 11, 2005,214.
142. Forriol, F., Denaro, L., Longo, U.G., Taira, H., Maffulli, N., Denaro, V. Bone lengthening osteogenesis, a combination of intramembranous and endochondral ossification: an experimental study in sheep. *Strategies Trauma Limb Reconstr* 5, 2010,71.
143. Horner, E.A., Kirkham, J., Wood, D., Curran, S., Smith, M., Thomson, B., et al. Long Bone Defect Models for Tissue Engineering Applications: Criteria for Choice. *Tissue Eng Part B Rev* 16, 2010,263.
144. Einhorn, T.A. Clinically applied models of bone regeneration in tissue engineering research. *Clin Orthop Relat Res*, 1999,S59.
145. Hansen, M., Mehler, D., Hessmann, M.H., Blum, J., Rommens, P.M. Intramedullary stabilization of extraarticular proximal tibial fractures: A biomechanical comparison of intramedullary and extramedullary implants including a new Proximal Tibia Nail (PTN). *J Orthop Trauma* 21, 2007,701.
146. Krettek, C., Schandelmaier, P., Miclau, T., Tscherne, H. Minimally invasive percutaneous plate osteosynthesis (MIPPO) using the DCS in proximal and distal femoral fractures. *Injury* 28, 1997,Sa20.
147. Gao, T.J., Lindholm, T.S., Kommonen, B., Ragni, P., Paronzini, A., Lindholm, T.C., et al. The use of a coral composite implant containing bone morphogenetic protein to repair a segmental tibial defect in sheep. *Int Orthop* 21, 1997,194.
148. Kirker-Head, C.A., Gerhart, T.N., Armstrong, R., Schelling, S.H., Carmel, L.A. Healing bone using recombinant human bone morphogenetic protein 2 and copolymer. *Clin Orthop Relat Res*, 1998,205.

149. Wefer, J., Wefer, A., Schrott, H.E., Thermann, H., Wippermann, B.W. Healing of autologous cancellous bone transplants and hydroxylapatite ceramics in tibial segment defects. Value of ultrasonic follow up. *Unfall chirurg* 103, 2000,452.
150. Meinel, L., Zoidis, E., Zapf, J., Hassa, P., Hottiger, M.O., Auer, J.A., et al. Localized insulin-like growth factor I delivery to enhance new bone formation. *Bone* 33, 2003,660.
151. Mastrogiacomo, M., Corsi, A., Francioso, E., Di Comite, M., Monetti, F., Scaglione, S., et al. Reconstruction of extensive long bone defects in sheep using resorbable bioceramics based on silicon stabilized tricalcium phosphate. *Tissue Eng* 12, 2006,1261.
152. Teixeira, C.R., Rahal, S.C., Volpi, R.S., Taga, R., Cestari, I.M., Granieiro, J.M., et al. Tibial segmental bone defect treated with bone plate and cage filled with either xenogeneic composite or autologous cortical bone graft. *Vet Comp Orthop Traumatol* 20, 2007,269.
153. Klaue, K., Knothe, U., Anton, C., Pfluger, D.H., Stoddart, M., Masquelet, A.C., et al. Bone regeneration in long-bone defects: tissue compartmentalisation? In vivo study on bone defects in sheep. *Injury* 40, 2009,S95.
154. Bella, C.A., N.N. Lucarelli, E. Dozza, B. Frisoni, T. Martini, L. Fini, M. Donati, D. . Osteogenic Protein-1 Associated with Mesenchymal Stem Cells Promote Bone Allograft Integration. *Tissue Eng Part A* 16, 2010,2967.
155. Bloemers, F.W., Blokhuis, T.J., Patka, P., Bakker, F.C., Wippermann, B.W., Haarman, H.J.T.M. Autologous bone versus calcium-phosphate ceramics in treatment of experimental bone defects. *J Biomed Mater Res Part B* 66B, 2003,526.
156. Sarkar, M.R., Augat, P., Shefelbine, S.J., Schorlemmer, S., Huber-Lang, M., Claes, L., et al. Bone formation in a long bone defect model using a platelet-rich plasma-loaded collagen scaffold. *Biomaterials* 27, 2006,1817.
157. Schneiders, W., Reinstorf, A., Biewener, A., Serra, A., Grass, R., Kinscher, M., et al. In Vivo Effects of Modification of Hydroxyapatite/Collagen Composites with and without Chondroitin Sulphate on Bone Remodeling in the Sheep Tibia. *J Orthop Res* 27, 2009,15.
158. van Loon, C.J., Buma, P., de Waal Malefijt, M.C., van Kampen, A., Veth, R.P. Morselized bone allografting in revision total knee replacement--a case report with a 4-year histological follow-up. *Acta Orthop Scand* 71, 2000,98.
159. Wang, J.S., Tagil, M., Aspenberg, P. Load-bearing increases new bone formation in impacted and morselized allografts. *Clin Orthop Relat Res*, 2000,274.
160. van der Donk, S., Buma, P., Verdonschot, N., Schreurs, B.W. Effect of load on the early incorporation of impacted morsellized allografts. *Biomaterials* 23, 2002,297.

161. Field, J.R., Mcgee, M., Stanley, R., Ruthenbeck, G., Papadimitrakis, T., Zannettino, A., et al. The efficacy of allogeneic mesenchymal precursor cells for the repair of an ovine tibial segmental defect. *Vet Comp Orthop Traumatol* 24, 2011,113.
162. Gugala, Z., Gogolewski, S. Healing of critical-size segmental bone defects in the sheep tibiae using bioresorbable polylactide membranes. *Injury* 33, 2002,71.
163. Maissen, O., Eckhardt, C., Gogolewski, S., Glatt, M., Arvinte, T., Steiner, A., et al. Mechanical and radiological assessment of the influence of rhTGF beta-3 on bone regeneration in a segmental defect in the ovine tibia: Pilot study. *J Orthop Res* 24, 2006,1670.
164. Liu, G., Zhao, L., Zhang, W., Cui, L., Liu, W., Cao, Y. Repair of goat tibial defects with bone marrow stromal cells and beta-tricalcium phosphate. *J Mater Sci Mater Med* 19, 2008,2367.

## **SECTION 2**

### **Chapter III MATERIALS & METHODS**

## **Materials and Methods**

The main aim of this chapter is to provide a general overview of the methodologies, materials, cells and animal models used in the experiments performed. Although, these are described in each of the chapters that follow in this thesis herein are provided further details. The layout of the present section is expected to provide a more comprehensive overview of the work performed.

### **3.1 Development of a new flow perfusion culture system**

Under the scope of this PhD thesis a new flow perfusion culture system, Bi-Directional Continuous Perfusion Bioreactor (BCPB), was designed, developed and optimized. This gave origin to an International patent application (1).

#### **3.1.1 Design philosophy**

The main objective was to develop a perfusion system that was capable of supporting the culturing of constructs of large dimensions promoting cell viability in the interior of scaffolds and simultaneously direct cellular activity through application of mechanical stimuli. For the development of this device several parameters were considered, such as: (I) easy handling/assembling in a flow chamber and easy fitting in a standard incubator), (II) easy sterilization of parts and maintenance of sterile condition throughout the culture period, (III) constituent parts washable and non toxic, (IV) transparent culturing chamber to allow easy visualization of the culture inside the incubator, (V) design preventing possible losses of pressure gradient, which would result in the flow reduction in the contact area of scaffolds with constituents parts inside the bioreactor, (VI) a flow rate that can be tightly controlled by a peristaltic pump, (VII) the flow system that allow the gases exchange without allowing the passage of possible contaminants to the interior of the system.

#### **3.1.2 Materials used in constituents parts**

The main parts of the BCPB are fabricated either from Plexiglass (Acrylic) or Polytetrafluoroethylene (PTFE). Plexiglass is the material used in the fabrication of the culture chamber of the BCPB. This material can be sterilized with ethylene oxide gas, formaldehyde or plasma and offers the advantage of being relatively transparent, allowing the visualization of the scaffold and the culture environment inside the bioreactor culture chamber.



In addition to this, it is readily machined to allow the fabrication of the unit and widely available in the market. The constituent parts that close the culture chamber as well as the parts that support the polycarbonate or the stainless steel 316L tube inside of bioreactor are made of PTFE which possess an excellent dimensional stability, even at high temperatures (up to 260°C or 300°C for short periods) making it suitable for sterilization by autoclaving, ethylene oxide gas, formaldehyde or plasma. PTFE possesses good mechanical properties and shows an excellent UV . Both Plexiglass and PTFE are biologically inert. For all these reasons, Plexiglass and PTFE are suitable materials for the production of cell culture devices.

Polycarbonate or Stainless steel 316L was used for the fabrication of the perforated coaxial tube that supports the scaffold. This material possesses high mechanical properties, is biologically inert, easily sterilized by autoclaving, ethylene oxide gas or formaldehyde, available in the market and easily machined.

### 3.1.3 Design description

The main difference between the BCPB and the bioreactors currently commercialized is the fact that the BCPB offers the possibility to control the flow rate and the pressure gradient inside and outside the large dimension scaffolds. This main advantage is directly related to the possibility of controlling the medium flow passage in the perforated tube to the inside of the scaffold and from there to the culture chamber and/or the passage of the medium circulating in the culture chamber to the inside of the scaffold, and from there to the perforated tube.

This innovative system (Figure 3.1) is composed by a cell culture chamber (Figure 3.2-1) with a cylindrical shape, made from acrylic (transparent) with four exits/entrance channels (Figure 3.2-1A) (Figure 3.2-1B) (Figure 3.2-1C) (Figure 3.2-1D) that can be used to connect three way valves, that will be connected to the silicone tubes. The tubing used to connect each component in the circuit is platinum-cured silicone tubing (Masterflex® tubing; Cole Parmer®). The platinum curing minimizes the amount of leachable chemicals, and has a relatively low-protein binding. These silicone tubing have a highly gas permeability to both carbon dioxide and oxygen, this way allowing proper gas exchange for oxygen delivery and maintenance of proper culture medium pH. These four exits/entrance channels may be used for: i) acoplacion of sensors for measurement of O<sub>2</sub>, CO<sub>2</sub>, Ph, temperature, etc.; ii) acoplacion of manometers to measure the pressure gradients; iii) harvesting of samples or inoculation of cells, or other substances, such as antibiotics growth factors etc.

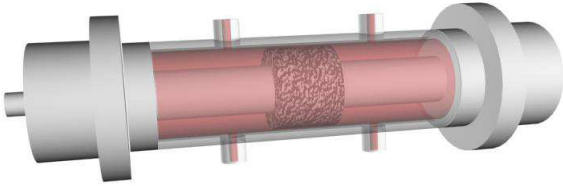


Figure 3.1: Design of the cellular culture chamber with the scaffold and culture medium.

In each of the two free extremities of the cell culture chamber, two lids (Figure 3.2-2) made of PTFE will be encased, being one of the lids composed of four distinct parts and the other one composed of five distinct parts. The part of the lid that is in direct contact with the cell culture chamber (Figure 3.2-2A) is responsible for preventing drainage of the culture medium, through the use of two O-rings; The second part (Figure 3.2-2B) works as a backstop of the part (Figure 3.2-2A) and presents an hexagonal form that is levelled with the part of the other lid, allowing the horizontal positioning of the bioreactor, when placed in a plain surface; The part that contains the rolling systems and the retainers (Figure 3.2-2C) has a cylindrical shape. In one of the lids, this part contains a gear-wheel (Figure 3.2-2D). Both lids contain in its interior a compartment comprising the rolling system (stainless steel) (Figure 3.2-3) and the silica retainer (Figure 3.2-4) that prevents medium drainage, allowing the coaxial perforated tube a rotational movement of 360 degrees (Figure 3.2-5). The part of the support system of the cell culture chamber (Figure 3.2-2E) has a cylindrical shape, and is connected by the support arm (Figure 3.2-13) that connects the cell culture chamber (through part Figure 3.2-2E) to the support base (Figure 3.2-14), that will keep the system suspended when its functioning, also having the function of allowing the 180-180 movement degrees, to which the cell culture chamber will be submitted. To allow the connection and fixation of the coaxial perforated tube to the main tubes (that provide the connection to the exterior tubes of the system) two parts (tubes) (Figure 3.2-6) (Figure 3.2-7) made of polycarbonate or stainless steel, are used. These tubes run through all the length of the system, including the support cell culture chamber, until reaching its exterior limit (Figure 3.2-11).

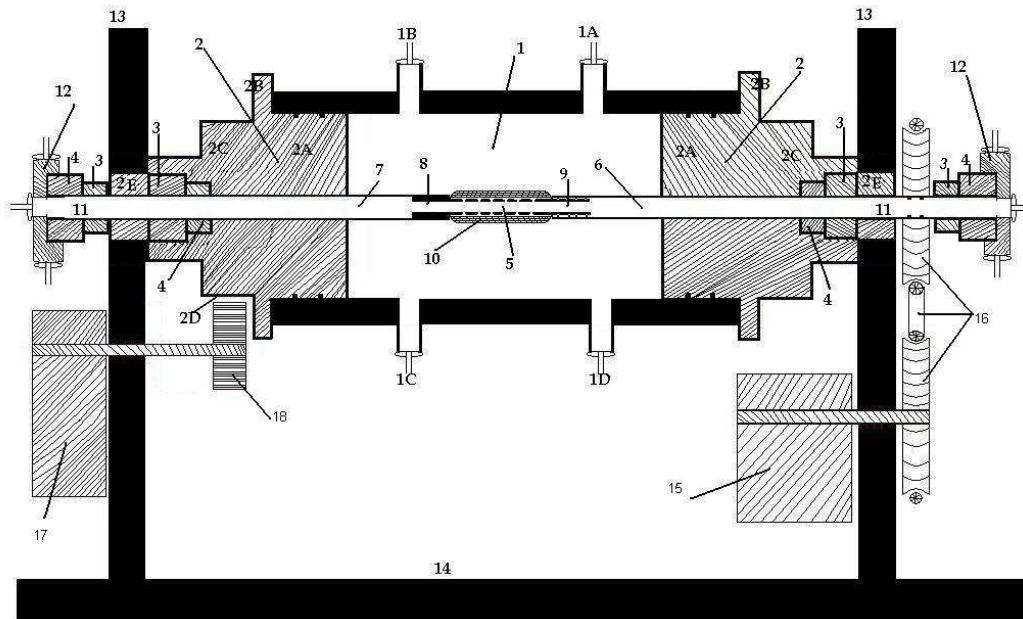


Figure 3.2: Overview of the design of the BCPB.

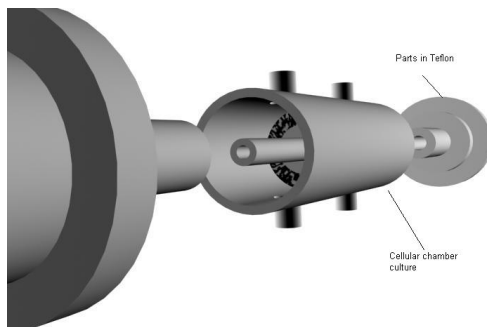


Figure 3.3: Two parts of extremities of the cellular chamber culture.

However, each lid has a different mechanism of connection to the perforated coaxial tube, being one of the connections carried through by screws (Figure 3.2-9 and Figure 3.3), and the other using a sliding fitting mechanism (Figure 3.2 -8 and Figure 3.3). Therefore, one of the ends of the coaxial perforated tube (Figure 3.2-5) has a screw, while the other has a mechanism of connection by sliding. The length and the number of orifices of the perforated tube is variable and will be determined by the size of the three-dimensional support (Figure 3.2-10; Figure 3.4 and Figure 3.5) that is intended to be used. This also determines the length to be slid for the coaxial tube in the interior of the part of connection to the system of bearing to establish a perfect tight-shut.

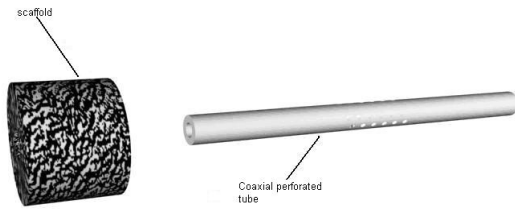


Figure 3.4: Coaxial perforated tube in polycarbonate or stainless steel and scaffold.

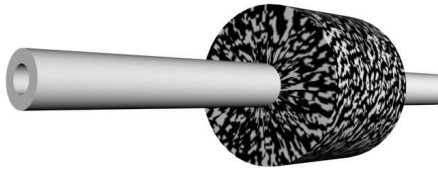


Figure 3.5: Scaffold size of the same size of the perforations in the tube.

The polycarbonate or stainless steel tubes that connect the perforated tube to the exterior (Figure 3.2-11), is linked to the continuous circular medium flow system through a three-way valve (Figure 3.2-12) in both sides of the cell culture chamber. However, the rotational movements of these tubes must be neutralized through the use of another rolling system (Figure 3.2-3) (Figure 3.2-4), in order to prevent the rolling up of all the tubes connected to them. Two engines are connected to the BCPB: the first one, engine 1 (Figure 3.2-17) is responsible for the rotational movement of 360 degrees, operating at a maximum speed of 52 rpm (coaxial perforated tube). This motor force is transmitted to the perforated tube through a pulley system (Figure 3.2-16). The second engine, engine 2 (Figure 3.2-17) is responsible for the rotational movement of 180-180 and 360 degrees, operating at a maximum of 52rpm (cell culture chamber); the force of this motor is transmitted to the Cell culture chamber through a gear-wheel system (Figure 3.2-18). For the functioning of the BCPB, a circular flow system was specifically designed. It is composed of a peristaltic pump (Figure 3.6-20), responsible for the positive flow gradient in the cellular culture chamber and the perforated coaxial tube, the pump driving the flow is a six-channel peristaltic pump (Cole Parmer®).

This pump gives accurate and consistent flow rates ranging from 0.1 to 10 mL/min with the tubing size used in our system (Cole Parmer® L/S 16), so it is possible with a single pump capable of pumping six different and independent bioreactors, with same flow per minute; b) a vacuum pump (Figure 3.6-21), that is responsible for the negative flow gradient in the cellular culture chamber and the perforated coaxial tube, a medium reservoir bottle of the peristaltic pump (Figure 3.6-22), a medium reservoir bottle of the vacuum pump (Figure 3.6-23), and a culture medium bottle collector (Figure 3.6-24). A three way valve will be located between the bottle collector and the reservoir bottle of the peristaltic pump, which will have to direct the flow of the bottle collector directly to the peristaltic pump, thus allowing the exchange of a new medium of culture for old medium of culture in the bottle reservoir of the peristaltic pump. Without this it would be necessary to stop all the flow system.

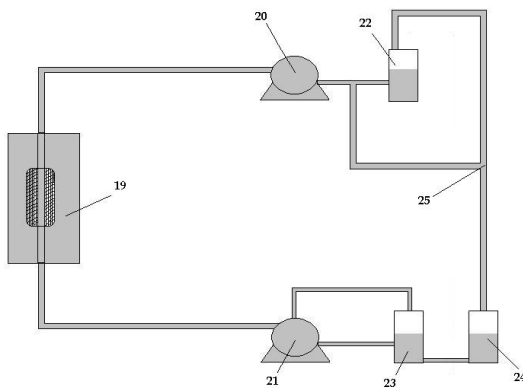


Figure 3.6: Overview of the BCPB circular flow system.

## 3.2 Scaffolds

### 3.2.1 Starch-poly ( $\epsilon$ -caprolactone)(SPCL) fiber-meshs scaffolds

SPCL fiber-mesh scaffolds were produced from a polymeric blend (30/70 wt %) of corn starch with the synthetic polymer PCL. Starch is one of the most abundant naturally occurring polymers that present excellent characteristics for application in the biomaterials field, such as low toxicity, biodegradability and biocompatibility (Martins et al, 2008). PCL, is a versatile, biocompatible and on another hand is a approved biodegradable polyester that has been used in the production of devices approved by the Food and Drug Administration (FDA)(2).

The combination of these two polymers in a blend confers increased biodegradability to PCL and improves the processability and mechanical properties of starch (3).

SPCL is a biodegradable polymer susceptible to be degraded by hydrolysis mainly catalysed by the enzymes lipase and  $\alpha$ -amylase (4, 5). Degradation studies of SPCL fibre-mesh scaffolds have been performed in solutions containing these hydrolytic enzymes in physiological concentrations (6). The results have shown that after 12 weeks of immersion the scaffolds were completely degraded. Furthermore, the products resultants from degradation are non toxic and are either metabolized via the tricarboxylic acid cycle or eliminated by direct renal secretion (4, 7) .

SPCL fibers are processed by melt spinning. An extruder equipped with a 12mm diameter screw is used with a 0.5 mm monofilament die. Die temperature are the 150°C and the screw speed 1 rpm. Extrusion is performed in the ambient environment. Hot fiber are driven into a cooling bath (water 13°C) and cold-drawn after the bath, using a caterpillar with a speed of 21 m/min and a winding unit with a speed of 28 m/min. Fibers are produced in the range 120–500  $\mu$ m diameter(6).

SPCL fiber meshes were prepared by a fiber bonding process consisting of cutting and sintering the fibers previously obtained by the above-described melt spinning method. Briefly, a selected amount of fibers will be placed in a glass mould and heated in an oven at 150°C/ 5 min. Immediately after removing the moulds from the oven, the fibers will be slightly compressed by a teflon cylinder (which runs within the mould) and then cooled at -20°C/ 5min.

The advantage of fibre-mesh design is the large surface area for cell attachment which also enables rapid diffusion of nutrients enhancing cell survival and growth (6). Another great advantage of SPCL fibre-mesh scaffold architecture and specially pore interconnectivity is its application in tissue-engineering strategies that involve the use of bioreactor cultures. Studies performed by Gomes et al, with a flow perfusion bioreactor, showed that SPCL fibre-mesh scaffold provided an appropriate matrix for the proliferation and osteogenic differentiation of rat bone marrow cells(8, 9). Furthermore, the fibre- mesh structure allowed a homogenous distribution of the cells and throughout deposition of mineralized matrix (9) when cultured under flow perfusion conditions.

A complementary study demonstrated the influence of porosity of these scaffolds in a flow perfusion bioreactor and concluded that the best outcome was obtained with SPCL fibre-mesh scaffolds with a porosity of 75%, rather than 50 % (8).

SPCL fiber mesh scaffolds, aiming at bone TE applications, have demonstrated great potential in this field (10-14).

### **3.3 Harvesting, isolation and culture of bone marrow mesenchymal stromal cells**

Mesenchymal stem cells (MSC) are an interesting candidate for cell-based therapeutics and regenerative medicine (15, 16). While several tissues remain an important source of therapeutic relevant differentiated cells, stem cells have emerged as a strong alternative due to their potential of expansion- self-renewal potential-and the fact that they can be obtained from autologous sources. Additionally, MSCs can be differentiated into a variety of connective tissues, including bone, cartilage, fat, muscle and tendon, when cultured with appropriated supplemented culture media and specific environments (17, 18).

In the studies described in this thesis we have used MSCs from rat and goat bone marrow. The experimental protocols to obtain the bone marrow aspirate were performed according to the guidelines and after approval by the National Ethical Committee for Laboratory Animals from the Direcção Geral da Agricultura.

#### **3.3.1 Harvesting, isolation and culture of rat bone marrow stromal cells (RBMSC's)**

Rat bone marrow stromal cells (RBMSC's) were used in the works described in chapter IV, which describes the behaviour of SPCL fiber mesh scaffolds seeded with these cells in the regeneration of critical sized defects in a rat model.

RBMSC's cells were obtained from femora of male Fisher rats weighing between 150-200g. Femora were washed 3 times in culture medium  $\alpha$ -MEM (Minimal Essential Medium) with added 50  $\mu$ g/ml gentamycin, 100  $\mu$ g/ml ampicillin and 0.3  $\mu$ g/ml fungizone. Epiphyses were cut off and diaphyses flushed out with 15 ml complete culture medium  $\alpha$ -MEM, supplemented with 10 % FCS (foetal calf serum, Gibco), 50  $\mu$ g/ml ascorbic acid (Sigma, Chemical Co., St.Louis, MO, USA), 50  $\mu$ g/ml gentamin, 100  $\mu$ g/ml ampicillin, 0.3  $\mu$ g/ml fungizone, 10 mM Na  $\beta$ -glycerophosphate and 10<sup>-8</sup> M dexamethasone (all Sigma). Cells were incubated in a humidified atmosphere of 95 % air, 5 % CO<sub>2</sub> at 37°C. The medium was changed three times a week.

After 7 days of primary culture, cells were detached using trypsin/ EDTA (0.25% w/v trypsin / 0.02% EDTA). The cells were concentrated by centrifugation at 1500 rpm for 5 minutes and resuspended in a known amount of media. Cells are counted and resuspended in complete medium.

### **3.3.2 Harvesting, isolation and culture of goat bone marrow stromal cells (GBMSC's)**

Goat bone marrow stromal cells were used in the works described in chapters V and VI, concerning the in vitro studies for assessing the feasibility of the developed bioreactor and the in vivo study that focused on assessing the behaviour of SPCL fiber mesh scaffolds seeded with these cell in the regeneration of critical sized defects in a goat model.

The iliac regions of the 6 adult goats were shaved and disinfected and animals were placed under general anaesthesia. Using a bone marrow aspiration needle (T-lok™ Angiotech Pharmaceuticals, Inc., USA) and a 10mL syringe, already containing 1mL heparin (5.000U.I, Heparin sodium, B. Braun Medical, Inc., USA), 10mL of bone marrow aspirate was harvested from the iliac crest of adult goats and transferred into a sterile tube and mixed with 30 ml basic culture medium – DMEM (Dulbecco's Modified Eagle's Medium) (Sigma-Aldrich, USA) supplemented with 10% fetal calf serum and 1% A/B (Invitrogen, Spain). GBMCs were centrifuged for 10 minutes at 1200 rpm and a dense cellular pellet was collected and cultured in a basic culture medium – DMEM (Dulbecco's Modified Eagle's Medium) (Sigma-Aldrich, USA) supplemented with 10% autologous serum isolated from goat peripheral blood and 1% A/B (Invitrogen, Spain)(13, 19). Four days after the harvesting procedure, cells were rinsed in a sterile phosphate buffered saline (PBS, Sigma, USA) solution and medium was changed. Then, cells were cryopreserved at 1P, expanded until 90% confluence and sub-cultured at 1P and 2P before seeding

#### **3.3.2.1 Cryopreservation of cells**

GBMSC's were cryoprezerved upon expansion until 90 % of confluence. At confluency, cells cultured in 75cm<sup>2</sup> flasks were enzymatically lifted with 3 ml of the 0.05 % trypsin-EDTA (Invitrogen, Spain), for 5 minutes in the incubator. After this the trypsin was neutralized by adding the same amount of basal culture medium (DMEM), and taking 10 µl of the cell suspension to count the number of cells with the Neubauer chamber; afterwards, the cell suspension was centrifuged at 1200 rpm at 4°C, the supernatant was



removed and the pellet was resuspended in the required volume of Foetal Bovine Serum (FBS) to obtain a final concentration of  $1 \times 10^6$  cells/ml. To each cryotube, 100 $\mu$ l of 10 % glycerol or dimethyl sulfoxide (DMSO) and 900 $\mu$ l of cell suspension were added. The cryotubes were placed at  $-80$  °C for 4 hours. After this the cryotubes were transferred into the liquid nitrogen container.

### **3.3.2.2 Replating cells after cryopreservation**

GBMSC's stored in a liquid nitrogen chamber ( $-196$ °C), at early passages and at high concentration maintain their characteristics and can be thawed and used when necessary. For this purpose, the cryotubes containing the cells are removed from the liquid nitrogen chamber, the culture medium is cooled in a glass container with ice, and the cryotubes are placed as quickly as possible in a thermostatic water bath at  $37$  °C, until it is partially thawed; after this the cryotubes are placed directly on ice, the cells are placed in a 15 ml tube and approximately 9 ml of cold culture medium is added, this cell suspension are centrifuged for 10 minutes at 12000 rpm at  $4$ °C, the supernatant is removed, and the pellet is resuspended in approximately 2 ml of culture medium. Finally, the cell suspension is transferred into 75 cm<sup>2</sup> culture flasks, and 15 ml culture medium (osteogenic or basal) was added.

### **3.3.3 Harvesting, isolation and culture of cat bone marrow stromal cells (CBMSC's)**

CBMSC's were used in the work reported in chapter VII which describes a case study where it was performed the application of an autologous stem cell therapy in the treatment of a tibial fracture gap in a cat.

Under general anaesthesia (ketamine HCl at 5 mg/kg IM and medetomidine at 80 $\mu$ /kg IM), maintained on isoflurane (2%) in oxygen(1500ml/min), 2ml of bone marrow (BM) was harvested from the femoral medullar cavity through the use of a biopsy needle (T-Lok <sup>TM</sup>). The cat bone marrow aspirate was mixed with 10ml of osteogenic media consisting of alfa-DMEM supplemented with osteogenic supplements namely,  $10^8$  M dexamethasone, 1% Antibiotics; 10%(FBS), 50 $\mu$ gml-1 ascorbic acid and 10mM  $\beta$ -glycerophosphate, and heparin (1/1000units) and the mixture was centrifuged (1200rpm/5 min). The pellet was removed and the cells were resuspended in the same media and seeded in two 75 cm<sup>2</sup> culture flasks and then placed inside an incubator.

Cells developed a fibroblastic-like morphology in visible symmetric colonies at about 4 days after initial plating. Non-adherent cells were removed with medium changes performed every 2-3 days. The osteoblastic differentiation was induced by culturing cells for 2 weeks in osteogenic medium.

### 3.4 Osteogenic differentiation

The differentiation of MSCs towards the osteogenic lineage is a highly programmed process that is well described *in vitro*. Usually it requires the supplementation of culture media with dexamethasone,  $\beta$ -glycerophosphate and ascorbic acid (16, 20). Dexamethasone (DEX) is routinely added to osteoprogenitor cells, having both inhibitory and stimulatory effects over skeletal cells.. It has also been suggested that even a transient exposure of stem cells to DEX may be effective in inducing and maintaining the osteoblastic phenotype (20). Glycerophosphate is the organic phosphate source, playing an important role in the mineralization process and modulation of osteoblast activities, namely on the alkaline phosphatase (ALP) activity and osteocalcin production. Ascorbic acid (AA) increases cell viability and is a cofactor in the hydroxylation of proline and lysine residues and is therefore necessary for the production of collagen (21). AA has also been demonstrated to increase ALP activity. Together with  $\beta$ -glycerophosphate, AA was found to be a prerequisite for the formation and mineralization of the extracellular matrix. The osteogenic culture medium that was used in several works of thesis (chapter IV;V,VI;VII) was composed of Alpha Modified Eagle Medium  $\alpha$  MEM (Sigma Aldrich, Germany), supplemented with 50  $\mu$ g/ml AA(Sigma Aldrich, Germany),  $10^8$  M Dexamethasone(Sigma Aldrich, Germany), 10 mM  $\beta$ -Glicerol Phosphate(Sigma Aldrich, Germany), 10 % FBS (Gibco,UK) and 1 % Antibiotic/Antimycotic (Gibco, UK), (designated in further sections as Osteogenic Medium).

### 3.5 “*In-Vitro*” biological testing

#### 3.5.1 Culture of Goat bone marrow stromal cells in SPCL constructs

##### 3.5.1.1 Seeding GBMSC's onto SPCL constructs

For the *in-vitro* and *in-vivo* goat studies (chapters V and VI) the polymer scaffolds were cut into disk of diameters of 16 mm and of thicknesses (3-4mm) with a inner cylindrical hole of 6mm (Figure 3.7).

All samples were sterilized by a standard procedure with ethylene oxide. The sterile samples were placed in 12-well cell culture plate (Costar® Corning; NY). Each sample was seeded with 300µl of a cell suspension containing  $1 \times 10^6$  GMBCs, prepared in osteogenic medium.

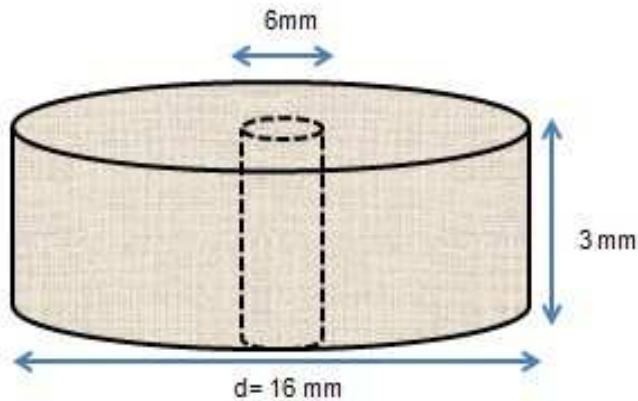


Figure 3.7. Schematic representation of the SPCL fiber-mesh scaffolds.

### 3.5.1.2 Static culture

For static culturing (controls), the SPCL scaffolds were placed in four 12 well non-adherents plates. A total of 14 samples were seeded with cell suspension for static culture for 14 days and 14 samples were seeded with cell suspension for static culture for 21 days. The well plates were transferred to the incubator and incubated overnight. The four 12 well plates of static culturing were taken out of the incubator and 10ml of osteogenic culture medium was added to each sample (static control). The scaffolds-cell was cultured for 14 days and 21 days. All GBMSC's-SPCL constructs were maintained in a 37 °C environment with 5% CO<sub>2</sub>. The culture medium was changed each 7 days.

### 3.5.1.3 Bioreactor culture

The plates containing cell-scaffolds constructs to be cultured in the bioreactor were carefully transferred to two BCPB's, in a flow laminar cabinet, as follows: each sample (3mm length and 16 mm diameter, with a inner hole of 6mm) was carefully inserted into the polycarbonate perforated tube and stacked until completing a total of 14 samples, corresponding to 42 mm length construct. The perforated tube with the construct was then connected to the two end parts of the bioreactor that aims to promote the hermetic and aseptic closure of the culture chamber; afterwards the main chamber of the bioreactor was connected to the flow system and slowly filled with the culture medium at a rate of 1ml/min, with the flow directed from inside the chamber to the perforated tube, enabling the medium to flow from outside to inside the cells-scaffold construct.

Finally, the whole system was transferred to the incubator (at 37°C environments with 5% CO<sub>2</sub>) where it was operated for 14 and 21 days. The culture chamber has a capacity for 216 ml of culture medium while the bottle reservoir has a capacity of 450 ml of medium; every week 400 ml of old medium were exchanged with 400 ml of fresh medium, without stopping medium flow in the bioreactor system. Each sample of the static group was cultured in the presence of 10 ml of culture medium which was changed every week.

### **3.6 “*In-Vitro*” characterization of the cultured cell-scaffolds constructs**

#### **3.6.1 Cell morphology – Scanning Electron Microscopy (SEM)**

The morphological analysis of cells growth, attachment, and distribution on the surface of the scaffolds was conducted by using SEM. To achieve these goals it is required the use of methods of fixation or stabilization of the cells on the scaffolds to obtain biological samples in their natural state. Due to the non-electric conductivity of those samples it is also needed to coat the samples with a conductive material such as gold or carbon. To overcome the limitation in the level of vacuum required for biological samples and/or the charging of non-conducting samples, a so-called environment SEM (E-SEM), was developed (Ziegler C, 2005). The constructs (scaffolds-cells) were fixed with 2.5 % Glutaraldehyde (Sigma, USA) in PBS solution during 1 hour at 4°C. Then, they were dehydrated through graded series of ethanol (70, 80, 90, 100 %) and let to dry overnight at room temperature. Finally, they were gold or carbon sputter coated (Fisons Instruments, model SC502; England) during 2 minutes at 15 mA, and analyzed by SEM (Leica Cambridge, model S360; England) equipped with an energy dispersive spectrometer (EDS; link-el-II).

#### **3.6.2 Cell viability assay**

The cellular viability on the scaffolds was assessed by a colorimetric assay named CellTiter 96<sup>®</sup> AQueos One Solution Cell Proliferation Assay (Promega, USA). The principle of this assay is based on the bioreduction of a tetrazolium compound [(3-(4,5-dimethylthiazol-2-yl)-5-(3-carboxymethoxyphenyl)-2(4-sulphophenyl)-2H-tetrazolium, inner salt(MTS)] into a brown formazan product that is soluble in culture medium (Cory et al., 1991). This conversion is accomplished by the production of nicotinamide adenosine dinucleotide phosphate (NADPH) or nicotinamide adenine dinucleotide (NADP) by the dehydrogenase enzymes existing in the metabolically active cells.

The quantity of formazan product measured by the amount of 490nm absorbance in a microplate reader (Bio-Tek, model Synergie HT; USA), after 3 hours of incubation at 37 °C. Three specimens per condition and per time point were characterized.

### 3.6.3 Cell proliferation assay

Determinations of Deoxyribonucleic acid (DNA) synthesis over time are frequently taken to be representative of the amount of cell proliferation (22). The most commonly used technique for measuring nucleic acid concentration is the determination of absorbance at 260nm ( $A_{260}$ ). The major disadvantages of the absorbance method are the large relative contribution of RNA and single-stranded DNA to the signal, the interference caused by contaminants commonly found in nucleic acid preparations, the inability to distinguish between DNA and Ribonucleic acid (RNA) and the relative insensitivity of the assay (an  $A_{260}$  of 0.1 corresponds to a 5 µg/ml double-stranded DNA solution). Alternatively, DNA content may be assayed by several fluorescence emissions, including reaction with DAPI, PicoGreen or Hoechst 33258.

In this work, cell proliferation was quantified by the total amount of double-stranded DNA (dsDNA) using an ultrasensitive fluorescent nucleic acid stain (23) during the culturing periods. For this, Quant-iT™ PicoGreen® dsDNA and RNA with minimal reagent was selected since it enables to quantify as little as 25 pg/ml of dsDNA with a standard spectrofluorometer and fluorescein excitation and emission wavelengths. The Quant-iT™ PicoGreen® dsDNA Assay Kit (Invitrogen™, Molecular Probes™, Oregon USA) was used according to the manufactures's instructions. Briefly, cells in the construct were lysed by osmotic and thermal shock and the supernatant used for the DNA quantification assay. A fluorescent dye, PicoGreen, was used because of its high sensitivity a specificity to double-stranded DNA. The fluorescence of the dye was measured at an excitation wavelength of 485/20 nm and at an emission wavelength 528/20 nm, in a microplate reader (Synergie HT, Bio-Tek; USA). Triplicates were made for each sample and per culturing time. The DNA concentration for each sample was calculated using time. The DNA concentration for each sample was calculated using a standard curve (DNA concentration ranging from 0.0 to 4.5µg/ml) relating quantity of DNA and fluorescence intensity.

### **3.6.4 Determination of alkaline phosphatase activity in cells – scaffold constructs**

The progression of differentiation can be assessed by biochemical assays. Routine assays involve the quantification of activity of alkaline phosphatase (ALP), a cell surface protein bound to the plasma membrane through phosphatidylinositol phospholipid complexes (21).

High ALP activity is associated with the active formation of mineralized matrix, and highest levels are found in the mineralization front of the bone healing process.

The ALP activity was determined for all time culture periods, using the same samples used for DNA quantification. Briefly, the activity of ALP was assessed using the *p*-nitrophenol assay. Nitrophenol phosphate disodium salt (pnPP;Fluka BioChemika, Austria), which is colourless, is hydrolysed by the alkaline phosphatase produced by the cells at pH 10.5 and temperature of 37 °C, to form free *p*-nitrophenol, which is yellow. The reaction was stopped by the addition of 2M NaOH (Panreac Quimica, Spain) and the absorbance read at 405 nm in a microplate reader (Bio-Tek, Synergie HT; USA). Standards were prepared with 10 µmol/ml *p*-nitrophenol (pNP;Sigma, USA) solution, to obtain a standard curve ranging from 0 to 0.4 nmol/ml/hr. Triplicates of each sample and standard were made, and the ALP concentrations read off directly from the standard curve.

### **3.6.5 Histological analysis**

The samples retrieved for the *in vitro* were rinsed in PBS, fixed in 4% formalin, dehydrated in a graded series of ethanol and embedded in methylmethacrylate (Technovit® 7100 NEW, Kulzer, DE). The procedure was based on the protocol provided by the manufacturer; following polymerization, sagittal microtome sections of 10 µm in thickness were prepared per implant. In order to observe cells and matrix formed, sections were stained with hematoxylin & eosin.

### **3.6.6 Light microscopy**

Stained constructs were observed under an optical microscope (BX61 Olympus Corporation, Germany) and images captured by a digital camera (DP70 Olympus Corporation, Germany).

### 3.6.7 Statistical analysis

The PASW Statistics18 software package (IBM, Somers, NY) was used for the statistical analysis. Descriptive values are presented as mean  $\pm$  SD unless stated otherwise. Kolmogorov-Smirnov test with Lilliefors significance correction was used to test the normality of the data. The one way ANOVA was used to determine if exist differences among the groups and Tukey test was used to assess the pairwise comparisons between groups. The statistical significance level considered was  $P < 0.05$ .

## 3.7 “*In-Vivo*” studies

Care and management of animals were conducted as per the guidelines of the Animal Ethics Committee and Supervision of Experiments on Animals.

### 3.7.1 Rat animal model

#### 3.7.1.1 Seeding rat bone marrow stromal cells in SPCL

##### constructs

For the in vivo rat study (chapter IV) the polymer scaffolds were cut into disk of diameters of 8 mm diameter and 2 mm of thicknesses. All samples were sterilized using ethylene oxide, as described above. The sterile samples were placed in 12–well cell culture plate (Costar® Corning; NY) and each sample was seeded with 200  $\mu$ l of a cell suspension containing 250.000 RBMSC's in osteogenic medium.

#### 3.7.1.2 Characterization of DNA in cell-seeded meshes

DNA assays (Invitrogen, Madrid, Spain) (n=6) were performed on day 0 and 1, after seeding of the RBMSCs onto SPCL scaffolds.. Culture medium was removed and meshes were washed twice with PBS. 1 ml of MilliQ was added to each sample. Cells were harvested by placing the scaffoldss with inoculated cells in a 1.5 ml tube. 1 ml of MilliQ was added to each sample. Cell suspension was frozen to  $-80^{\circ}\text{C}$ , heated to  $37^{\circ}\text{C}$ , frozen to  $-80^{\circ}\text{C}$  again and stored at  $-80^{\circ}\text{C}$  until usage.

DNA standard curve was made with Salmon testes DNA. 100  $\mu$ l of sample or standard were added to 100  $\mu$ l Picogreen working solution. The samples were incubated for 5 minutes at room temperature in the dark.

After incubation, DNA was measured using a fluorescence microplate reader (Bio-Tek instruments, Winooski, VT, USA) with excitation filter 365 nm and emission filter 450 nm. The quantity of DNA was correlated to the number of cells, using the standard curve of cell number versus the measured emission.

### **3.7.1.3 Animal surgical procedures**

Thirty inbred male Fisher rats (250g; Charles River, Barcelona, Spain) were used, in which each rat received one implant in a circular critical size cranial defect of 8 mm. The implantation periods were 4 and 8 weeks and the rats were divided into three groups: SPCL meshes loaded with osteoblast-like cells, SPCL meshes and empty defects (only 8 weeks).

The care and use of laboratory animals were performed according to the national guidelines after approval by the national ethical committee for laboratory animals and conducted in accordance with European standards on animal welfare. During the entire study, adequate measures were taken to minimize any pain and discomfort. One animal was housed in each cage and the proper intake of fluids and food were monitored on a daily basis. Also, the animals were observed for signs of pain, infection and proper activity. Surgery was performed under general inhalation anesthesia, induced by 4% isoflurane and maintained with 2.5% isoflurane by a non-rebreather mask. The rats were monitored with an oxy-pulse meter during surgery. To minimize postoperative pain, buprenorfine (Temgesic®) (0.05 mg/kg s.c.) was administered postoperatively.

After anesthesia the rats were immobilized on their abdomen and the skull was washed and disinfected with iodine. A longitudinal incision was made down to the periosteum from the nasal bone to the occipital protuberance, and soft tissues were sharp-dissected to visualize the cranial periosteum. Subsequently, a midline incision was made in the periosteum and the periosteum was undermined and lifted off the parietal skull. To create a central full thickness bone defect in the parietal cranium, a hollow trephine bur (ACE dental implant systems, Paço D'Arcos, Portugal) with an outer diameter of 8.0 mm in a dental hand piece was used. The bone defect was carefully drilled under continuous cooling with physiologic saline and without damaging of the underlying dura. Then, the created bone segment was carefully removed, without damaging the underlying sagittal sinus.



Following insertion of the implants the periosteum was closed using resorbable MonoPlus® 4-0 suture materials (BBraun, Portugal). Subsequently, the skin was closed using the same resorbable sutures. Eventually, the rats were euthanized 4 or 8 weeks after surgery by an overdose of thiopentone (Tiopental, BBraun, Portugal).

### **3.7.2 Characterization of the samples retrieved from in vivo study performed in a rat model**

#### **3.7.2.1 Micro-CT analysis**

Before implantation and after retrieving the cranium including the implanted samples, specimens were scanned and analyzed using microcomputed tomography ( $\mu$ CT) (SkyScan 1072 high-resolution micro-CT, SkyScan, Kontich, Belgium). The data from the initial scanning were used to quantify the total porosity of the implants.

After retrieving the implants, the quantitative evaluation of newly formed bone was calculated by determining a region of interest (ROI), which was set between the pre-existing bone and the implants. Within this ROI, new bone formation was distinguished from pre-existing bone and composite through structure and color differences. New bone formation was expressed in  $\text{mm}^3$ , using standardization of the 3-dimensional region of interest.

#### **3.7.2.2. Histology**

After scanning the implants with the microCT, implants were prepared for histological evaluation. The samples were dehydrated in a graded series of ethanol, decalcified and embedded in paraffin. After hardening, sagittal microtome sections of 5  $\mu\text{m}$  in thickness were prepared per implant. The sections were stained with hematoxylin and eosin or Masson's trichrome solution, which is frequently used as bone-specific staining. Subsequently, sections were investigated with a light microscope.

#### **3.7.2.3. Statistical analyses**

Statistical analyses were performed with GraphPad® InStat 3.05 software (GraphPad Software Inc., San Diego, CA, USA) using an one-way analyses of variance (ANOVA) with a Tukey multiple comparison post test.

### 3.7.3 Goat animal model

Six goats, 2-year-old females (n=2 in each group), with an average weight of 25 kg (ranged, 23–27.5 kg) were used. Animals were kept in separate cages with free access to food and water. Cylindrical critical size defects were performed in the tibial shafts, with the main purpose of comparing the new bone formation in defect implanted with GBMSC's-SPCL constructs cultured either in the flow perfusion bioreactor or under static conditions. Therefore three study groups were considered: Bioreactor group (6 and 12 weeks); Static (6 and 12 weeks) and empty defect (6 and 12 weeks). Autologous approach culture was used in this study, ie, animals were implanted with constructs containing the cells that were previously harvested from each animal.

#### 3.7.3.1 Cell seeding onto SPCL scaffolds

As described in previous section 3.5.1.1. A total of 56 samples were seeded.

#### 3.7.3.2 Static Culture Groups

The SPCL scaffolds were placed in four 12 well non-adherents plates. A total of 14 samples were seeded with 300  $\mu$ l of a cell suspension containing  $1 \times 10^6$  cells in basal medium composed of  $\alpha$ -MEM (Minimal Essential Medium) with 10 % FCS (foetal calf serum, Gibco), 50  $\mu$ g/ml gentamycin, 100  $\mu$ g/ml ampicillin and 0.3  $\mu$ g/ml fungizone (all from Sigma) for static culture 6 weeks group and 14 samples for static culture 12 weeks group. The well plates were transferred to the incubator and incubated overnight. The four well plates were then transferred to the incubator and three hours after seeding it was added 1.6 ml of basal medium to each well and incubated overnight. After this the 12 well plates of static culturing were taken out of the incubator the basal medium was removed and 10ml of osteogenic culture medium was added to each sample (static control). The scaffolds-cell was cultured for 14 days. All GBMC–SPCL constructs were maintained in a 37 °C environment with 5% CO<sub>2</sub>. The culture medium was changed each 7 days.

#### 3.7.3.3 Bioreactor culture groups

The SPCL scaffolds were placed in four 12 well non-adherents plates (Costar; Becton-Dickinson). A total of 14 samples were seeded with 300  $\mu$ l of a cell suspension containing  $1 \times 10^6$  cells in basal medium for bioreactor culture for 14 days (6 weeks implantation group) and additional 14 samples for bioreactor culture for 14 days (12 weeks implantation group).

The four well plates were then transferred to the incubator and three hours after seeding it was added 1.6 ml of basal medium to each well and incubated overnight. The four 12 well plates of bioreactor culturing were taken out of the incubator and were then carefully transferred to two bioreactors to which were added 216 ml of osteogenic culture medium in each bioreactor. The scaffolds-cell was cultured for 14 days. All GBMSC's–SPCL constructs were maintained in a 37 °C environment with 5% CO<sub>2</sub>. The culture medium was changed each 7 days.

### 3.7.3.4 Animal surgical procedures

The animals were premedicated with intramuscular injection medetomidine hydrochloride (Domitor®, Pfizer, Portugal) at 0.11mg/kg body weight, and ketamine hydrochloride (Imalgene®, Merial, Portugal) at 10mg/kg body weight.

Thiopentone (Tiopental®, BBraun, Portugal) sodium at 5mg/kg body weight intravenously was given for induction of anesthesia. Antibiotic therapy with Cephazolin (Cefazolin® 500mg, Sagent, Portugal), 10 mg/kg was administered subcutaneously as prophylactic antibiotics. The animals were intubated immediately with size n° 9 Magill endotracheal tube. Anesthesia was maintained with increments of medetomidine hydrochloride and ketamine hydrochloride dose-effect every 20–30 min. The animals were fixed in the right lateral position on an operating table. Asepsis of the skin after shaving was done with chlorhexidine (LifoScrub®, BBraun, Portugal) solution and wrapped using sterile technique, a skin incision of 15 cm length along the right tibia was made and the tibia was exposed using a standard medial approach. The periosteum was elevated and a 40 mm bone segment was excised from the mid diaphyseal region using an oscillating saw under abundant irrigation. A stainless steel biological healing plate of 7 holes (Servive Portugal, Valencia) and cortical screws of 3.5 mm and 16 mm in length more wire banding (Cerclagem) techniques were used for immobilization of the bone. The GBMSC's–SPCL constructs by bioreactor perfusion culture were placed into the right tibia defects (bioreactor group, 6 and 12 weeks). The GBMSC's–SPCL constructs for culture in static state (static group, 6 and 12 weeks) and control group (empty defect, 6 and 12 weeks) were implanted into the right tibia by the same procedure. The surround soft tissue and skin (intra-dermal suture) incision was closed with uninterrupted sutures with absorbable synthetic monofilament suture (MonoPlus®, BBraun, Portugal).

Limb immobilization was performed with the use of a modified Robert Jones bandage for a week. During the first week after surgery, cephazolin (10 mg/kg) was routinely administered intramuscularly once a day and the physical exams of all the animals were conducted daily. The animals were sacrificed at 6 and 12 weeks with an injection of high doses of thiopentone (Tiopental, BBraun, Portugal).

### **3.7.4 Characterization of the samples retrieved from in vivo study performed in a goat model**

#### **3.7.4.1 Digital radiography**

In vivo, digital radiography of all the goats were taken in the immediate postoperative, 6, and 12 weeks post operation. Standard mediolateral and craniocaudal radiographic views of the right tibia were obtained using a radiography machine (Philips<sup>®</sup>, Corp.), all exposure were taken at 50 kVp for 2.5 mAs, and each image was immediately reviewed using a diagnostic imaging software (CrystalView<sup>®</sup>).

To ensure diagnostic quality of exposure and positioning. The changes of radiopacity in and around the GBMC–SPCL constructs at the defect and bone union at the cut-ends of the original tibias were analyzed. Radiographs of the tibia removed from the goats were taken by routine procedures.

#### **3.7.4.2 Micro-CT**

The formation of mineralized tissue in the GBMSC's–SPCL constructs explants was evaluated using a high-resolution  $\mu$ -CT Skyscan 1072 scanner (Skyscan, Konitich, Belgium). Each sample was scanned in high-resolution mode with a pixel size of 17.58 $\mu$ m and exposure time of 1.6ms. The x-ray source was set at 52 keV of energy and 163 $\mu$ A of intensity. Approximately 400 projections were acquired over a rotation of 180<sup>o</sup> with a rotation step of 0.45<sup>o</sup>. Each one of these projections were segmented into binary images with dynamic threshold of 220-255 (grey values) to assess new bone formation. These data sets were used for morphometric analysis (CT analyser, v1.51.5 SkyScan) and to build the 3D models (ANT 3D creator, v2.4 SkyScan). The distribution and quantification of the new bone formation in the scaffolds was assessed by 3 D virtual models that were created, visualized and registered using both image processing software's (CT analyser and ANT 3D creator).

### 3.7.4.3 SEM

Cell adhesion and morphology at the surface of the GBMSC's–SPCL constructs explants were also analysed by SEM. Scaffolds were washed in 0.15M phosphate buffered saline and fixed in 2,5 % glutaraldehyde in phosphate buffered saline for 1 hours at 4°C. After rinsing 3 times in phosphatase buffered saline, the scaffolds were dehydrated using a series of graded ethanol (70, 80, 90, and 100%) and let to dry overnight at room temperature.

Finally, they were gold or carbon sputter coated (Fisons Instruments, model SC502; England) during 2 minutes at 15 mA, and analyzed by SEM (Leica Cambridge, model S360; England) equipped with an energy dispersive spectrometer (EDS;link-el-II).

### 3.7.4.4 Histological analysis

The samples retrieved were rinsed in PBS, fixed in 4% formalin, dehydrated in a graded series of ethanol and embedded in paraffin, sagittal microtome sections of 5 µm in thickness were prepared per implant. In order to observe cells and matrix formed, sections were stained with hematoxylin & eosin and Masson trichrome, which are frequently used as bone-specific staining. Samples were then visualized under a light microscope and images taken with an attached camera.

### 3.7.4.5 Light microscopy

Stained constructs were observed under an optical microscope (BX61 Olympus Corporation, Germany) and images captured by a digital camera (DP70 Olympus Corporation, Germany).

### 3.7.4.6 Statistical analysis

The PASW Statistics18 software package (IBM, Somers, NY) was used for the statistical analysis. Descriptive values are presented as mean  $\pm$  SD unless stated otherwise. Kolmogorov-Smirnov test with Lillefors significance correction was used to test the normality of the data. The one way ANOVA was used to determine if exist differences among the groups and Tukey test was used to assess the pairwise comparisons between groups. The statistical significance level considered was  $P < 0.05$ .

### 3.7.5 Cat animal model

#### 3.7.5.1 Cells harvesting, culturing and implantation

CBMSC's cells, harvested/isolated and cultured as previously described in section 3.3.3, were enzymatically lifted with 3 ml of trypsin after reaching 80%- 90% of confluence at passage 3 (p3), centrifuged (1200rpm/5min) and the pellet was removed. A cells suspension containing  $9 \times 10^6$  cells in 0, 6 ml of phosphate-buffered saline (PBS) solution was prepared and injected in the gap site using a 1mL sterile syringe.

#### 3.7.5.2 Osteogenic differentiation - Determination of the alkaline phosphatase activity

To characterize the osteogenic differentiation in vitro, cells were cultured in 6 well plates at a density of  $3 \times 10^5$  cells/well. Plates with osteogenic medium for days 0, 7(first week) and 21(third week), changing the medium every 2-3 days. ALP activity of the CBMSC was measured to evaluate osteoblastic-like differentiation; for this purpose, the samples were collected on days 0, 7(first week) and 21(third week), washed twice with a sterile PBS solution and transferred into 1.5 ml microtubes containing 1ml of ultra pure water; the tubes containing the cells samples were then incubated for 1h at 37 °C in a water -bath and then stored in a -80 °C freezer until testing. For the ALP assay, 20µl of each sample plus 60µl of substrate solution (0.2% (w/v) *p*-nitrophenyl (*p*NP) phosphate in a substrate buffer: 1 M diethanolamine HCL, at pH 9.8) was placed in each well of a 96-well plate were added 20µl of sample plus 60µl of substrate solution: 0.2% (w/v) *p*-nitrophenyl (*p*NP) phosphate in a substrate buffer: 1 M diethanolamine HCL, at pH 9.8. The plate was then incubated in the dark for 45 min at 37 °C. After the incubation period, 80 µl of a stop solution (2M NaOH containing 0.2 mM ethylenediaminetetraacetic acid (EDTA), was added to each well. Standards were prepared with 10µmol ml<sup>-1</sup> *p*NP and the stop solutions in order to achieve final concentrations ranging between 0 and 0.3µmol<sup>-1</sup>. Triplicates were made for each sample and standard. Absorbance was read at 405 nm Microplate ELISA Reader and sample concentrations were read off from standard graph.

### **3.7.5.3 Osteogenic differentiation- Alizarin red staining**

To assess mineralization,  $3 \times 10^5$  cells/well cultured in 6-well plates with osteogenic medium for different time points 7(first week) and 21(third week) were stained with Alizarin Red (Fluca, Germany).

## **3.7.6 Characterization performed upon cells implantation**

### **3.7.6.1 Radiography**

To visualize the development of the mineralization in the gap site, X-rays (X-rays: Cosmos BS, Philips Medical Systems, Carlsbad, CA) were carried out and all exposure were taken at 48 kVp for 2.5 mAs were performed at days 0, 7(first week) and 21(third week) upon cells implantation.

### **3.7.6.2 Determination of alkaline phosphatase activity in cat blood serum**

Assessment of ALP In vivo was carried out by harvest of 2 ml of peripheral blood serum for assay in IDEXX VetTest® chemistry analyzer in days 0 (day of the application of the cells), 7(first week) and 21(third week).

## References

1. Gardel, L., Gomes, M., Reis, R. Bi-Directional Continuous Perfusion Bioreactor for Tridimensional Culture Of Mammal Tissue Substitutes. Applicant: Association For The Advancement Of Tissue Engineering And Cell based Technologies & Therapies, nº 097936249- 1521 PCT/PT 2009000063, 2008.
2. Aronin, C.E.P., Cooper, J.A., Jr., Sefcik, L.S., Tholpady, S.S., Ogle, R.C., Botchwey, E.A. Osteogenic differentiation of dura mater stem cells cultured in vitro on three-dimensional porous scaffolds of poly(epsilon-caprolactone) fabricated via co-extrusion and gas foaming. *Acta Biomater* 4, 2008,1187.
3. Pashkuleva, I., Azevedo, H.S., Reis, R.L. Surface structural investigation of starch-based biomaterials. *Macromol Biosci* 8, 2008,210.
4. Azevedo, H.S., Gama, F.M., Reis, R.L. In vitro assessment of the enzymatic degradation of several starch based biomaterials. *Biomacromolecules* 4, 2003,1703.
5. Martins, A.M., Pham, Q.P., Malafaya, P.B., Sousa, R.A., Gomes, M.E., Raphael, R.M., et al. The Role of Lipase and alpha-Amylase in the Degradation of Starch/Poly(epsilon-Caprolactone) Fiber Meshes and the Osteogenic Differentiation of Cultured Marrow Stromal Cells. *Tissue Eng Part A* 15, 2009,295.
6. Gomes, M.E., Azevedo, H.S., Moreira, A.R., Ella, V., Kellomaki, M., Reis, R.L. Starch-poly(epsilon-caprolactone) and starch-poly(lactic acid) fibre-mesh scaffolds for bone tissue engineering applications: structure, mechanical properties and degradation behaviour. *J Tissue Eng Regen Med* 2, 2008,243.
7. Kweon, H., Yoo, M.K., Park, I.K., Kim, T.H., Lee, H.C., Lee, H.S., et al. A novel degradable polycaprolactone networks for tissue engineering. *Biomaterials* 24, 2003,801.
8. Gomes, M.E., Holtorf, H.L., Reis, R.L., Mikos, A.G. Influence of the porosity of starch-based fiber mesh scaffolds on the proliferation and osteogenic differentiation of bone marrow stromal cells cultured in a flow perfusion bioreactor. *Tissue Eng* 12, 2006,801.
9. Gomes, M.E., Sikavitsas, V.I., Behraves, E., Reis, R.L., Mikos, A.G. Effect of flow perfusion on the osteogenic differentiation of bone marrow stromal cells cultured on starch-based three-dimensional scaffolds. *J Biomed Mater Res Part A* 67A, 2003,87.
10. Alves, C.M., Yang, Y., Carnes, D.L., Ong, J.L., Sylvia, V.L., Dean, D.D., et al. Modulating bone cells response onto starch-based biomaterials by surface plasma treatment and protein adsorption. *Biomaterials* 28, 2007,307.
11. Marques, A.P., Cruz, H.R., Coutinho, O.P., Reis, R.L. Effect of starch-based biomaterials on the in vitro proliferation and viability of osteoblast-like cells. *J Mater Sci Mater Med* 16, 2005,833.



12. Santos, M.I., Tuzlakoglu, K., Fuchs, S., Gomes, M.E., Peters, K., Unger, R.E., et al. Endothelial cell colonization and angiogenic potential of combined nano- and micro-fibrous scaffolds for bone tissue engineering. *Biomaterials* 29, 2008,4306.
13. Rodrigues, M.T., Gomes, M.E., Viegas, C.A., Azevedo, J.T., Dias, I.R., Guzon, F.M., et al. Tissue-engineered constructs based on SPCL scaffolds cultured with goat marrow cells: functionality in femoral defects. *J Tissue Eng Regen Med* 5, 2011,41.
14. Rodrigues, M.T., Martins, A., Dias, I.R., Viegas, C.A., Neves, N.M., Gomes, M.E., et al. Synergistic effect of scaffold composition and dynamic culturing environment in multilayered systems for bone tissue engineering. *J Tissue Eng Regen Med*, 2012.
15. Satija, N.K., Gurudutta, G.U., Sharma, S., Afrin, F., Gupta, P., Verma, Y.K., et al. Mesenchymal stem cells: molecular targets for tissue engineering. *Stem Cells Dev* 16, 2007,7.
16. Salgado, A.J., Oliveira, J.T., Pedro, A.J., Reis, R.L. Adult stem cells in bone and cartilage tissue engineering. *Curr Stem Cell Res Ther* 1, 2006,345.
17. Pittenger, M.F., Mackay, A.M., Beck, S.C., Jaiswal, R.K., Douglas, R., Mosca, J.D., et al. Multilineage potential of adult human mesenchymal stem cells. *Science* 284, 1999,143.
18. Bianco, P., Riminucci, M., Gronthos, S., Robey, P.G. Bone marrow stromal stem cells: nature, biology, and potential applications. *Stem Cells* 19, 2001,180.
19. Oliveira, J.M., Rodrigues, M.T., Silva, S.S., Malafaya, P.B., Gomes, M.E., Viegas, C.A.A., et al. Novel hydroxyapatite/chitosan bilayered scaffold for osteochondral tissue-engineering applications: scaffold design and its performance when seeded with goat bone marrow stromal cells. *Biomaterials* 27, 2006,6123.
20. Jaiswal, N., Haynesworth, S.E., Caplan, A.I., Bruder, S.P. Osteogenic differentiation of purified, culture-expanded human mesenchymal stem cells in vitro. *J Cell Biochem* 64, 1997,295.
21. Hofmann, S., Kaplan, D., Vunjak-Novakovic, G., Meinel, L. Tissue Engineering of Bone. In: Vunjak-Novakovic G, Freshney RI, editors *Culture of cells for tissue Engineering* New Jersey: John Wiley & Sons, Inc 2006,pg. 323.
22. Freshney, R.I. Citotoxicity. In Freshney RI, editor *Culture of animal cells: A Manual of Basic Technique* Fifth ed: John Wiley& Sons, Inc. , 2005,pg. 359.
23. Chadwick, R.B., Conrad, M.P., McGinnis, M.D., JohnstonDow, L., Spurgeon, S.L., Kronick, M.N. Heterozygote and mutation detection by direct automated fluorescent DNA sequencing using a mutant Taq DNA polymerase. *Biotechniques* 20, 1996,676.



## SECTION 3

### Chapter IV

#### **Osteogenic properties of starch poly( $\epsilon$ -caprolactone) (SPCL) fiber meshes loaded with rat bone marrow stromal stem cells (RBMSCs) in a rat critical-sized cranial defect**

This chapter is based on the following publication: Link\* DP, Gardel\* LS, Correlo VM, Gomes ME, Reis RL. Osteogenic properties of starch poly( $\epsilon$ -caprolactone) (SPCL) fiber meshes loaded with rat bone marrow stromal stem cells (RBMSCs) in a rat critical-sized cranial defect. 2012 submitted.

\*These authors contributed equally to this work



## **Abstract**

Bone marrow stromal cells (BMSCs) are able to differentiate into the osteogenic lineage and together with a suitable scaffold, these cell-scaffold constructs can aid the bone regeneration process. A suitable scaffold could be starch poly( $\epsilon$ -caprolactone) (SPCL) fiber meshes, which have shown a high potential to support bone formation in previous in vitro and in vivo studies. However, previous in vivo studies were limited to subcutaneous and non-critical sized orthotopic defect models. Therefore, the aim of this study was to assess the effect of these scaffolds alone or combined with rat bone marrow stromal cells (RBMSCs) in the regeneration of a critical size cranial defect in a rat model. Therefore, SPCL fiber meshes were pre-loaded with RBMSCs and subsequently implanted in a critical-sized cranial defect in male Fisher rats. Empty defects and defects filled with cell-free scaffolds were used as controls groups. After four and eight weeks of implantation, samples were analyzed to assess new bone formation by means of MicroCT and histological analysis.

In general, histological analyses revealed that all study groups showed new bone formation from the defect edges towards the interior of the defects. Also, bone was formed in the center of the scaffolds, especially in the groups containing pre-loaded RBMSCs. MicroCT reconstructions showed that bone formation increased over time and was enhanced with the inclusion of pre-loaded RBMSCs compared to SPCL scaffolds alone. According to these results, the pre-loaded RBMSCs contributed to the bone regeneration process in a critical-sized bone defect. Furthermore, SPCL fiber meshes proved to be a very suitable material to use for bone regeneration purposes.

## 4.1 Introduction

Autologous and allogeneous bone grafts are still the method of choice for the treatment of bone defects caused by trauma, disease or tumor resection. However, both of these methods are associated with significant clinical problems, like donor site morbidity and the possible transfer of diseases, respectively. In view of this, innovative tissue engineering techniques have been introduced, which include the use of stem cells in combination with a suitable scaffold to create tissue substitutes in vitro.(1, 2) These stem cells are commonly derived from bone marrow stroma, which provides a cellular reservoir for the regeneration of bone tissue. Unfortunately, a limitation in the use of bone marrow cells for bone tissue engineering is the relatively low number of osteoprogenitor cells in the marrow stroma. Culturing bone marrow stromal cells in osteogenic media has shown to provide good expansion rates of osteoprogenitor cells and can eventually lead to a pre-differentiated state of these cells, which have shown to have a positive influence in the bone regeneration process in vivo.(3, 4) The majority of these bone tissue engineered constructs include stem cells in combination with natural and synthetic scaffolds.(5, 6) These scaffolds provide mechanical support and serve as a substrate to which cells attach, and subsequently proliferate and undergo differentiation. Specifically in bone tissue engineering strategies, these scaffolds support bone formation by serving as a guide for new bone growth along the scaffold surface and hence bridge the gap between bone ends.(7) Whereas in non-critical sized defects, implantation of scaffolds or cells alone could be sufficient to support new bone formation, in critical-sized defects the bone regeneration process requires a combination of cells of the osteoblastic lineage with a porous scaffold to stimulate bone formation from within the construct.(8-10) For the present study, it was selected a scaffold based on a polymeric blend of starch poly ( $\epsilon$ -caprolactone) (SPCL), which proved to be biocompatible and biodegradable.(11) SPCL can be processed by melt-spinning to create fibers which can be combined, under the influence of temperature and pressure, into physical bonded fiber meshes. These fiber meshes exhibit a high surface area combined with high pore interconnectivity, that enables adequate diffusion of nutrients and waste while maintaining sufficient mechanical properties and thus allows cell attachment and proliferation.(12) Previous studies showed that SPCL fiber meshes supported bone-like tissue formation in vitro (13, 14) and enhanced the regeneration of a non-critical sized orthotopic defect(15), while only showing a moderate inflammatory response in a subcutaneous and intramuscular study in rats.(16)

Critical-sized cranial defects in rats constitute a well-known and established animal model to assess the potential of tissue engineered constructs to induce new bone formation/regeneration.(17-19) Thus, in this study, SPCL fiber meshes were pre-loaded with RBMSCs and subsequently implanted in a rat critical-sized cranial defect. Empty defects and defects filled with cell-free scaffolds were used as control groups. After four and eight weeks of implantation, samples were analyzed to assess new bone formation by means of MicroCT and histological analysis. The pre-loaded RBMSCs are expected to contribute to the bone regeneration process in a critical-sized bone defect, while SPCL fiber meshes are envisioned to provide an adequate support for cells adhesion/proliferation and also for new tissue ingrowth, upon implantation.

## **4.2 Materials and Methods**

### **4.2.1 Scaffolds preparation**

Polymeric fibers based on SPCL (a 30:70 w/w% blend of starch with poly( $\epsilon$ -caprolactone)) were obtained by melt spinning. An extruder equipped with a 12mm diameter screw was used with a 0.5 mm monofilament die. Die temperature was 150°C and the screw speed 1 rpm. Extrusion was performed in an ambient environment. Hot fiber was driven into a cooling bath (water 13°C) and cold-drawn after the bath, using a caterpillar with a speed of 21 m/min and a winding unit with a speed of 28 m/min. Fibers were produced with diameter in the range of 120–500  $\mu$ m.

SPCL fiber meshes were prepared by a fiber bonding process consisting of cutting and sintering the fibers previously obtained by the above-described melt spinning method.(12) Briefly, a selected amount of fibers were placed in a glass mould and heated in an oven at 150°C; immediately after removing the moulds from the oven, the fibers were slightly compressed by a teflon cylinder (which runs within the mould) and then cooled at -20°C. All samples were cut into cylindrical mesh samples of 8 mm diameter and 2 mm height and sterilized using ethylene oxide.

## 4.2.2 Cell isolation and seeding into scaffolds

Rat bone marrow stromal cells (RBMSCs) were obtained from femora of male Fisher rats weighing between 150-200g. Femora were washed 3 times in culture medium  $\alpha$ -MEM (Minimal Essential Medium) with added 50  $\mu$ g/ml gentamycin, 100  $\mu$ g/ml ampicillin and 0.3  $\mu$ g/ml fungizone. Epiphyses were cut off and diaphyses flushed out with 15 ml of osteogenic culture medium composed of  $\alpha$ -MEM supplemented with 10 % FCS (foetal calf serum, Gibco), 50  $\mu$ g/ml ascorbic acid (Sigma, St.Louis, MO, USA), 50  $\mu$ g/ml gentamin, 100  $\mu$ g/ml ampicillin, 0.3  $\mu$ g/ml fungizone, 10 mM Na  $\beta$ -glycerophosphate and  $10^{-8}$  M dexamethasone (all Sigma). Cells were incubated in a humidified atmosphere of 95 % air, 5 % CO<sub>2</sub> at 37°C and the culture medium was changed three times a week.

After 7 days of primary culture, cells were detached using trypsin/ EDTA (0.25% w/v trypsin / 0.02% EDTA). The cells were concentrated by centrifugation at 1500 rpm for 5 minutes and resuspended in a known amount of osteogenic medium. The cell suspension was seeded onto the SPCL fiber meshes at a density of 250.000 cells per sample. Cell-seeded samples were characterized in terms of DNA content and ALP activity in same day of seeding and 1 day after seeding, i.e., at the time they were implanted.

## 4.2.3 Characterization of cell-seeded meshes

### 4.2.3.1 DNA quantification

DNA quantification assays (Invitrogen, Madrid, Spain) (n=6) were performed on day 0 and 1, after seeding of the RBMSCs onto SPCL scaffolds. Culture medium was removed, the cell seeded meshes were washed twice with PBS and 1 ml of MilliQ was added to each sample. Cell-seeded meshes were frozen to -80°C, heated to 37°C, frozen to -80°C again and stored at -80°C until usage.

DNA standard curve was made with Salmon testes DNA. 100  $\mu$ l of sample or standard were added to 100  $\mu$ l Picogreen working solution. The samples were incubated for 5 minutes at room temperature in the dark. After incubation, DNA was measured using a fluorescence microplate reader (Bio-Tek instruments, Winooski, VT, USA) with excitation filter 365 nm and emission filter 450 nm. The quantity of DNA was correlated to the number of cells, using the standard curve of cell number versus the measured emission.



#### 4.2.4 Surgery

Thirty inbred male Fisher rats (250g; Charles River, Barcelona, Spain) were used for the study. A single circular critical size cranial defect of 8 mm was performed in each rat, which were divided into three study groups, implanted for 4 and 8 weeks: i) group implanted with SPCL meshes loaded with RBMSCs, ii) group implanted with SPCL meshes alone (without cells) and iii) group with defects left empty. The care and use of laboratory animals were performed according to the national guidelines after approval by the national ethical committee for laboratory animals and conducted in accordance with National and European standards on animal welfare. During the entire study, adequate measures were taken to minimize any pain and discomfort. One animal was housed in each cage and the proper intake of fluids and food were monitored on a daily basis. Also, the animals were observed for signs of pain, infection and proper activity. Surgery was performed under general inhalation anesthesia, induced by 4% isoflurane and maintained with 2.5% isoflurane by a non-rebreather mask. The rats were monitored with an oxy-pulse meter during surgery. To minimize pain, buprenorfine (Temgesic®) (0.05 mg/kg s.c.) was administered postoperatively.

After anesthesia the rats were immobilized on their abdomen and the skull was washed and disinfected with iodine. A longitudinal incision was made down to the periosteum from the nasal bone to the occipital protuberance, and soft tissues were sharp-dissected to visualize the cranial periosteum. Subsequently, a midline incision was made in the periosteum and the periosteum was undermined and lifted off the parietal skull. To create a central full thickness bone defect in the parietal cranium, a hollow trephine bur (ACE dental implant systems, Paço D'Arcos, Portugal) with an outer diameter of 8.0 mm in a dental handpiece was used. The bone defect was carefully drilled under continuous cooling with physiologic saline and without damaging of the underlying dura. Then, the created bone segment was carefully removed, without damaging the underlying sagittal sinus. Following insertion of the implants the periosteum was closed using resorbable MonoPlus® 4-0 suture materials (BBraun, Portugal)(Figure 1 A, B and C). Subsequently, the skin was closed using the same resorbable sutures. The rats were euthanized 4 or 8 weeks after surgery by an overdose of pentobarbital.

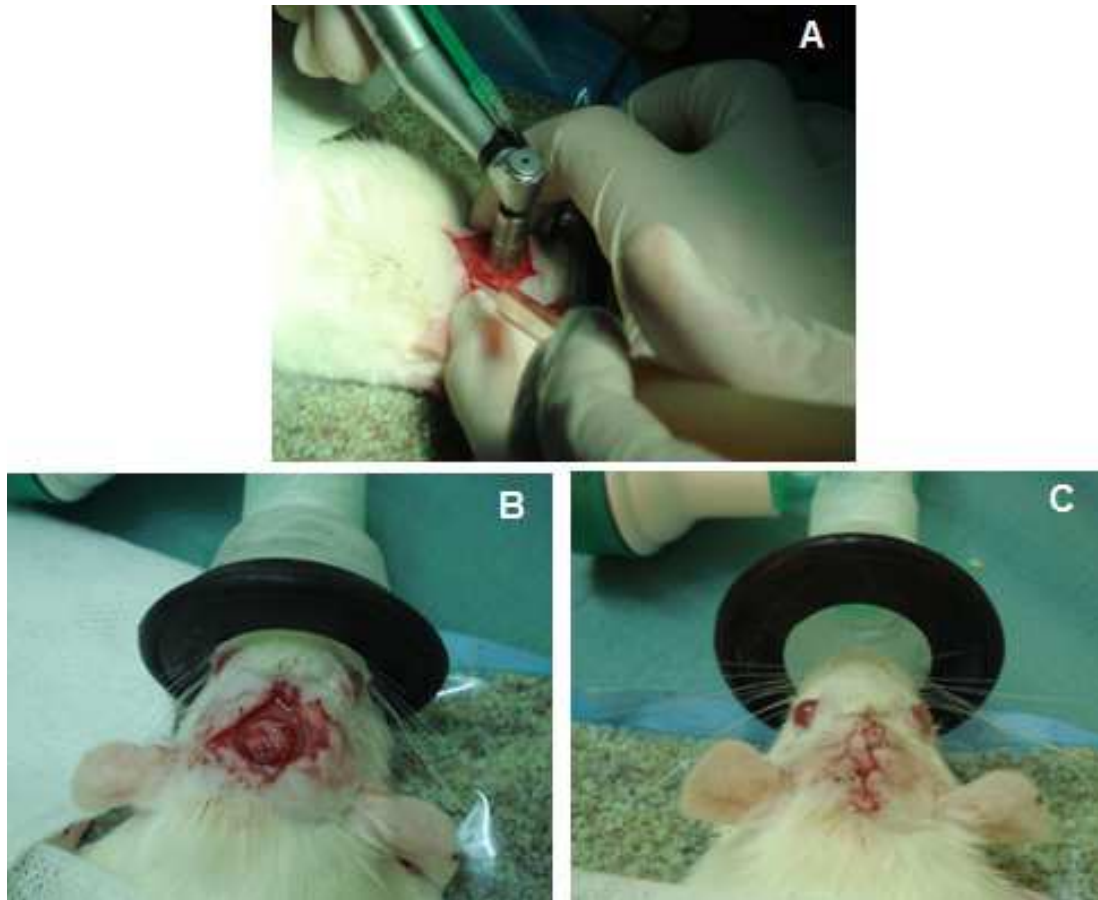


Figure 4.1. Surgical approach and implantation of the scaffold.

## 4.2.5 Characterization of the explants

### 4.2.5.1 MicroCT

After retrieving the cranium including the implanted samples, specimens were fixated in 4% formalin solution (pH=7.4) and scanned using microcomputed tomography ( $\mu$ CT) (SkyScan 1072 high-resolution micro-CT, SkyScan, Kontich, Belgium). The data from the initial scanning (non-implanted SPCL samples) was used to quantify the total porosity of the implants. After retrieving the implants, the quantitative evaluation of newly formed bone was calculated by determining a region of interest (ROI), which was set between the pre-existing bone and the implants. Within this ROI, new bone formation was distinguished from pre-existing bone and composite through structure and color differences. New bone formation was expressed in  $\text{mm}^3$ , using standardization of the 3-dimensional region of interest.

#### 4.2.5.2 Histology

After scanning the explants with the microCT, samples were prepared for histological evaluation. The samples were dehydrated in a graded series of ethanol, decalcified and embedded in paraffin. After hardening, sagittal microtome sections of 5  $\mu\text{m}$  in thickness were prepared per implant. The sections were stained with hematoxylin and eosin or Masson's trichrome solution, which is frequently used as bone-specific staining. Subsequently, sections were analyzed under a light microscope.

#### 4.2.6 Statistical analyses

Statistical analyses were performed with GraphPad® InStat 3.05 software (GraphPad Software Inc., San Diego, CA, USA) using an one-way analyses of variance (ANOVA) with a Tukey multiple comparison post test.

### 4.3 Results

SEM examination showed that RBMSCs adhered and were well-spread on the surface of the SPCL fibers, one day after seeding. DNA analyses showed that the cell seeding suspension contained  $231 \pm 3$  ng/ml DNA, whereas the DNA quantity after 1 day of culturing on the SPCL fiber meshes was  $159 \pm 24$  ng/ml DNA. Therefore, the calculated seeding efficiency was 69%, resulting that approximately 172.500 RBMSCs (of the 250.000 that were seeded) were efficiently seeded onto the SPCL fiber meshes. (Figure 4.2)

Implant characterization before implantation	
Porosity	62.5%, mean pore diameter 275 $\mu\text{m}$
Seeding solution	$231 \pm 3$ ng/ml DNA
After 1 day of culturing	$159 \pm 24$ ng/ml DNA

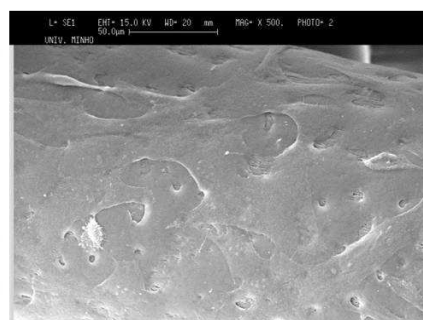


Figure 4.2. Implant characterization and SEM picture before implantation after 1 day of culturing.

### 4.3.1 In vivo experiment

#### 4.3.1.1 General observations

During surgery and when the implants were inserted into the cranial defect, some infiltration of blood in the SPCL fiber meshes occurred. Also, some implants were completely press-fitted into the critical-sized cranial defect, where others were less press-fitted. From the thirty-two male Fisher rats, two rats died during surgery, due to heavy blood loss after cutting the main cerebral sinus. All other rats remained in good health and did not show any wound complications. At retrieval, the cranial implants were all covered by periosteum and implants remained intact. No inflammatory signs or adverse tissue reactions were macroscopically observed.

#### 4.3.1.2 MicroCT

Before implantation, MicroCT reconstructions showed that SPCL fiber meshes exhibited an average overall porosity of 62.5% with a mean pore diameter of 275  $\mu\text{m}$ . After retrieving the implants with their surrounding tissue, samples were scanned with the MicroCT. Reconstructions of the obtained scans showed that after 4 weeks of implantation, new bone formation in the implants loaded with SPCL seeded with RBMSCs was  $5.99 \pm 4.09 \text{ mm}^3$ , while SPCL without cells showed  $3.83 \pm 1.70 \text{ mm}^3$  of new bone formation. After 8 weeks of implantation new bone formation was  $7.35 \pm 3.15 \text{ mm}^3$  in the implants containing RBMSCs, while SPCL without cells showed  $4.91 \pm 2.51 \text{ mm}^3$  new bone (Figure 4.3 and 4.4).

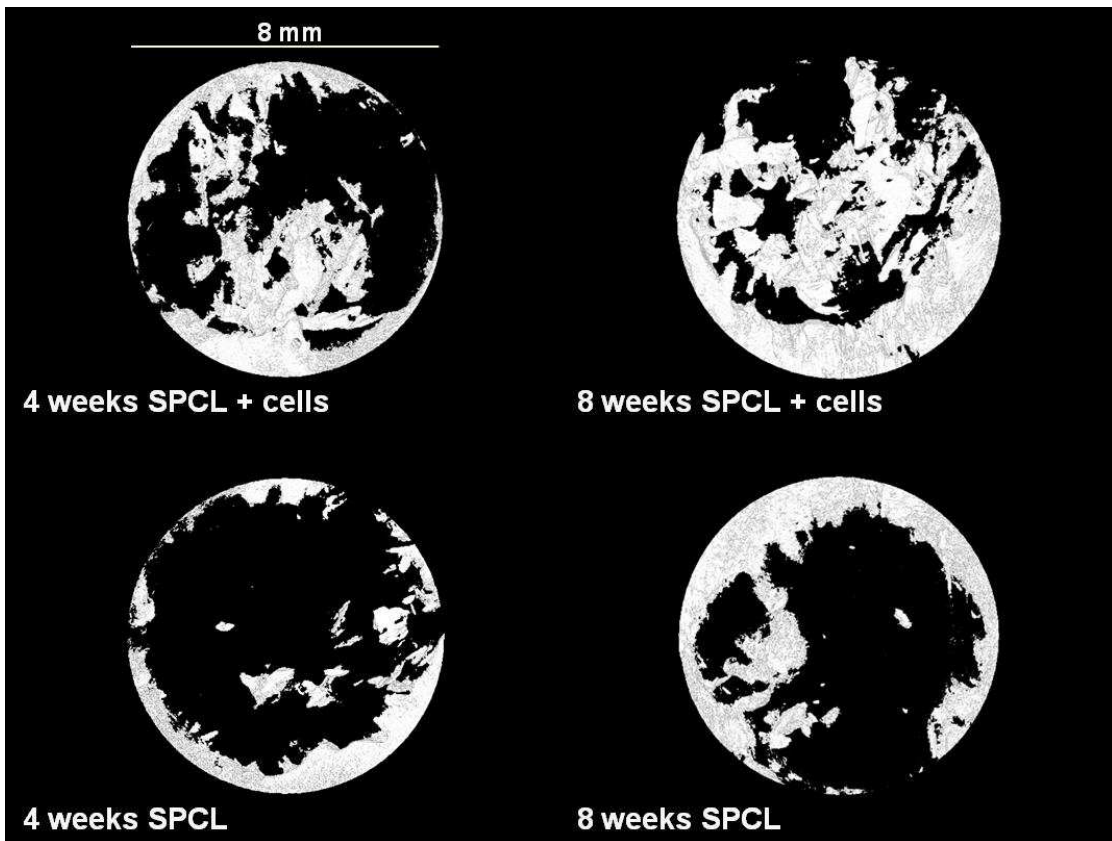


Figure 4.3. MicroCT reconstructions of the various implant formulations.

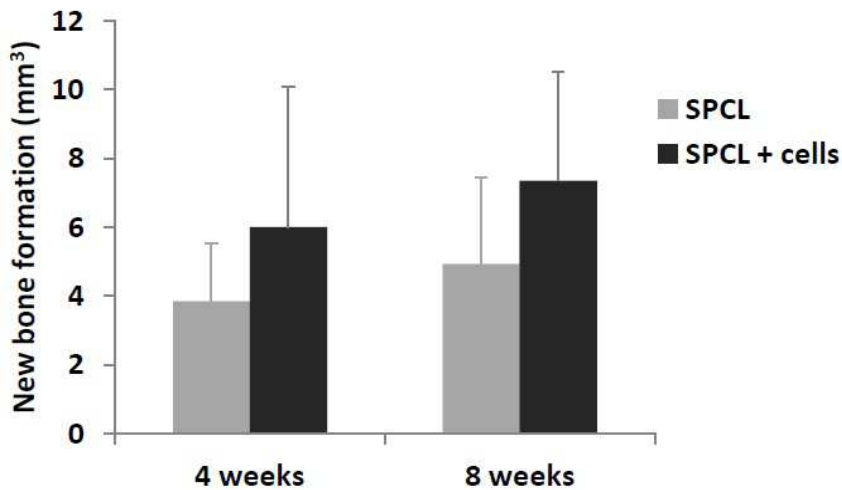


Figure 4.4. MicroCT quantification of the new bone formation of the various implant formulations.

#### 4.3.1.3 Histology

Light microscopic analysis of the obtained histological sections showed that after four weeks of implantation, minimal bone ingrowth from the cranial bone into the SPCL fiber meshes (without cells) had occurred. The SPCL meshes loaded with RBMSCs showed limited bone ingrowth from the cranial bone after four weeks of implantation, but some bone formation was found in the center of the implants.

The SPCL fiber meshes showed some new bone formation from the cranial bone after eight weeks of implantation and also some bone formation at the cerebral side of the implants occurred. However, no bridging of the entire defect was observed. The SPCL implants loaded with RBMSCs showed some new bone formation from the cranial bone into the implants and also bone was formed in the center of the implants, after 8 weeks of implantation. Although some bone formation at the cerebral side of the implants occurred, no bone bridging of the defect was noted. Empty defects showed minimal bone formation and no bone bridging were observed, confirming that the created defects were critical-sized. At all implantation periods, fibrous tissue between implants and cranial bone was observed, especially when there was no close contact between implant and bone. (Figure 4.5)

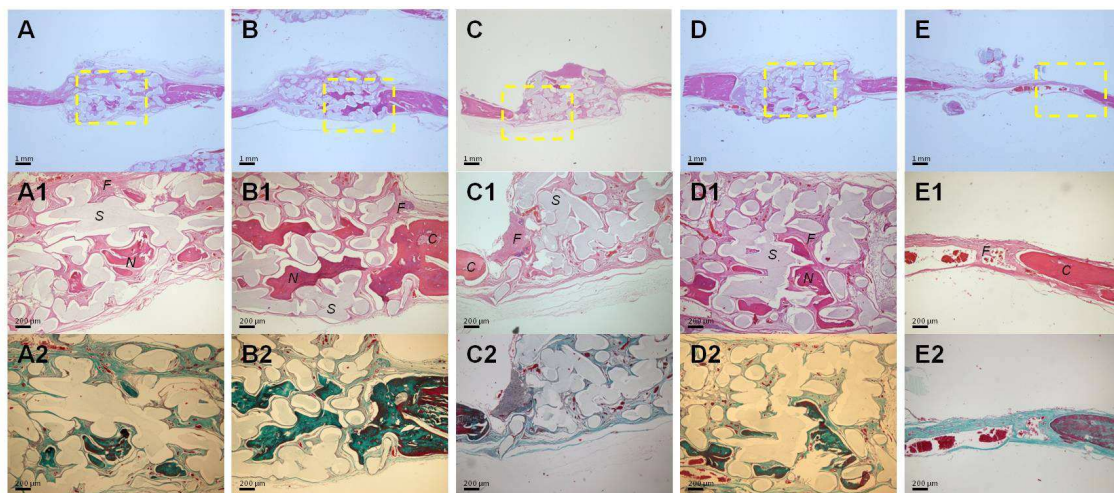


Figure 4.5. Histological sections stained with hematoxylin and eosin (first two rows) and Masson's trichrome (bottom row) of SPCL fiber meshes loaded with MSCs after four (A) and eight (B) weeks of implantation. Four (C) and eight (D) weeks of implantation of SPCL fiber meshes and empty controls (E) after eight weeks were stained as well. C = cranial bone; F = fibrous tissue; N = newly formed bone; S = SPCL fibers

#### 4.4 Discussion

Current drawbacks of cell-based bone tissue engineering approaches are the low yield of autologous cells with bone inducing capacities and the lack of standardized methods for expansion as well as for differentiation of bone progenitor cells. As a consequence, the reproducibility and predictability in human patients is low. Several solutions have already been suggested to solve this problem, like the use of cell selection (20, 21) or dynamic cell culturing (flow perfusion system).(22, 23) Furthermore, an autologous approach avoids immune responses that might jeopardize the recipient and also avoids adverse effects on the bone regeneration process. Still, the final cell population has to be incorporated in a scaffold material that possesses osteoconductive properties. For bone regeneration purposes, the ideal scaffold material is considered to be bioactive, slowly biodegradable, moldable and easy to apply. Also, the success of a scaffold material relies on an adequate porosity, and pores must be interconnective to allow bone and vascular ingrowth, diffusion of nutrients and waste removal. In our study, the used SPCL fiber meshes exhibit an interconnective porous network that seems to benefit cell ingrowth enabling access to nutrients, as well as the removal of metabolic wastes. However, the seeding efficiency of the SPCL fiber meshes was nearly 70%. This means a loss of about 30% on the cell seeding on the SPCL fiber meshes, suggesting that a downside of the interconnective porous network is that some cells go easily through the fiber meshes during seeding, without attaching to the SPCL. Especially when there is only a limited amount of cells available, a preferred solution could be to confine the scaffolds to a device that prevents cell suspension leakage. Also in a lesser extent, increasing the fiber content, increasing the fiber diameter, or mixing the SPCL fiber meshes with nano-sized fibers, could improve the cell seeding efficiency.(24, 25) Nonetheless, the results still showed that the relatively small number of cells implanted ( $1700 \text{ cells/cm}^3$ ) do benefit the bone regeneration process, whereas previous studies used a significant higher amount of seeded cells ( $>10.000 \text{ cells/cm}^3$ ) to get comparable results in a rat critical-sized cranial defect.(25, 26)

During surgery, when the implants were placed into the cranial defect, some infiltration of blood in the SPCL fiber meshes occurred. This could potentially influence the bone regeneration inside the implants. However, the effect of blood on bone repair remains controversial. To mimic the blood clot formation, platelet rich plasma (PRP) is a commonly used experimental approach, although results are not conclusive. Some studies claim that the effect of platelet rich plasma is impairing bone regeneration (27, 28), whereas other studies report a stimulated early bone repair (29, 30).

Also, some studies indicate that diluted amounts of PRP present in a bone graft stimulate bone formation, once it is dosed in a optimal concentration (30-32). Therefore, a moderate infiltration of blood could be beneficial for bone regeneration. In our study, new bone formation was present especially after 8 weeks of implantation. However no significant differences were observed between groups containing SPCL scaffolds loaded with RBMSCs compared to SPCL scaffolds without loaded cells. The lack of significant differences between the experimental groups might be explained by the infiltration of blood, as the growth factors present in the blood clot could contribute to the recruitment of osteogenic precursor cells, diminishing the effect of the loaded RBMSCs in the implants. Another reason for the lack of significant differences is that pre-seeded cells loaded on implants are essential in the early stages of bone regeneration, but eventually the hosts' own cells are responsible for the new bone formation, rather than the pre-seeded RBMSCs. In fact, it has been reported that pre-seeded RBMSCs indirectly contribute to the new bone formation by means of releasing growth factors, which in turn, recruit other cell types and therefore do not directly participate in new bone formation.(31, 33, 34)

Furthermore, some implants were more efficiently press-fitted into the critical-sized cranial defect than others, thus, not all implanted constructs were tightly in contact with the surrounding bone. More bone formation was observed when close contact between implant and bone was detected, compared to implants with less contact between the implant and the cranial bone. Previous studies showed that implant fixation is an important factor in the bone regeneration process.(17, 35) Lacking an optimal contact between bone and an implant causes fibrous tissue formation and therefore delays the bone forming process. This explains the relatively large standard deviation between implants from the same implantation group and further explains why the difference between the experimental groups is not significant.

However, MicroCT reconstructions showed that there is a clear trend, although not statistically significant, for increased bone formation in the defects filled with SPCL scaffolds seeded with RBMSCs, as compared to defects filled with SPCL scaffolds alone, at both 4 and 8 weeks of implantation. In fact, all experimental groups observed bone regeneration from the defect edges towards the interior of the implants but only in the groups with the pre-loaded RBMSCs, bone formation was also observed in the center of the implants. However, the additional amount of bone formed in the center of the implants was not sufficient to led to statistical significant differences between both groups



## 4.5 Conclusions

In general, histological analyses revealed that all study groups showed new bone formation from the defect edges towards the interior of the defects. Also, new bone was formed in the center of the scaffolds, especially in the groups containing pre-loaded RBMSCs. MicroCT reconstructions showed that bone formation increased over time and was enhanced with the inclusion of pre-loaded RBMSCs compared to SPCL scaffolds alone. According to these results, the pre-loaded RBMSCs contributed to the bone regeneration process in a critical-sized bone defect. Furthermore, SPCL fiber meshes proved to be a very suitable material to use for bone regeneration purposes.

## References

1. Tortelli, F., Cancedda, R. Three-dimensional cultures of osteogenic and chondrogenic cells: a tissue engineering approach to mimic bone and cartilage in vitro. *Eur Cell Mater* 17, 2009,1.
2. Zhang, Z. Bone regeneration by stem cell and tissue engineering in oral and maxillofacial region. *Frontiers of medicine* 5, 2011,401.
3. Ben-David, D., Kizhner, T., Livne, E., Srouji, S. A tissue-like construct of human bone marrow MSCs composite scaffold support in vivo ectopic bone formation. *J Tissue Eng Regen Med* 4, 2010,30.
4. Jones, E., Yang, X. Mesenchymal stem cells and bone regeneration: current status. *Injury* 42, 2011,562.
5. Gamie, Z., Tran, G.T., Vyzas, G., Korres, N., Heliotis, M., Mantalaris, A., et al. Stem cells combined with bone graft substitutes in skeletal tissue engineering. *Expert Opin Biol Ther*, 2012.
6. Zippel, N., Schulze, M., Tobiasch, E. Biomaterials and mesenchymal stem cells for regenerative medicine. *Recent Pat Biotechnol* 4, 2010,1.
7. Bodde, E.W., Habraken, W.J., Mikos, A.G., Spauwen, P.H., Jansen, J.A. Effect of polymer molecular weight on the bone biological activity of biodegradable polymer/calcium phosphate cement composites. *Tissue Eng Part A* 15, 2009,3183.
8. Bruder, S.P., Kraus, K.H., Goldberg, V.M., Kadiyala, S. The effect of implants loaded with autologous mesenchymal stem cells on the healing of canine segmental bone defects. *J Bone Joint Surg Am* 80, 1998,985.
9. Rodrigues, M.T., Lee, B.K., Lee, S.J., Gomes, M.E., Reis, R.L., Atala, A., et al. The effect of differentiation stage of amniotic fluid stem cells on bone regeneration. *Biomaterials* 33, 2012,6069.
10. Yuan, J., Zhang, W.J., Liu, G., Wei, M., Qi, Z.L., Liu, W., et al. Repair of canine mandibular bone defects with bone marrow stromal cells and coral. *Tissue Eng Part A* 16, 2010,1385.
11. Marques, A.P., Cruz, H.R., Coutinho, O.P., Reis, R.L. Effect of starch-based biomaterials on the in vitro proliferation and viability of osteoblast-like cells. *J Mater Sci Mater Med* 16, 2005,833.
12. Gomes, M.E., Azevedo, H.S., Moreira, A.R., Ella, V., Kellomaki, M., Reis, R.L. Starch-poly( $\epsilon$ -caprolactone) and starch-poly(lactic acid) fibre-mesh scaffolds for bone tissue engineering applications: structure, mechanical properties and degradation behaviour. *J Tissue Eng Regen Med* 2, 2008,243.

13. Gomes, M.E., Holtorf, H.L., Reis, R.L., Mikos, A.G. Influence of the porosity of starch-based fiber mesh scaffolds on the proliferation and osteogenic differentiation of bone marrow stromal cells cultured in a flow perfusion bioreactor. *Tissue Eng* 12, 2006,801.
14. Gomes, M.E., Sikavitsas, V.I., Behravesh, E., Reis, R.L., Mikos, A.G. Effect of flow perfusion on the osteogenic differentiation of bone marrow stromal cells cultured on starch-based three-dimensional scaffolds. *J Biomed Mater Res A* 67, 2003,87.
15. Rodrigues, M.T., Gomes, M.E., Viegas, C.A., Azevedo, J.T., Dias, I.R., Guzon, F.M., et al. Tissue-engineered constructs based on SPCL scaffolds cultured with goat marrow cells: functionality in femoral defects. *J Tissue Eng Regen Med* 5, 2011,41.
16. Santos, T.C., Marques, A.P., Horing, B., Martins, A.R., Tuzlakoglu, K., Castro, A.G., et al. In vivo short-term and long-term host reaction to starch-based scaffolds. *Acta Biomater* 6, 2010,4314.
17. Link, D.P., van den Dolder, J., van den Beucken, J.J., Habraken, W., Soede, A., Boerman, O.C., et al. Evaluation of an orthotopically implanted calcium phosphate cement containing gelatin microparticles. *J Biomed Mater Res A* 90, 2009,372.
18. Cornejo, A., Sahar, D.E., Stephenson, S.M., Chang, S., Nguyen, S., Guda, T., et al. Effect of Adipose Tissue-Derived Osteogenic and Endothelial Cells on Bone Allograft Osteogenesis and Vascularization in Critical-Sized Calvarial Defects. *Tissue Eng Part A* 10, 2012, [Epub ahead of print].
19. Song, K., Rao, N.J., Chen, M.L., Huang, Z.J., Cao, Y.G. Enhanced bone regeneration with sequential delivery of basic fibroblast growth factor and sonic hedgehog. *Injury* 42, 2011,796.
20. Rada, T., Gomes, M.E., Reis, R.L. A novel method for the isolation of subpopulations of rat adipose stem cells with different proliferation and osteogenic differentiation potentials. *J Tissue Eng Regen Med* 5, 2011,655.
21. Mihaila, S.M., Frias, A.M., Pirraco, R., Rada, T., Reis, R.L., Gomes, M.E., et al. Human Adipose Tissue-Derived SSEA-4 Sub-Population Multi-Differentiation Potential Towards the Endothelial and Osteogenic Lineages. *Tissue Eng Part A* accepted.
22. Bjerre, L., Bungler, C., Baatrup, A., Kassem, M., Mygind, T. Flow perfusion culture of human mesenchymal stem cells on coralline hydroxyapatite scaffolds with various pore sizes. *J Biomed Mater Res A* 97, 2011,251.
23. Goncalves, A., Costa, P., Rodrigues, M.T., Dias, I.R., Reis, R.L., Gomes, M.E. Effect of flow perfusion conditions in the chondrogenic differentiation of bone marrow stromal cells cultured onto starch based biodegradable scaffolds. *Acta Biomater* 7, 2011,1644.

24. Tuzlakoglu, K., Bolgen, N., Salgado, A.J., Gomes, M.E., Piskin, E., Reis, R.L. Nano- and micro-fiber combined scaffolds: a new architecture for bone tissue engineering. *J Mater Sci Mater Med* 16, 2005,1099.
25. Santos, M.I., Tuzlakoglu, K., Fuchs, S., Gomes, M.E., Peters, K., Unger, R.E., et al. Endothelial cell colonization and angiogenic potential of combined nano- and micro-fibrous scaffolds for bone tissue engineering. *Biomaterials* 29, 2008,4306.
26. Yoon, E., Dhar, S., Chun, D.E., Gharibjanian, N.A., Evans, G.R. In vivo osteogenic potential of human adipose-derived stem cells/poly lactide-co-glycolic acid constructs for bone regeneration in a rat critical-sized calvarial defect model. *Tissue Eng* 13, 2007,619.
27. Giovanini, A.F., Gonzaga, C.C., Zielak, J.C., Deliberador, T.M., Kuczera, J., Goringher, I., et al. Platelet-rich plasma (PRP) impairs the craniofacial bone repair associated with its elevated TGF-beta levels and modulates the co-expression between collagen III and alpha-smooth muscle actin. *J Orthop Res* 29, 2011,457.
28. Giovanini, A.F., Deliberador, T.M., Gonzaga, C.C., de Oliveira Filho, M.A., Gohringer, I., Kuczera, J., et al. Platelet-rich plasma diminishes calvarial bone repair associated with alterations in collagen matrix composition and elevated CD34+ cell prevalence. *Bone* 46, 2010,1597.
29. Gerard, D., Carlson, E.R., Gotcher, J.E., Jacobs, M. Effects of platelet-rich plasma on the healing of autologous bone grafted mandibular defects in dogs. *J Oral Maxillofac Surg* 64, 2006,443.
30. Gerard, D., Carlson, E.R., Gotcher, J.E., Jacobs, M. Effects of platelet-rich plasma at the cellular level on healing of autologous bone-grafted mandibular defects in dogs. *J Oral Maxillofac Surg* 65, 2007,721.
31. Choi, B.H., Zhu, S.J., Kim, B.Y., Huh, J.Y., Lee, S.H., Jung, J.H. Effect of platelet-rich plasma (PRP) concentration on the viability and proliferation of alveolar bone cells: an in vitro study. *Int J Oral Maxillofac Surg* 34, 2005,420.
32. Nagata, M.J., Messoria, M., Pola, N., Campos, N., Vieira, R., Esper, L.A., et al. Influence of the ratio of particulate autogenous bone graft/platelet-rich plasma on bone healing in critical-size defects: a histologic and histometric study in rat calvaria. *J Orthop Res* 28, 2010,468.
33. Tasso, R., Augello, A., Boccardo, S., Salvi, S., Carida, M., Postiglione, F., et al. Recruitment of a host's osteoprogenitor cells using exogenous mesenchymal stem cells seeded on porous ceramic. *Tissue Eng Part A* 15, 2009,2203.
34. Tasso, R., Fais, F., Reverberi, D., Tortelli, F., Cancedda, R. The recruitment of two consecutive and different waves of host stem/progenitor cells during the development of tissue-engineered bone in a murine model. *Biomaterials* 31, 2010,2121.

35. Link, D.P., van den Dolder, J., Jurgens, W.J., Wolke, J.G., Jansen, J.A. Mechanical evaluation of implanted calcium phosphate cement incorporated with PLGA microparticles. *Biomaterials* 27, 2006,4941.

## **SECTION 4**

### **Chapter V**

#### **A Novel Bidirectional Continuous Perfusion Bioreactor for the culture of large sized bone tissue engineered constructs**

This chapter is based on the following publication:\_Gardel LS, Serra LA, Gomes ME., Reis RL A Novel Bidirectional Continuous Perfusion Bioreactor for the culture of large sized bone tissue engineered constructs. Submitted 2012



## **Abstract**

This work reports the development and preliminary assessment of a new bioreactor for the culturing of large sized 3D scaffolds–cells constructs aimed at applications in bone tissue engineering. The Bidirectional Continuous Perfusion Bioreactor (BCPB) was designed to promote the mechanical stimulation of cells through the creation of shear forces induced by flow perfusion, using different pressure gradients, controlled by a peristaltic pump. Additionally, it provides the possibility of varying both perfusion flow rate and direction. However, the main innovation of the system herein presented consists in the possibility of culturing scaffolds of large dimensions that can be suitable for the regeneration of critical size defects, as the control of flow perfusion and pressure gradient in the inside/outside of the scaffold, enables a culture environment that favours the access to nutrients and removal of metabolic wastes of the cells located in the inner regions. The functionality of the developed system was preliminarily evaluated by culturing starch/polycaprolactone (SPCL) fibers mesh scaffolds with previously seeded goat bone marrow stromal cells (GBMSC's) for 14 and 21 days. For this purpose, cylindrical blocks (16mm of diameter) of cell-seeded scaffolds were stacked into a 42 mm thick construct. Static cultured constructs were used as controls. The samples resulting from these experiments were characterized concerning DNA content, ALP activity and cell morphology/distribution using scanning electron microscopy and histological analysis. The results showed higher ALP activity levels in the bioreactor cultures than those obtained under static conditions. However, the number of cells (obtained from DNA amounts) in constructs cultured in the bioreactor showed lower values compared to static cultures, suggesting that static conditions tend to privilege the metabolic pathway for cellular proliferation while dynamic conditions tend to privilege the metabolic pathway for osteogenic differentiation. Histologically, it was observed that the migration was improved and homogenous cell distribution was observed in the bioreactor groups. In conclusion, these results demonstrate the feasibility and the benefit of culturing cell/SPCL constructs in this BCPB system.



## 5.1 Introduction

A major challenge in the translation of tissue engineered bone grafts to viable clinical treatments of osseous defects has been the need to grow large, fully viable grafts that are several centimetres in size. The current size limitations are primarily due to the limited transport of metabolites to cells within the core regions of the graft that prevents cell survival and proliferation. Traditionally, in two-dimensional (2D) cell culture techniques (e.g., Petri dishes and culture flasks), a monolayer of cells is in continuous contact with the culture medium, and simple diffusion is sufficient to maintain cell viability (1), but these conditions are clearly inadequate for culturing cells seeded onto three-dimensional (3D) tissue engineering scaffolds. Given the clinical need to use 3D tissue constructs of large dimensions, the use of perfusion bioreactors has shown evident advantageous over static culturing, as these systems usually allow a more efficient transfer of nutrients and oxygen, stimulating the development of homogeneous tissue cultured *in vitro* for subsequent implantation. Whereas the primary role of perfusion has been to increase the transport rates of nutrients, metabolites, and oxygen to and from the cells, interstitial flow of medium has the additional benefit of providing hydrodynamic shear stress induced stimulation, a known regulatory factor of bone development and function (2). In fact, several previous studies, have demonstrated that the use of bioreactors with a flow medium favours bone-like tissue formation within 3D tissue constructs (3-6). However, these works have focused on culturing small constructs, not addressing the clinical need for developing grafts that can be used in the regeneration of critical sized defects. Based in this approach, we aimed to develop and optimize *in vitro* conditions to create functional bone tissue in 3D tissue constructs of large dimensions. For this purpose we designed and developed a new perfusion bioreactor named Bidirectional Continuous Perfusion Bioreactor (BCPB), presenting an innovative and advanced design. The BCPB creates mechanical cellular stimulus through the generation of shear forces due to medium flow perfusion using different pressure gradients, controlled by peristaltic pumps. Additionally, it provides the possibility of varying both perfusion flow rate/flow direction through rotational forces generated by mechanical engines specifically designed for the BCPB. Furthermore, the flow-perfusion bioreactor is a scalable technology that should support porous scaffolds of any thickness.

This is, in fact the main innovation of the BCPB, as it enables the possibility of culturing scaffolds of large dimensions, since the systems allows the control of flow perfusion and pressure gradient inside and outside of the scaffold, providing the adequate access to nutrients and removal of metabolic wastes of the cells located in the inner regions of thick 3D constructs, thereby maintaining cell viability and activity. The feasibility of this new flow-perfusion bioreactor in sustaining “thick” 3D tissue constructs that approaches sizes of surgical importance was also addressed in the present work. For this purpose, constructs composed of SPCL (a blend of starch and polycaprolactone) fiber meshes of 16 mm diameter (with a 6mm interior hole) and 3 mm thick, were seeded with  $1 \times 10^6$  goat marrow stromal cells (GBMCSs) and stacked, completing a 42 mm thick 3D tissue construct. After 14 and 21 days of culture in the bioreactor at a flow rate of 1 ml/min, the samples were collected for MTS, DNA and ALP assays, histological analysis and scanning electron microscopy (SEM). Static cultured constructs were used as controls. The results obtained demonstrated that this new flow-perfusion bioreactor provides adequate conditions to enable cells distribution into the core of a thick scaffold and stimulates osteogenic differentiation of GBMSC’s. It is envisioned that this bioreactor may lead to significant advances in bone tissue engineering, enabling the culture of 3D constructs of large dimensions with different scaffolds compositions and with stem cells of different sources

## **5.2. Materials and Methods**

### **5.2.1 Flow-perfusion bioreactor design philosophy**

The main aim of this work was to develop a new flow perfusion system for culturing 3D-scaffolds of large dimensions for bone tissue engineering, thus a system that would enable cellular distribution into a thick construct, enabling maintenance of cell viability/functionality in the interior of the scaffold. In order to develop such system, several other basic requirements were considered: this should be easily sterilized and maintained in sterile conditions throughout the culture period, the system should be reasonable easy to operate and deliver the flow through the scaffolds enabling a controllable, repeatable, and reliant rate of flow to meet the envisioned requirements.

The designed and developed perfusion bioreactor was named BiDirectional Continuous Perfusion Bioreactor (BCPB) and is mainly composed of the following elements: (1) One single culture chamber that enables culturing cell-seeded 3D constructs of large dimensions, up to 120 mm in length and 60 mm in diameter (2) a perfusion flow system that allows controlling the medium flow passage from the inside of the scaffold to the culture chamber and/or the passage of the medium circulating in the culture chamber to the inside of the scaffold, enabling the access to nutrients by the cells in the scaffold interior as well as the removal of their metabolic products.

For this purpose, the systems uses a perforated tube (Fig 5.1 A and B) into which the scaffold is inserted; Then by manipulating the flow directions, using the peristaltic and vacuum pumps, it is possible to direct the perfusion of medium into the interior of the construct and/or from there to the culture chamber. This is the system feature that is expected to assure a uniform cellular distribution in the construct, enabling an adequate access to nutrients and removal of metabolic wastes.

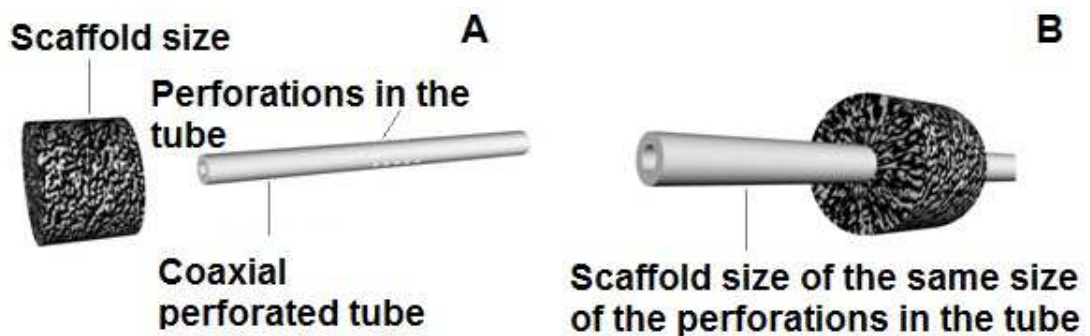


Figure 5.1. A) Coaxial perforated tube in polycarbonate and scaffold. B) Scaffold positioned in the tube.

### 5.2.2. Construction and functioning of the BCPB

The BCPB is constituted by a cell culture chamber (Figure 5.2A) made of acrylic, transparent, with four output/inputs connected to three-way valves that are connected to silicone tubes (to allow the passage of the culture medium); these three-way valves enable the possibility of connecting syringes for antibiotics and growth factors inoculation and/or connecting sensors for pressure,  $O_2$ ,  $CO_2$ , Ph and glucose. In each end of the cell culture chamber, a part made of teflon is connected to promote a hermetic and waterproof sealing.

These parts present an hexagonal form that, when levelled with the other part, allows the linear positioning of the bioreactor when placed on a flat surface; these parts also have a round and smooth shape section, that allows the support of the entire system in arms that connect to the support base, keeping the whole system sustained when operating inside of the incubator (Figure 5.2B). To hold the constructs/samples in the culture chamber, it is used a perforated coaxial tube made of polycarbonate that can have variable length and number of holes, depending on the size of the three-dimensional construct to be used (Figure 5.1 A and B).

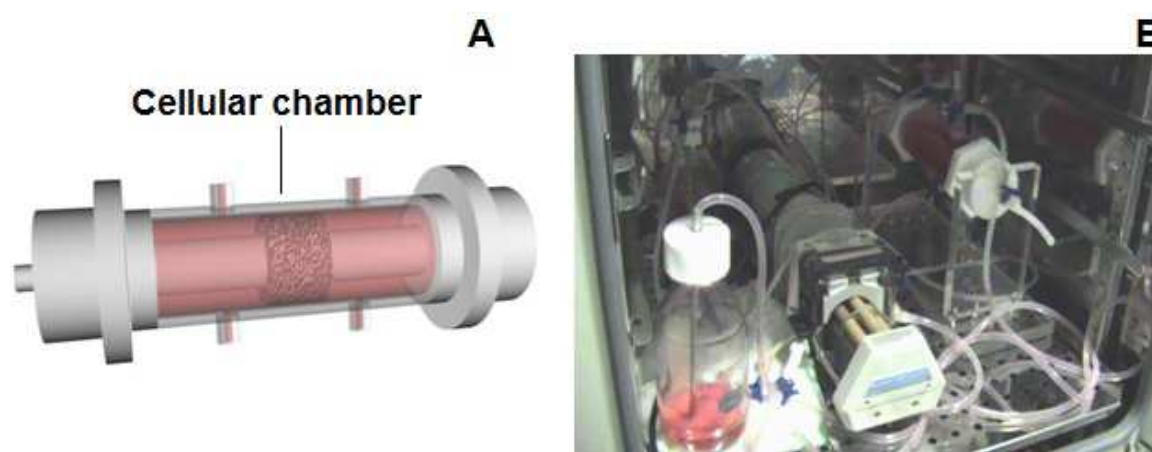


Figure 5.2. A) Representation of the cell culture chamber with the scaffolds inserted in the perforated tube and filled with medium culture. B) Picture of the complete BiDirectional Continuous Perfusion Bioreactor (BCPB) system under operation in a CO<sub>2</sub> incubator.

The perforated coaxial tube, coming from within the bioreactor is connected to the continuous circular flow system through a three-way valve. The circular flow system (Figure 5.3) is composed of a peristaltic pump responsible for the positive flow gradient, a vacuum pump responsible for the negative flow gradient and a collector bottle for the culture medium; additionally, a reservoir bottle is associated to the peristaltic pump, and another reservoir bottle to the vacuum pump. The balance between positive and negative gradient within the bioreactor is monitored by connecting a pressure gauge to the cell culture chamber and the vacuum pump can be adjusted to maintain the pressure gauge within the bioreactor at zero. The exchange of the flow direction is performed by changing the positioning of the tubes (connected to the peristaltic and vacuum pump) in the two inputs in the bioreactor.

A three-way valve is positioned between the collector bottle and the reservoir bottle of the peristaltic pump, which will function, when desired, directing the flow from the bottle directly to the peristaltic pump, allowing to exchange the culture medium, without being necessary to stop the entire flow system.

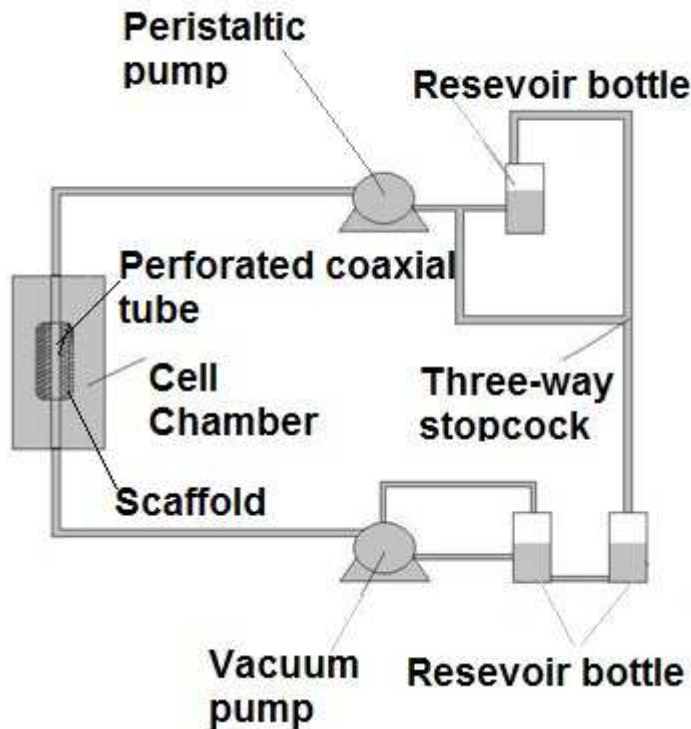


Figure 5.3. Schematic representation of the flow system “circuit” that is associated with the continuous bi-directional flow bioreactor

### 5.2.3 Preliminary evaluation of the bioreactor functionality

#### 5.2.3.1 Scaffolds design and preparation

The polymer scaffolds used in this study are based on a biodegradable polymer blend of starch and polycaprolactone (SPCL) that has been intensively investigated for tissue engineering applications (7-11). The 3D scaffolds were produced from melt spun fibers by a fibre-bonding method into mesh structures with a porosity of ~75%, as described previously (5, 6). SPCL fiber mesh scaffolds have shown very promising results for bone tissue regeneration in previous studies (8, 11-17).

In the present study, SPCL fiber meshes were cut into samples disks of 16mm diameter and 3mm of thicknesses with a 6mm interior hole; this inner hole allows the

samples/constructs to be positioned within the bioreactor by inserting them into the polycarbonate perforated tube, enabling the bidirectional medium flow, from the interior of the constructs to the outside (culture chamber) or from outside to the interior of the samples (Figure 5.4).

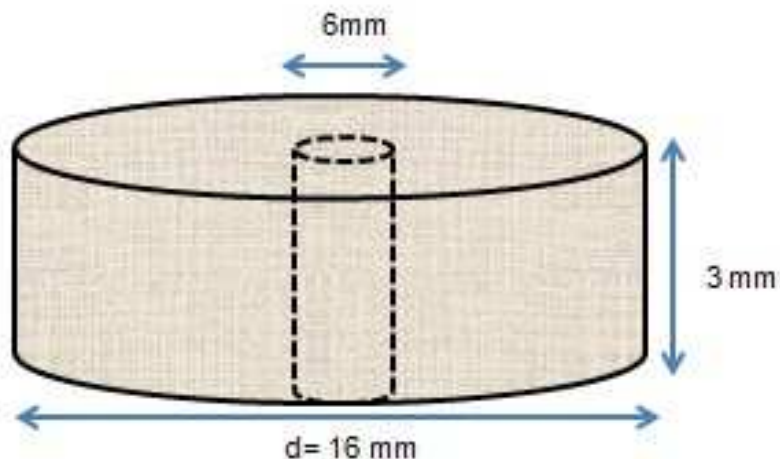


Figure 5.4. Schematic representation of the SPCL fiber-mesh scaffolds samples used in this study.

### 5.2.3.2 Cell seeding of scaffolds

GBMSC's were isolated and expanded in vitro as previously described (8). The sterile SPCL fiber mesh samples were placed in non adherent 12 well -plate (Costar<sup>®</sup> Corning; NY). A total of 56 samples were seeded with a 300 $\mu$ l cell suspension containing  $1 \times 10^6$  cells in basal medium composed of  $\alpha$ -MEM (Minimal Essential Medium) with 10 % FCS (foetal calf serum, Gibco), 50  $\mu$ g/ml gentamycin, 100  $\mu$ g/ml ampicillin and 0.3  $\mu$ g/ml fungizone were added (all sigma) The well plates were then transferred to the incubator and three hours after seeding 1.6 ml of basal medium was added to each well and incubated overnight. (at 37  $^{\circ}$ C environment with 5% CO<sub>2</sub>) to allow cell attachment. In the following day, the cell-scaffolds constructs were either transferred to the bioreactor or kept in static conditions. In the later case, 10 mL of osteogenic medium composed of  $\alpha$ -MEM, supplemented with 10 % FCS (foetal calf serum, Gibco), 50  $\mu$ g/ml ascorbic acid (Sigma, St.Louis, MO, USA), 50  $\mu$ g/ml gentamin, 100  $\mu$ g/ml ampicillin, 0.3  $\mu$ g/ml fungizone, 10 mM Na  $\beta$ -glycerophosphate and  $10^{-8}$  M dexamethasone (all Sigma), was added to each well, in order to try to approximate the construct-mediums volume ratio to the one in the bioreactor(15 ml per sample). The culture medium was changed each 7 days.

### 5.2.3.3 Bioreactor culture

The plates containing cell-scaffolds constructs to be cultured in the bioreactor were carefully transferred to two BCPB's, in a laminar flow cabinet, as follows: each sample (3mm length and 16 mm diameter, with a inner hole of 6mm) was carefully inserted into the polycarbonate perforated tube and stacked until completing a total of 14 samples, corresponding to a 42 mm length construct. The perforated tube with the construct was then connected to the two end parts of the bioreactor that aims to promote the hermetic and aseptic closure of the culture chamber. Afterwards the main chamber of the bioreactor was connected to the flow system and slowly filled with the culture medium at a rate of 1ml/min, with the flow directed from inside the chamber to the perforated tube, enabling the medium to flow from outside to inside the cells-scaffold construct. Finally, the whole system was transferred to the incubator (at 37°C environments with 5% CO<sub>2</sub>) where it was operated for 14 and 21 days. The culture chamber has a capacity for 216 ml of culture medium while the bottle reservoir has a capacity of 450 ml of medium; every week 400 ml of old medium were exchanged with 400 ml of new medium, without stopping medium flow in the bioreactor system. Each sample of the static group was cultured in the presence of 10 ml of culture medium which was changed every week.

#### **5.2.4. –Characterization of cell-scaffolds constructs**

At the end of time point of culture, cell-scaffolds constructs were collected for DNA (n=3 per group and time point), ALP (n=3 per group and time point), and MTS (n=3 per group and time point), assays, for SEM (n=2 per group and time point), and for histological analysis (n=3 per group and time point). Each sample was carefully and aseptically removed from the polycarbonate perforated tube and washed 3 times in PBS.

##### **5.2.4.1 Cell proliferation and viability analysis**

The scaffolds-cells constructs retrieved at the end of each time point, were rinsed 3 times with PBS, placed in a vial containing 3 ml of ultrapure water and frozen at -80°C overnight; after this were lysed by osmotic and thermal shock and the supernatant used for the DNA quantification assay. DNA concentration was measured using the Quant-iT™ Picogreen® dsDNA Assay Kit (Invitrogen™, Molecular Probes™, Oregon USA).A description of the assay can be found elsewhere (18). Triplicates were made for each sample and per culturing time.

The DNA concentration for each sample was calculated using a standard curve (DNA concentration ranging from 0.0 to 4.5µg/ml) relating quantity of DNA and fluorescence intensity.

The cellular viability was assessed by a colorimetric assay named CellTiter 96<sup>®</sup> AQueos One Solution Cell Proliferation Assay (Promega, USA). The principle of this assay is based on the bioreduction of a tetrazolium compound [(3-(4,5-dimethylthiazol-2-yl)-5-(3-carboxymethoxyphenyl)-2(4-sulphophenyl)-2Htetrazolium, inner salt(MTS)] into a brown formazan product that is soluble in culture medium (19). This conversion is accomplished by the production of nicotinamide adenosine dinucleotide phosphate (NADPH) or nicotinamide adenine dinucleotide (NADP) by the dehydrogenase enzymes existing in the metabolically active cells. The quantity of formazan product measured by the amount of 490nm absorbance in a microplate reader (Bio-Tek, model Synergie HT; USA). Three specimens per condition and per time point were characterized.

#### **5.2.4.2 Determination of alkaline phosphatases (ALP) activity of cells on scaffolds**

The ALP activity was determined for all time culture periods, using the same samples used for DNA quantification. The activity of ALP was assessed using the *p*-nitrophenol assay. Nitrophenol phosphate disodium salt (pnPP;Fluka BioChemika, Austria), was hydrolysed by the alkaline phosphatase produced by the cells to form free *p*-nitrophenol. Standards were prepared with 10  $\mu\text{mol/ml}$  *p*-nitrophenol(pNP;Sigma, USA) solution, to obtain a standard curve ranging from 0 to 0.4  $\mu\text{molALP}/\mu\text{DNA/h}$ . Triplicates of each sample and standard were made, and the ALP concentrations were read directly from the standard curve.

#### **5.2.4.3 Cell morphology analysis**

The morphological analysis of cells as well as their growth, attachment, and distribution on the surface of the scaffolds was performed with a Scanning Electron Microscopy (SEM). For this purpose, the scaffolds-cells constructs were rinsed 3 times with PBS and then fixed with 2.5 % Glutaraldehyde (Sigma,USA) in PBS solution during 1 hour at 4°C; after this, samples were dehydrated through a graded series of ethanol and let to dry overnight at room temperature. Finally, samples were gold sputter coated (Fisons Instruments, model SC502; England), and analyzed with SEM (Leica Cambridge, model S360; England)-



#### **5.2.4.4 Histological analysis**

The cell-scaffolds samples were rinsed in PBS, fixed in 4% formalin, and embedded in methacrylate (Technovit® 7100 NEW, Kulzer, DE) The procedure was based on the protocol provided by the manufacturer and cut into 10 µm sections. In order to observe cells and the formed matrix, sections were stained with hematoxylin & eosin. Samples were then visualized under a light microscope and images taken with an attached camera.

#### **5.2.5 Statistical Analysis**

The PASW Statistics18 software package (IBM, Somers, NY) was used for the statistical analysis. Descriptive values are presented as mean ± SD unless stated otherwise. Kolmogorov-Smirnov test with Lilliefors significance correction was used to test the normality of the data. The one way ANOVA test was used to determine statistically significant differences among the groups and Tukey test was used to assess the pairwise comparisons between groups. The statistical significance level considered was  $P < 0.05$ .

### **5.3. Results**

#### **5.3.1 Alkaline phosphatases activity**

The osteogenic phenotypic expression of cells was evaluated by a colorimetric assay for alkaline phosphatase activity. The Figure (5.5 A) shows the ALP activity results corresponding to day 0, day 14 and day 21 of culturing in the bioreactor and static condition. The ALP activity registered for samples resulting from flow cultures at day 14 was statistically significantly higher as compared to all other groups [day 0 ( $P=0.015$ ); day 14 static ( $P=0.015$ ); day 21 static ( $P=0.016$ ) and day 21 flow ( $P=0.004$ )]. The maximum and minimum ALP activity registered was higher for flow perfusion conditions when compared to static culture at all time points (Figure 5.5 B), clearly suggesting that bone cell phenotype expression was stimulated under dynamic flow. Under static conditions a low level of ALP activity was registered which remained unchanged over the culture period studied.

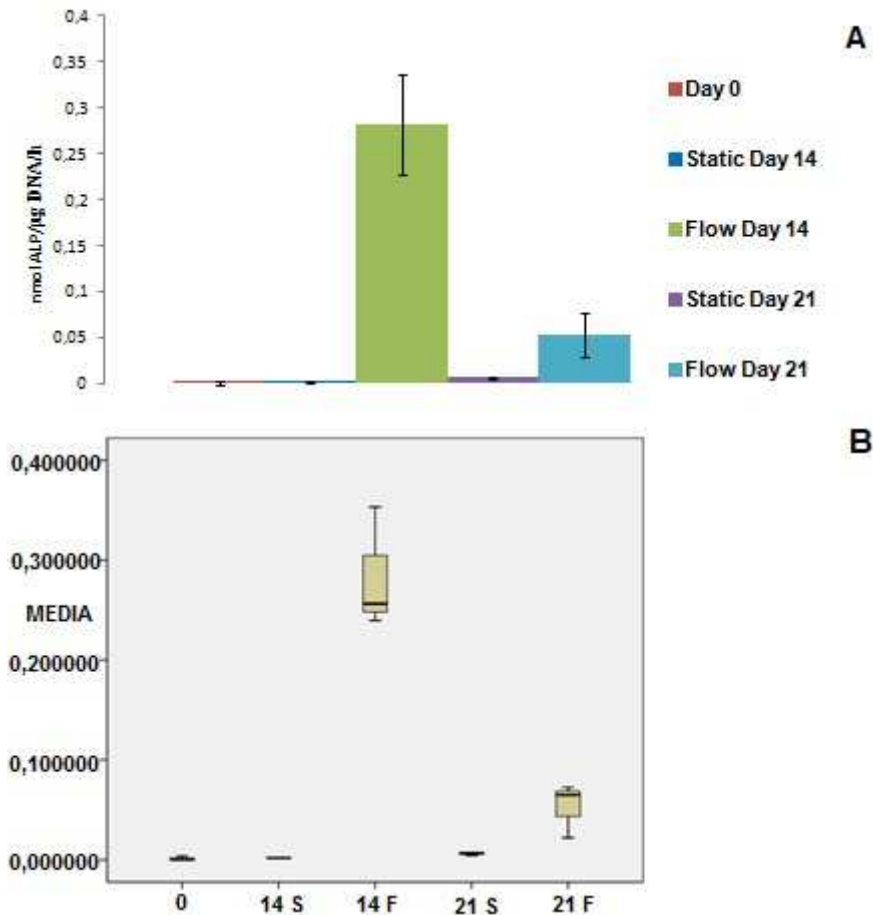


Figure 5.5. ALP activity in static and flow culture (A), and maximum and minimum ALP activity values expressed (B).

### 5.3.2 Cell proliferation

DNA quantification results showed higher cellular content in constructs cultured in static conditions, as compared to those cultured in the flow perfusion bioreactor (Figure 5.6 A). It was registered a statistical significant difference between constructs retrieved at day 14 after static culture and constructs retrieved at day 14 after flow culture ( $P=0.010$ ); and similarly, between day 21 static and day 21 flow ( $P=0.027$ ). However, under static conditions, statistical increase of DNA concentration over time was not registered, as observed when comparing the results between day 14 static and day 21 static ( $P=0.645$ ). Nevertheless, the Figure 5.6A shows an increase in DNA concentration between day 14 and day 21 in constructs cultured in the flow perfusion bioreactor, although it was not found a significant difference between these two groups ( $P=0.185$ ).

However, it is possible to observe in figure (5.6 B) that the maximum and minimum DNA concentration values, corresponding to the construct cultured for 21 days under flow perfusion are higher than the 14 days flow, demonstrating a trend for cellular proliferation over time in the bioreactor culture.

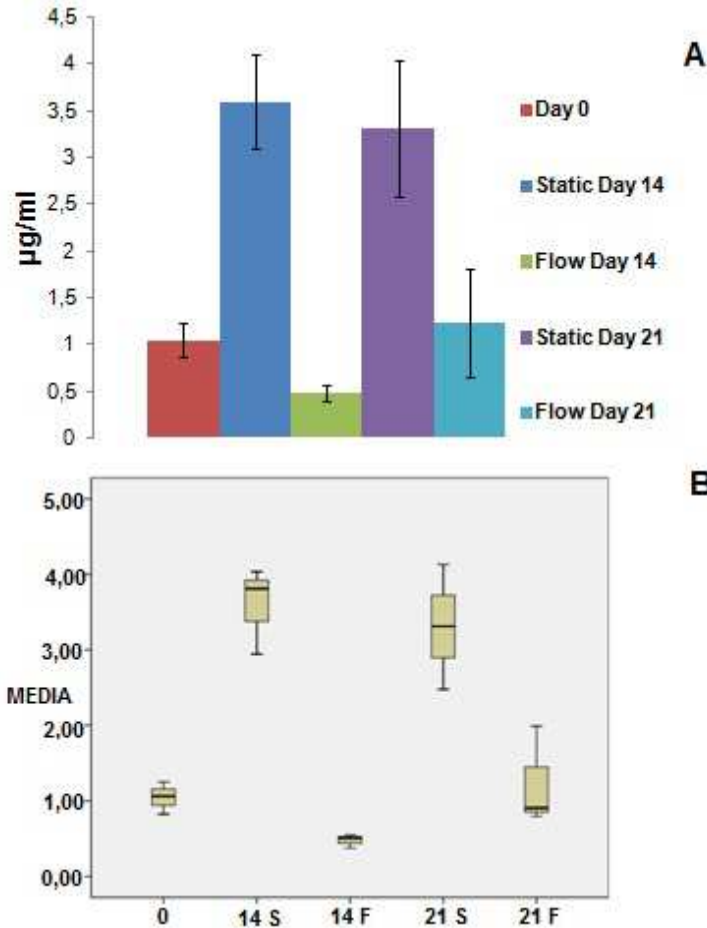


Figure 5.6. DNA concentration in static and flow culture (A) and maximum and minimum DNA concentration values expressed (B).

### 5.3.3 Cellular viability

MTS quantification results showed a tendency for higher cellular viability under static conditions, which is in good agreement with DNA results (Figure 5.7). In fact, an enhanced cell metabolic activity in static cultures was observed as compared to flow cultures, at day 14 ( $P < 0.001$ ) and at day 21 ( $P = 0.005$ ). Under static conditions there seems to be an increase in the metabolic activity between day 14 and day 21, but this increase was not significantly different ( $P = 0.176$ ). Similarly, an increase in cells metabolic activity between day 14 and day 21 under flow was registered, although it was also not found a significant difference between these two groups ( $P = 0.163$ ).

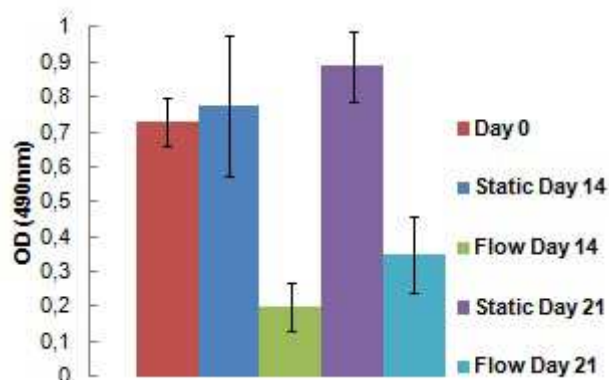


Figure5.7. MTS quantification in static and flow culture

### 5.3.4 Cell Morphology

The cell adhesion and distribution in the scaffolds was visualized using SEM. Analysis from day 0 (control) showed that cells accumulated mainly on the surface of the GBMSC's–SPCL constructs (Figure5.8). However, after 14 and 21 days of culture under bioreactor culture, the cells occupied predominantly the interior of GBMC–SPCL constructs. The cells are clearly forming layers evenly distributed around the GBMSC's–SPCL constructs (Figure 5.9 A and B/ Figure 5.10 A and B). SEM analysis of the static groups showed that fewer cells were present within the GBMSC's–SPCL constructs interior where probably the nutrients are insufficient to maintain cell viability (Figure 5.11 A and B).

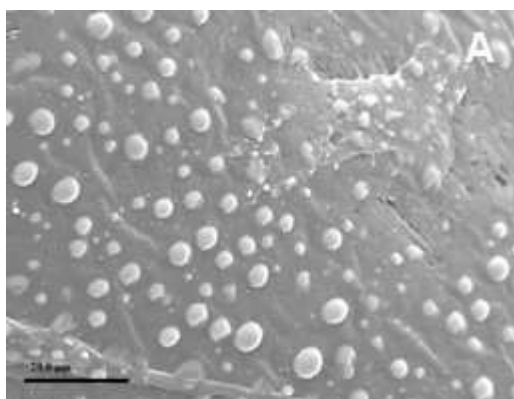


Figure5.8. A) Cells in the interior of the scaffolds in day 0, x1000.

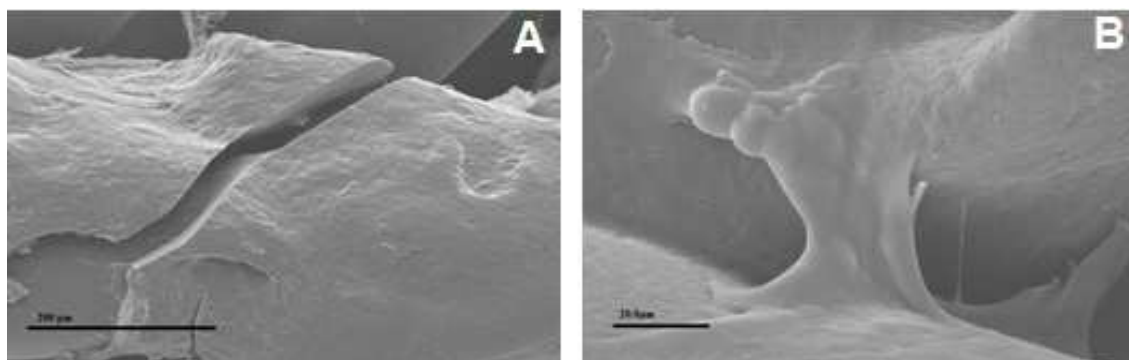


Figure 5.9. A) Cells in the interior of the scaffolds in day 14 flow, x 200. B) Day 14 flow, x1000.

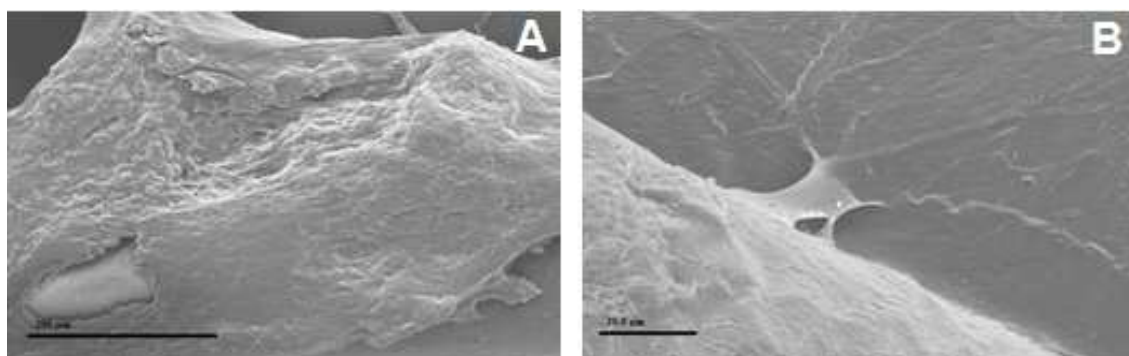


Figure 5.10. A) Cells in the interior of the scaffolds in day 21 flow, x200. B) Day 21 flow, x1000.

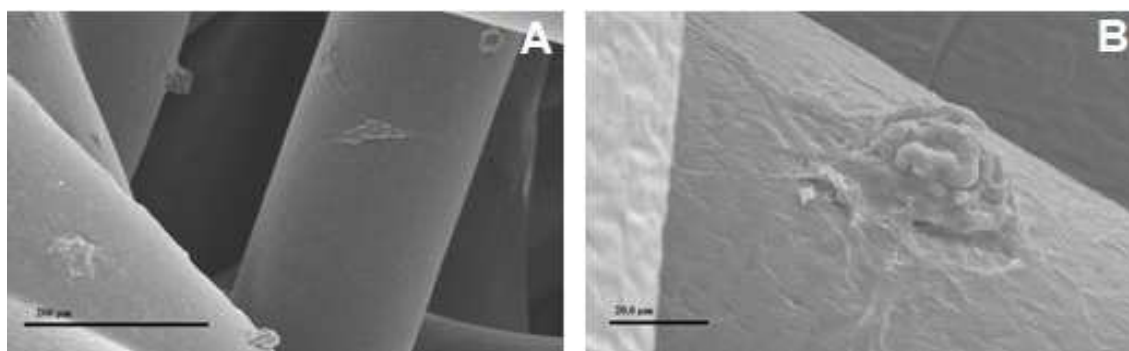


Figure 5.11. A) Cells in the interior of the scaffolds in day 14 static, x200. B) Day 21 static, x1000.

### 5.3.5 Histological analysis

The observation of sections stained with H&E (Figure 5.12 A and B), shows that there was cell proliferation and distribution and ECM formation in the GBMSC's-SPCL constructs cultured under perfusion in 14 and 21 days, which suggests the importance of the bioreactor system to stimulate cell growth and uniform distribution.

Under static culture, few cells were found in the samples sections, and these showed little ability to synthesizes ECM after 14 and 21 days of culture (Figure 5.13 A and B).

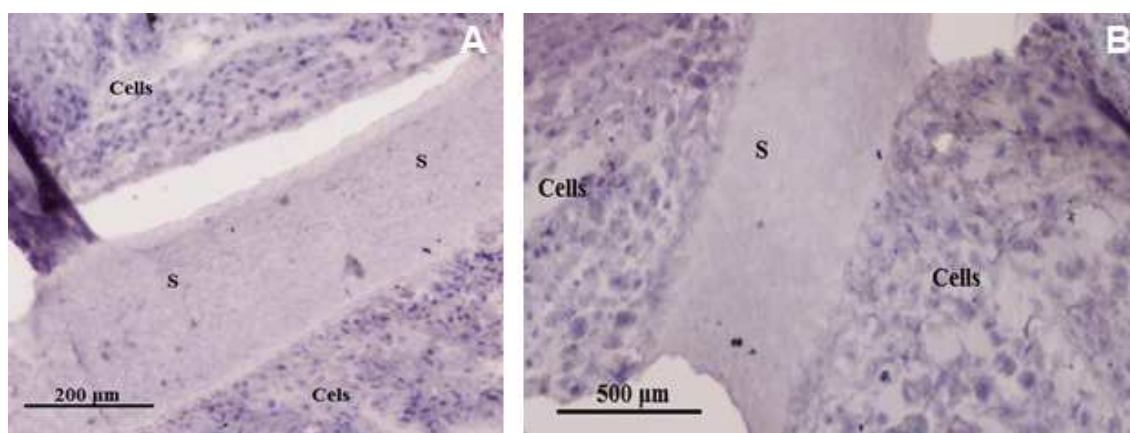


Figure 5.12. Sections of cell-scaffold constructs cultured in the bioreactor and stained with H&E: (A) 14 days; (B) 21 days of culture. S: Scaffold.

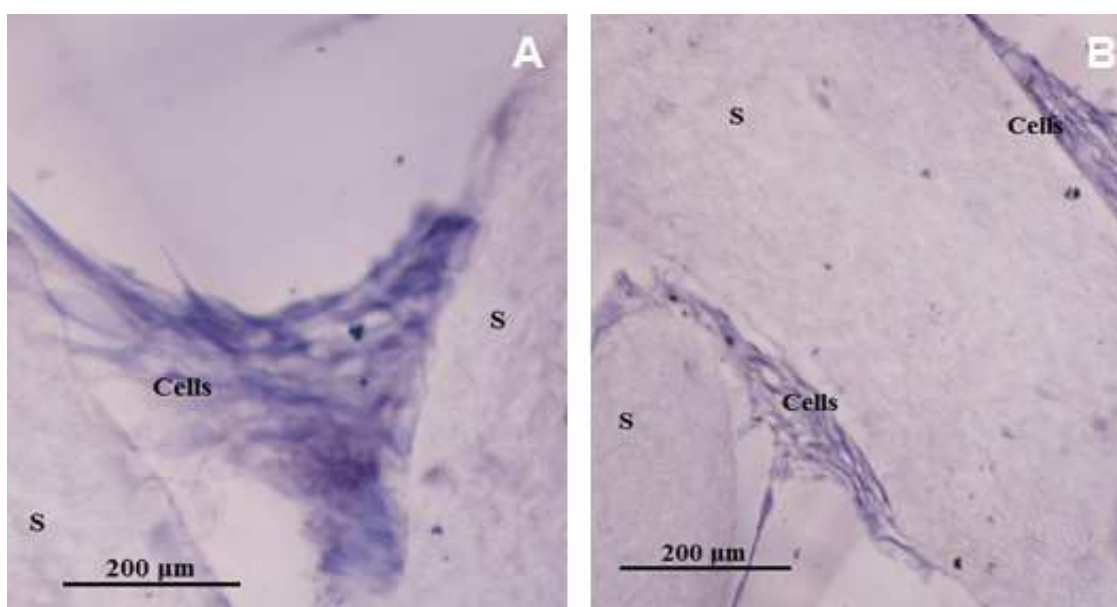


Figure 5.13. Sections of cell-scaffold constructs cultured in static conditions and stained with H&E: (A) 14 days; (B) 21 days of culture. S: Scaffold.

## 5.4. Discussion

The viability of tissue engineered constructs grown in vitro is limited by strict requirements in terms of oxygen and nutrients supply and metabolic waste elimination from the inner regions of the constructs (20, 21). In recent years, many different types of bioreactors such as spinner flasks, perfusion bioreactors and rotating wall vessel (RWV) bioreactors have been proposed to meet these requirements, but have been beset by various limitations. The use of spinner flasks resulted in improved fluid flow through a simple design (22-24), although the turbulence generated can be detrimental for seeded cells and newly laid down ECM (25, 26). Rotating wall vessel (RWV) bioreactors (27-29), which generate low shear forces and 3D high mass transfer capacity, are prone to problems of non-homogenous cellular growth and ECM deposition. In addition, during the free floating culture, collision between the scaffolds and the bioreactor walls can induce cellular damage and disrupt cellular attachment and matrix deposition on the scaffolds (25, 30, 31). Several studies have been reported using perfusion bioreactors in the last decade (1, 4-6, 30, 32-41). However, in most of these studies, the authors report the use of perfusion bioreactors to culture cell-seeded 3D scaffolds that are limited to the use of small three-dimensional (3D) scaffolds [volume ( $\pi \times r^2 \times h$ )], hence creating a limitation to their possible clinical use, indispensable for the future development of this scientific field, as we see in the graphic (Figure 5.14).

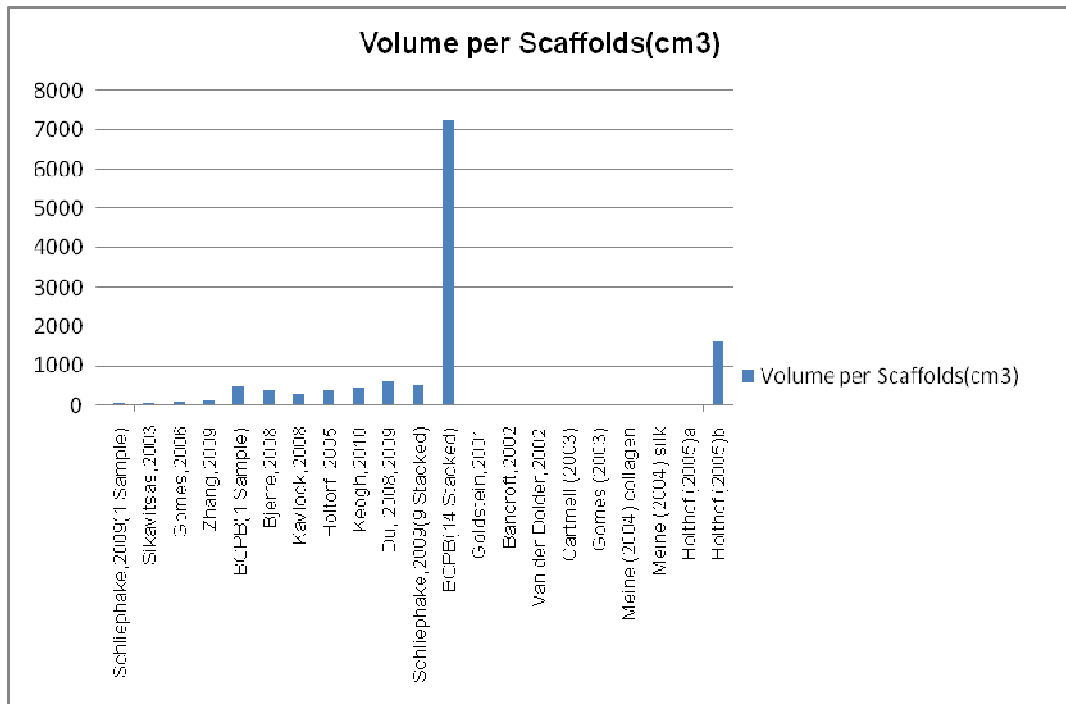


Figure 5.14: Graphical representation of the scaffolds volume cultured in several bioreactors reported in literature, as compared to the newly developed BCPB.

Apart from the bioreactor described by Zhang *et al*, 2009, all other studies (1, 4-6, 30, 32, 34, 36, 37, 39-41) describe the use of bioreactors that comprehend individual chamber bioreactors, and Zhang's single chamber bioreactor allows culturing only small scaffolds (144 cm<sup>3</sup> each). The bioreactor described by Schliephake *et al.*, 2009, uses 9 scaffolds (59 cm<sup>3</sup> each) stacked to form small scaffolds of (531 cm<sup>3</sup> total), in a single chamber. In this study we described the design and development of a new bioreactor (BCPB), where the samples are cultured in a single chamber that allows using scaffolds of variable and large dimensions. Herein we described studies on the preliminary evaluation of this bioreactor, in which we have used SPCL fiber meshes scaffolds that were stacked to form a scaffold of 42 mm length and 16 mm in diameter (7252 cm<sup>3</sup>). To the author's knowledge, the BCPB is the first bioreactor described in the literature, enabling the culture of 3D's scaffolds with dimensions meeting the requirements of critical sized defects, and thus with potential to use in real clinical situations.



The amounts of DNA registered during the experimental time of culture, demonstrated significant lower values for the constructs cultured in the bioreactor, indicating that cell proliferation was probably affected by dynamic flow conditions. However this decrease can also be explained by the procedure required to stack the GBMSC's-SPCL constructs in the coaxial perforated tube before placing them inside the single chamber for flow culture, as the use of tweezers to hold the samples is susceptible to induce cellular damage and/or disrupt cellular attachment on the scaffolds. This drawback of the procedure might be overcome in future studies, performing the seeding directly in the system. Furthermore, it is well known that when MSCs differentiate, the proliferation rate is expected to decrease because a higher amount of cellular energy is directed to the synthesis of ECM matrix proteins rather than for cell replication and proliferation. Thus, the decrease in cellular proliferation can also be seen as a direct association of the increase in ALP activity in GBMSC's (8). Although the results show an increase in DNA values between day 14 and day 21 for the bioreactor cultures, suggesting that BCPB (perfusion culture) promotes cell proliferation, no statistic difference was found between the two groups. ALP activity assay revealed increased amounts in all time point of flow cultures, and these values were statistically different when compared the control group (day 0), showing the osteogenic phenotypic expressions of cells cultured in the BCPB. A significant increase in ALP activity was also registered upon 14 days of culture in the bioreactor, followed by a decline at 21 days, corresponding to a common behavior in the process of osteogenic differentiation of MSCs (32, 42, 43).

However, this ALP activity profile was not observed in static conditions, indicating that static culturing did not provide the necessary conditions to initiate the osteogenic differentiation of the MSCs. These findings are in good agreement with other previous studies that have demonstrated the improved osteogenic differentiation in a dynamic bioreactor environment over a static culture system, due to the shear stresses induced by flow perfusion, which stimulate osteogenic programming in mesenchymal stem cells (9, 37, 44-46). SEM micrographs revealed that GBMSC's seeded onto SPCL fibers, appeared to completely and preferentially covered the fibbers on the interior of the scaffolds cultured in the bioreactor, and cells showed greater spreading and adhesion in the entire depth of the structure, exhibiting abundant cellular connections in the interior of the scaffolds. In contrast, SEM showed that in static conditions, cells tend to agglomerate and do not spread on the scaffolds structure.

Histological examination of the samples supported SEM findings, showing that under the flow perfusion culture cells proliferated, grow and distributed throughout the GBMSC's–SPCL constructs, while under static culture the cells proliferated only in the surface of the GBMSC's–SPCL constructs.

## 5.5. Conclusions

One of the challenges in bone tissue engineering is to create a large-scale tissue engineered graft in vitro to repair large bone defects. However, one of the main obstacles in tissue engineering is to ensure that cells survival in the interior of the large scaffolds, which is clearly impossible under static culture conditions. To date, most tissue-engineering research has been constrained to using scaffolds small dimensions (2mm in thickness or less), which are easily sustainable by medium convection or static culture methods.

In this article, we described and evaluated the design of a novel flow perfusion bioreactor system for sustaining “thick” 3D scaffolds that approach sizes of clinical relevance. Specifically, as proof of principle, we tested large cylindrical scaffolds (42mm in length, 16 mm in diameter and 3 mm thick). Preliminary experiments showed that the BCPB enabled cells survival and proliferation in the GBMSC's–SPCL constructs, demonstrating that this new flow perfusion system was superior to static culture conditions for large-scale cell-construct culture. Due to their size, without effective fluid flow, these GBMSC's–SPCL constructs would probably suffer central core cells necrosis. The continuous cell proliferation under the flow perfusion culture showed that the perfusion system ensures the cell proliferation for at least 21 days.

Additionally, this newly designed BCPB perfusion system is composed of parts that can be easily assembled under sterile conditions, avoiding possible contaminations during culture. Thus, the BCPB demonstrated to be a simple and efficient system for enabling the culture of large-scale scaffolds and for the obtention of highly functional constructs for bone regeneration applications.

## References

1. van den Dolder, J., Bancroft, G.N., Sikavitsas, V.I., Spauwen, P.H., Jansen, J.A., Mikos, A.G. Flow perfusion culture of marrow stromal osteoblasts in titanium fiber mesh. *J Biomed Mater Res Part A* 64, 2003,235.
2. Grayson, W.L., Marolt, D., Bhumiratana, S., Frohlich, M., Guo, X.E., Vunjak-Novakovic, G. Optimizing the medium perfusion rate in bone tissue engineering bioreactors. *Biotechnol and Bioeng* 108, 2011,1159.
3. Grayson, W.L., Bhumiratana, S., Cannizzaro, C., Chao, P.H.G., Lennon, D.P., Caplan, A.I., et al. Effects of Initial Seeding Density and Fluid Perfusion Rate on Formation of Tissue-Engineered Bone. *Tissue Eng Part A* 14, 2008,1809.
4. Marolt, D., Augst, A., Freed, L.E. Bone and cartilage tissue constructs grown using human bone marrow stromal cells, silk scaffolds and rotating bioreactors. *Biomaterials* 27, 2006,6138.
5. Gomes, M.E., Bossano, C.M., Johnston, C.M., Reis, R.L., Mikos, A.G. In vitro localization of bone growth factors in constructs of biodegradable scaffolds seeded with marrow stromal cells and cultured in a flow perfusion bioreactor. *Tissue Eng* 12, 2006,177.
6. Gomes, M.E., Holtorf, H.L., Reis, R.L., Mikos, A.G. Influence of the porosity of starch-based fiber mesh scaffolds on the proliferation and osteogenic differentiation of bone marrow stromal cells cultured in a flow perfusion bioreactor. *Tissue Eng* 12, 2006,801.
7. Pashkuleva, I., Azevedo, H.S., Reis, R.L. Surface structural investigation of starch-based biomaterials. *Macromol Biosci* 8, 2008,210.
8. Rodrigues, M.T., Gomes, M.E., Viegas, C.A., Azevedo, J.T., Dias, I.R., Guzon, F.M., et al. Tissue-engineered constructs based on SPCL scaffolds cultured with goat marrow cells: functionality in femoral defects. *J Tissue Eng Regen Med* 5, 2011,41.
9. Gomes, M.E., Sikavitsas, V.I., Behraves, E., Reis, R.L., Mikos, A.G. Effect of flow perfusion on the osteogenic differentiation of bone marrow stromal cells cultured on starch-based three-dimensional scaffolds. *J Biomed Mater Res Part A* 67A, 2003,87.
10. Gomes, M.E., Azevedo, H.S., Moreira, A.R., Ella, V., Kellomaki, M., Reis, R.L. Starch-poly(epsilon-caprolactone) and starch-poly(lactic acid) fibre-mesh scaffolds for bone tissue engineering applications: structure, mechanical properties and degradation behaviour. *J Tissue Eng Regen Med* 2, 2008,243.
11. Marques, A.P., Cruz, H.R., Coutinho, O.P., Reis, R.L. Effect of starch-based biomaterials on the in vitro proliferation and viability of osteoblast-like cells. *J Mater Sci Mater Med* 16, 2005,833.

12. Gomes, M.E., Ribeiro, A.S., Malafaya, P.B., Reis, R.L., Cunha, A.M. A new approach based on injection moulding to produce biodegradable starch-based polymeric scaffolds: morphology, mechanical and degradation behaviour. *Biomaterials* 22, 2001,883.
13. Santos, M.I., Tuzlakoglu, K., Fuchs, S., Gomes, M.E., Peters, K., Unger, R.E., et al. Endothelial cell colonization and angiogenic potential of combined nano- and micro-fibrous scaffolds for bone tissue engineering. *Biomaterials* 29, 2008,4306.
14. Martins, A.M., Pham, Q.P., Malafaya, P.B., Sousa, R.A., Gomes, M.E., Raphael, R.M., et al. The Role of Lipase and alpha-Amylase in the Degradation of Starch/Poly(epsilon-Caprolactone) Fiber Meshes and the Osteogenic Differentiation of Cultured Marrow Stromal Cells. *Tissue Eng Part A* 15, 2009,295.
15. Santos, T.C., Marques, A.P., Horing, B., Martins, A.R., Tuzlakoglu, K., Castro, A.G., et al. In vivo short-term and long-term host reaction to starch-based scaffolds. *Acta Biomater* 6, 2010,4314.
16. Rodrigues, M.T., Martins, A., Dias, I.R., Viegas, C.A., Neves, N.M., Gomes, M.E., et al. Synergistic effect of scaffold composition and dynamic culturing environment in multilayered systems for bone tissue engineering. *J Tissue Eng Regen Med*, 2012.
17. Alves, C.M., Yang, Y., Carnes, D.L., Ong, J.L., Sylvia, V.L., Dean, D.D., et al. Modulating bone cells response onto starch-based biomaterials by surface plasma treatment and protein adsorption. *Biomaterials* 28, 2007,307.
18. Bancroft, G.N., Sikavitsas, V.I., van den Dolder, J., Sheffield, T.L., Ambrose, C.G., Jansen, J.A., et al. Fluid flow increases mineralized matrix deposition in 3D perfusion culture of marrow stromal osteoblasts in a dose-dependent manner. *Proc Natl Acad Sci U S A* 99, 2002,12600.
19. Cory, A.H., Owen, T.C., Bartrop, J.A., Cory, J.G. Use of an Aqueous Soluble Tetrazolium Formazan Assay for Cell-Growth Assays in Culture. *Cancer Commun* 3, 1991,207.
20. Martin, Y., Vermette, P. Bioreactors for tissue mass culture: design, characterization, and recent advances. *Biomaterials* 26, 2005,7481.
21. Martin, I., Wendet, D., Heberer, M. The roles of bioreactor in tissue engineering. *Trends Biotechnol* 22, 2004,80.
22. Stiehler, M., Bunger, C., Bastrup, A., Lind, M., Kassem, M., Mygind, T. Effect of dynamic 3-D culture on proliferation, distribution, and osteogenic differentiation of human mesenchymal stem cells. *J Biomed Mater Res Part A* 89, 2009,96.
23. Song, K., Liu, T., Cui, Z., Li, X., Ma, X. Three-dimensional fabrication of engineered bone with human bio-derived bone scaffolds in a rotating wall vessel bioreactor. *J Biomed Mater Res Part A* 86, 2008,323.

24. Mygind, T., Stiehler, M., Baatrup, A., Li, H., Zoua, X., Flyvbjerg, A., et al. Mesenchymal stem cell ingrowth and differentiation on coralline hydroxyapatite scaffolds. *Biomaterials* 28, 2007,1036.
25. Chen, H.C., Hu, Y.C. Bioreactors for tissue engineering. *Biotechnol Lett* 28, 2006,1415.
26. Sikavitsas, V.I., Bancroft, G.N., Mikos, A.G. Formation of three-dimensional cell/polymer constructs for bone tissue engineering in a spinner flask and a rotating wall vessel bioreactor. *J Biomed Mater Res* 62, 2002,136.
27. Yu, X.J., Botchwey, E.A., Levine, E.M., Pollack, S.R., Laurencin, C.T. Bioreactor-based bone tissue engineering: The influence of dynamic flow on osteoblast phenotypic expression and matrix mineralization. *Proc Natl Acad Sci U S A* 101, 2004,11203.
28. Granet, C., Laroche, N., Vico, L., Alexandre, C., Lafage-Proust, M.H. Rotating-wall vessels, promising bioreactors for osteoblastic cell culture: comparison with other 3D conditions. *Med Biol Eng Comput* 36, 1998,513.
29. Molnar, G., Schroedl, N.A., Gonda, S.R., Hartzell, C.R. Skeletal muscle satellite cells cultured in simulated microgravity. *In Vitro Cell Dev Biol Anim* 33, 1997,386.
30. Sikavitsas, V.I., Bancroft, G.N., Holtorf, H.L., Jansen, J.A., Mikos, A.G. Mineralized matrix deposition by marrow stromal osteoblasts in 3D perfusion culture increases with increasing fluid shear forces. *Proc Natl Acad Sci U S A* 100, 2003,14683.
31. Goldstein, A.S., Juarez, T.M., Helmke, C.D., Gustin, M.C., Mikos, A.G. Effect of convection on osteoblastic cell growth and function in biodegradable polymer foam scaffolds. *Biomaterials* 22, 2001,1279.
32. Keogh, M.B., Partap, S., Daly, J.S., O'Brien, F.J. Three hours of perfusion culture prior to 28 days of static culture, enhances osteogenesis by human cells in a collagen GAG scaffold. *Biotechnol and Bioeng* 108, 2011,1203.
33. Du, D.J., Furukawa, K.S., Ushida, T. 3D Culture of Osteoblast-Like Cells by Unidirectional or Oscillatory Flow for Bone Tissue Engineering. *Biotechnol and Bioeng* 102, 2009,1670.
34. Schliephake, H., Zghoul, N., Jager, V., van Griensven, M., Zeichen, J., Gelinsky, M., et al. Bone formation in trabecular bone cell seeded scaffolds used for reconstruction of the rat mandible. *Int J Oral Maxillofac Surg* 38, 2009,166.
35. Zhang, Z.Y., Teoh, S.H., Chong, W.S., Foo, T.T., Chng, Y.C., Choolani, M., et al. A biaxial rotating bioreactor for the culture of fetal mesenchymal stem cells for bone tissue engineering. *Biomaterials* 30, 2009,2694.
36. Sailon, A.M., Allori, A.C., Davidson, E.H., Reformat, D.D., Allen, R.J., Warren, S.M. A Novel Flow-Perfusion Bioreactor Supports 3D Dynamic Cell Culture. *J Biomed Biotechnol*, 2009.

37. Bjerre, L., Bunger, C.E., Kassem, M., Mygind, T. Flow perfusion culture of human mesenchymal stem cells on silicate-substituted tricalcium phosphate scaffolds. *Biomaterials* 29, 2008,2616.
38. Du, D., Furukawa, K., Ushida, T. Oscillatory perfusion seeding and culturing of osteoblast-like cells on porous beta-tricalcium phosphate scaffolds. *J Biomed Mater Res Part A* 86, 2008,796.
39. Kavlock, K.D., Goldstein, A.S. Effect of pulsatile flow on the osteogenic differentiation of bone marrow stromal cells in porous scaffolds. *Biomed Sci Instrum* 44, 2008,471.
40. Holtorf, H.L., Jansen, J.A., Mikos, A.G. Flow perfusion culture induces the osteoblastic differentiation of marrow stromal cell-scaffold constructs in the absence of dexamethasone. *J Biomed Mater Res Part A* 72A, 2005,326.
41. Holtorf, H.L., Sheffield, T.L., Ambrose, C.G., Jansen, J.A., Mikos, A.G. Flow perfusion culture of marrow stromal cells seeded on porous biphasic calcium phosphate ceramics. *Ann Biomed Eng* 33, 2005,1238.
42. Oliveira, J.M., Rodrigues, M.T., Silva, S.S., Malafaya, P.B., Gomes, M.E., Viegas, C.A.A., et al. Novel hydroxyapatite/chitosan bilayered scaffold for osteochondral tissue-engineering applications: scaffold design and its performance when seeded with goat bone marrow stromal cells. *Biomaterials* 27, 2006,6123.
43. Zhang, Z.Y., Teoh, S.H., Teo, E.Y., Chong, M.S.K., Shin, C.W., Tien, F.T., et al. A comparison of bioreactors for culture of fetal mesenchymal stem cells for bone tissue engineering. *Biomaterials* 31, 2010,8684.
44. Datta, N., Pham, Q.P., Sharma, U., Sikavitsas, V.I., Jansen, J.A., Mikos, A.G. In vitro generated extracellular matrix and fluid shear stress synergistically enhance 3D osteoblastic differentiation. *Proc Natl Acad Sci U S A* 103, 2006,2488.
45. Kurpinski, K., Chu, J., Hashi, C., Li, S. Anisotropic mechanosensing by mesenchymal stem cells. *Proc Natl Acad Sci U S A* 103, 2006,16095.
46. Park, J.S., Chu, J.S., Cheng, C., Chen, F., Chen, D., Li, S. Differential effects of equiaxial and uniaxial strain on mesenchymal stem cells. *Biotechnol Bioeng* 88, 2004,359.



## SECTION 5

### Chapter VI

#### **Assessing the repair of critical size bone defects performed in a goat tibia model using tissue engineered constructs cultured in a bi-directional flow perfusion bioreactor**

This chapter is based on the following publication: Gardel LS, Afonso M, Frias C, Correia-Gomes C, Serra LA, Gomes ME, Reis RL. Assessing the repair of critical size bone defects performed in a goat tibia model using tissue engineered constructs cultured in a bi-directional flow perfusion bioreactor. Submitted 2012





## **Abstract**

This work aims to evaluate the in vivo performance of a tissue engineered bone substitute obtained by culturing cell–scaffold constructs in a flow perfusion bioreactor, specifically designed to enable the culture of large constructs, envisioning the regeneration of critical sized defects. Therefore, SPCL (a blend of starch with polycaprolactone) fibre mesh scaffolds were seeded with goat bone marrow stromal cells (GBMSCs) and cultured in the perfusion bioreactor for 14 days using osteogenic medium. Static cultures were also performed as controls. After 14 days, the constructs (42 mm length and 16 mm in diameter) were implanted in critical size defects performed in the tibial bone of six adult goats from which the bone marrow had been collected previously. Explants were retrieved after six and twelve weeks of implantation and characterized using scanning electron microscopy, energy dispersive spectroscopy, micro-CT and radiographic analysis to assess tissue morphology and calcification. Explants were also histologically analysed, using hematoxylin & eosin and Masson trichrome staining. The results obtained provided relevant information about the performance and functionality of SPCL–GBMSCs constructs in a critical sized orthotopic defect performed in a large animal model - the goat model - and demonstrated that the culture of the SPCL scaffolds with the autologous cells in perfusion culture can provide a good alternative therapy for the healing and regenerative process of bone critical sized defects.

## 6.1. Introduction

In the field of orthopedics there is a significant number of surgical and clinical problems such as trauma, infections, and surgical treatment of tumors that lead to critical-sized defects difficult to solve (1, 2). Currently, these problems are treated using bone grafting techniques including autologous, allogeneic and bone transport methods (Ilizarov technique). However these techniques present major limitations requiring the pursuit of alternatives for the management of critical size bone defects, with the latest approach being the use of tissue engineering strategies. Tissue Engineering technology aims at the creation of tissue substitutes by the deliberate and controlled stimulation of selected target cells through a systemic combination of molecular and mechanical signals provided by a support material and by the culturing environment (3, 4). The general bone tissue engineering is based on the use of Mesenchymal Stem Cells (MSCs), most often obtained from the bone marrow, associated with 3D scaffolds. The MSCs are multipotent, but are present in strikingly low quantities in bone marrow (5) and thus it is usually necessary to expand MSCs in vitro before implantation, to obtain a clinically relevant number of cells. The scaffold must provide an appropriate environment (interconnected porosity, chemical composition, surface topography) to facilitate the ingrowth of cells and vascular tissue and must be biodegradable with a rate in par with *de novo* tissue regeneration (6). Several advanced culturing systems, mostly perfusion bioreactors, have been described in the literature in recent years to culture bone constructs (7-16) with clear advantages over the traditional static culturing methodologies. Unfortunately, the vast majority of these culture systems are designed for engineering small cell-scaffolds constructs, measuring only few millimeters. Consequently, these perfusion systems are not capable of meeting the real clinical needs existing in the field of orthopedic surgery that is to solve the problem of the BMSC's nutrition supply in the center of large 3D scaffolds that can be used in critical-sized defects regeneration. Thus, in this study we describe the use of a new Bi-directional continuous perfusion bioreactor (BCPB) that allows culturing large scaffolds. Constructs composed of goat bone marrow stroma cells seeded onto 3D polymeric scaffolds were cultured using this bioreactor and then implanted into 42-mm-sized defects in a tibial goat model. In general, the histological analysis of the explants (stained with Hematoxylin & Eosin and Masson's trichrome) showed homogeneous distribution and more new bone formation in the defects implanted with constructs cultured in the perfusion bioreactor.

Micro-ct 3D image reconstructions also showed new bone formation and deposition around the constructs cultured in perfusion conditions, while bone formation was not detectable in defects implanted with constructs that were statically cultured.

Although complete bony union was not radiographically observed in any defect, it was possible to visualize bone in the early stages of development in defects filled with constructs cultured in perfusion conditions after 12 weeks of implantation. These data indicate that BCFB can be used for enhancing the functionality of tissue engineered constructs and thus enabling enhanced bone regeneration in real critical-sized bone defects.

## **6.2. Materials and Methods**

### **6.2.1 GBMSC's harvesting, isolation and culture**

Six (6) goats were anesthetized, with intramuscular injection medetomidine hydrochloride (Domitor<sup>®</sup>, Pfizer, Portugal) at 0.11mg/kg of body weight, and ketamine hydrochloride (Imalgene<sup>®</sup>, Merial, Portugal) at 10mg/kg of body weight. Thiopentone (Tiopental<sup>®</sup>, BBraun, Portugal) sodium at 5mg/kg of body weight was administered intravenously given for general anesthesia. After this, the region of the dorsal iliac crest was aseptically prepared and 2 mL of bone marrow (BM) was harvested using a biopsy needle (T-Lok<sup>™</sup>) and mixed with 100 IU/mL heparin. The goat BM aspirate was mixed with 10ml of basal media consisting of  $\alpha$ -DMEM with 10% fetal calf serum and the mixture was centrifuged (1200rpm/5 min). The pellet was removed and the cells were resuspended in the same media and seeded in two 150 cm<sup>2</sup> culture flasks and then placed inside an incubator. Cells developed a fibroblastic-like morphology in visible symmetric colonies at about 4 days after initial plating. Non adherent cells were removed with medium changes performed every 2-3 days. Cells were cultured at 37°C in a 5% CO<sub>2</sub> atmosphere at 95% humidity. On reaching confluence, cells were passed with 0.05% trypsin. GBMSC's cells were enzymatically lifted with 3 ml of trypsin after reaching 80%-90% of confluence at passage 4 (p4), were centrifuged (1200rpm/5min) and the pellet was removed. A cells suspension containing of 1x10<sup>6</sup> cells in 300  $\mu$ l of  $\alpha$ -DMEM with 10% fetal calf serum was prepared to seed onto each scaffold (SPCL fiber – meshes) used for the study.

### 6.2.2 Scaffold design and preparation

In this study a fiber mesh scaffold based on a biodegradable polymeric blend of starch and polycaprolactone (SPCL) that has been extensively investigated for bone tissue engineering applications (17-22) was used. The 3D scaffolds were produced by a fiber-bonding method into mesh structures with a porosity of ~75%, as described previously (15, 16), and cut into disks of 16mm diameters and 3mm of thicknesses with a 6mm interior hole. The interior hole was performed with two main objectives, the first is to allow the samples to be positioned within the bioreactor through insertion of the scaffolds into the perforated tube enabling the use of a bidirectional flow from inside to outside or outside to inside of the samples; the second goal is to mimic the role of the medullar canal in the long bones, allowing the passage of blood vessels and thus support the development of a functional bone tissue into the samples upon implantation (Figure 6.1). All samples were sterilized using ethylene oxide.

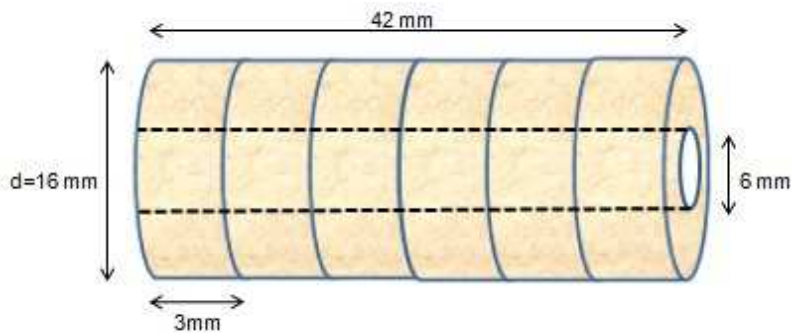


Figure 6.1. Schematic representation of the SPCL fiber-meshes stacked into a scaffold of critical sized defect dimensions

### 6.2.3 Flow-perfusion bioreactor design

The flow perfusion bioreactor used in this study was developed by the 3B's Research Group and named Bi-Directional Continuous Perfusion Bioreactor (BCPB). It has an innovative design which consists in the use of a rigid tube, where the scaffold is inserted, with perforations in the central part, equivalent to the length of the three-dimensional scaffold (of large and variable dimensions) that is used. This tube is connected to a circular system that is responsible for promoting the medium flow from the interior to the exterior of the three-dimensional support (linked to the peristaltic pump) or from the exterior to the interior of the three-dimensional medium.

This tube is positioned co-axially within a single cell culture chamber with exits /entrances hermetically closed, connected to the same circular system, which allows the control of the flow and of the pressure gradient inside the chamber and the perforated tube. In this experiment two BCPB systems were used, at a continuous flow rate of 1 ml/min.

#### **6.2.4 GBMSC's seeding onto SPCL scaffolds and bioreactor culture**

The SPCL scaffolds were placed in 12 well non-adherents plates (Costar; Becton-Dickinson). A total of 56 samples were seeded with 300  $\mu$ l of a cell suspension containing  $1 \times 10^6$  cells in basal medium composed of  $\alpha$ -MEM (Minimal Essential Medium) with 10 % FCS (foetal calf serum, Gibco), 50  $\mu$ g/ml gentamycin, 100  $\mu$ g/ml ampicillin and 0.3  $\mu$ g/ml fungizone (all from Sigma), for either static or bioreactor culture during 14 days prior to implantation for 6 or 12 weeks. The well plates were then transferred to the incubator and three hours after seeding 1.6 ml of basal medium was added to each well and the plates were left to incubate overnight. The 12 well plates containing cell-scaffolds for static culture were kept in the same incubator for 14 days, in osteogenic medium, with weekly medium change. The osteogenic medium was composed of  $\alpha$ -MEM, supplemented with 10 % FCS (foetal calf serum, Gibco), 50  $\mu$ g/ml ascorbic acid (Sigma, St.Louis, MO, USA), 50  $\mu$ g/ml gentamin, 100  $\mu$ g/ml ampicillin, 0.3  $\mu$ g/ml fungizone, 10 mM Na  $\beta$ -glycerophosphate and  $10^{-8}$  M dexamethasone (all Sigma). The plates containing cell-scaffolds constructs to be cultured in the bioreactor were carefully transferred to two BCPB's, in a laminar flow cabinet, as follows: each sample (3mm length and 16 mm diameter), with a inner hole of 6mm was carefully inserted into the polycarbonate perforated tube and stacked until completing a total of 14 samples, corresponding to a 42 mm length construct. The perforated tube with the inserted construct, was then connected to the two end parts of the bioreactor that assure the hermetic and aseptic closure of the culture chamber; subsequently these were connected to the system flow and the culture chamber was slowly filled with the culture medium at a rate of 1ml/min, with a direction from inside the chamber to the perforated tube, which will cause a flow direction from outside to inside the scaffold. Finally, the system was transferred to an incubator (at 37  $^{\circ}$ C environment with 5% CO<sub>2</sub>).

A 14 days of the culture period inside of bioreactor was selected to surpass the 'cusp of viability in static culture' (determined in previous studies to be 4 days), such that experimental duration would be sufficient to detect any measureable difference among static and flow cultures viability (23). This culture period is also comparable to that of previous in vitro investigations (10, 24) and other ex vivo studies found in the literature (25). The culture chamber has a capacity for 216 ml of culture medium while the bottle reservoir was filled up to 450 ml of medium; every week 400 ml of medium were exchanged with 400 ml of fresh medium, without stopping the medium flow in the bioreactor system. Each sample of the static group was cultured in the presence of 10 ml of culture medium which was changed every week.

#### **6.2.4.1 Characterization of cell viability in seeded scaffolds**

To ensure the reliability of seeding, 3 samples (day 0), of each group were collected for studies of cell viability, for this DNA, MTS and SEM assay were performed using previously reported methods (15, 26, 27).

#### **6.2.5 Animal surgical procedures**

Care and management of animals was conducted as per the guidelines of the Institutional Animal Ethics Committee and the Committee for the Purpose of Control and Supervision of Experiments on Animals. Six goats, 2-year-old female (n=2 in each group), with an average weight of 25 kg (ranged, 23–27.5 kg) and fed in separate cages with free access to food and water, were used in this study. The animals were premedicated with intramuscular injection of medetomidine hydrochloride (Domitor<sup>®</sup>, Pfizer, Portugal) at 0.11mg/kg of body weight, and ketamine hydrochloride (Imalgene<sup>®</sup>, Merial, Portugal) at 10mg/kg of body weight. Thiopentone (Tiopental<sup>®</sup>, BBraun, Portugal) sodium at 5mg/kg of body weight was given intravenously for induction of anesthesia. Cephazolin (Cefazolin<sup>®</sup> 500mg, Sagent), 10 mg/kg was administered subcutaneously as prophylactic antibiotics. The animals were intubated immediately with size n<sup>o</sup> 9 Magill endotracheal tube. Anesthesia was maintained with increments of medetomidine hydrochloride and ketamine hydrochloride dose-effect every 20–30 min. The animals were in right recumbency on the operating table.

Asepsis of the skin after shaving was achieved with a chlorhexidine (LifoScrub<sup>®</sup>, BBraun, Portugal) solution and wrapped using a sterile technique. A skin incision of 15 cm length was made along the right tibia and the tibia was exposed using a standard medial approach.

A 42 mm bone segment (with periosteum included) was excised from the mid diaphyseal region using an oscillating saw under abundant irrigation (Figure.6.2A). A stainless steel biological healing plate of 7 holes with 3.5 cortical screws and cerclage (Servive Portugal<sup>®</sup>, Valencia), were used for immobilization of the bone (Figure 6..2B). The 3D cell - scaffolds (42 mm length and 16 mm in diameter) constructs were placed into the right tibia defects divided into bioreactor group (6 and 12 weeks), static group, (6 and 12 weeks) (Figure 6..2C) and control group (empty defect, 6 and 12 weeks) (Figure 6..2D) by the same procedure. The surrounding soft tissue and skin incision was closed with uninterrupted sutures using absorbable synthetic monofilament suture (MonoPlus<sup>®</sup>, BBraun, Portugal). During the first week after surgery, cephazolin (Kefzolan<sup>®</sup>) (10 mg/kg) and 0.2mg/kg butorphanol (Torbugesic<sup>®</sup>) were routinely administered intramuscularly once a day and the physical states of all the animals were also closely monitored. All animals recovered successfully from surgery, remained in good health, and the implants remained stably fixed and in correct positioning (Figure 6.3 A,B,C). The animals were sacrificed at 6 and 12 weeks with injection of high doses of thiopentone (Tiopental<sup>®</sup>, BBraun, Portugal).

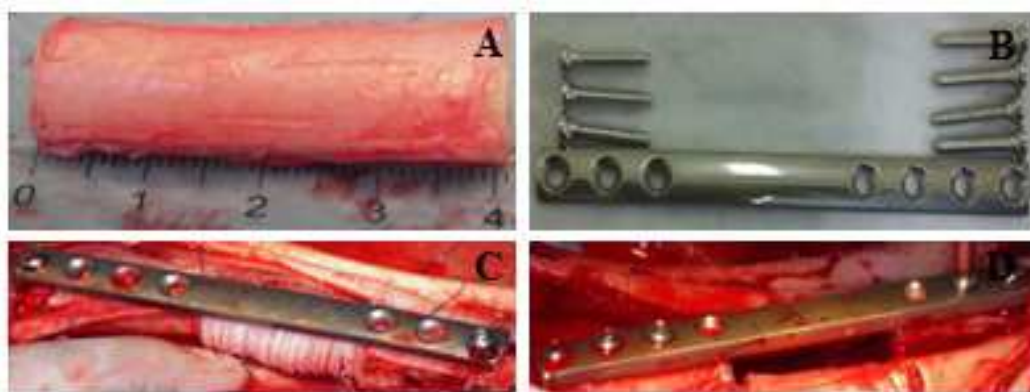


Figure6.2. (A) Bone fragment removed together with the periosteum; (B) Osteosynthesis material applied to the tibia; (C) Implantation of the biomaterial in tibia bone and fixation with osteosynthesis material; (D) Empty defect (control group).



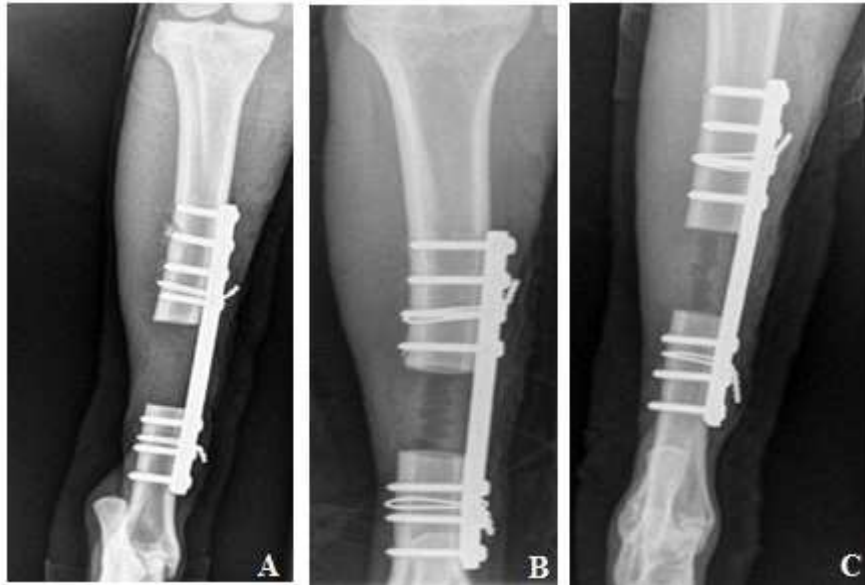


Figure 6.3. X-ray obtained immediately after surgery, showing the correct positioning of the bone fixation device. (A) Control group (empty defect); (B) Static group; (C) Bioreactor group. In B and C images it is possible to visualize radiographically the cells-scaffolds constructs implanted within the defect.

## 6.2.6 Characterization of explants from in vivo studies

### 6.2.6.1 Radiographic analysis

In vivo digital X-rays of all the groups were obtained in the immediate postoperative, and at 6 and 12 weeks post operation using an X-ray equipment (PHILIPS Corp). Exposure was at 50 kVp for 2.5 mAs, using diagnostic imaging software (CrystalView®). The differences in radiopacity in and around the 3D scaffolds at the defect and bone union at the cut-ends of the original tibias were analyzed. Radiographs of the tibia removed from the goats were obtained by routine procedures.

### **6.2.6.2 Scanning Electron Microscopy (SEM) and Energy-Dispersive X-ray Spectroscopy (EDS) analysis**

The morphological analysis of cells growth, attachment, and distribution on the surface of the scaffolds was performed by SEM (Leica Cambridge, model S360; England) and measurements of the amount of calcium and phosphorous in samples were performed by Energy Dispersive Spectroscopy (EDS) in a link-el-II equipment. For this purpose, the constructs (scaffolds-cells) were fixed with 2.5 % Glutaraldehyde (Sigma,USA) in PBS solution, dehydrated through a graded series of ethanol, let to dry overnight at room temperature and finally gold sputter coated (Fisons Instruments, model SC502; England).

### **6.2.6.3 Micro-CT analysis**

The formation of mineralized tissue in the explants was evaluated using a high-resolution  $\mu$ -CT Skyscan 1072 scanner (Skyscan, Konitich, Belgium). Each sample was scanned in a high-resolution mode with a pixel size of 17.58 $\mu$ m and exposure time of 1.6ms. The x-ray source was set at 52 keV of energy and 163 $\mu$ A of intensity. Approximately 400 projections were acquired over a rotation of 180 $^{\circ}$  with a rotation step of 0.45 $^{\circ}$ . Each one of these projections were segmented into binary images with dynamic threshold of 55-225 (grey values) to assess new bone formation. These data sets were used for morphometric analysis (CT analyser, v1.51.5 SkyScan); for this purpose a cylinder (6 mm in diameter) between the outer and inner edge of each scaffold analyzed was designated as region of interest (ROI); the new bone formation was measured and calculated by percentage of object volume values (total volume values/object volume values). The distribution and quantification of the new bone formation in the scaffolds was assessed by 3D virtual models that were created, visualized and registered using both image processing software's (CT analyser and ANT 3D creator).

#### **6.2.6.4 Histological analysis**

Following euthanasia, the implants and their surrounding tissue were retrieved and prepared for histological evaluation. The explants were rinsed in PBS, fixed in 4% formalin solution, dehydrated in a graded series of ethanol and embedded in paraffin. Then 5  $\mu\text{m}$  sections were obtained with a microtome and stained with hematoxylin & Eosin (HE) and Masson Trichrome (MT) which is frequently used as a bone-specific staining. Samples were then visualized under a light microscope and images taken with an attached camera.

#### **6.2.7 Statistical analysis**

The PASW Statistics18 software package (IBM, Somers, NY) was used for the statistical analysis. Descriptive values are presented as mean  $\pm$  SD unless stated otherwise. Kolmogorov-Smirnov test with Lilliefors significance correction was used to test the normality of the data. The one way ANOVA test was used to determine statistically significant differences among the groups and the Tukey test was used to assess the pairwise comparisons between groups. The statistical significance level considered was  $P < 0.05$ .

### **6.3. Results**

#### **6.3.1 Cell adhesion and viability of scaffolds**

MTS (Figure 6.4 A) and DNA (Figure 6.4 B) quantification results of samples from day 0 (control), showed that there was no apparent difference between the results for each group. In fact, the ANOVA test for DNA and MTS results did not detect statistically significant differences among all samples for the selected statistical level ( $P < 0.05$ ), suggesting that the seeding technique used was effective to all groups. SEM picture (Figure 6.4 C), shows adhesion and cellular distribution along the SPCL fiber after the seeding.

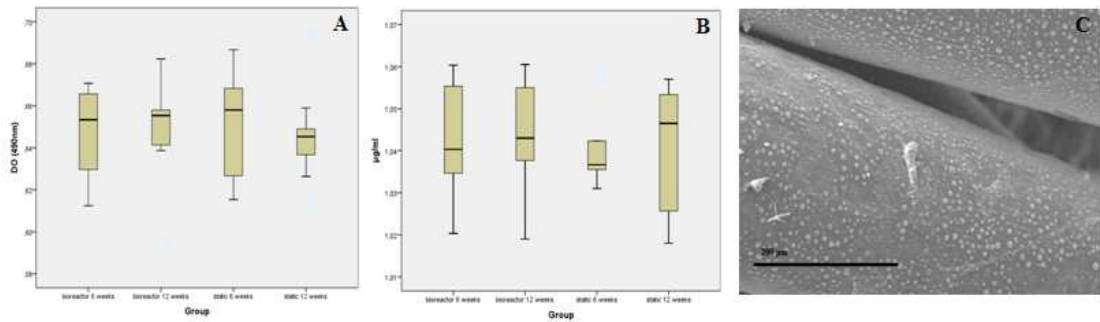


Figure6.4. (A) Boxplot of MTS quantification from all groups, day 0;(B) Boxplot of DNA quantification from all groups, day 0;(C) SEM photomicrographs obtained from cell seeded SPCL samples at day 0.

### 6.3.2 Radiographic analysis

After 6 weeks of implantation it was possible to visualize that the bone fixation device remained in the same position (figure 6.5) as immediately after surgery (Figure 6.3). No bony union was visualized between proximal/distal bone fragments in any groups, and it was also not possible to radiographically detect any early bone healing (Figure 6.5 A,B,C).

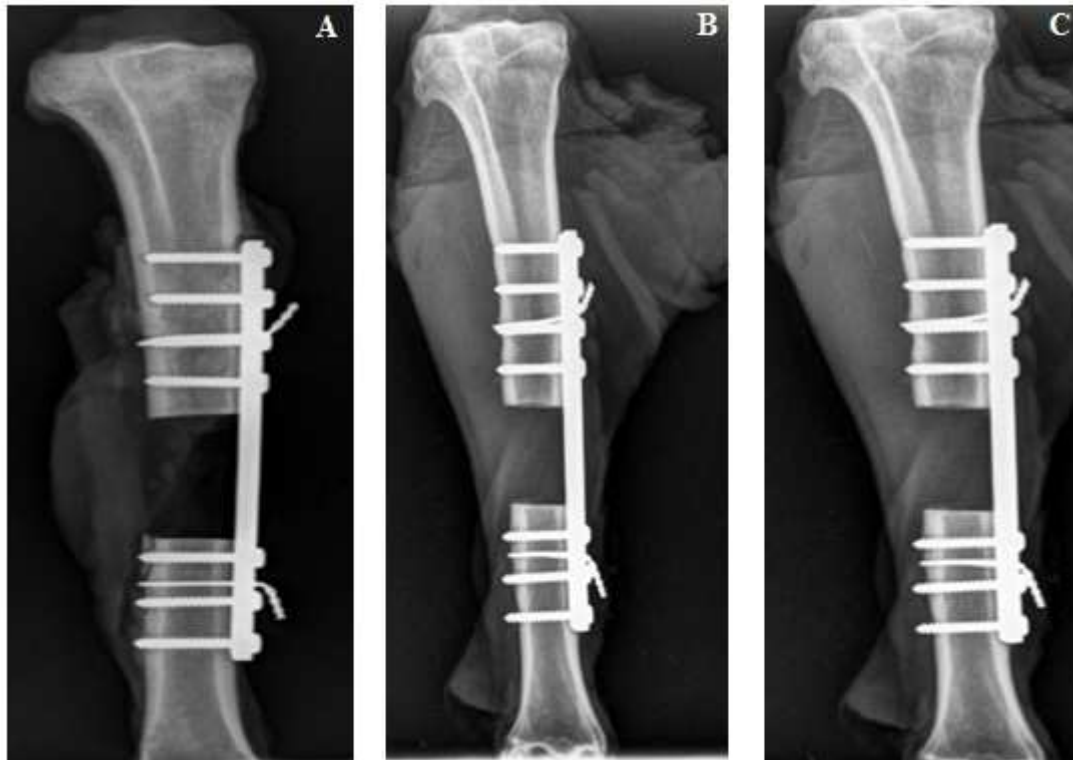


Figure6.5. Radiographs obtained after 6 weeks of implantation: (A) Control- empty defect (B) Static group (C) Bioreactor group.

After 12 weeks of implantation, it was possible to visualize that the bone fixation device remained in the same position as of immediately after surgery (figure 6.6). However, in the control group, it is apparent that the device bone fixation was subjected to strong mechanical forces (angulation, rotation and shears forces bone) active in the empty bone defect. The entire weight of the limb (bone) was supported by the device, which resulted in a strong bone resorption at the bone screws-plate and bone interface, in both the proximal/distal bone fragments. In distal fragment it is possible to see that this reaction was more intense (Figure 6.6 A). Probably if the time of study was broader the collapse of this device would occur. In the static group, unlike what happened with the empty defect (control), it was not visualized bone resorption between the screw-plate and bone. Probably this reaction did not occur because of the division of bone forces between the device and the 3D scaffold, and no early bone healing was detected radiographically (Figure 6.6 B). In the bioreactor group it is possible to radiographically visualize bone deposition in the vicinity of the cut edges of the proximal fragment (inside the biomaterial) and distal fragment (medially under the bone plate), but bone resorption was also not visualized (Figure 6.6 C). In any of the study groups was possible to radiographically visualized complete bony union between proximal/distal bone fragments.



Figure6.6. Radiographs obtained after 12 weeks of implantation: (A) Control-empty defects weeks; (B) Static; (C) Bioreactor.

### 6.3.3 SEM analysis

SEM photomicrographs were obtained from samples retrieved from the region indicated by the white arrows in the X-ray images depicted in the Figure 6.7, which were obtained at the moment of euthanasia for the static and bioreactor groups, after 6 and 12 weeks of implantation.



Figure 6.7. Radiographs obtained after implantation: (A) Static 6/ weeks group; (b) Static/12 weeks group; (C) Bioreactor/6 weeks group; (D) Bioreactor/12 weeks group.



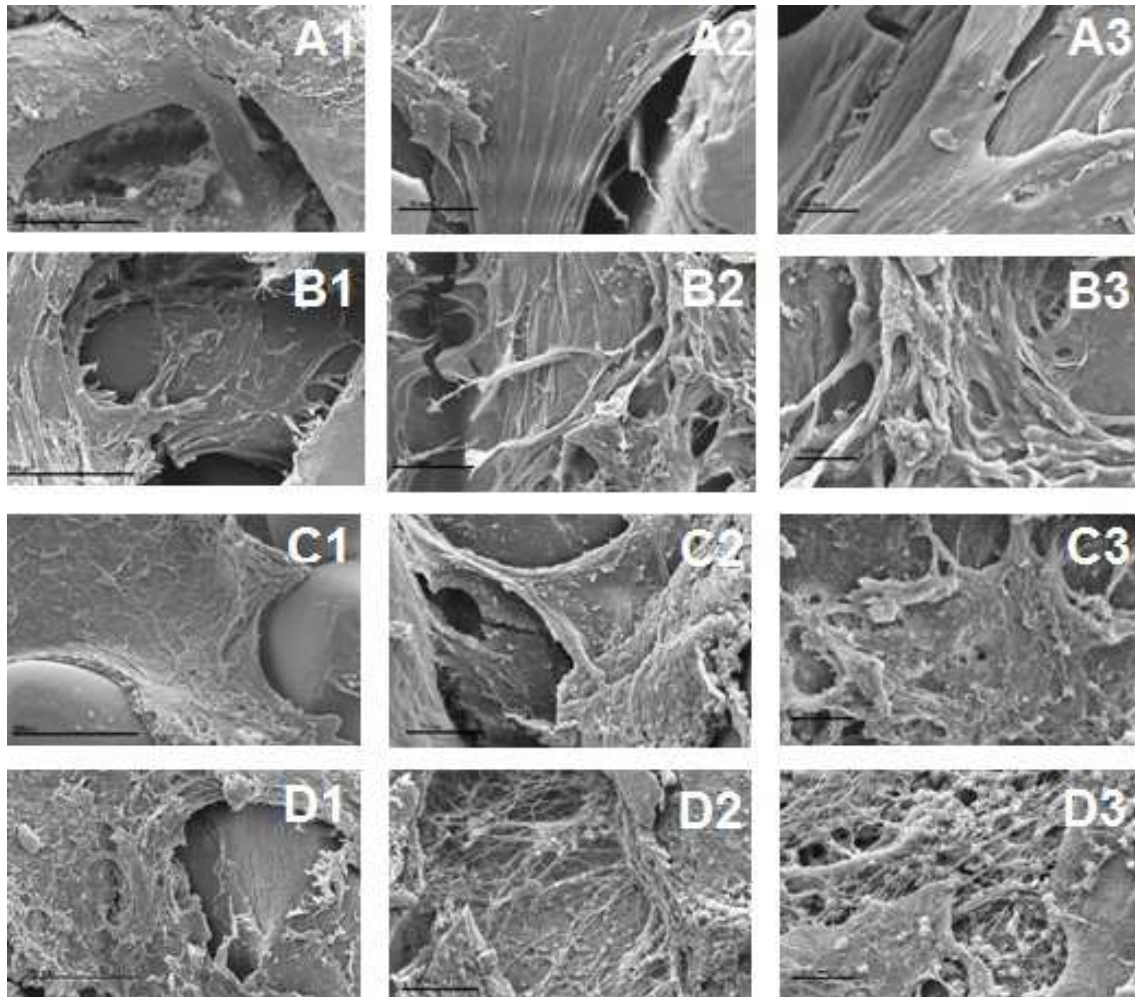


Figure 6.8. SEM photomicrographs of the cell-scaffold constructs retrieved upon implantation: (A) Static 6 weeks [A1 (x200),A2 (x500),A3 (x1000)]; (B) Static 12 weeks [B1 (x200),B2 (x500),B3 (x1000)]; (C) Bioreactor 6 weeks [C1(x200),C2(x500),C3(x1000)] and (D) Bioreactor 12 weeks (D1 (x200),D2 (x500),D3 (x1000)).

SEM (Figure 6.8), showed the formation of dense sheets of tissue crossing adjacent fibers of SPCL meshes, mostly for the longer periods of implantation in both static and bioreactor groups (12 weeks) (Figure 6.8 B1-B3 and D1-D3). Cells embedded in a matrix were observed covering the fibers surface, but also colonizing the inner pores/regions of the scaffold. Nevertheless, in the constructs cultured in the bioreactor groups, it was also possible to observe the formation of a layer of calcified globular accretions associated with collagen bundles, deposited on and into of the scaffolds (Figure 6.8 C1-C3 and D1-D3), that is more evident after 12 weeks of implantation (Figure 6.8 D1-D3).

Analysis of the EDS spectra obtained from samples corresponding to bioreactor 6 weeks group (Figure 6.9 A), bioreactor 12 weeks group (Figure 6.9 B), static 6 weeks (Figure 6.9 C) and static 12 weeks group (Figure 6.9 D) allowed to detect an increment of the calcium (Ca) and phosphorus (P) elements that corresponding to the deposition of a mineralized matrix. By observation of the figure (6.9 B) it is possible to detect that the graphic corresponding to the bioreactor 12 week surgical group shows a higher increase of Ca and P in the SPCL-cell construct when compared to other groups.

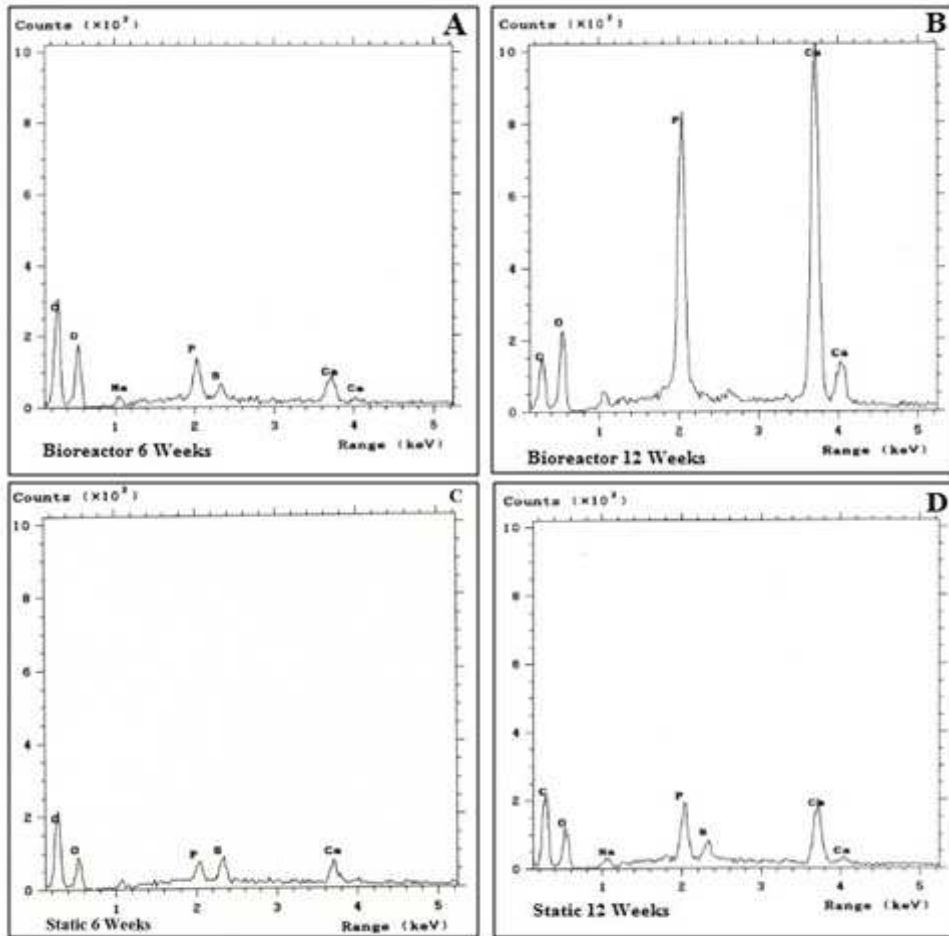


Figure 6.9. EDS spectra for Bioreactor 6 weeks group (A), Bioreactors 12 weeks group (B), Static 6 weeks group (C) and Static 12 weeks group (D).



#### 6.3.4. Micro-CT analysis

In figure 6.10, it is possible to visualize four representative images of SPCL-cells constructs retrieved from the in vivo experiments and analyzed by micro-ct. These images were obtained precisely in the region of the interface among the proximal/distal bone and the scaffolds. In both bioreactor study groups (6 and 12 weeks) it was possible to detect development and deposition of lamellar bone tissue in this bone defect borders, but only in the 12 weeks group bioreactor it was possible to visualize a high degree of bone calcification. This calcification not only occurred on the surface of the scaffold but also inside, suggesting the important role of the homogenous distribution of the cells in the scaffolds and their active metabolism and osteogenic differentiation, when cultured in the flow perfusion bioreactor. The results of the morphometric measurements in the 3D analysis of the new bone formation in all samples were analyzed using a threshold ranging from 120 (lower grey) to 225 (upper grey). However, with this threshold value it was not possible to obtain data from the static group. The data obtained from the bioreactor group (6 and 12 weeks), showed that the bioreactor 12 weeks group was filled for  $10 \pm 3\%$  of their volume with bone. In contrast, the bioreactor 6 weeks group showed  $0.9 \pm 1.4\%$  of the bone. Statistical evaluation revealed that significantly more bone was present in bioreactor 12 weeks group compared with bioreactor 6 weeks group ( $P=0.009$ ).

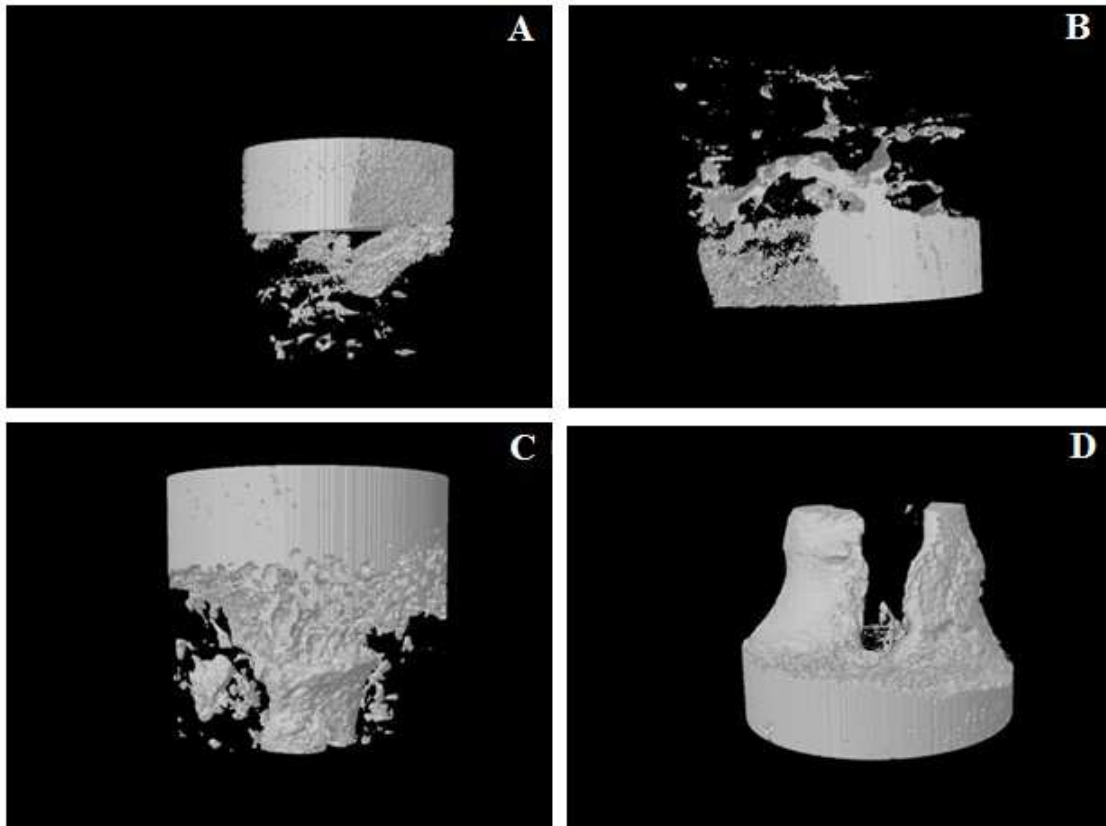


Figure 6.10:  $\mu$ -CT 3D virtual models images of the region corresponding to the bone interfaces with SPCL-Cells constructs. A) Interface between proximal fragment and scaffolds bioreactor 6 weeks group; B) Interface between distal fragment and scaffolds bioreactor 6 weeks group; C) Interface between proximal fragment and scaffolds bioreactor 12 weeks group and D) Interface among distal fragment and scaffolds bioreactor 12 weeks group.

### 6.3.5 Histological analysis

Upon harvesting of the explants, a thin fibrous capsule surrounding all scaffolds groups was observed. No inflammatory reaction was observed inside or around the implants. No bone formation could be observed macroscopically. Histologically (Figures 6.11 and 6.12), after 6 weeks of implantation in static and bioreactor group, matrix deposition, revascularization and neovascularization (small vessels with thick endothelium) were observed inside the scaffolds in both experimental groups. The matrix was red stained (similar to bone tissue), but lacked osteocyte-like cells and was not surrounded by osteoid with active osteoblasts.

Mineralized-like matrix deposition was mainly found at the scaffolds edges that were in direct contact with the bone, in the bioreactor group 6 weeks. In the same samples, it was possible to observe revascularization and neovascularization (Figure 6.11 A and B). Furthermore, for static surgical group 6 weeks, no connection or union of bone with scaffolds was observed (Figure 6.11 C and D).

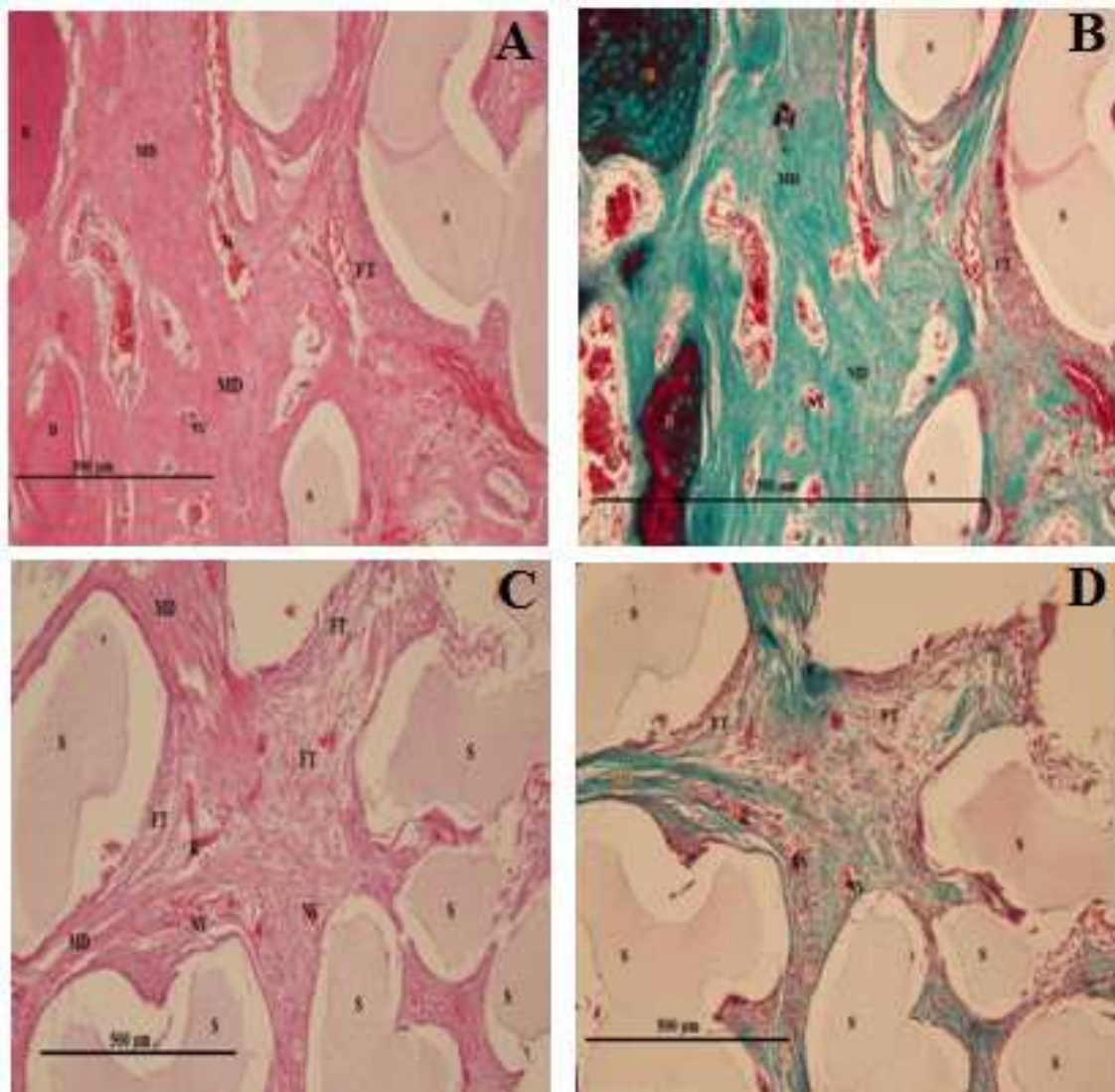


Figure 6.11. Light microscopy images of cell-scaffolds sections corresponding to the bioreactor groups after 6 weeks implantation (HE (A) and MT (B) and static groups after 6 weeks implantation (H&E(C) and MT(D). Bone (B); Matrix Deposition (MD); Fibrous Tissue (FT); Revascularization (R); Neovascularization (NV); SPCL fiber-meshes (S).

After 12 weeks of implantation, revascularization and neovascularization of blood vessels into scaffolds porosity was found in both experimental groups, but bone formation and bone marrow was only observed in the bioreactor groups (Figure 6.12 E and F). In static groups, fibrous tissue and mineralized-like matrix deposition could be observed (Figure 6.12 G and H), but new bone formation was not observed.

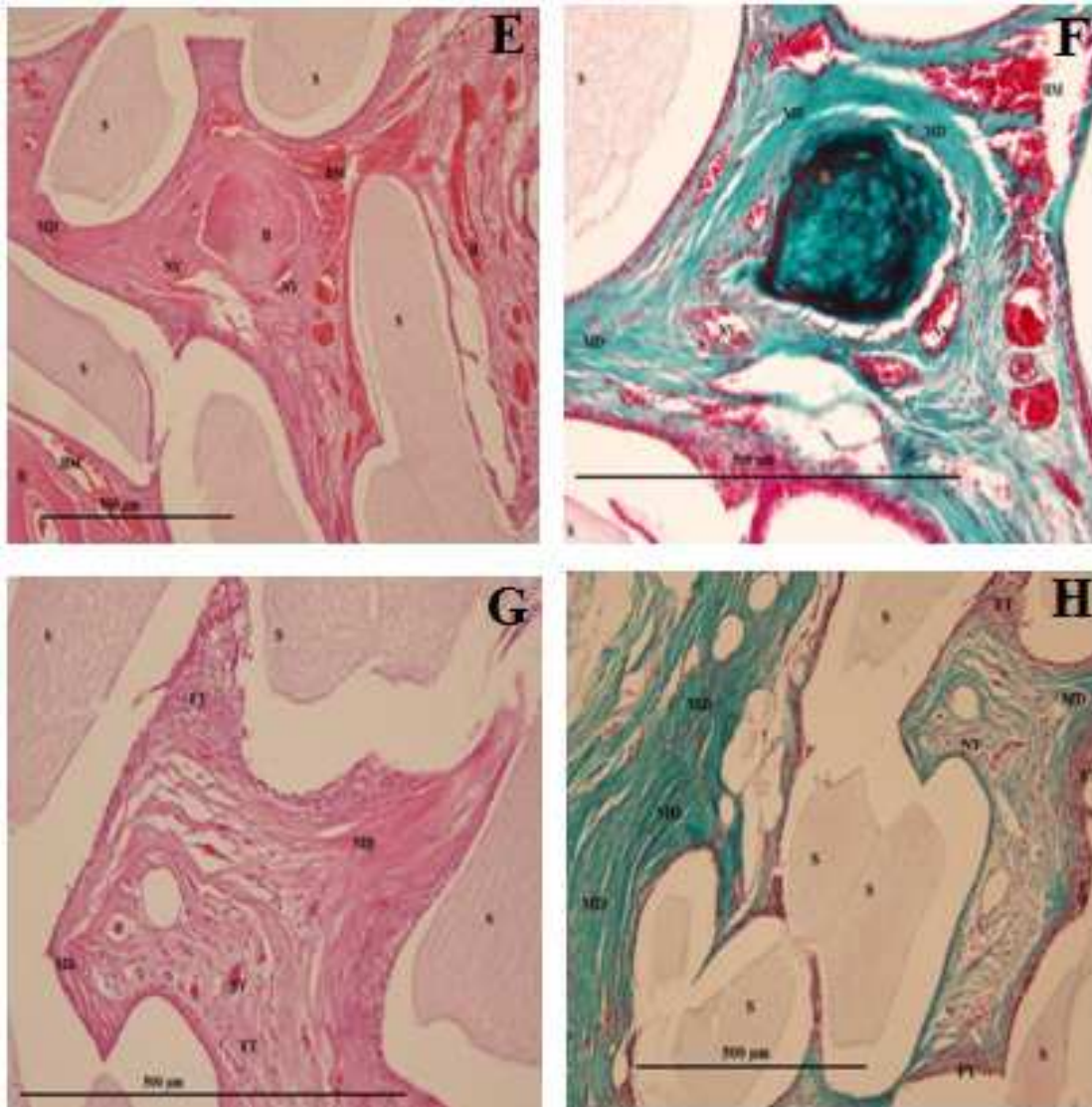


Figure 6.12. Light microscopy images of cell-scaffold constructs sections corresponding to bioreactor groups after 12 weeks implantation (HE (E) and MT (F)), and static groups after 12 weeks of implantation. Bone (B); Bone Marrow (BM); Matrix Deposition (MD); Revascularization (R); Neovascularization (NV); SPCL fiber-meshes (S).



## 6.4. Discussion

In the present work, aimed to observe the effect of using SPCL fibre mesh scaffolds seeded with GBMSC's cultured in a flow perfusion bioreactor, specifically designed to enable the culture of large sized constructs, in the regeneration of critical size defects (42mm in length) performed in goat tibial diaphysis. Goat has a metabolic rate and bone remodeling rate similar to that of human's presenting a suitable animal model for testing human implants and materials. The constructs were cultured in the bioreactor with osteogenic medium for a period of 14 days, determined based on earlier studies, which revealed that this period of time enabled the initiation of osteogenic differentiation of cells in SPCL fiber meshes (24). All animals survived and no signs of infection or inflammation were found nearby the implantation areas 12 weeks after implantation. X-ray images obtained after the surgery and on the day of euthanasia, demonstrated that the choice of primary bone fixation device was correct. The critical defects implanted with GBMSC's–SPCL constructs can be compared to a complicated comminuted fracture in which the fracture site is unlikely to contribute substantially to the transfer of load during weight-bearing, and thus the plate must essentially support all of the forces transmitted through the limb. This requires a very rigid, strong plate-bone construction. These transmissions of forces were easily visible in the control animals (with defects left empty) after 12 weeks of implantation, where it's visible the stress caused by the plate-screws in the proximal/distal bone fragments. In higher strain environments, cellular differentiation favors osteoclasts and chondrogenesis or fibrogenesis. This was not visualized in other study group animals (control 6 weeks and static 6 weeks), which can probably be explained by the short time of the weight-bearing of the limb, since during the first two weeks a limb immobilization by a modified Robert-Jones bandage was applied in the operated limb (of the all animals). However, this was not observed in the groups that were implanted for longer periods of time (static 12 weeks and bioreactor 12 weeks), due to the biomechanical sustenance provided by the SPCL constructs(20), that supported the load together with the bone fixation device, since it was loaded with the purpose of compressing the stacked GBMSC's–SPCL constructs. The X-ray results confirm that during the time of the study there was no bone union among the proximal/distal bone fragments in all the study animals, and it was only possible to visualize radiographically bone formation in both proximal/distal bone fragments, in the defects treated with constructs cultured in the bioreactor, upon 12 weeks of implantation.

However, the results obtained from  $\mu$ -CT 3D virtual models images showed a representative volumetric bone formation among the proximal/distal bone fragments and GBMSC's–SPCL constructs cultured in the bioreactor, after 6 weeks of implantation.

This might be explained by the fact that  $\mu$ -CT is a much more sensitive method for detection of bone formation and mineralization than x-ray. In the defects filled with constructs cultured in the bioreactor after 12 weeks of implantation, where bone formation is radiographically visible and mineralization in both proximal and distal bone fragments, the  $\mu$ -CT 3D virtual models images of this same region show a much more intense and compact bone formation and mineralization. In fact, these 3D images corroborate with the SEM observations and EDS analysis spectra, which showed matrix mineralization in the GBMSC's–SPCL constructs cultured under perfusion, even after the shortest implantation time (6 weeks); in this group, a layer of calcified globular accretions associated with collagen bundles was deposited on and into the scaffolds, but this was even more evident in the defects filled with constructs cultured in the bioreactor, 12 weeks after implantation. Additionally, connection and integration of newly formed bone directly with the original proximal/distal bone fragments of the tibia (as shown in micro-CT 3D images) will result in rapid stabilization of the implant. As consequence, it can support further growth of bone through the scaffolds. These findings are clinically very relevant, because this will ensure the mechanical integrity of the constructs, protect and assist the distribution of forces among the bone fixation device and the large dimensions implanted construct.

Histological analysis also illustrated that bone marrow and bone formation (osteoid) inside the SPCL fiber meshes only occurred in the defects treated with bioreactor cultured constructs, after 12 weeks of implantation. Furthermore, occlusion of pores of the GBMSC's–SPCL constructs was not observed, possibly allowing the continuous exchange of oxygen, nutrients, and removal of metabolites that is expected to facilitate neovascularization. Morphometrical measurements demonstrated a higher new bone formation in the scaffolds cultured under perfusion, suggesting that GBMSC's–SPCL constructs cultured under a flow perfusion bioreactor exhibit a higher osteogenic potential in vitro and in vivo. Several other studies show that perfusion culturing of cell/scaffold constructs has a positive effect on cell proliferation and osteogenic differentiation (16, 28), but few studies have analyzed the effect of constructs cultured under these conditions upon implantation onto an orthotopic defect. Furthermore, studies focusing on orthotopic models are typically conducted using non critical size defects.

This methodology is very important to obtain information on the biocompatibility of the biomaterial used (immunologic and inflammatory reactions), to define optimal *in vitro* culture conditions before implantation and to analyze the importance of the number of cells and their differentiation stage at the moment of the cell-construct implantation. However, the results provided by non-critical size defect models, do not provide a complete answer regarding the feasibility (biomechanical behavior) of the cell-scaffold construct, when it is selected to be implanted in a critical size defect. In this study we have analyzed the role of cell-scaffolds constructs cultured in a perfusion bioreactor upon implantation in a critical size defect. The results obtained showed that bone development was enhanced with the perfusion culture of the constructs, demonstrating the importance of the culturing conditions in the *in vivo* functionality of the constructs composed of GBMSC's and SPCL scaffolds. Furthermore, it was demonstrated that SPCL fibre mesh scaffolds showed an appropriate biomechanical behavior, providing an adequate tissue 3D support for the regeneration of bone in critical size defects. The results of this study also confirm previous findings (18) on the biocompatibility of SPCL fiber meshes and their suitability for bone regeneration.

To the author's knowledge, no reference can be found to other studies that have used a single culture chamber perfusion bioreactor for culturing scaffolds of large dimensions and subsequently implanted it in a critical size defect performed on large animal models. With this study, we also show that bone formation was enhanced in the presence of GBMSC's–SPCL constructs cultured under a flow perfusion bioreactor in comparison to static groups in an orthopedic critical sized defect.

Consequently, we conclude that inoculating SPCL fiber meshes and osteogenic cells cultured in a perfusion system can improve the bone healing capacity of this tissue engineered construct and demonstrates that the use of this perfusion culture system is a valuable and convenient tool for applications in bone regeneration. Most perfusion bioreactors described in the literature do not enable the culture of large constructs and few studies have reported on the *in vivo* functionality of such constructs using critical size defects on large animal models. The BCPB demonstrated its potential as an important tool that fulfills the expectations for the successful culture of large bone tissue engineered substitutes.

## References

1. Green, S.A., Jackson, J.M., Wall, D.M., Marinow, H., Ishkanian, J. Management of segmental defects by the Ilizarov intercalary bone transport method. *Clin Orthop Relat Res*, 1992,136.
2. Giannoudis, P.V., Pountos, I. Tissue regeneration. The past, the present and the future. *Injury* 36 Suppl 4, 2005,S2.
3. Nair, M.B., Varma, H., Shenoy, S.J., John, A. Treatment of goat femur segmental defects with silica-coated hydroxyapatite--one-year follow-up. *Tissue Eng Part A* 16, 2010,385.
4. Williams, D.F. On the mechanisms of biocompatibility. *Biomaterials* 29, 2008,2941.
5. Pittenger, M.F., Mackay, A.M., Beck, S.C., Jaiswal, R.K., Douglas, R., Mosca, J.D., et al. Multilineage potential of adult human mesenchymal stem cells. *Science* 284, 1999,143.
6. Salgado, A.J., Coutinho, O.P., Reis, R.L. Bone tissue engineering: state of the art and future trends. *Macromol Biosci* 4, 2004,743.
7. Keogh, M.B., Partap, S., Daly, J.S., O'Brien, F.J. Three hours of perfusion culture prior to 28 days of static culture, enhances osteogenesis by human cells in a collagen GAG scaffold. *Biotechnol and Bioeng* 108, 2011,1203.
8. Du, D.J., Furukawa, K.S., Ushida, T. 3D Culture of Osteoblast-Like Cells by Unidirectional or Oscillatory Flow for Bone Tissue Engineering. *Biotechnol and Bioeng* 102, 2009,1670.
9. Schliephake, H., Zghoul, N., Jager, V., van Griensven, M., Zeichen, J., Gelinsky, M., et al. Bone formation in trabecular bone cell seeded scaffolds used for reconstruction of the rat mandible. *Int J Oral Maxillofac Surg* 38, 2009,166.
10. Sillon, A.M., Allori, A.C., Davidson, E.H., Reformat, D.D., Allen, R.J., Warren, S.M. A Novel Flow-Perfusion Bioreactor Supports 3D Dynamic Cell Culture. *J Biomed Biotechnol*, 2009.
11. Bjerre, L., Bunger, C.E., Kassem, M., Mygind, T. Flow perfusion culture of human mesenchymal stem cells on silicate-substituted tricalcium phosphate scaffolds. *Biomaterials* 29, 2008,2616.
12. Du, D., Furukawa, K., Ushida, T. Oscillatory perfusion seeding and culturing of osteoblast-like cells on porous beta-tricalcium phosphate scaffolds. *J Biomed Mater Res Part A* 86, 2008,796.



13. Grayson, W.L., Bhumiratana, S., Cannizzaro, C., Chao, P.H., Lennon, D.P., Caplan, A.I., et al. Effects of initial seeding density and fluid perfusion rate on formation of tissue-engineered bone. *Tissue Eng Part A* 14, 2008,1809.
14. Kavlock, K.D., Goldstein, A.S. Effect of pulsatile flow on the osteogenic differentiation of bone marrow stromal cells in porous scaffolds. *Biomed Sci Instrum* 44, 2008,471.
15. Gomes, M.E., Bossano, C.M., Johnston, C.M., Reis, R.L., Mikos, A.G. In vitro localization of bone growth factors in constructs of biodegradable scaffolds seeded with marrow stromal cells and cultured in a flow perfusion bioreactor. *Tissue Eng* 12, 2006,177.
16. Gomes, M.E., Holtorf, H.L., Reis, R.L., Mikos, A.G. Influence of the porosity of starch-based fiber mesh scaffolds on the proliferation and osteogenic differentiation of bone marrow stromal cells cultured in a flow perfusion bioreactor. *Tissue Eng* 12, 2006,801.
17. Pashkuleva, I., Azevedo, H.S., Reis, R.L. Surface structural investigation of starch-based biomaterials. *Macromol Biosci* 8, 2008,210.
18. Rodrigues, M.T., Gomes, M.E., Viegas, C.A., Azevedo, J.T., Dias, I.R., Guzon, F.M., et al. Tissue-engineered constructs based on SPCL scaffolds cultured with goat marrow cells: functionality in femoral defects. *J Tissue Eng Regen Med* 5, 2011,41.
19. Gomes, M.E., Sikavitsas, V.I., Behravesh, E., Reis, R.L., Mikos, A.G. Effect of flow perfusion on the osteogenic differentiation of bone marrow stromal cells cultured on starch-based three-dimensional scaffolds. *J Biomed Mater Res Part A* 67A, 2003,87.
20. Gomes, M.E., Azevedo, H.S., Moreira, A.R., Ella, V., Kellomaki, M., Reis, R.L. Starch-poly(epsilon-caprolactone) and starch-poly(lactic acid) fibre-mesh scaffolds for bone tissue engineering applications: structure, mechanical properties and degradation behaviour. *J Tissue Eng Regen Med* 2, 2008,243.
21. Marques, A.P., Cruz, H.R., Coutinho, O.P., Reis, R.L. Effect of starch-based biomaterials on the in vitro proliferation and viability of osteoblast-like cells. *J Mater Sci Mater Med* 16, 2005,833.
22. Santos, T.C., Marques, A.P., Horing, B., Martins, A.R., Tuzlakoglu, K., Castro, A.G., et al. In vivo short-term and long-term host reaction to starch-based scaffolds. *Acta Biomater* 6, 2010,4314.
23. Davidson, E.H., Reformat, D.D., Allori, A., Canizares, O., Janelle Wagner, I., Saadeh, P.B., et al. Flow perfusion maintains ex vivo bone viability: a novel model for bone biology research. *J Tissue Eng Regen Med* Nov 3. doi: 10.1002/term.478. [Epub ahead of print]. 2011., 2011.

24. Gardel, L.S., Dias, A., Link, D.P., Serra, L.A., Gomes, M.E., Reis, R.L. Development of an novel bidirectional continuous perfusion bioreactor (BCPB) for culturing cells in 3D scaffolds. *Histology and Histopathology Cellular and Molecular Biology* 26, 2011,70.
25. David, V., Guignandon, A., Martin, A., Malaval, L., Lafage-Proust, M.H., Rattner, A.M., V., et al. Ex Vivo bone formation in bovine trabecular bone cultured in a dynamic 3D bioreactor is enhanced by compressive mechanical strain. *Tissue Eng Part A* 14, 2008,117.
26. Costa, P.F., Martins, A., Neves, N.M., Gomes, M.E., Reis, R.L. A novel bioreactor design for enhanced stem cells proliferation and differentiation in tissue engineered constructs. *Tissue Eng Part A* 14, 2008,802.
27. Rodrigues, M.T., Martins, A., Dias, I.R., Viegas, C.A., Neves, N.M., Gomes, M.E., et al. Synergistic effect of scaffold composition and dynamic culturing environment in multilayered systems for bone tissue engineering. *J Tissue Eng Regen Med*, 2012.
28. Goldstein, A.S., Juarez, T.M., Helmke, C.D., Gustin, M.C., Mikos, A.G. Effect of convection on osteoblastic cell growth and function in biodegradable polymer foam scaffolds. *Biomaterials* 22, 2001,1279.



## **SECTION 6**

### **CHAPTER VII**

## **Autologous stem cell therapy for the treatment of a tibial fracture gap in a cat.**

This chapter is based on the following publication: Gardel LS, Afonso M, Serra LA, Gomes ME, Reis RL .Autologous stem cell therapy for the treatment of tibial fracture gap in a cat. Submitted 2012



## **ABSTRACT**

Autologous stem cell therapy is a new field of veterinary medicine regenerative that involve harvesting, proliferation and differentiation of stem cells, most often from the bone marrow our adipose tissue, for posterior application in the same patient. This work describes a successful clinical treatment of a tibial fracture gap in a cat using an autologous stem cell therapy (ASCT). Bone marrow (BM) was harvested from the femoral medullar cavity. Cat Bone Marrow Stromal Cells (CBMSC's) were cultured in osteogenic medium for a pre--differentiation into osteoblasts, before applying the cells suspension percutaneously in the fracture site. Alkaline phosphatase (ALP) assay and alizarin red staining were used to assess osteogenic differentiation/mineralization of in vitro cultured cells and X-rays were performed to follow up bone repair. The postoperative of an orthopaedic patient requires a degree of reduction of movement of the member affected until the clinic union occurs, which is very difficult to achieve for most patients In this study it was shown that two weeks after the application of the autologous stem cell therapy (ASCT) in the gap fracture, the animal developed a callus with high opacity and also developed a clinical bone union that allowed the animal to fully utilize the affected limb. Thus ASCT should be considered as a successful adjuvant therapy for rapid repair in large gap sites.

## 7.1 INTRODUCTION

Autologous Stem Cell Therapy (ASCT) is a field of regenerative veterinary medicine that involves harvesting tissue, such as bone marrow, from the patient, isolating the stem cells, and administering the cells back to the patient, with or without in vitro expansions and/or differentiation. It has been described in humans (1-3) dogs (4-7), and horses (8-10) to treat orthopaedics conditions. Cat bone marrow stem cells (CBMSCs) are multipotent adult stem cells and have become an important cell source for cell therapy and engineered tissue repair. Their osteogenic differentiation potential has been well characterized in vitro (11). With an increasing feline pet population that currently exceeds the canine pet population, veterinary practitioners and specialists are expected to treat a growing variety and number of fractures involving the humerus, radius/ulna, femur, and tibia/fibula (12). Fractures of the tibia are common in cats (about 20 % of all fractures) (13). Diaphyseal fractures of the tibia are encountered frequently (14). They are most often caused by trauma, but occasionally spontaneous fractures occur, being frequently accompanied by diaphyseal fractures of the fibula. These are not addressed during tibial fracture repair. Posttraumatic synostoses between the tibia and fibula have no negative effect on the clinical outcome (15). External fixators are widely used for the treatment of tibial injuries since there is little soft-tissue coverage of the crus (16). In one study, closed reduction and external skeletal fixation of comminuted tibial fractures resulted in a 27% shorter fracture healing period compared with an open approach and plate osteosynthesis (17).

This case report describes the successful clinical treatment of a cat with a large fracture gap after percutaneous application of the CBMCs pre-differentiated into osteoblasts, clearly demonstrates that the use of ASCT can help shorten fracture healing time.

## 7.2 CASE REPORT

A 3 years-old female sterilized European cat weighing 7.200kg, presented a high-impact fracture of the medial shaft of the right tibia due to a fall from a height of 15 meters, which was stabilized using External Skeletal Fixation type II (ESF), applied through a closed approach performed by the referring veterinarian, was referred to the Veterinary Medical Teaching Clinical (UPVET) at the ICBAS-University of Porto, Porto (UP), two days after the surgery because of a small collapse in the ESF utilized, for application of ASCT. Thoracic radiographs, hematologic, biochemical and urinalysis profiles were within normal parameters. After craneo-caudal radiography projections (Figure 7.1) of the affected limb, a lateral displacement in the axial focus of fracture was observed and a large bone gap was visualized (Latero-lateral projections were made but due to overlapping of the bone fixation device, not was possible to visualize displacement). This usually indicates a long time for repair or it can lead to a non union. In this clinical situation, it is very important to assure a significant reduction in the mobility of the patients. However this is very difficult to achieve in most cases. This small collapse was probably caused by the method selected (smooth pins rather than positive threaded pins), associated with the inability of owners to keep the patient in cage rest. With this in mind, it was decided to apply a cellular therapy with the goal of enhancing fracture healing in a shorten time.



Figure7.1. Craneo-caudal radiography projections of the affected limb, where it is observed a lateral displacement in the axial focus of fracture.



Under general anaesthesia (ketamine HCl, Merial, Sintra, PT) at 5 mg/kg IM and medetomidine (Virbac, Sintra, PT) at 80µg/kg IM), maintained on isoflurane (Abbott laboratories, Amadora, PT) (2%) in oxygen (1500ml/min), 2ml of bone marrow (BM) was harvested from the femoral medullar cavity through the use of a biopsy needle (T-Lok™ Angiotech, Vancouver, British Columbia, CA, USA). The cat bone marrow aspirate was mixed with 10ml of osteogenic media consisting of alpha-DMEM (Sigma-Aldrich, St. Louis, USA) supplemented with osteogenic supplements namely, 10<sup>-8</sup> M dexamethasone (Sigma-Aldrich, St. Louis, USA), 1% Antibiotics (Sigma, St. Louis, USA); 10% Fetal bovine serum (Invitrogen, Burlington, ON, CA) 50µg/ml-1 ascorbic acid (Sigma, St. Louis, USA) and 10mM β-glycerophosphate (Sigma, St. Louis, USA), and heparin (BBraun medical, Barcarena, PT) (1/1000units) and the mixture was centrifuged (1200rpm/5 min). The pellet was removed and the cells were resuspended in the same media and seeded in two 75 cm<sup>2</sup> culture flasks and then placed inside an incubator. Cells developed a fibroblastic-like morphology in visible symmetric colonies at about 4 days after initial plating. Nonadherent cells were removed with medium changes performed every 2-3 days. The osteoblastic differentiation was induced by culturing cells for 2 weeks.

CBMSC's cells were enzymatically lifted with 3 ml of trypsin after reaching 80%-90% of confluence at passage 3 (p3), centrifuged (1200rpm/5min) and the pellet was removed. A cells suspension containing 9x10<sup>6</sup> cells in 0,6 ml of phosphate-buffered saline (PBS) (Sigma, St. Louis USA) solution was prepared to be injected in the gap site using a 1mL sterile syringe (Figure 7.2).



Figure 7.2. Syringe containing the cells suspension, used for the application of the cells in fracture gap.

To characterize the osteogenic differentiation *in vitro*, cells were cultured in 6 well plates at a density of  $3 \times 10^5$  cells/well. Plates with osteogenic medium for days 0, 7 (first week) and 21 (third week), changing the medium every 2-3 days. ALP activity of the CBMSC's was measured to evaluate osteoblastic-like differentiation; for this purpose, the samples were collected on days 0, 7 (first week) and 21 (third week), washed twice with a sterile PBS solution and transferred into 1.5 ml microtubes containing 1ml of ultra pure water; the tubes containing the cells samples were then incubated for 1h at 37 °C in a water -bath and then stored in a -80 °C freezer until testing. For the ALP assay, 20µl of each sample plus 60µl of substrate solution 0.2% (w/v) *p*-nitrophenyl (*p*NP) phosphate (Sigma, St. Louís USA) in a substrate buffer: 1 M diethanolamine HCL (Merck, Darmstadt, DE), at pH 9.8 was placed in each well of a 96-well plate. The plate was then incubated in the dark for 45 min at 37 °C. After the incubation period, 80 µl of a stop solution (2M NaOH) (Panreac, Barcelona, ES) containing 0.2 mM ethylenediaminetetraacetic acid (EDTA) (Sigma, St. Louís, USA), was added to each well. Standards were prepared with  $10 \mu\text{mol ml}^{-1}$  *p*NP and the stop solutions in order to achieve final concentrations ranging between 0 and  $0.3 \mu\text{mol}^{-1}$ . Triplicates were made for each sample and standard. Absorbance was read at 405 nm Microplate ELISA Reader (Synergie HT, Bio-Tek Instruments, Inc, Winooski, USA) and sample concentrations were read off from standard graph. To asses mineralization, cells cultured in 6-well plates with osteogenic medium for different time points were stained with Alizarin Red (Fluca, GE).

Assessment of ALP *In vivo* was carried out by harvest of 2 ml of peripheral blood serum for assay in IDEXX VetTest® chemistry analyzer (Barcelona, ES) in days 0 ( day of the application of the cells), 7 (first week) and 21 (third week). To visualize the development of the mineralization in the gap site, X-rays (Philips Medical Systems, Carlsbad, CA) were carried out at days 0, 7 (first week) and 21 (third week) upon cells implantation.

### 7.3 RESULTS

The CBMSCs presented a high *in vitro* osteoblastic-like differentiation potential, similarly to others studies carried out in mouse (18), rabbits (19), dogs (20), goats (21) sheep (22) and human (23).

The high ALP activity registered after two weeks of *in vitro* culture in osteogenic media - day 0 (day of application) – demonstrated that these cells are undergoing osteoblastic differentiation. The synthesis of ALP has the main function of stimulating the extracellular matrix formation, carried out by osteoblasts through mineral deposition (mineralization).

This phenomenon can be evidenced by the gradual decrease of ALP activity registered at day 7 (first week of implantation) and day 21 (third week of implantation) in cells cultured in vitro (Figure 7.3).

The Alizarin red staining was performed after day 21 (three weeks) of culture, showing the mineralization of the cells at this stage (Figure 7.4).

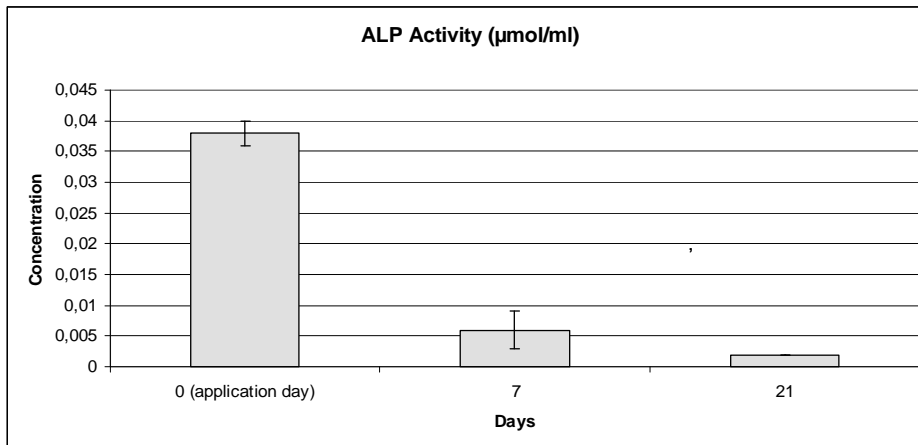


Figure 7.3. ALP activity in cells cultured in vitro, in osteogenic medium, at the day of implantation (after expansion for 2 weeks in osteogenic medium) and at 7 and 21 days of subsequent culturing.

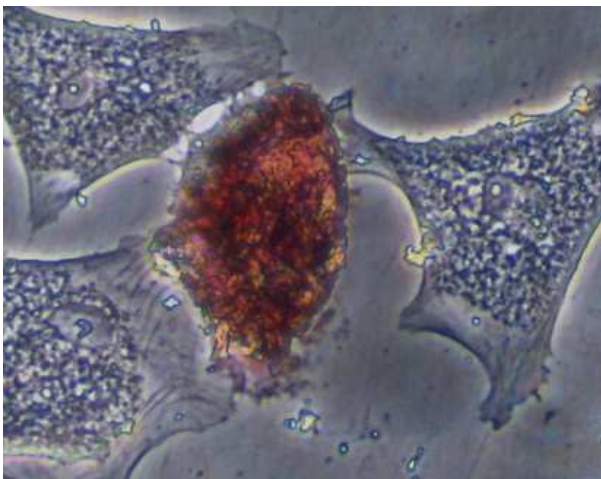


Figure 7.4. Alizarin red staining of the cat bone marrow cells after 3 weeks of in vitro culture in osteogenic medium

Values of the ALP activity measured in blood serum cat immediately before the application of the cells were within normal values reported for feline species. Abnormal values of the ALP (2 times or more) are indicative of pathological changes in bone, muscle, liver and reproductive tissues. The effect of the CBMSCs implanted was evidenced by the increase of ALP activity in cat serum registered at day 7 (first week) and day 21 (three week) after cell application (Figure 7.5).

In fact, stem cells have great tropism for the injured site and participate in tissue regeneration by differentiating into specific cell types that are necessary in the damaged tissue, producing anabolic effects, stimulating neovascularization, recruiting additional stem cells and promoting anti-inflammatory effects (by secreting great levels of immunomodulatory and trophic agents) (24, 25). Thus, this increase in serum ALP is probably associated with an enhanced regeneration and bone healing at the fracture site. These findings are supported by the results displayed in the X-rays images, which showed an excellent outcome of the applied autogenic therapy.

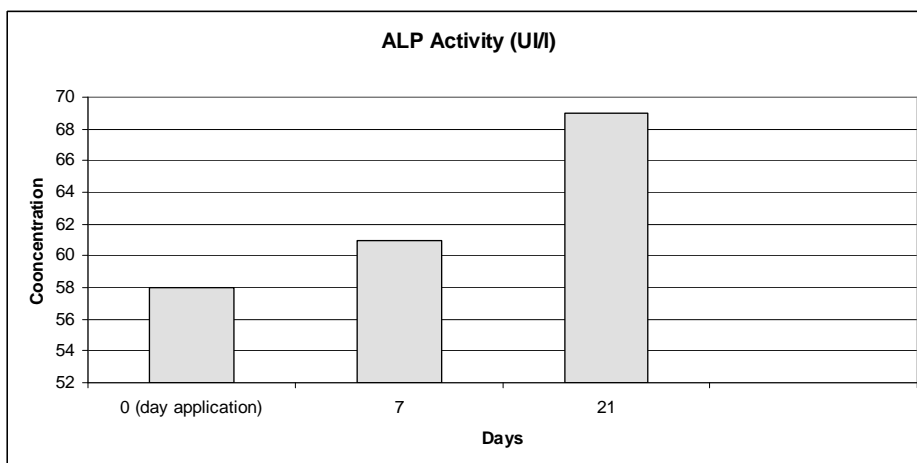


Figure 7.5. ALP activity in blood serum of the cat, measured at the day of the application of the cells (day 0) and 7 and 21 days after application.

Specifically, in the X-ray images (Figure 7.6 A,B and C), the formation of new bone is easily identified as demonstrated by the rounded tops of fracture distal and proximal as well as the gradual increase in opacity within the focus of fracture, caused by the formation and deposition of calcium, characteristic of bone formation. After 3 weeks of the cells application, the radiographs showed satisfactory healing of the tibia, bone consolidation was observed (lamellar bone), and the animal had full use of the affected limb, was then given directions to the referring veterinarian to remove the ESF.

The owners reported that there were not any signs of pain or lameness of the limb six months after application, and no side effects (inflammation) were visualized at the application site. Eighteen months after application, radiographs showed a medial deviation and recurvatum deformity of the tibial bone (Figure 7.7), caused initially after the surgery by the difficulty of the owners to keep the patient in cage rest, but the cat walked normally and without lameness. The joint mobilization was pain free and the range-of-motion in flexion and extension was similar to the contralateral limb.

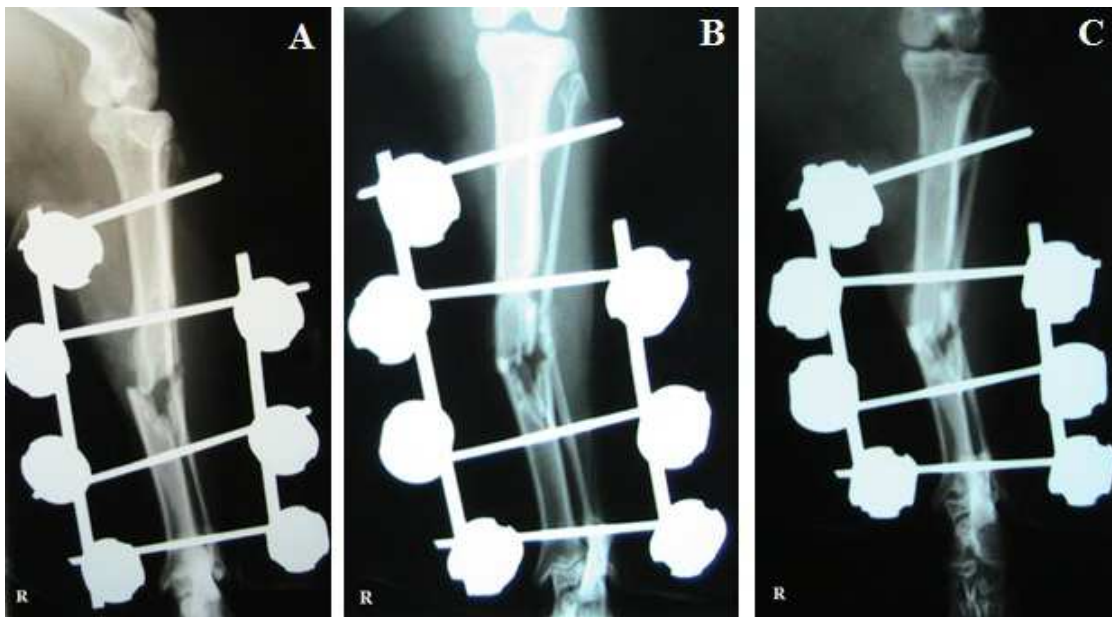


Figure 7.6. Crano-caudal radiographic projections obtained at: (A) day 0 (day of cells application); (B) after 1 weeks of cells application in the fracture site; (C) after 3 weeks of cells application in the fracture site.



Figure 7.7. Craneo-caudal and latero-medial radiographic projections showing a medial deviation and recurvatum deformity of the tibial bone after eighteen months of follow-up.

#### 7.4 CONCLUSION

A major challenge for the owners of an orthopaedic veterinary patient is to keep the pet on the recommended laid down by the veterinary surgeon preventing it from doing high impact exercises, climbing up/down stairs, preventing slips on smooth floor, etc., during the first weeks of postoperative. Therefore these recommendations are very difficult to be strictly followed in most cases, which can lead to collapse of the bone fixation method selected according to the different classification of the long bone fractures types. This highlights the importance of a good planning of the fixation method type to select before surgery. Stem cell therapy is currently being used as an alternative treatment in various pathologies related to bone. This case report demonstrates that CBMCs differentiated into osteoblasts applied at the fracture site allows a rapid bone healing and functional return bone tissue, and thus ASCT should be considered as a new successful adjuvant therapy for a quick treatment of long-bone fracture in the orthopaedic surgery of small animals.

## REFERENCES

1. Kim, S.J., Shin, Y.W., Yang, K.H., Kim, S.B., Yoo, M.J., Han, S.K., et al. A multi-center, randomized, clinical study to compare the effect and safety of autologous cultured osteoblast(Ossron) injection to treat fractures. *BMC Musculoskelet Disord* 12, 2009,10.
2. Hernigou, P., Poignard, A., Beaujean, F., Rouard, H. Percutaneous autologous bone-marrow grafting for nonunions. Influence of the number and concentration of progenitor cells. *J Bone Joint Surg Am* 87, 2005,1430.
3. Voegelé, T.J., Voegelé-Kadletz, M., Esposito, V., Macfelda, K., Oberndorfer, U., Vecsei, V., et al. The effect of different isolation techniques on human osteoblast-like cell growth. *Anticancer Res* 20, 2000,3575.
4. Yamazoe, K., Mishima, H., Torigoe, K., Iijima, H., Watanabe, K., Sakai, H., et al. Effects of atelocollagen gel containing bone marrow-derived stromal cells on repair of osteochondral defect in a dog. *J Vet Med Sci* 69, 2007,835.
5. Yan, Z., Hang, D., Guo, C., Chen, Z. Fate of mesenchymal stem cells transplanted to osteonecrosis of femoral head. *J Orthop Res* 27, 2009,442.
6. Black, L.L., Gaynor, J., Adams, C., Dhupa, S., Sams, A.E., Taylor, R., et al. Effect of intraarticular injection of autologous adipose-derived mesenchymal stem and regenerative cells on clinical signs of chronic osteoarthritis of the elbow joint in dogs. *Vet Ther* 9, 2008,192.
7. Black, L.L., Gaynor, J., Gahring, D., Adams, C., Aron, D., Harman, S., et al. Effect of adipose-derived mesenchymal stem and regenerative cells on lameness in dogs with chronic osteoarthritis of the coxofemoral joints: a randomized, double-blinded, multicenter, controlled trial. *Vet Ther* 8, 2007,272.
8. Koch, T.G., Berg, L.C., Betts, D.H. Current and future regenerative medicine - principles, concepts, and therapeutic use of stem cell therapy and tissue engineering in equine medicine. *Can Vet J* 50, 2009,155.
9. Arnhold, S.J., Goletz, I., Klein, H., Stumpf, G., Beluche, L.A., Rohde, C., et al. Isolation and characterization of bone marrow-derived equine mesenchymal stem cells. *Am J Vet Res* 68, 2007,1095.
10. O'Rielly, J.L., Bertone, A.L., Genovese, R.L. Treatment of a chronic comminuted fracture of the fibula in a horse. *J Am Vet Med Assoc* 212, 1998,396.
11. Martin, D.R., Cox, N.R., Hathcock, T.L., Niemeyer, G.P., Baker, H.J. Isolation and characterization of multipotential mesenchymal stem cells from feline bone marrow. *Exp Hematol* 30, 2002,879.

12. Harari, J. Treatments for feline long bone fractures. *Vet Clin North Am Small Anim Pract* 32, 2002,927.
13. Boudrjeau, R.J. Fractures of the tibia and fibula. In: Slatter D editors *Textbook of Small Animal Surgery*, Vol 2. Philadelphia: Saunders, 2003,pp. 2144.
14. Piermattei, D.L., Flo, G.L. *Fractures of the tibia and fibula*. 2006.
15. Schwarz, G. Fractures of the tibial diaphysis. In: Johnson AN, Houlton JEF, Vannini R, editors: *AO Principles of Fracture Management in the Dog and Cat* New York, NY: Thieme, 2005,319.
16. Marcellin-Little, D.J. External skeletal fixation. In: Slatter D editors *Textbook of Small Animal Surgery Vol 2*, Philadelphia, PA, Saunders;, 2003,818.
17. Dudley, M., Johnson, A.L., Olmstead, M. Open reduction and bone plate stabilization, compared with closed reduction and external fixation, for treatment of comminuted tibial fractures: 47 cases (1990-1995) in dogs. *J Am Vet Med Assoc* 211, 1997,1008.
18. Gao, C., Seuntjens, J., Kaufman, G.N., Tran-Khanh, N., Butler, A., Li, A., et al. Mesenchymal stem cell transplantation to promote bone healing. *J Orthop Res*, 2012.
19. Kim, S.J., Chung, Y.G., Lee, Y.K., Oh, I.W., Kim, Y.S., Moon, Y.S. Comparison of the osteogenic potentials of autologous cultured osteoblasts and mesenchymal stem cells loaded onto allogeneic cancellous bone granules. *Cell Tissue Res* 347, 2012,303.
20. Sun, B., Ma, W., Su, F., Wang, Y., Liu, J., Wang, D., et al. The osteogenic differentiation of dog bone marrow mesenchymal stem cells in a thermo-sensitive injectable chitosan/collagen/beta-glycerophosphate hydrogel: in vitro and in vivo. *J Mater Sci Mater Med* 22, 2011,2111.
21. Wang, C., Wang, Z., Li, A., Bai, F., Lu, J., Xu, S., et al. Repair of segmental bone-defect of goat's tibia using a dynamic perfusion culture tissue engineering bone. *J Biomed Mater Res Part A* 92, 2010,1145.
22. Feitosa, M.L., Fadel, L., Beltrao-Braga, P.C., Wenceslau, C.V., Kerkis, I., Kerkis, A., et al. Successful transplant of mesenchymal stem cells in induced osteonecrosis of the ovine femoral head: preliminary results. *Acta Cir Bras* 25, 2010,416.
23. Leonardi, E., Devescovi, V., Perut, F., Ciapetti, G., Giunti, A. Isolation, characterisation and osteogenic potential of human bone marrow stromal cells derived from the medullary cavity of the femur. *Chir Organi Mov* 92, 2008,97.
24. Caplan, A.I. "What's in a name?" *Tissue Eng Part A* 16, 2010,2415.
25. Ribitsch, I., Burk, J., Delling, U., Geissler, C., Gittel, C., Julke, H., et al. Basic Science and Clinical Application of Stem Cells in Veterinary Medicine. *Adv Biochem Eng Biotechnol* 123, 2010,219.





**SECTION 7**

**Chapter VIII**

**GENERAL CONCLUSION**



## CONCLUSIONS

The work developed under the scope of this thesis enabled to achieve results that led to several conclusions concerning the main objectives of this thesis, which are summarized below:

### *1) Importance of bone marrow MSCs and scaffold material in the regeneration of critical sized defects*

The *in vivo* study performed in a rat model was designed to assess the influence of the 3D scaffolds loaded/non loaded with rat bone marrow stromal cells and cultured in static conditions with osteogenic medium in the regeneration of a rat calvarial critical size defect. For this purpose, the scaffold materials that was select to use in this thesis - starch/polycaprolactone (SPCL) fiber meshes - pre-loaded with RBMSCs or alone, were implanted in a the rat critical-sized cranial defects, for two different periods of implantation, namely four and eight weeks. Results obtained by Micro-CT reconstructions and histological analysis showed that bone formation increased over the implantation time and was enhanced in the defects filled with the scaffolds pre-loaded with RBMSCs as compared to SPCL scaffolds alone.

These results showed that the pre-loaded RBMSCs contributed to the bone regeneration process in a critical-sized bone defect, possibly by the release of factors that induce the recruitment of osteoprogenitor cells rather that participating directly in the new bone formed. SPCL fiber mesh scaffolds have also proved to be a suitable scaffold for bone engineering. In summary, this study clearly demonstrated that the regeneration of critical size bone defects requires the presence of both osteoprogenitor cells and a suitable scaffold.

### *2) Development a flow perfusion bioreactor BCPB:*

A major challenge in the translation of tissue engineered bone grafts to viable clinical treatments of osseous defects has been the need to grow large, fully viable grafts that are several centimetres in size. This was the main motivation for the development of the flow perfusion Bioreactor (BCPB) under this thesis. The BCPB presents an innovative design that has proven to create mechanical cellular stimulus (described in chapter V,VI) through the generation of shear forces due to medium flow perfusion using different pressure gradients, controlled by peristaltic pumps. Furthermore, the flow-perfusion bioreactor is a scalable technology that should support the culture of porous scaffolds with large dimensions, up to 120 mm in length and 60 mm in diameter, which constitutes the main innovation of this system.

The culture of large sized constructs is enabled by the control of flow perfusion and pressure gradient from inside to outside of the scaffold and vice-versa, providing the adequate access to nutrients and removal of metabolic wastes of the cells located in the inner regions of thick 3D constructs, thereby maintaining cell viability and activity.

Most tissue-engineering research has been constrained to using scaffolds of small dimensions (2mm in thickness or less), which are easily sustainable by medium convection or static culture methods. The experiments performed in this thesis showed that the BCPB enabled cells survival and proliferation in constructs of the 42mm in length, 16 mm in diameter and 3 mm thick, demonstrating that this new system flow perfusion is superior to the static culture for large-scale cell-construct culture.

*3) Functionality of the developed bioreactor: Effect of culture conditions provided by the newly developed flow perfusion bioreactor versus static condition, on the proliferation, distribution and differentiation of GBMSC's seeded onto SPCL fiber mesh scaffolds.*

This *in vitro* study described under chapter V was planned to evaluate the feasibility of the newly developed flow perfusion bioreactor system for sustaining “thick” 3D scaffolds that approach sizes of clinical relevance in the orthopaedic field. Specifically, as proof of principle, it were cultured in the bioreactor large cylindrical scaffolds (42mm in length, 16 mm in diameter and 3 mm thick), seeded with goat bone marrow stromal cells (GBMSCs), and compared to scaffolds cultured under static conditions. Results showed that the BCPB enabled GBMSC's survival and proliferation in the GBMSC's–SPCL constructs, and enabled superior outcomes as compared to the static culture conditions, particularly regarding GBMSCs osteogenic differentiation. Thus, the BCPB demonstrate be a simple and efficient system for enabling to culture large-scale scaffolds and obtain highly functional constructs for bone regeneration applications.

*4) Assessment of the in vivo functionality of constructs cultured in the newly developed bioreactor, using a critical size defect performed in a large animal*

The *in vivo* study described under chapter VI, performed in a goat model, demonstrated that 14 days of flow perfusion culturing of SPCL scaffolds-GBMSCs constructs induces differences in the functionality of the resulting constructs upon implantation in a critical size defect.

The results obtained showed that bone development was enhanced with the perfusion culture of the constructs of large dimension, demonstrating the importance of the culturing conditions in the in vivo functionality of the constructs composed of GBMSC's and SPCL scaffolds. Furthermore, it was demonstrated that SPCL fibre mesh scaffolds enabled an appropriate biomechanical environment, providing an adequate tissue 3D support for the regeneration of bone in critical size defects. Thus, in summary, it was concluded that inoculating SPCL fiber meshes and osteogenic cells cultured in a perfusion system can improve the bone healing capacity of this tissue engineered constructs and demonstrates that the use of this perfusion culture system is a valuable and convenient tool for applications in bone regeneration.

*5) Studying autologous stem cell therapy of CBMSCs when applied in the treatment of a tibial fracture gap in a cat. Case report*

A major challenge in orthopedic veterinary surgery is to keep the pet on the recommended laid down by the veterinary surgeon preventing it from doing high impact exercises, during the first weeks of postoperative.

With know-how obtained along of this thesis, it was possible to assess, in a clinical case-study the application of an autologous stem cell therapy to enhance bone healing in a cat feline patient who presented a large gap fracture after fixing bone with external skeletal fixation type II. For this purpose, cat bone marrow stromal cells were harvested from the femoral medullar cavity through the use of a biopsy needle and pre-differentiated in osteoblasts-like cells. A cells suspension containing  $9 \times 10^6$  cells was injected in the gap site. The animal developed a callus with high opacity identified radiographically and also developed a clinical bone union that allowed the animal to fully utilize the affected limb two weeks after the application of the autologous stem cell therapy.

***Final concluding remarks:***

Accordingly to all the above mentioned findings it was possible to conclude that the work carried out in the scope of this thesis resulted in the development of a novel flow perfusion bioreactor that enables to culture large sized constructs allowing to obtain functional bone tissue-like substitutes for the regeneration of critical size defects. To the author's knowledge, no reference can be found to other studies that have used a single culture chamber perfusion bioreactor for culturing scaffolds of large dimensions and subsequently implanted it in a critical size defect performed on large animal model.

The results obtained have also clearly demonstrated the important capabilities of the bone marrow stromal cells and SPCL as a 3D scaffold with high osteogenic potential within the area of bone tissue engineering. Finally it was shown that the application of autologous pre-differentiated stem cells presents itself as an alternative and adjuvant therapy for the repair of bone tissue.